Rylene Bisimide-Diarylethene Photochromic Systems for Non-destructive Memory Read-out

Dissertation zur Erlangung des
naturwissenschaftlichen Doktorgrades
der Julius-Maximilians-Universität Würzburg

vorgelegt von

Martin Berberich

aus Amorbach

Würzburg 2012

Eingereicht bei der Fakultät für Chemie und Pharmazie am:

10.08.2012

1. Gutachter: Prof. Dr. Frank Würthner

2. Gutachter: Prof. Dr. Markus Sauer

der schriftlichen Arbeit

1. Prüfer: Prof. Dr. Frank Würthner

2. Prüfer: Prof. Dr. Markus Sauer

3. Prüfer: Prof. Dr. Tobias Brixner

des öffentlichen Promotionskolloquiums

Tag des öffentlichen Promotionskolloquiums:

29.10.2012

Doktorurkunde ausgehändigt am:

_____

Wer nichts als Chemie versteht,

versteht auch die nicht recht.

Georg Christoph Lichtenberg

(1742–1799)

List of Abbreviations

A	acceptor
AIBN	azobisisobutyronitrile
APCI	atmospheric-pressure chemical ionization
BOC	*N-tert*-butoxycarbonyl
c	closed form of photochrome
CI	conical intersection
CT	charge transfer
CV	cyclic voltammetry
D	donor
DAE	diarylethene
DAE_C	closed form of diarylethene
DAE_O	open form of diarylethene
DBN	1,5 diazabicyclo[4.3.0]non-5-ene
DCC	*N,N'*-dicyclohexylcarbodiimide
DCTB	2-[(2*E*)-3-(4-*tert*-butylphenyl)-2-methylprop-2-enylidene]malononitrile
diglyme	1-methoxy-2-(2-methoxyethoxy)ethane
DMF	*N,N*-dimethylformamide
DMSO	dimethyl sulfoxide
ESI	electrospray ionization
FRET	Förster resonance energy transfer
FWHM	full width half maximum
HOMO	highest occupied molecular orbital
HRMS	high resolution mass spectrometry
IC	internal conversion
ISC	intersystem crossing
lit.	literature
LUMO	lowest unoccupied molecular orbital
MALDI	Matrix-assisted laser desorption/ionization
MCH	methylcyclohexane
*m*CPBA	*meta*-chloroperoxybenzoic acid
mp	melting point
MS	mass spectrometry
NBS	*N*-bromosuccinimide
NIR	near infrared
NMP	*N*-methyl-2-pyrrolidone
NMR	nuclear magnetic resonance

o	open form of photochrome
OMEM	organic memory
Oxone®	$2KHSO_5 \cdot KHSO_4 \cdot K_2SO_4$
PET	photoinduced electron transfer
PBI	perylene bisimide
PSS	photostationary state
RC	ring closure
ref.	reference
RO	ring opening
RT	reaction time
rt	room temperature
S_0	singlet ground state
S_1	first singlet excited state
SEC	spectroelectrochemistry
SOMO	singly occupied molecular orbital
T_1	lowest triplet state
TBAHFP	tetrabutylammonium hexafluorophosphate
TBI	terrylene bisimide
TC-SPC	time-correlated single-photon counting
THF	tetrahydrofuran
TMP	2,2,6,6-tetramethylpiperidine
TOF	time-of-flight
UV	ultraviolet
vis	visible
VR	vibrational relaxation

Abbreviations for NMR characterization

|	
ap	*anti*-parallel isomer of diarylethene
brs	broad singlet
d	doublet
dd	doublet of doublets
m	multiplet
p	parallel isomer of diarylethene
s	singlet
sept	septet
t	triplet
TMS	tetramethylsilane

7

Table of Contents

1   Introduction and Aim of the Thesis

The demand for advanced data storage methods has increased dramatically during the last decade. The development of computer technologies and memory systems with large storage capacity and fast read-write efficiencies is in a footrace with the increasing need for technologies such as high-resolution photography, high-definition (HD) film techniques and the miniaturization for laptops, tablet PCs and smartphones. An emerging memory method that has potential for high bit density is based on single organic molecules, which are photoswitchable between two thermally stable isomers. This molecular property is known as photochromism and derived from the Greek words *phos* for light and *chroma* for color. Photochromism was initially defined by Yehuda Hirshberg in the 1950s as "a reversible transformation of a chemical species induced in one or both directions by absorption of electromagnetic radiation between two forms (isomers) having different absorption spectra".[1]

The high potential of photochromic systems for organic memories (OMEM) has been convincingly demonstrated by Parthenopoulos and Rentzepis in 1989 with a three-dimensional data storage system based on photochromic spirobenzopyran embedded in a polymer matrix.[2] Following this seminal work several new photochromic systems have been developed for high-density information storage on a molecular level.[3] In regard to our present work, one particularly relevant photochromic dyad system consisting of a switchable diarylethene (DAE) unit and a fluorescent bis(phenylethynyl)anthracene dye was reported by Irie, Fukaminato and coworkers.[4] In this particular system, emission of the dye unit could be turned on and off repeatedly by isomerization of the photochromic DAE unit upon irradiation with light of two different wavelengths. With an additional third light source of a different wavelength, the respective fluorescent or non-fluorescent state can be obtained as the "read-out" signal, resulting in a binary emissive "1" and non-emissive "0" code. For one of the photochromic isomers, intramolecular Förster resonance energy transfer (FRET) from the excited dye quenches the emission, while this process cannot occur in the other, fluorescent isomer. One detrimental effect of the intramolecular fluorescence quenching by FRET, however, is the concomitant excitation of the ring-closed form of the photochromic dyad during the read-out process, resulting in undesirable ring opening. Thus, energy transfer may induce the photochromic back reaction of the ring-closed form to the ring-open one during reading of the fluorescence intensity and such energy-transfer-based memory systems lead to destructive read-out.

Emission quenching based on intramolecular photoinduced electron transfer (PET)[5] may circumvent such a destructive read-out pathway. Some examples of electron-transfer switching with different photochromic units have been reported in the literature. However, so far such switching systems lack a thermally bistable photochrome or an efficient fluorophore to monitor electron transfer by fluorescence quenching.[6] An interesting system has been published by Tsuchiya, where an electron-rich and an electron-poor porphyrin are connected by an azobenzene bridge allowing modulation of the donor-acceptor distance by photoinduced *cis-trans* isomerization.[7] Electron

transfer was observed only in the *cis* isomeric form because of a markedly reduced distance between the porphyrin units. One major drawback of azobenzene-based systems is the lack of thermal stability of the *cis* isomer. A few years ago, nearly simultaneously in the preceding diploma work[8] (see dyad **1o**/**1c** in Scheme 1) and in a publication of Fukaminato and Irie,[9] a concept for fluorescence photoswitching by intramolecular electron transfer based on dyads of photochromic DAE and fluorescent perylene bisimide (PBI) dye was proposed. The basic idea behind this concept is that the ring-open and ring-closed isomers of the photochromic DAE moiety exhibit different redox properties and the electron transfer from fluorescent PBI dye is thermodynamically favorable only to one of the two DAE isomers.
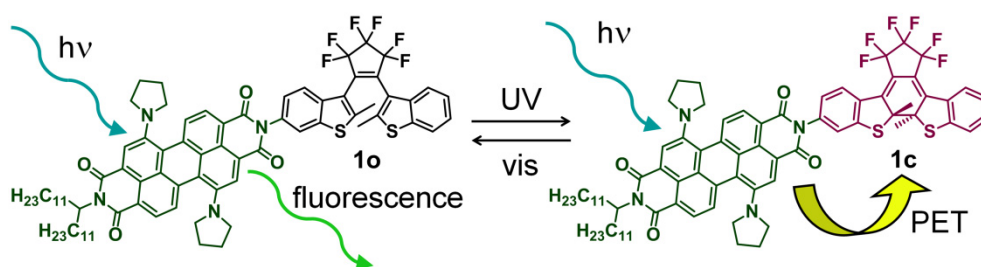
Scheme 1. Photoswitching of fluorescence by intramolecular electron transfer in a diarylethene-perylene bisimide photochromic system **1o**/**1c**.[8b]

Due to the fact that several DAE derivatives also show electrochromic behavior upon oxidation,[10] the DAE unit of a photochromic donor-acceptor dyad may act as the electron acceptor. In an optimal case, electron transfer from a fluorescent dye to the DAE unit of a Dye–DAE dyad would be exergonic only for the Dye^+–DAE_C^- but not for Dye^+–DAE_O^- charge transfer (CT) state (Figure 1). The stabilization and, therefore, the thermodynamically favored formation of a CT state can be dramatically influenced by the nature of the environment (*e.g.* polarity and rigidity). With an appropriately designed system, it would then be possible to read, write and erase optical memory without destructive read-out using light sources of three different wavelengths.
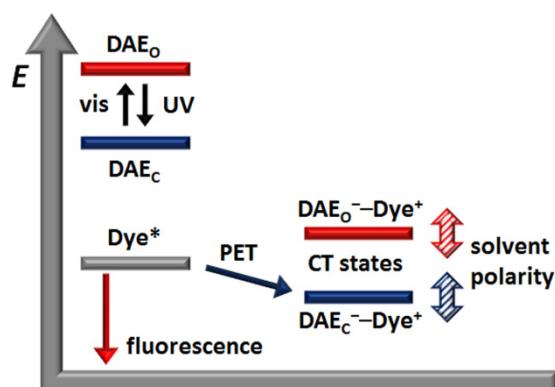
Figure 1. Schematic energy diagram for the fluorescent open form (red line) and the non-fluorescent closed form (blue line) of DAE–Dye conjugate.[11]

Each of the previously reported photoswitching systems based on this concept suffer from certain disadvantages, such as low fluorescence quantum yield, photocyclization by triplet state population, small driving force for fluorescence-quenching PET, or low photostability.[8-9,12] For instance, PBI– DAE dyad **1o/1c** (Scheme 1) has the disadvantage of low fluorescence quantum yield ($\Phi_{fl} = 14\%$ in dichloromethane) and low photostability of the 1,7-dipyrrolidino-substituted PBI, leading to decomposition of this moiety upon continuing irradiation.[8]

Since our initial communication,[8b] efforts to develop photoswitching systems with superior properties were made by employing photostable rylene bisimide dyes with high fluorescence quantum yields and by varying the optical and electronic properties of the switching DAE unit. The present thesis describes the synthesis and characterization of two novel photochromic systems **2o/2c** and **3o/3c** (Scheme 2). The photoswitching properties of these systems are investigated in detail by steady-state and time-resolved spectroscopy, while the driving force for the emission quenching PET has been estimated by Rehm-Weller equation.[13]
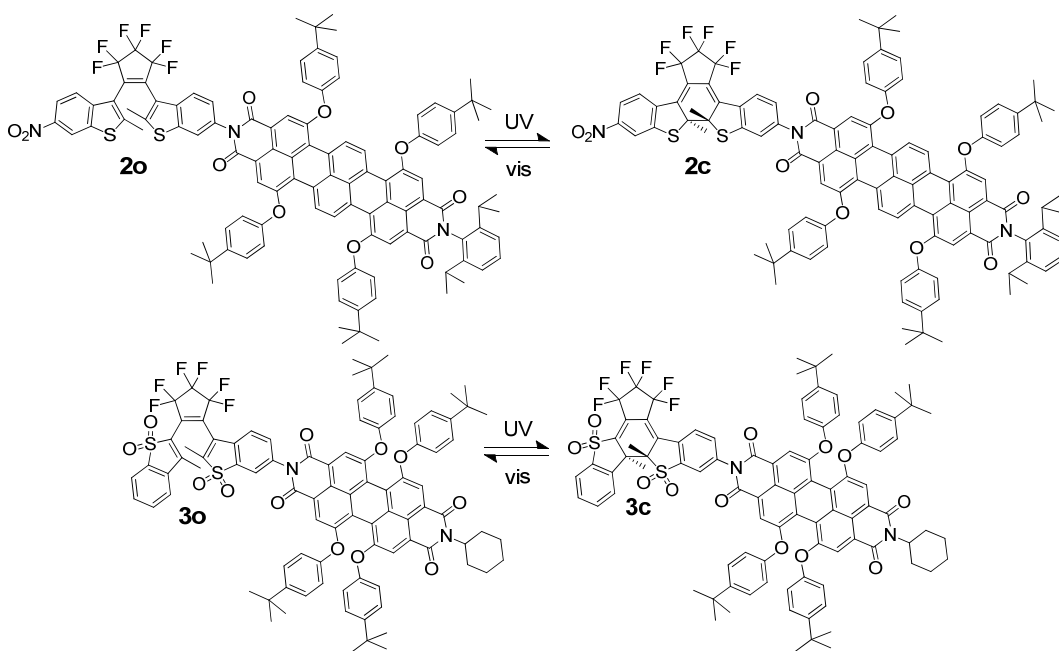
Scheme 2. Open and closed form of new photochromic compounds **2o/2c** and **3o/3c** composed of a photoswitchable diarylethene and a fluorescent rylene bisimide unit.

Chapter 2 gives an overview of photochromism with a particular focus on diarylethenes. In this context, the design, energetics of the switching process, and the redox behavior of this outstanding class of photochromes will be introduced. The important terms energy and electron transfer will be summarized to gain a better understanding of the last section of this chapter. In this a literature survey will systematically present photochromic systems composed of two or three units for the photoinduced control of intramolecular energy or electron transfer, in some cases already in respect to data storage application.

Chapter 3 compares the spectroscopic and electronic properties of three literature known and four new electron-poor DAEs and judges about their applicability for electron-transfer photoswitches.

Chapter 4 introduces the first photochromic system **2o/2c** (Scheme 2) based on a tetraaryloxy-substituted terrylene bisimide (TBI) as photostable, electron-rich emissive moiety and a DAE photoswitch. The synthesis and the investigation of the photoswitching properties by UV/vis absorption and fluorescence spectroscopy, and cyclic voltammetry are reported and discussed. Furthermore, the photostability of the present system has been tested by repeating switching cycles performed by alternating irradiation with UV and visible light. With the DAE–TBI dyad **2**, a photochromic system enabling excellent control of the fluorescence intensity of the TBI unit by switching between the two states of the DAE unit and high photostability over multiple switching cycles was achieved

Chapter 5 presents an optimized system **3o/3c** (Scheme 2) with superior properties by employing 1,6,7,12-tetraaryloxy PBI dyes and a DAE moiety with oxidized thiophene 1,1-dioxide subunits. The optical and photophysical properties of this dyad were studied in detail by steady-state and time-resolved spectroscopy. Solvent-dependent studies revealed outstanding switching behavior between the two states with very different fluorescence properties (*i.e.* quantum yields of 95% and 5%, respectively), as well as non-destructive read-out and excellent fatigue resistance are proven for this photochromic system.

Chapter 6 compares the two new photochromic systems **2o/2c** and **3o/3c** to all other literature known dyads, which were designed for photoswitching of fluorescence by photoinduced electron transfer containing perylene bisimide dyes as emitting unit.

The thesis is summarized in English and in German in **Chapter 7** and concludes with an **Appendix**, which contains supplementary information for Chapter 4.

References

[1]   Y. Hirshberg, *C. R. Hebd. Seances Acad. Sci.* **1950**, *231*, 903-904.

[2]   a) D. A. Parthenopoulos, P. M. Rentzepis, *Science* **1989**, *245*, 843-845; b) F.-K. Bruder, R. Hagen, T. Rölle, M.-S. Weiser, T. Fäcke, *Angew. Chem. Int. Ed.* **2011**, *50*, 4552-4573.

[3]   a) T. A. Golovkova, D. V. Kozlov, D. C. Neckers, *J. Org. Chem.* **2005**, *70*, 5545-5549; b) M. Bossi, V. Belov, S. Polyakova, S. W. Hell, *Angew. Chem. Int. Ed.* **2006**, *45*, 7462-7465; c) G. Jiang, S. Wang, W. Yuan, L. Jiang, Y. Song, H. Tian, D. Zhu, *Chem. Mater.* **2006**, *18*, 235-237; d) T. Fukaminato, T. Umemoto, Y. Iwata, S. Yokojima, M. Yoneyama, S. Nakamura, M. Irie, *J. Am. Chem. Soc.* **2007**, *129*, 5932-5938; e) J. H. Hurenkamp, J. J. D. de Jong, W. R. Browne, J. H. van Esch, B. L. Feringa, *Org. Biomol. Chem.* **2008**, *6*, 1268-1277; f) S. F. Yan, V. N. Belov, M. L. Bossi, S. W. Hell, *Eur. J. Org. Chem.* **2008**, 2531-2538; g) J. Fölling, S. Polyakova, V. Belov, A. van Blaaderen, M. L. Bossi, S. W. Hell, *Small* **2008**, *4*, 134-142; h) J. Cusido, E. Deniz, F. M. Raymo, *Eur. J. Org. Chem.* **2009**, 2031-2045; i) R. Métivier, S.

Badré, R. Méallet-Renault, P. Yu, R. B. Pansu, K. Nakatani, *J. Phys. Chem. C* **2009**, *113*, 11916-11926; j) J. Kärnbratt, M. Hammarson, S. Li, H. L. Anderson, B. Albinsson, J. Andréasson, *Angew. Chem. Int. Ed.* **2010**, *49*, 1854-1857; k) B. Seefeldt, K. Altenhoner, O. Tosic, T. Geisler, M. Sauer, J. Mattay, *Photochem. Photobiol. Sci.* **2011**, *10*, 1488-1495; l) T. Fukaminato, *J. Photochem. Photobiol., C* **2011**, *12*, 177-208.

[4]   a) M. Irie, T. Fukaminato, T. Sasaki, N. Tamai, T. Kawai, *Nature* **2002**, *420*, 759-760; b) T. Fukaminato, T. Sasaki, T. Kawai, N. Tamai, M. Irie, *J. Am. Chem. Soc.* **2004**, *126*, 14843-14849.

[5]   a) *Supramolecular Photochemistry* (eds. Balzani, V.; Scandola, F.), Ellis Horwood, New York, **1991**; b) *Fundamentals of Photoinduced Electron Transfer* (ed. Kavarnos, G. J.), VCH Publishers Inc, New York, **1993**; c) *Electron Transfer in Chemistry* (ed. Balzani, V.), Wiley-VCH, Weinheim, **2001**; d) N. Mataga, H. Chosrowjan, S. Taniguchi, *J. Photochem. Photobiol., C* **2005**, *6*, 37-79.

[6]   a) J. M. Endtner, F. Effenberger, A. Hartschuh, H. Port, *J. Am. Chem. Soc.* **2000**, *122*, 3037-3046; b) A. J. Myles, N. R. Branda, *J. Am. Chem. Soc.* **2001**, *123*, 177-178; c) Y. Terazono, G. Kodis, J. Andréasson, G. Jeong, A. Brune, T. Hartmann, H. Dürr, A. L. Moore, T. A. Moore, D. Gust, *J. Phys. Chem. B* **2004**, *108*, 1812-1814; d) F. M. Raymo, M. Tomasulo, *Chem. Soc. Rev.* **2005**, *34*, 327-336.

[7]   S. Tsuchiya, *J. Am. Chem. Soc.* **1999**, *121*, 48-53.

[8]   a) M. Berberich, Diploma Thesis, University of Würzburg, Würzburg (Germany), **2007**; b) M. Berberich, A.-M. Krause, M. Orlandi, F. Scandola, F. Würthner, *Angew. Chem. Int. Ed.* **2008**, *47*, 6616-6619.

[9]   Y. Odo, T. Fukaminato, M. Irie, *Chem. Lett.* **2007**, *36*, 240-241.

[10]   a) A. Peters, N. R. Branda, *J. Am. Chem. Soc.* **2003**, *125*, 3404-3405; b) A. Peters, N. R. Branda, *Chem. Commun.* **2003**, 954-955; c) W. R. Browne, J. J. D. de Jong, T. Kudernac, M. Walko, L. N. Lucas, K. Uchida, J. H. van Esch, B. L. Feringa, *Chem. Eur. J.* **2005**, *11*, 6414-6429; d) W. R. Browne, J. J. D. de Jong, T. Kudernac, M. Walko, L. N. Lucas, K. Uchida, J. H. van Esch, B. L. Feringa, *Chem. Eur. J.* **2005**, *11*, 6430-6441; e) Y. Moriyama, K. Matsuda, N. Tanifuji, S. Irie, M. Irie, *Org. Lett.* **2005**, *7*, 3315-3318; f) G. Guirado, C. Coudret, M. Hliwa, J.-P. Launay, *J. Phys. Chem. B* **2005**, *109*, 17445-17459.

[11]   M. Berberich, F. Würthner, *Chem. Sci.* **2012**, *3*, 2771-2777.

[12]   a) T. Fukaminato, T. Doi, M. Tanaka, M. Irie, *J. Phys. Chem. C* **2009**, *113*, 11623-11627; b) T. Fukaminato, M. Tanaka, T. Doi, N. Tamaoki, T. Katayama, A. Mallick, Y. Ishibashi, H. Miyasaka, M. Irie, *Photochem. Photobiol. Sci.* **2010**, *9*, 181-187; c) T. Fukaminato, T. Doi, N. Tamaoki, K. Okuno, Y. Ishibashi, H. Miyasaka, M. Irie, *J. Am. Chem. Soc.* **2011**, *133*, 4984-4990.

[13]   A. Z. Weller, *Z. Phys. Chem.* **1982**, *133*, 93-98.

2   State of Knowledge and Literature Survey

2.1   Photochromism

In Nature, photoswitchable organic compounds enable humans' vision process and control the permeability of ion channels in some species.[1] In the human eye, the Schiff base of 11-*cis*-retinal (see **1cis** in Scheme 1), the chromophore of the biological pigment rhodopsin, isomerizes to the all-*trans* form upon irradiation, bleaching the color. The reverse reaction of this particular photoswitch compound, is not governed by light but is driven by a chemical stimulus.
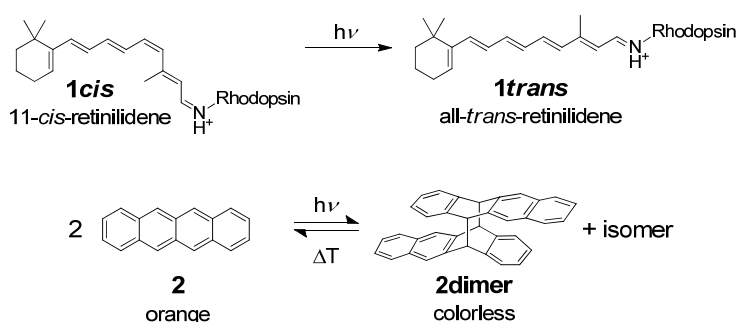
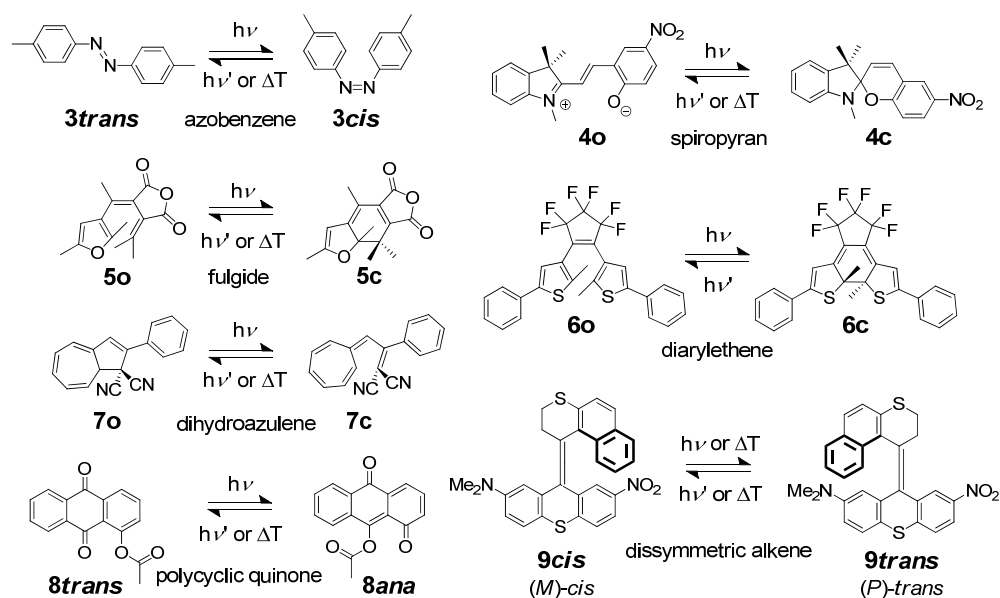**Scheme 1.** Initial examples of photochromic compounds.

Another example of photochromism in Nature is the protein channelrhodopsin, which acts as light-gated ion channel within the membranes of green alga *Chlamydomonas reinhardtii*. The photoisomerization from all-*trans*-retinal, found within the protein, to 13-*cis*-retinal enables sodium ions to pass through the membrane. The related protein bacteriorhodopsin, found in the cell membrane of *Halobacterium salinarum*, "pumps" protons through the channel upon irradiation and thereby establishes a proton gradient across the membrane. With this approach, the protein plays an important role as a converter of solar energy into chemical energy for phototrophs.

The first report on photochromic compounds was published by Fritsche in the middle of the 19th century.[2] He described the light-induced dimerization of tetracene **2** (see Scheme 1) and thus observed a color change from orange to colorless. The respective back reaction to the colored form is thermally activated. One hundred years later, Corning Glass Works developed the first commercially available photochromic lenses, called Bestlite[TM], in 1960. Glasses with such lenses become dark upon irradiation with sunlight and return to a colorless state in the absence of intense radiation.

The term photochromism was initially defined by Yehuda Hirshberg in the 1950s as "a reversible transformation of a chemical species induced in one or both directions by absorption of electromagnetic radiation between two forms (isomers) having different absorption spectra".[3] This molecular property of being switchable between two thermally stable isomers is derived from the Greek words *phos* for light and *chroma* for color. Contemporary photochromic compounds (see

Scheme 2) range from the best-known azobenzenes **3**,[4] which undergo photoinduced *cis-trans* isomerization, to spiropyrans **4**,[5] fulgides **5**,[6] and diarylethenes[7] **6** that undergo six π-electron pericyclic reactions from the so called ring-open to the respective ring-closed form upon irradiation. Less developed examples of photochromic compounds are dihydroazulenes **7**, polycyclic quinones **8**, and dissymmetric alkenes **9**, which are impressively used for molecular motors.[8]

**Scheme 2**. Examples of different photochromic compounds.

The drawback of most photochromic molecules is the thermally promoted back reaction, *i.e.* thermochromism, even under exclusion of light. Molecules with two thermally stable isomers, *i.e.* bistability, that do not show any isomerization up to 80 °C are qualified as P-type photochromes.[7a] Those with at least one thermally reversible isomer are denoted as T-type. The cyclization and the respective cycloreversion quantum yield describe the ratio of absorbed photons inducing the isomerization reaction and can distinctly differ for the same compound. Besides the thermal bistability, the fatigue resistance is one of the most important properties of photochromic compounds. In this context, the repeatable cycle number describes the number of switching cycles, *e.g.* from open to closed form of a diarylethene (denoted as DAE) and *vice versa*, at which the absorbance change of one isomer decreases to only 80% of the first cycle.[7a] Even a low side reaction quantum yield of 0.001 leads to 63% decomposition after 1000 switching cycles. Values of more than 10000 for the repeatable cycle number denote photochromes with a good fatigue resistance.

Besides the change of color, in other words the absorption behavior, several properties of the compound can be reversibly changed by isomerization. These are emission, oxidation/reduction potentials, dielectric constants, refractive indices and the geometrical structures.[7a,9] This exceptional possibility of triggering molecular properties reversibly upon irradiation with light at different

wavelengths has led to a multitude of applications for such compounds in recent years, *e.g.* molecular motors,[8a] photochromically controlled motion of living organisms,[10] and data storage.[11]

2.2   Diarylethenes

While most of the known photochromic compounds exhibit equilibrating thermal back reactions, diarylethene (DAE) derivatives offer highly desirable thermal bistability in both ring-open (denoted as DAE_O) and ring-closed (denoted as DAE_C) forms, making them unique among photochromic molecular systems.[8b] Another intriguing property of DAEs is their excellent fatigue resistance towards repeated switching cycles.[5a] DAEs, first introduced in 1988 by Masahiro Irie *et al.*,[12] are generally composed of two aromatic rings, mainly thiophenes or benzo[*b*]thiophenes that are connected by a carbon-carbon double bond bridge, the latter usually is a part of a five-membered ring like perfluorocyclopentene or maleimide. *cis*-Stilbene **10cis** can be seen as "parent" molecule for DAEs, however, three main problems occur when using *cis*-stilbene: *cis-trans* isomerization, due to the fact that the *trans*-stilbene **10trans** is preferred by energetics; irreversible oxidative degradation after ring closure to phenanthrene **11** and thermal cycloreversion because of lack in thermal bistability (see Scheme 3).

10trans   **10cis**   **10c**   **11**
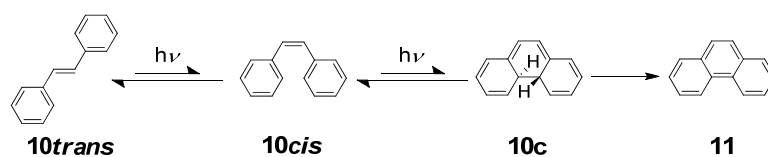
Scheme 3. Isomerization, photochromism and rearomatization of stilbene.

Approaches for solving these problems are "locking" the *cis* orientation by the incorporation of a 5-membered ring at the C–C double bond and "protecting" the *ortho* positions of the phenyl rings, which are susceptible to oxidation leading to rearomatization, by the use of methyl groups (see **12o**/**12c** in Scheme 4). However, these improvements are not sufficient to ensure thermal bistability, which makes DAEs unique. Replacing the phenyl groups by heterocyclic rings increases the thermal stability due to the difference in the aromatic stabilization energy of the heteroaromatic and phenyl rings obtained in the ring-opening process.

**12o**   **12c**   X = NH, O, S
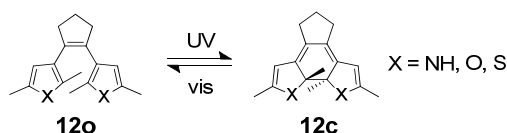
Scheme 4. Open and closed form of basic DAE.

Bistability is imparted, when the energy difference between the open, aromatic form and the closed, conjugated one is small, resulting in a higher isomerization barrier. The precondition for

achieving bistability is a low aromatic stabilization energy for the aromatic part, which exists with thiophene, thiazole, and benzo[*b*]thiophene substituents and not for benzene, pyrrole or indole substituents. Actually, thiophenes and benzenes reveal a high degree of aromaticity with high resonance energy per carbon, whereas furans and pyrroles possess a low degree of aromaticity due to the high electronegativity of the oxygen or nitrogen disturbing the resonance delocalization. Although, resonance energy and aromatic stabilization energy for such DAE systems are related, resonance energy is not a reliable gauge for predicting bistability of photochromic compounds.

Figure 1 illustrates the correlation diagrams for the conrotatory ring closure and ring opening of a heteroaryl- (left side) and an aryl-substituted DAE (right side). The higher energy difference for the lowest state of the phenyl-substituted compound leads to a low activation energy for the thermal back reaction, *i.e.* ring opening, while the barrier increases for the heteroaryl-substituted DAE.
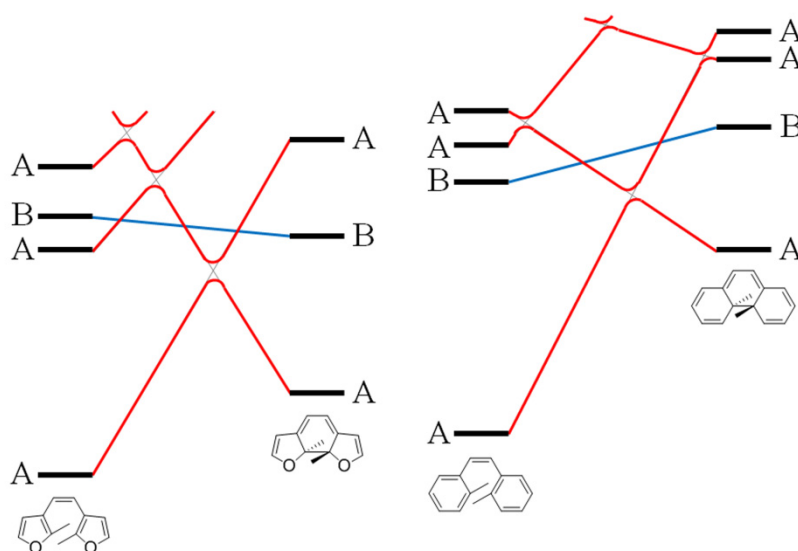

Figure 1. Energetic scheme for conrotatory ring closure and ring opening of a heteroaryl- and an aryl-substituted DAE. Different electronic states with same symmetry, *i.e.* A or B, are able to correlate; those with same symmetry cannot cross. Reprinted with permission from ref.[7a] Copyright 2000 American Chemical Society.

For thiophene substituted DAEs, the energetic levels of open and closed form are nearly balanced and accordingly, the respective barrier is higher. Exemplary for this enormous thermal bistability is DAE **6o**/**6c** (Scheme 5) with a barrier for ring opening of 139 kJ mol^{-1} and therefore, a half-life of the closed form at 30 °C of 1900 years. The respective pyrrole analog has a have-life of only 37 s.[7a]
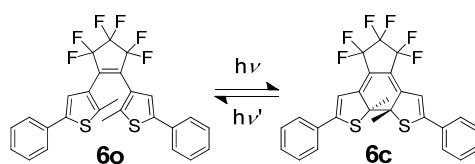
**Scheme 5.** Ring-open **6o** and ring-closed form **6c** of 1,2-bis(5-phenylthiophen-3-yl)-perfluorocyclopentene.

Irie and Mohri published the first thermally irreversible and fatigue resistant photochromic diarylethene in 1988.[12] They synthesized *cis*-1,2-dicyano-1,2-bis(2,4,5-trimethyl-3-thienyl)ethene **13o** and transferred the cyano groups to an anhydride function by heating the compound to the boiling point in a solution mixture of basic aqueous potassium hydroxide and ethylene glycol monoethyl ether (Scheme 6).
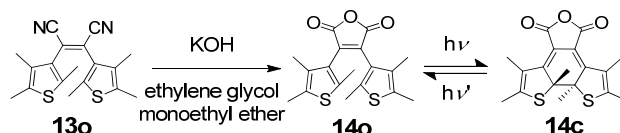
Scheme 6. Synthesis and photochromism of 2,3-bis(2,3,5-trimethyl-3-thienyl)maleic anhydride **14o/14c**.[12]

The absorption maximum of the colored closed form **14c** is 560 nm and no changes in the visible absorption at this wavelength or in the NMR spectrum were observed at 80 °C. Even the dicyano precursor **13o** showed photochromic behavior with an absorption maximum of the closed form at around 512 nm. NMR-studies revealed, that for this molecule, the *Z–E* isomerization is negligible upon irradiation with ring-closing light at 405 nm.[12]

While the open form of a diarylethene exhibits two rotamers, parallel **15o-p** and *anti*-parallel **15o-ap**, only the *anti*-parallel one may undergo the orbital-controlled six π-electron pericyclic isomerization upon irradiation to afford the ring-closed form **15c** (see Scheme 7). Only this *anti*-parallel conformation allows the right orbital overlap of the bond forming molecular orbitals, thus enabling the photochemical conrotatory reaction according to the Woodward-Hoffmann rules.[13]
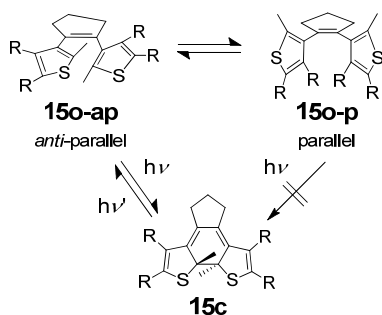
Scheme 7. Parallel and *anti*-parallel open form and closed form DAE.

Both rotamers for the open form have different shifts in the ^{1}H NMR spectra, most pronounced for the methyl group at the thiophene substituent. For the *anti*-parallel rotamer, the methyl group attached to one thiophene substituent is situated directly above the middle of the other thiophene ring and the diamagnetic circular current, which operates against the external magnetic field, leads to an up-shift of the proton signals of the methyl group (apCH_3: ~2.2 ppm in deuterated chloroform) compared to the signals of the parallel form (pCH_3: ~2.5 ppm). When rotation of the thiophene units is strictly limited due to introduction of bulky groups, there exists three atropisomers of the open form: the *meso* parallel

one and two racemic *anti*-parallel ones (*S,S* and *R,R*), which could be separated by HPLC on chiral columns.[14] Furthermore, two different forms of the ring-closed form of a DAE are imaginable. In agreement with the Woodward-Hoffmann rules,[13] the photochemical conrotatory ring closure (**16c-trans**) forces the two methyl groups at the newly formed six-membered ring into a *trans*-conformation; however, both *cis*- and *trans*-isomers are accessible by electrochromic ring closure (see Scheme 8 and Chapter 2.3)
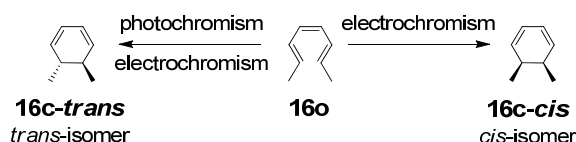
Scheme 8. Photo- and electrochromically induced conrotatory and electrochromically induced disrotatory ring closure.

Since the open form isomer of DAE absorbs predominantly in the short-wave spectral region, its ring closure can be initiated by irradiation with UV light. The ring closure of DAE results in an extension of the π-system and thus the ring-closed isomer possesses longer wavelength absorption bands (see Figure 2). Accordingly, the ring-opening reaction of the closed form can be triggered by irradiation with visible light.
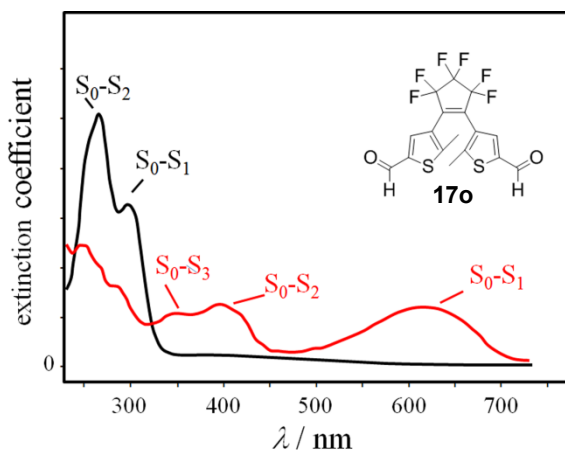
Figure 2. Exemplary absorption spectra for ring-open (black line) and ring-closed DAE **17o** (red line). The transitions from ground to excited states are denoted as S_0–S_1, S_0–S_2, and S_0–S_3, respectively. Reprinted with permission from ref.[15] Copyright 2000 Elsevier.

Structural variation of the basic diarylethenes often results in distinct changes in the absorption properties of the respective closed form in the visible region. The closed form of "normal" diarylethene **18c** with the perfluorocyclopentene bridge in the 3-position of the thiophene shows a more bathochromic absorption maxima (534 nm) in the visible region than the "inverse" diarylethenes **19c/20c**, that have the bridge connected to the 2-position of one or both thiophenes, respectively. The

inverse diarylethene **19c** reveals a absorption maximum at 425 nm, which is more than 100 nm less than the "normal" diarylethene **21c** with a maximum at 534 nm (Figure 3).[7a]

22c   **19c**   **20c**   **21c**   **18c**
398 nm   425 nm   469 nm   526 nm   534 nm
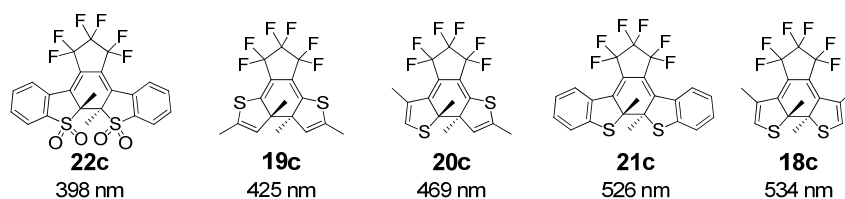
Figure 3. Comparison of the absorption wavelength maxima of the closed forms of different "normal" and "inverse" diarylethenes.

Also the oxidation state of the sulfur atoms of the thiophene has an distinct influence on the absorption maximum. Therefore, the "normal" benzo[*b*]thiophene substituted diarylethene **21c** reveals a maximum at 526 nm, while this maximum is shifted by more than 100 nm to 398 nm for the benzo[*b*]thiophene 1,1-dioxide substituted compound **22c**.[16]

Ring-closure quantum yields of DAEs are generally much greater (between 0.2 to 0.5) compared to the ring-opening values (< 0.2), which can be explained by taking a look at the energetics of this photo-induced reactions. The ring closure happens barrier-free through a conical intersection (CI) after excitation to the S_1 state (see Figure 4).[15]
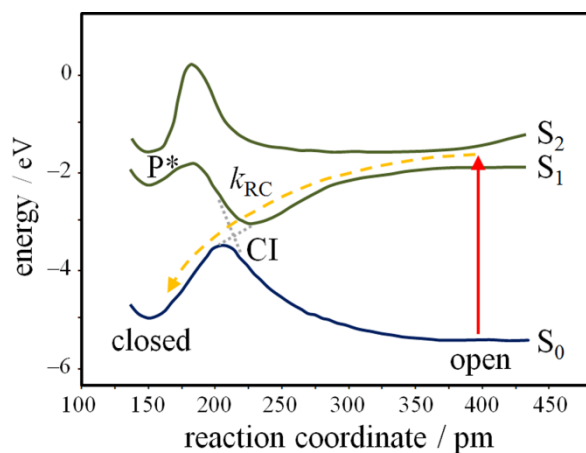
Figure 4. Illustrative scheme for the potential energy surfaces of photoinduced ring closure. The red arrow represents the light-induced excitation of the open-form DAE while the yellow, dashed arrow displays the subsequent ring closure. CI = conical intersection; P* = precursor for ring-opening reaction; RC = ring closure. Reprinted with permission from ref.[15] Copyright 2000 Elsevier.

Therefore, the main decimation factor for the ring-closure quantum yield is the proportion of the open form, which exists as non-reactive parallel rotamer. The respective ring-opening reaction reveals a distinctly lower quantum yield on account of the fact that a short-lived species is formed after excitation to the S_1 state. The subsequent ring opening does not take place barrier-free, and the ratio

between ring opening and direct relaxation to the ground state without isomerization depends on the transition state between the initial excited state (C*) and the CI (see Figure 5).[17]
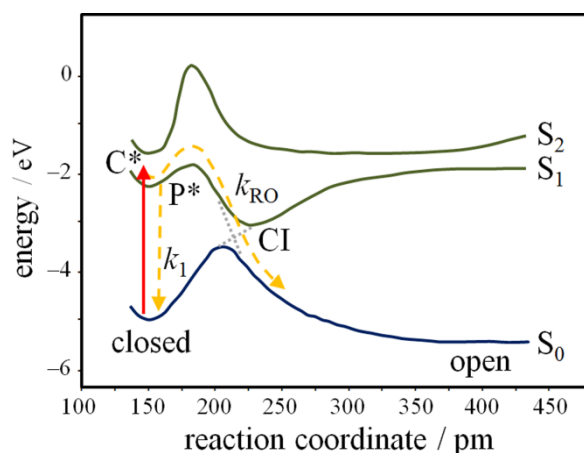
Figure 5. Illustrative scheme for the potential energy surfaces of photoinduced ring opening. The red arrow represents the light-induced excitation of the closed-form DAE while the yellow, dashed arrows display the subsequent ring opening or the ordinary relaxation to the ground state. C* = initial excited state; CI = conical intersection; P* = precursor for ring-opening reaction; RO = ring opening. Reprinted with permission from ref.[17] Copyright 1999 Elsevier.

Therefore, for the ring opening, in contrast to ring closure, a short-lived species can be detected by ultrafast spectroscopic techniques. An increase in the π-system of a DAE further decreases the ring-opening quantum yield due to a decrease of the excitation density at the central photoreactive unit and of the excited state lifetime.[18] Appreciable temperature dependence of the ring-closure rates could not be observed, whereas the ring-opening quantum yield increases with temperature. The ring-opening quantum yields strongly depend on the wavelength of excitation, due to an excess of vibronic energy at shorter wavelengths. Therefore, the photochrome with anhydride bridge **14c** (see Scheme 6) has a ring-opening quantum yield in tetrachloromethane upon excitation at 633 nm of 0.04, which is distinctly smaller than upon excitation at 546 nm where the value is 0.15.[12] This, however, seems to be contradicted by the fact that vibrational relaxation in solution should be very fast and chemical reactions can rarely compete with the relaxation process.[12] The energetics of DAEs explain the fast ring closure and the comparatively inefficient ring opening; however, the whole situation is the other way around for "inverse" DAEs, *i.e.* a high quantum yield for ring opening and distinctly lower values for ring closure.

The ease of photoswitching between thermally stable ring-open and ring-closed DAE isomers has resulted in their application in different optoelectronic devices.[4d,7b,9,19] Moreover, by implementing DAE chemistry, exciting recent concepts such as reversible switching of conductance,[20] photoprogrammable organic light-emitting diodes (OLEDs),[21] bulk optical transistors,[22] integration in nano-particles[23] and quantum dots,[24] molecular logic devices,[25] *anti*-counterfeiting technology,[26]

and imaging of living cells by single-molecule photoswitching[27] have recently been developed, and more interestingly, the photochromically controlled motion of living organisms has been demonstrated.[10] Hirshberg mentioned for the first time the possibility of a chemical memory by utilizing the reversible switching between colored and colorless forms of an organic compound upon irradiation in 1956.[28] The high potential of photochromic systems for optical data storage has been convincingly demonstrated by Parthenopoulos and Rentzepis in 1989 with a three-dimensional memory system based on photochromic spirobenzopyran embedded in a polymer matrix.[11,29] Followed by this seminal work, several new photochromic systems containing DAEs have been developed for high-density data storage on a molecular level (see Chapter 2.6).[30]

2.3   Electrochromic Behavior and Redox Properties of Diarylethenes

Photochromic compounds often exhibit electrochromic behavior, *i.e.* ring closing or opening driven by electrochemistry, and thus the electrochromism of these compounds has been investigated in detail in recent years.[31] Electrochemical transformations are not bound by the Woodward-Hoffmann rules like photochemical transformations. Therefore, upon ring closure of DAEs, the electrochromically generated closed forms exist in two isomers. The methyl groups in the 2-position at the thiophene subunits can point in the same direction, denoted as the *cis*-isomer, or in the opposite direction, denoted as the *trans*-isomer (see Scheme 9). The respective photochemical ring closure facilitates only formation of the *trans*-isomer.

Guirado *et al.* synthesized and investigated the electrochromic behavior by cyclic voltammetry of a variety of DAEs.[32] The photochromes **23o/23c** have either perfluoro- or perhydrocyclopentene bridges, which possess only inductive effects, and different electron-donating or electron-withdrawing substituents, *i.e.* chloro, iodo, trimethylsilyl, thiophenoxy, formyl, carboxyl and ethynylanisyl groups, in 5-position at the thiophene subunits (see Scheme 9). Due to the fact that the HOMO (highest occupied molecular orbital) increases in energy upon ring closure, the ionization potential of the closed forms is smaller than for the open forms, and therefore, the former can be oxidized at lower potentials than the latter for the whole range of DAEs.
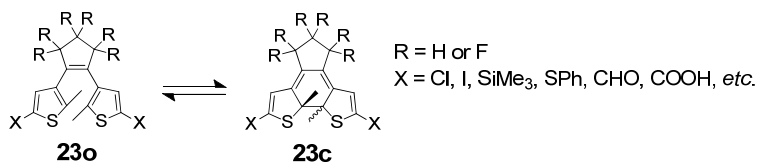

Scheme 9. Range of DAEs with perfluoro- or perhydrocyclopentene bridge and electron-donating or electron-withdrawing substituents in the 5-position of the thiophene subunits.[32]

Two possible reaction pathways, *i.e.* an intermolecular and an intramolecular one, can be obtained upon oxidation of the open isomers. One pathways results in dimerization of the radical cations in the

5-position, which is limited to the halogen-substituted DAEs. On the other hand, the once oxidized DAE reacted intramolecularly to its cyclic form, which is subsequently oxidized again at the same potential, yielding the stable dication. This observation was shown for the thiophenoxy-substituted DAE **24** in Scheme 10. The radical-cation intermediate revealed a lower activation barrier for the cyclization, because depleting the HOMO of its electrons reduces the secondary *anti*-bonding interactions between the reactive carbons, analogous to the photochemical pathway.
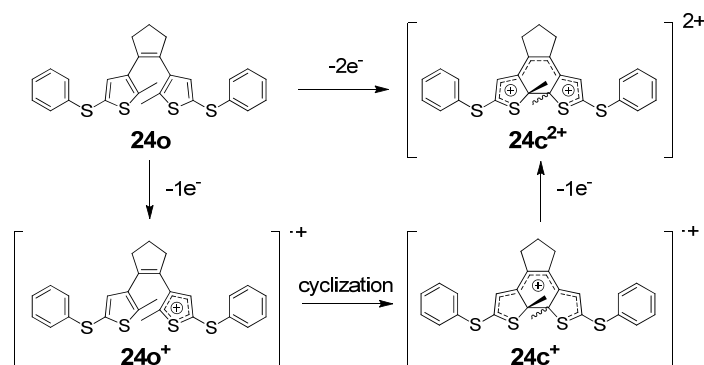
Scheme 10. Electrochromic ring closure of thiophenoxy-substituted DAE **24** and further oxidation to the dication (the positive charge(s) were delocalized over the whole molecules).[32]

Just as upon oxidation of the open forms, two different behaviors can be observed for the respective closed forms upon oxidation. In some cases the radical cation or dication of the DAEs was stable and the positive charge(s) were delocalized over the whole molecule, inducing a slight color change. In other cases oxidation triggered the ring-opening reaction and bleaching. Ring opening was favored for DAEs containing a perfluorocyclopentene bridge and electron-withdrawing substituents, due to the fact that removal of an electron destabilizes the carbon-carbon σ-bond. The ring-open radical cation is a better oxidizing agent than the ring-closed starting material, and therefore, the cation is quickly reduced to the neutral form which could even lead to further oxidation of neutral closed forms and subsequent ring opening.[32]

Figure 6 summarizes the effect of the substituents on the electrochromic behavior of the observed DAEs. Oxidation of the ring closed forms below 0.8 V generates stable charged species, while oxidation above this potential leads to ring opening. Oxidation of the ring-open DAEs leads to the ring-closed isomers with the exception of the DAEs containing iodine or chlorine in the 5-position. Iodine and chlorine substituted DAEs undergo radical initiated oligomerization upon oxidation yielding to the respective dimer, trimer, *etc*.
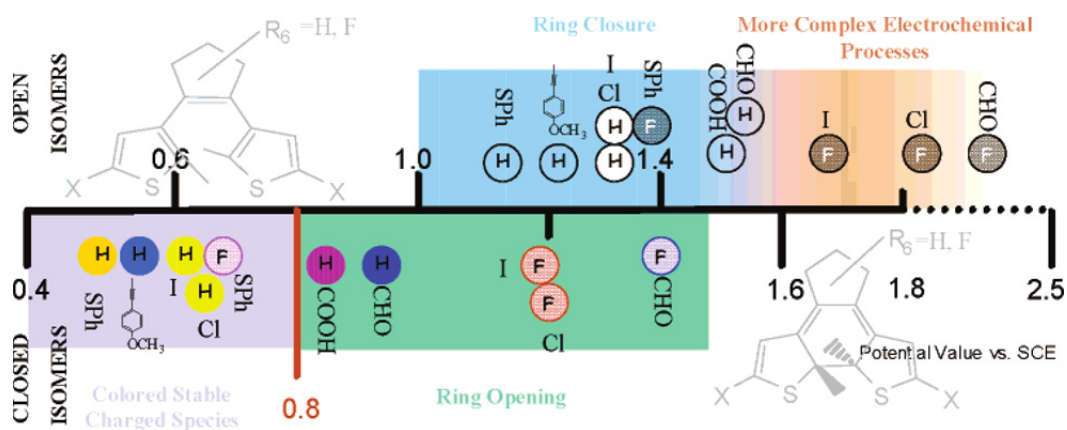
Figure 6. Electrochromic behavior upon oxidation of different ring-open (row above) and ring-closed (row below) DAEs. Perhydro- or perfluorocyclopentene bridges were denoted as H or F in a circle and the respective color of the circle signifies the color of the closed form in solution. The substituents at the 5-position of the thiophene subunits were also given at the particular first oxidation potential. Reprinted with permission from ref.[32] Copyright 2005 American Chemical Society.

Examples of electrochromic behavior upon reduction are rare. Branda *et al*. introduced a dicationic DAE **25** with two pyridinium groups in the 5-position of the thiophene subunits and observed ring closure upon reduction (see Scheme 11).[33] Just as in the case of oxidative electrochromism, reductive ring closure also led to the respective *trans*- and *cis*-isomer of the closed form. Drawbacks of this very specialized system are the lack of thermal stability for both closed forms, *i.e. cis*- and *trans*-isomers, and the steady decomposition of the closed *cis*-isomer.
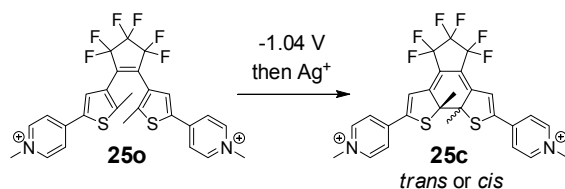
Scheme 11. First example for electrochromic ring closure of a DAE **25** upon reduction.[33]

The group of Feringa investigated substitution effects on the electronic properties of DAEs.[34] While replacing the central perfluorocyclopentene (**26**) bridge with a perhydrocyclopentene (**27**) bridge has little influence on the photochemical properties (see Figure 7), the redox properties are distinctly different. Although ring closure of DAE **27** takes place upon oxidation of the open isomer, ring opening is observed for the closed form of DAE **26** upon oxidation. However, electron-withdrawing groups, *i.e.* anisyl, in 5-position of the thiophene subunit enables oxidative ring closure for DAE **26**. The bridging cyclopentene units are redox-inactive, but do inductively affect the electron density of the central alkene group. A perfluorocyclopentene bridge acts as an electron-withdrawing group, whereas a perhydrocyclopentene bridge acts as an electron-donating group.
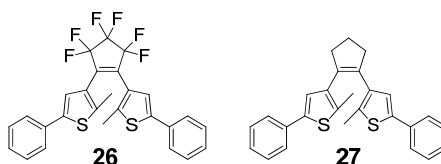
Figure 7. DAE containing perfluorocyclopentene (**26**) or perhydrocyclopentene (**26**) bridge.

The group of Feringa reported in another study the effects of various substituents located at 5-position of the thiophene subunit on the redox properties.[34b] They synthesized and investigated a series of compounds containing different substituents in the *para*-position of the external phenyl rings (*cf.* Figure 7). The electronic properties of the substituents range from electron withdrawing, *i.e.* cyano, to electron donating, *i.e.* methoxy, and several in between. Substituents in the 5-position of the thiophene subunits have a major influence on the HOMO to LUMO (lowest unoccupied molecular orbital) energy gap for open and closed forms. Therefore, electron-donating groups favor ring closure upon oxidation and electron-withdrawing groups favor ring opening by stabilization or destabilization of the respective cationic or dicationic state.

In conclusion, isomerization results in a large change in the energy gap between the HOMO and LUMO, significantly altering the electronic properties of the DAEs. This ability enables applications like optically switchable OTFT (organic thin-film transistor) devices *via* energy-level phototuning[35] and reversible photoswitching of conductance.[36] For non-destructive memory devices based on an electron-transfer process, it is important that this DAE moiety acts as the electron-accepting component to prevent disadvantageous electrochromic behavior. Non-destructive implies that data reading has no influence on the isomeric state of the DAE-based memory device.

2.4   Photochromic Compounds as Prototypes for Data Storage Systems

A necessary prerequisite of organic compounds for optical memory systems is the reversible switching of physical properties like emission, transmission, reflectance, *etc.* induced by a photochemical reaction.[7a] Therefore, photochromic molecules, and especially thermally bistable DAEs, should be ideal for such applications. Another condition is that the respective read-out signal must be obtained without influencing the isomeric state of the photochrome. A number of more or less practicable concepts for data storage on the molecular level were proposed in recent years and are summarized below.

The closed form of some DAEs (for example see compound **28c** in Scheme 12) possess exceptional intense IR absorption bands for C-C double bonds at around 1495 cm^{-1}. These intense IR absorptions do not occur in the same extent for the open form.[37] While the photochromic reactions are initiated upon irradiation with UV or visible light, the read-out process may occur in the energetically lower IR region. Data reading in the IR region does not have an influence on the isomeric state, *i.e.* the system

provides non-destructive read-out capability. However, the wavelength is a relevant factor for optical data storage, and therefore, IR read-out limits the approachable density.

Scheme 12. Photochromic DAE for data storage application by detection of intensive IR-bands.[37]

Monitoring changes in optical rotation is a further possible alternative for non-destructive read-out. Due to the fact that the closed forms of DAEs are chiral, they are appropriate candidates for chiroptical devices. Therefore, the group of Branda named two important conditions: 1) the photochromes should exhibit significantly contrasting optical rotating strengths between their two states; and 2) the photochromic reactions should maximize the formation of only one stereoisomer.[38] They introduced a DAE system **29o** (see Scheme 13) with two oxazoline substituents, which preorient the thiophene subunits with respect to each other when two of them form a complex **(29o)$_2$·Cu$_2$** with two copper(I) cations. Thus, ring closure yields a single diastereomer **29c^2**, *i.e.* (*S,S*)-(*S,S*), with a selectivity of 86%. Several spectral regions in the optical rotary dispersion (ORD) spectra of the open and closed forms of the copper(I) complex provide distinct differences in rotation, *i.e.* at 450 and 475 nm. Thus, the system exhibits potential for non-destructive read-out by non-invasive stimulation of these isomers in optical regions where both isomers are transparent. However, the stability of the complexes and complexity of the read-out restricts the applicability of such systems.

Scheme 13. Copper-complex **15Cu** of photochromic DAE for non-destructive read-out of the optical rotation signal.[38]

The group of Lehn proposed a non-destructive read-out possibility by applying a write-lock-read-unlock-erase cycle.[39] Their dual-mode system, based on DAE **30** (see Scheme 14), can be stimulated by two different reversible processes, *i.e.* photochromically by light and electrochromically by redox reactions. The colorless open form of the DAE, **30o** with two hydroxy groups, does not react

electrochemically in a range of −1 V to +1 V. The blue colored closed form **30c**, which can be obtained upon UV irradiation (λ_{max} = 312 nm), can be seen as an extended hydroquinone and reacts to the respective extended quinone upon oxidation at +1 V. The photochromic back reaction is blocked for the received system **30c^{ox}**, which can be unlocked upon reduction at −1 V. The ring opening is triggered upon irradiation at wavelengths above 600 nm. Because only the changes in absorption were provided without fluorescence data, no useful read-out signal was reported. Despite photochrome **30** exhibiting a wealth of elegant photochromic and electrochromic switching behavior, the complexity of the multi-step electrochemical locking and unlocking limits the applicability of the system.
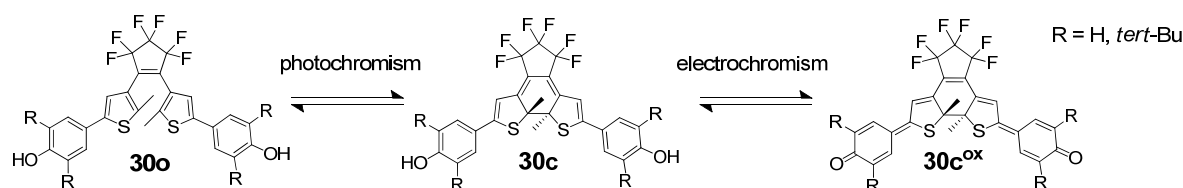
Scheme 14. Photochromic DAE **30** with the possibility of "locking" the closed form by oxidation.[39]

Therefore, changing the fluorescence properties might be the ideal route to achieve non-destructive read-out signals for optical memories. Photoisomerization of a DAE from the open to the closed form and *vice versa* causes significant changes of the structural and electronic character, and can therefore be accompanied by noticeable changes in emission intensity. If the fluorescence intensity of the two states of a DAE exhibits a significant difference in intensity, the emission intensity may be used as the read-out signal for memory storage systems. The group of Lehn synthesized and characterized a group of photochromic DAEs with six and eight conjugated thiophene units (*e.g.* compound **31o** in Figure 8).[40] While the closed form of compound **31c** revealed a broad absorption band with a maximum at 698 nm and showed only negligible fluorescence, the respective open form with an absorption maximum at 451 nm, emits strongly with a maximum at 604 nm (exact fluorescence quantum yields are not given by the authors).
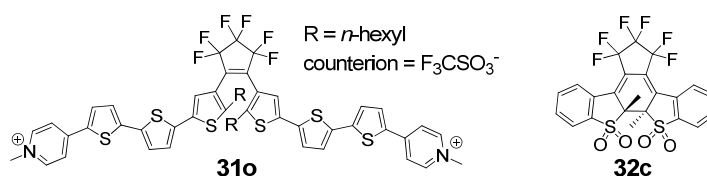

Figure 8. Photochromic DAEs, which show either a fluorescent open form (**31o**) or a fluorescent closed form (**32c**).[16,40b]

Although systems such as **31o** have been described as presenting "much potential for the sensitive non-destructive reading of optically stored data",[40b] because "reading" of the fluorescent state might be possible by excitation of inactive absorption bands for the photoisomerization excitation, fluorescence competes with the photoisomerization in the same range of the optical spectrum leading

to disadvantageous reactions. While **31o** shows fluorescence for the open-ring isomer, the oxidized DAE **32c** revealed fluorescence only for the ring-closed form (see Figure 8). Oxidation of 1,2-bis(2-methyl-1-benzo[*b*]thiophene-3-yl)perfluorocyclopentene, which is not emitting in both isomeric states, gives compound **32**, which possesses an almost non-fluorescent open form but a closed form with a twenty times higher fluorescence intensity.[16] However, such DAEs with oxidized thiophene or benzo[*b*]thiophene units often show a reduced stability, *e.g.* DAE **32c** tends to remain in a colored, closed form.

The group of Tian used the phosphorescence instead of the fluorescence as read-out signal for non-destructive read-out.[41] They synthesized a diarylethene-based tetraazaporphyrin system **33o/33c** with up to four photochromic subunits (see Scheme 15). The all-open form **33o** is phosphorescent with a maximum at 620 nm upon excitation at 400 nm, which might induce no photoisomerization at this wavelength, while irradiation at 350 nm produces the non-phosphorescent, closed form **33c**. The cyclic back reaction was induced upon irradiation at 660 nm. Data concerning quantum yields or the on/off ratio were not given by the authors. Similar structures containing magnesium or palladium as the central ion revealed fluorescence quantum yields below 10% and an approximate on/off ratio of emission at 689 nm of 10:1 for the magnesium derivative but low photostability.[42]
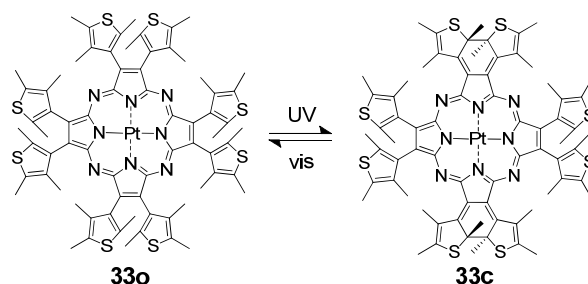

Scheme 15. Photochromic diarylethene-tetraazaporphyrin hybrid **33o/33c**.[41]

The summarized drawbacks for DAEs with one emissive and one non-emissive state as media for data storage applications are photoisomerization during reading of the emission state and low fluorescence contrast in most cases. Based on the idea of controlling the emission behavior of a fluorophore upon triggering the isomeric state of an attached photochrome, Saika *et al.* synthesized a system **34E/34Z** containing two emissive pyrenes and a photochromic thioindigo base body in 1992 (see Scheme 16).[43] The *E*-isomer revealed monomeric emission of the pyrene fluorophore, while the isomerization to the *Z*-form reduced the distance between both pyrene units and allows the formation of an intramolecular excimer, which caused excimer emission. Neither thermal stability, nor distinguishable emission bands for monomer and excimer were available.
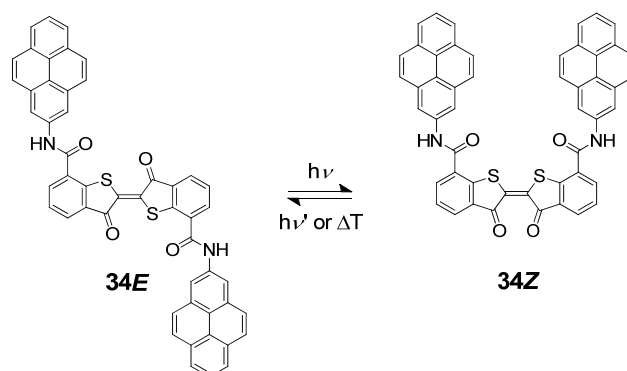
Scheme 16. Photochromic thioindigo **34E**/**34Z** containing two pyrene units.[43]

The group of Lehn published a tungsten complex **35o** with a photochromic DAE ligand,[44] which exhibited a seven times higher fluorescence intensity for the closed form (7%) than for the open form (1%) (see Figure 9). In general, [W(CO)$_5$L] complexes with an additional pyridine derivative as ligand L are fluorescent at room temperature only with electron-withdrawing substituents in the *para* position to the pyridine ring. This is the case for the open form of the DAE as a ligand, whereas ring closure effects the energetics of the DAE and therefore, quenches emission.[44b]
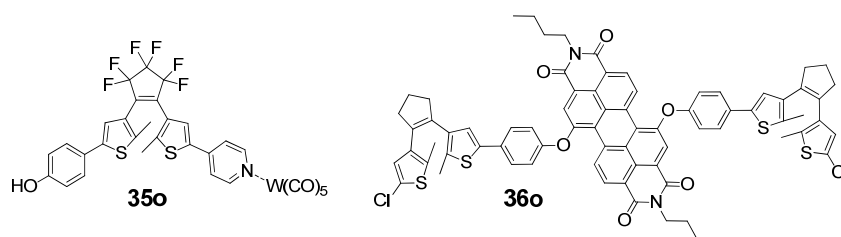

Figure 9. Tungsten complex **35o** containing photochromic DAE ligand[44] and triad **36o** containing two DAE photochromes attached to the bay position of a PBI fluorophore.[26]

Recently, the group of Tian attached two DAE units at the bay position of an emissive perylene bisimide (PBI) dye (see compound **36o** in Figure 9).[26] While the open form revealed a fluorescence quantum yield of only 5% in tetrahydrofuran (THF), the respective closed ring-closed isomer has a value of 37%. However, both quantum yields are far away from unity, which can be obtained for diphenoxy-substituted PBI fluorophores.[45] A possible explanation for the different quenching behavior is that the electrons of the DAE units, which are "flowing towards the PBI unit" in the case of the open form of the photochromes with a HOMO localized over both DAE units and the PBI core, were "pulled back" due to the increased π-conjugation of the closed isomers of the DAEs.[26] Such systems cannot be seen as useful for non-destructive read-out data storage due to the interaction between PBI and DAE subunits but are better suited for *anti*-counterfeiting technology.

An interesting concept was published by the group of Rentzepis.[46] They synthesized and investigated the dyad system **37o**/**37c** composed of a photochromic fulgimide and a fluorescent oxazine unit (see Scheme 17). The fluorescence intensity of the dye is strongly dependent on the

31

polarity of the fulgimide photochrome, which possesses a non-polar, open and a polar, closed isomer. Ring closing and ring opening can be obtained upon irradiation at 400 and 530 nm, respectively. The absorption band of the oxazine dye at 650 nm and the respective emission band at 700 nm are completely separated and are situated more bathochromic than the spectral regions for the isomerization of the photochrome, and therefore, the fluorophore can be excited independently. In the non-polar, open form, the fluorescence intensity of the oxazine, which exhibits better fluorescence in a non-polar environment, is "several times" higher than for the closed form. Exact fluorescence quantum yields and ratios were not provided by the authors (quantum yields between 0.2 and 1.5% in alcoholic solvents were given for either the open or the closed form).[46]
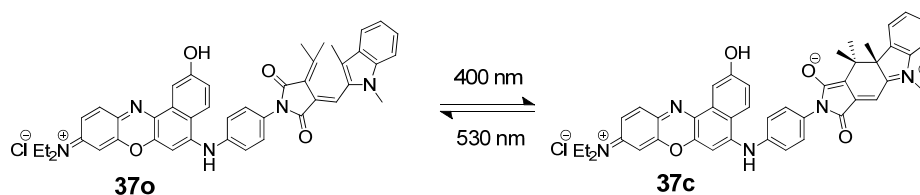
Scheme 17. Switchable polarity of photochrome influences fluorescence intensity of emitter.[46]

Kärnbratt *et al.* gave an example for a photochromic supramolecular memory with non-destructive read-out.[30j] They described photoswitch **38o/38c** based on a pyridine-substituted DAE and a porphyrin dimer (see Scheme 18). While, the more rigid closed form **38c** was connected only once to the porphyrin dimer, ring opening allowed linkage to both porphyrins, and therefore, induced a distortion of the linear dimer. The supramolecular structure containing the open form of the DAE exhibited an additional intense absorption band with a maximum at 748 nm, which is more bathochromic than the absorption band of the closed form of the DAE unit. Upon excitation at 748 nm of the closed isomer with the linear porphyrin dimer the emission intensity measured at 755 nm is *circa* 5 times higher than for the open form, and isomerization between both forms can be triggered by light. However, a memory device composed of **38** embedded within a rigid polymeric environment might inhibit the distinct structural changes necessary for the fluorescence regulation of **38**.


Ar = 3,5-di(octyloxy)phenyl
R = Si(C$_6$H$_{13}$)$_3$
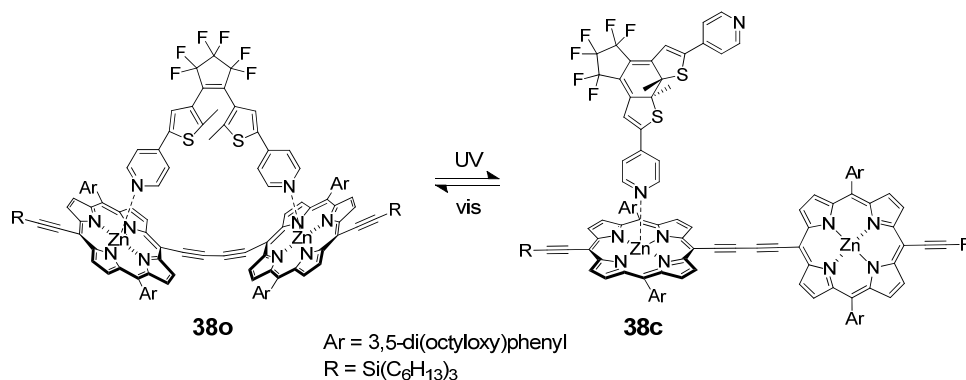
Scheme 18. Photochromic supramolecular memory based on a porphyrin dimer and a pyridine-substituted DAE.[19i]

None of the examples presented here is perfect for data storage applications. Each compound either lacks a good on/off ratio of the read-out signal, exhibits a destructive read-out process or has other drawbacks such as poor thermal stability. Further examples for non-destructive read-out concepts in photoswitchable systems, which seems to be of even less practical use, like the "reversible light-induced change of refractive indices in DAE-containing glassy nematic liquid crystals"[47] or the "photochromic switching of excited-state intramolecular proton-transfer fluorescence"[48] were not covered in this overview. Chapter 2.6 highlights promising systems for data storage applications based on fluorescence quenching by photochromically controlled energy or electron transfer in dyad or triad systems. Before such systems are summarized, the important terms with respect to energy- and electron-transfer processes are briefly introduced in Chapter 2.5.

## 2.5   Excursion: Photoinduced Energy- and Electron-Transfer Processes

Different relaxation processes can occur after photoexcitation to higher electronic states of a molecule. Besides the emission of a photon from the S_1 state, *i.e.* fluorescence, or the non-radiative release of thermal energy, *i.e.* vibrational relaxation (VR) subsequent to internal conversion (IC) from the S_1 to the S_0 state, triplet or charge-transfer states can be populated by intersystem crossing (ISC) or electron transfer.[49] Starting from these states, either VR or radiative processes like phosphorescence from the T_1 state and CT emission are possible. The important processes are shown in the Jablonski diagram in Figure 10. The common occurrence of deactivation pathways often results in considerably decreased fluorescence quantum yields and reduced fluorescence lifetimes. The rate constants for the VR are in a range of 0.1–10 ps, for fluorescence between 0.1 and 10 ns, and for phosphorescence larger than 100 μs.
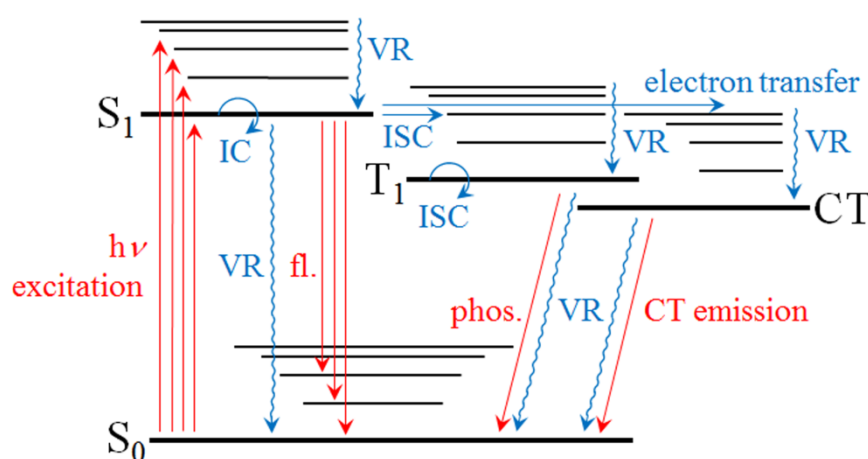
Figure 10. Jablonski diagram containing electron transfer as deactivation pathway; CT = charge-transfer state, fl. = fluorescence, IC = internal conversion (*i.e.* from S_1 to S_0), ISC = intersystem crossing (*i.e.* from S_1 to T_1 and from T_1 to S_0), phos. = phosphorescence, VR = vibrational relaxation; blue arrows denote non-radiative transitions and red arrows describe radiative processes, respectively.

Energy-transfer processes are also potential pathways for the deactivation of excited molecules. The radiative or "trivial" energy transfer is a two-stage process involving a donor unit emitting a photon that is subsequently absorbed by a nearby acceptor unit. Prerequisites for such phenomena are high concentration of the acceptor and partial overlap of the emission spectrum of the donor and the absorption spectrum of the acceptor. Indeed, much more important processes are non-radiative Förster resonance energy transfer (FRET) and Dexter energy transfer.

Förster theory[50] describes the energy transfer as a resonance process between two coupled oscillators that are relatively far away from each other on a molecular scale. This through-space energy transfer is based on dipole-dipole interaction of the transition dipoles, *i.e.* a coulombic mechanism, and requires spectral overlap of the emission band of the donor and the absorption band of the acceptor (see Figure 11).
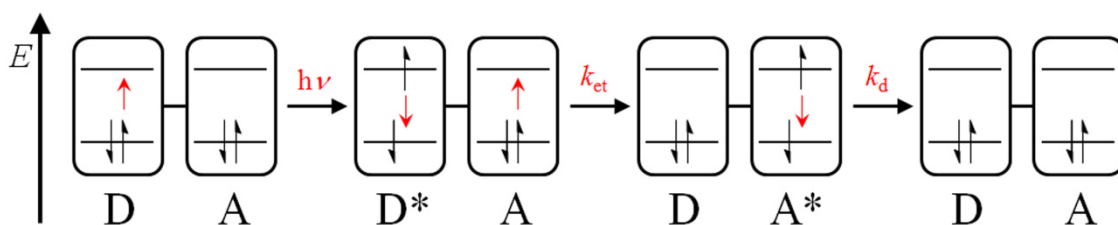

Figure 11. Schematic illustration of the successive steps of FRET upon excitation by light in a donor-acceptor system, *i.e.* excitation of the donor, energy transfer from donor to acceptor, and deactivation of the acceptor; k_d = rate constant for deactivation of excited acceptor, k_{et} = rate constant for energy transfer process.

The rate constant k_{FRET} can be calculated from the donor-acceptor distance r_{DA}, the quantum yield ϕ_D and the lifetime of the donor excited state τ_D in absence of the acceptor, the relative orientation κ^2 of the transition dipole moments of the donor and acceptor, and the refractive index n of the solvent (see Equation (1)). Another variable is the overlap integral $J(\lambda)$, which describes the spectral overlap of the emission band of the donor and the absorption band of the acceptor by means of the normalized fluorescence spectrum and the wavelength-depended extinction coefficient of the acceptor.

$$k_{FRET} = \frac{\phi_D \kappa^2}{\tau_D r_{DA}^6} \left(\frac{9000(\ln 10)}{128 \pi^5 N_A n^4} \right) J(\lambda) \tag{1}$$

The orientation factor κ^2 can be obtained with Equation (2), which contains the angle θ_{DA} between transition dipole moments of donor μ_D and acceptor μ_A, and the respective angles of the dipole vectors of donor θ_D and acceptor θ_A and the connecting line r_{DA} (see Figure 12).

$$\kappa^2 = \left(\cos \theta_{DA} - 3 \cos \theta_D \cos \theta_A \right)^2 \tag{2}$$
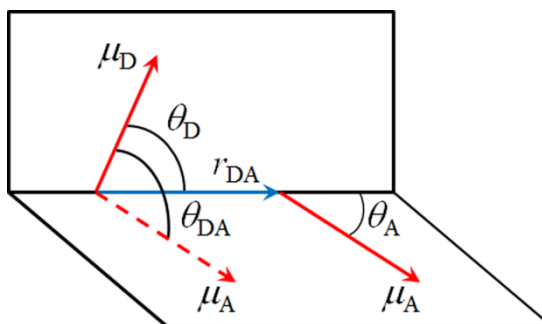
Figure 12. Dependence of the orientation factor κ^2 on the directions of the transition dipole vectors of donor μ_D and acceptor μ_A.

The factor κ^2 reaches a maximum value of 4 for collinear alignment of the dipole moments, a minimum value of 0, *i.e.* no energy transfer, in the case of *e.g.* perpendicular orientation, and a value of 2/3 for the statistical distribution, where donor and acceptor units can freely rotate around the connecting axis.

The Förster distance R_0^6 (Equation (3)) denotes the distance between donor and acceptor, at which FRET takes place for half of the excited molecules, while emission or other radiationless processes occur for the other half.

$$R_0^6 = \frac{9000(\ln 10)}{128\pi^5 N_A n^4} \kappa^2 \phi_D J(\lambda) \tag{3}$$

The efficiency of the FRET process E_{FRET} can be determined with the help of Förster distance R_0^6 and the donor-acceptor distance r_{DA} (Equation (4)). FRET occurs at rather large donor-acceptor distances of 10–60 Å due to a distance dependence of r_{DA}^{-6}.

$$E_{FRET} = \frac{R_0^6}{R_0^6 + r_{DA}^6} \tag{4}$$

By comparison, the much less important Dexter energy transfer[51] appears only at rather short distances of 5–10 Å. Subsequent to the excitation of the donor, a double-electron exchange between the LUMOs of donor and acceptor and the respective HOMOs takes place (see Figure 13). The resulting excited acceptor will finally be radiatively or non-radiatively deactivated. This "through-bond" energy transfer is based on an exchange mechanism that requires overlap of the molecular orbitals.
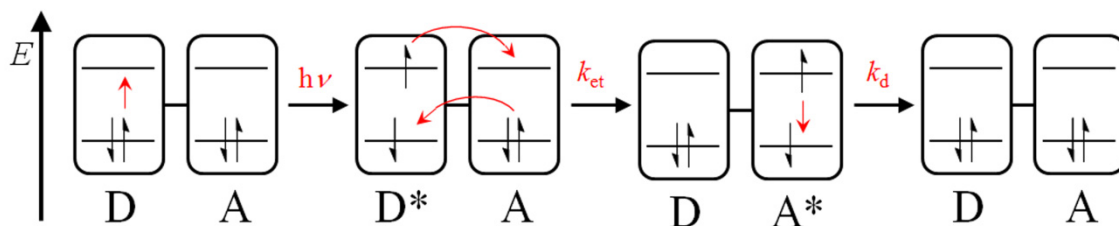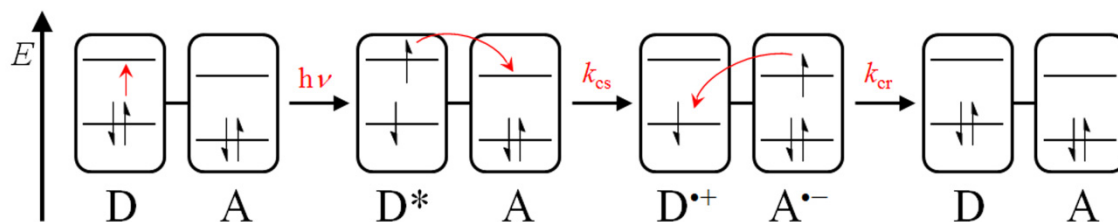
Figure 13. Schematic illustration of the successive steps of Dexter energy transfer upon excitation by light in a donor-acceptor system, *i.e.* excitation of the donor, electron exchange between donor and acceptor, and deactivation of the acceptor; k_d = rate constant for deactivation of excited acceptor, k_{et} = rate constant for energy transfer process.

Due to the fact that electron density decreases exponentially with increasing distance from the nucleus, the rate constant k_{DET} also decreases exponentially with increasing donor-acceptor distance r_{DA}. The rate constant k_{DET} (Equation (5)) can be calculated with the help of the constant K, which describes the specific orbital interactions, the sum of the van der Waals radii of donor and acceptor L, and the spectral overlap integral $J(\lambda)$, which was described in the case of FRET. Dexter energy transfer is favored in the case of small distances, when triplet states are formed, and consequently FRET is not possible.

$$k_{DET} = \frac{2\pi}{h} K e^{-\frac{2r_{DA}}{L}} J(\lambda) \tag{5}$$

The energy migration process between excitonically coupled, identical molecules will not be considered within this thesis.

Electron transfer processes, which occur upon irradiation, are denoted as photoinduced electron transfer (PET) and were convincingly described by the classical Marcus theory.[52] The PET process is in competition to other deactivation processes like fluorescence and the already mentioned energy transfer processes. Figure 14 schematically illustrates the PET process, starting with excitation upon irradiation, followed by charge separation by electron transfer from the excited donor to the LUMO of the acceptor and finally charge recombination by direct electron transfer or driven by the surrounding environment. As a consequence of the charge-separation step, a short-lived radical cation of the donor and a radical anion of the acceptor are formed, *i.e.* a charge-transfer state (CT state).

Figure 14. Schematic illustration of the successive steps of PET upon excitation by light in a donor-acceptor system, *i.e.* excitation of the donor, electron transfer from donor to acceptor, charge recombination; k_{cs} = rate constant for charge separation, k_{cr} = rate constant for charge recombination.

However, it should be pointed out that two possibilities for the formation of the CT state exist. On the one hand, electron transfer from the LUMO or, in this instance, SOMO, *i.e.* singly occupied molecular orbital, of the excited donor to the LUMO of the acceptor, is denoted as oxidative PET (see left side of Figure 15). In this case, the excited donor is a better reducing agent than in the ground state. On the other hand, electron transfer from the HOMO of the donor to the HOMO of the excited acceptor, is denoted as reductive PET (see right side of Figure 15). Accordingly, the excited acceptor is a better oxidizing agent than in the ground state.
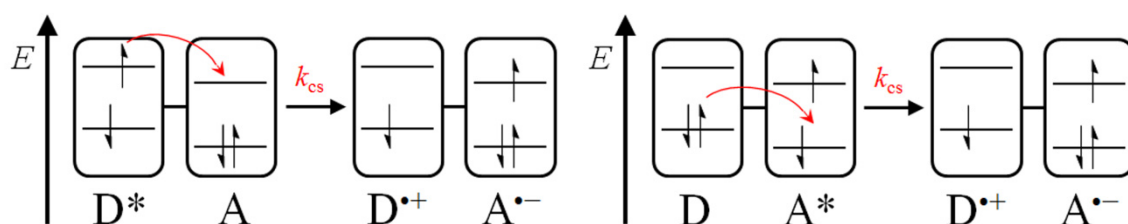
Figure 15. Schematic drawings of oxidative PET (left side) and reductive PET (right side) upon excitation of either the donor or the acceptor unit.

The initial state, *i.e.* D*–A, and final state, *i.e.* $D^{\bullet+}$–$A^{\bullet-}$, of the system can be presented as potential curves in the form of harmonic oscillators. In this case, two general types of interactions between these curves must be distinguished: (i) the adiabatic electron transfer without intersection of both parabolas, when strong electronic coupling V_{DA} occurs; and (ii) diabatic (also called non-adiabatic) electron transfer at low electronic coupling V_{DA} with crossing curves (see Figure 16). The difference between both adiabatic curves sums to $2V_{DA}$. The reorganization energy λ denotes the energy, which is necessary for the rearrangement of the geometry of the molecule, *i.e.* inner reorganization energy λ_i, and the reorientation of the solvent molecules due to their usually dipolar character, *i.e.* outer reorganization energy λ_o, subsequent to the charge transfer.
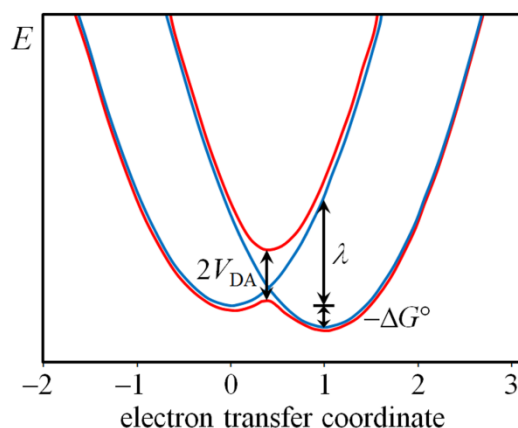
Figure 16. Reaction coordinate for adiabatic (red curves) and diabatic (blue curves) electron transfer process; $\Delta G°$ = Gibbs free energy for diabatic electron transfer, λ = reorganization energy, V_{DA} = coupling energy.

The thermodynamic aspects of electron-transfer processes were described by Rehm and Weller[53] and the kinetics by the Marcus theory,[52] which is based on the diabatic approach. The kinetic rate constant for PET k_{ET} can be obtained according to Eyring theory for the transition state by means of the free activation enthalpy $\Delta G^{\ddagger}$ (Equation (6)) and prefactor k_0, which includes the weak electronic coupling V_{DA}.

$$k_{ET} = k_0 e^{-\frac{\Delta G^{\ddagger}}{k_B T}} \tag{6}$$

The free activation enthalpy $\Delta G^{\ddagger}$ can be replaced by Equation (7), which contains the Gibbs free energy $\Delta G°$ and the reorganization energy λ (see Figure 17).

$$\Delta G^{\ddagger} = \frac{(\lambda + \Delta G°)^2}{4\lambda} \tag{7}$$

The rate constant k_{ET} for electron transfer increases with a larger $-\Delta G°$ value and by decreasing the barrier $\Delta G^{\ddagger}$ (denoted as Marcus normal region, see Figure 17a) up to a maximum when $-\Delta G°$ is equal to the reorganization energy λ (denoted as barrier-free electron transfer, see Figure 17b). When $-\Delta G°$ falls below the reorganization energy the activation barrier begins to increase and deceleration of the electron transfer process is observed. Thus, increasing the driving force, *i.e.* $-\Delta G°$, for the electron transfer decreases the rate constant in the Marcus-inverted region (see Figure 17c). The lifetime of charge-separated states can be prolonged by the design of appropriate systems with charge separation in the Marcus normal region and respective charge recombination in the Marcus inverted region.
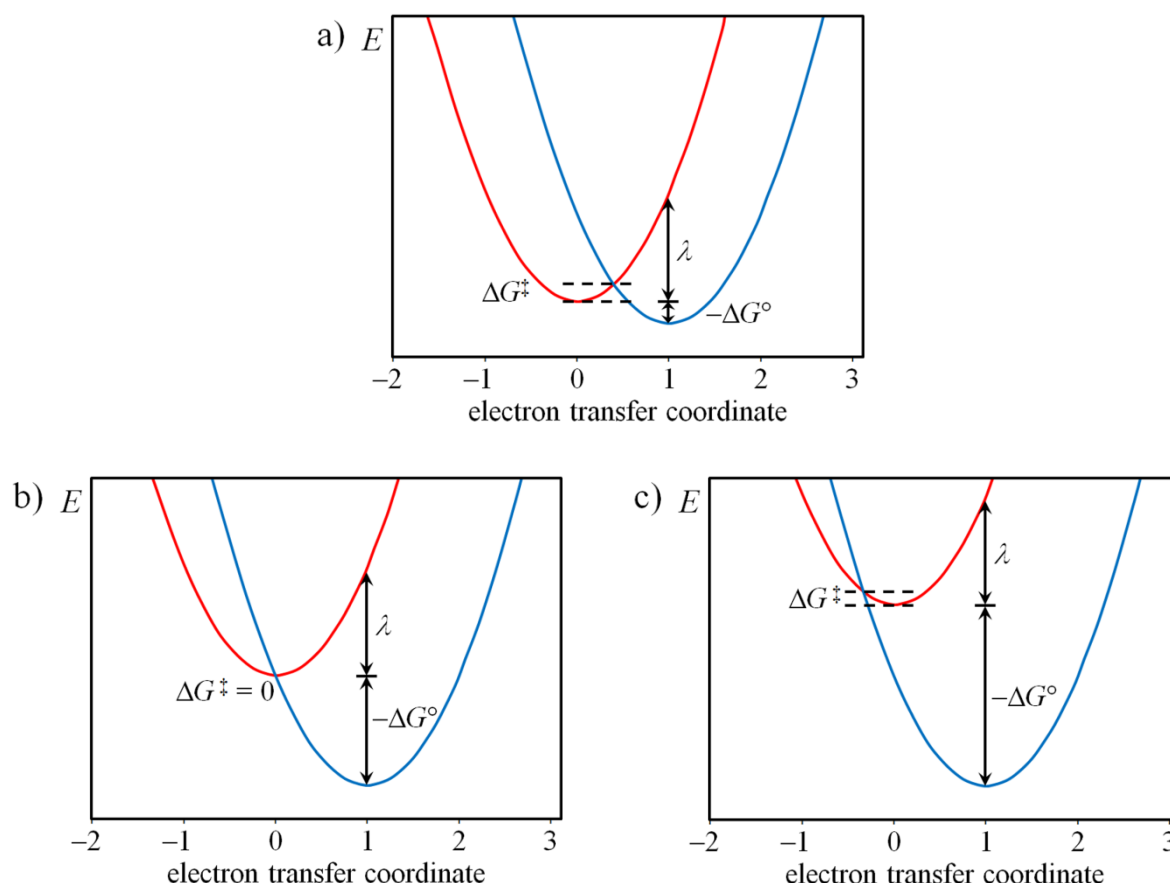
Figure 17. Potential curves for electron transfer processes (a) in the Marcus normal region, (b) barrier free ($\Delta G^{\ddagger} = 0$), and (c) in the Marcus inverted region; $\Delta G^{\ddagger}$ = free activation enthalpy, ΔG° = Gibbs free energy, λ = reorganization energy.

The Rehm-Weller equation or "Gibbs energy of photoinduced electron transfer" can be applied to quantify the thermodynamic driving force for photoinduced electron-transfer processes (Equation (8)).[54] One prerequisite to enable electron transfer upon excitation is that the supplied photoenergy must be larger than the sum of energy, which is necessary to oxidize the donor and to reduce the acceptor.

$$\Delta G^{\circ} = e\left[E_{ox}(D) - E_{red}(A)\right] - E_{00} - \frac{e^2}{4\pi\varepsilon_0\varepsilon_S R_{CC}} - \frac{e^2}{8\pi\varepsilon_0}\left(\frac{1}{r^+} + \frac{1}{r^-}\right)\left(\frac{1}{\varepsilon_{ref}} - \frac{1}{\varepsilon_S}\right) \qquad (8)$$

The variables of Rehm-Weller equation are denoted as $E_{ox}(D)$ and $E_{red}(A)$ and represent the first oxidation potential of the donor and first reduction potential of the acceptor, respectively. The term E_{00} signifies the spectroscopic excited state energy, while R_{CC} is the distance between the centers of the donor and acceptor moieties. The effective ionic radii of the donor radical cation and acceptor radical anion are labeled as r^+ and r^-, respectively. The dielectric constant of the reference solvent used in electrochemistry is denoted as ε_{ref}, while ε_S is the dielectric constant of the respective solvent applied

in the spectroscopic investigation. If the same solvents were used in cyclic voltammetry and spectroscopy studies, the solvent related fourth term can be neglected.

The understanding of energy- and electron-transfer processes is of great importance for developing artificial photosynthesis, organic photovoltaics, and light-emitting diodes. Chapter 2.6 summarizes photochromic systems for switching of fluorescence by such energy- or electron-transfer processes.

2.6   Photochromically Controlled Switching of Fluorescence by Energy or Electron Transfer

Energy transfer-based fluorescence quenching upon photoisomerization between open and closed form of a photochrome was initially demonstrated by the group of Effenberger in 1993 fusing the triad **39o/39c** composed of an anthracene donor, a photochromic fulgide, and a coumarin acceptor (see Scheme 19).[55] The fluorescence of the coumarin unit was triggered by the isomeric state of the fulgide. Excitation of the anthracene led to an effective energy transfer to the coumarin and subsequent fluorescence from the coumarin when the fulgide was in the open form. In the ring closed form, energy transfer from the excited anthracene to the fulgide photochrome was observed, effectively quenching the coumarin emission. One drawback of the system is that the excitation of the anthracene unit, which was performed in the UV region at 320 nm, and the generation of the ring-closed form upon irradiation must be performed in the same spectral region.
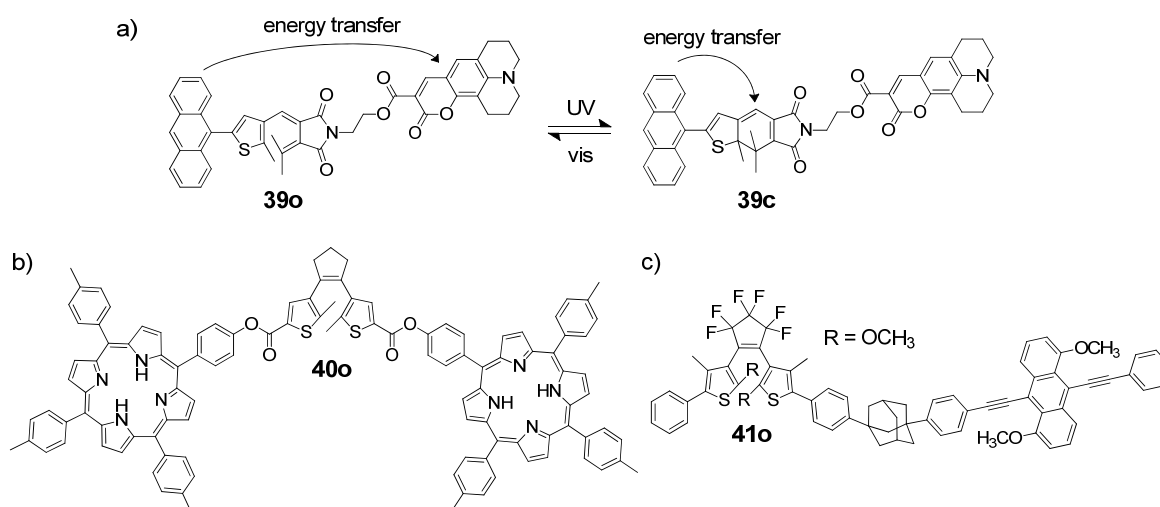

Scheme 19. (a) Photochromic energy-transfer triad **39o/39c**, containing an anthracene donor, a fulgide as switching unit, and a coumarin acceptor, (b) triad **40o** composed of a DAE and two porphyrin fluorophores, and (c) dyad **41o**, which consists of a DAE and an emissive bis(phenylethynyl)anthracene dye.[55-56]

Another fluorophore reported by Branda, *i.e.* triad **40o** composed of two emissive porphyrins and a DAE photochrome (see Scheme 19), was excited directly and fluorescence-quenching energy transfer takes place only for one isomer of the respective photochrome.[56a] However, photoswitching from open to closed from and *vice versa* revealed a rather moderate on/off ratio of roughly 2 : 1 in toluene. Neither FRET nor another reason was given as explanation for the observed quenching by the authors.

Furthermore, continuous read-out of the fluorescence signal of the closed form led to complete, undesired ring-opening.

One particularly relevant photochromic dyad showing enhanced function from **40**, was reported by Masahiro Irie, Tuyoshi Fukaminato, and coworkers in 2002.[56b,c] In this system **41o** (see Scheme 19), consisting of a switchable DAE unit and a fluorescent bis(phenylethynyl)anthracene dye linked by an adamantane bridge, emission of the dye unit could be turned on, *i.e.* 76% fluorescence quantum yield for the open form in toluene, and off, *i.e.* <0.1% for the closed form, repeatedly by isomerization of the photochromic DAE unit upon irradiation with light of two different wavelengths. With an additional third light source of a different wavelength, the respective fluorescent or non-fluorescent state can be obtained as the "read-out" signal, resulting in a binary emissive "1" and non-emissive "0" code. The emission in this process is quenched by an effective intramolecular FRET from the excited dye to only one of the photochromic isomers (see Figure 18) due to a good overlap of the emission band of the fluorophore and the absorption band of the closed form of the DAE unit in the visible region. One detrimental effect of the intramolecular fluorescence quenching by FRET, however, is the concomitant excitation of the ring-closed form of the photochromic dyad during the read-out process, resulting in undesirable ring opening. Thus, energy transfer may induce the photochromic back reaction of the ring-closed form to the ring-open one during reading of the fluorescence intensity, and such energy-transfer-based memory systems lead to destructive read-out.
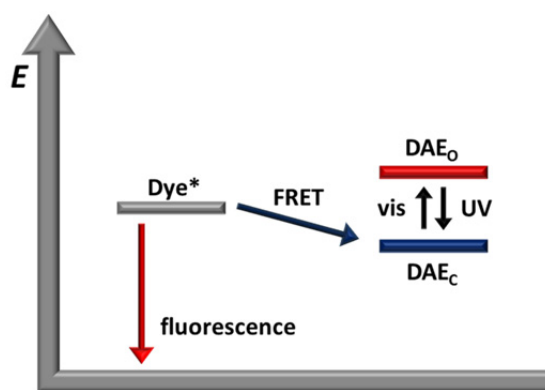

Figure 18. Schematic illustration of energy diagram for the fluorescent open form (red line) and the non-fluorescent closed form (blue line) of Dye–DAE conjugate.

The authors have chosen methoxy substituents in the 2-position instead of the common methyl groups (residue R of compound **41o** in Scheme 19) to decrease the ring-opening quantum yield dramatically ($< 8 \times 10^{-5}$).[56c] Due to this strategy, the disadvantageous cyclic back reaction upon selective excitation of the fluorophore does not attract attention, but switching performance of the system drastically dropped down. The lack in photostability of the emitter unit further restricted the usage of this system.[30l]

The first report of a PBI dye being used as a fluorophore unit for a photochromic dyad was by Fukaminato *et al.* in 2006 (**42o** in Figure 19).[57] They used a special DAE containing a maleic

anhydride bridge instead of the perfluorocyclopentene bridge to attach the aniline-functionalized PBI emitter at the imide position. While the open form of the system showed a fluorescence quantum yield of almost unity in methylcyclohexane (MCH), the value for the pure closed form was negligible. However, upon irradiation of the open isomer with UV light ($\lambda_{max} = 313$ nm) only a moderate conversion with 24% of the ring-closed form in the photostationary state (PSS) could be obtained. The system revealed an interesting fluorescence behavior upon increasing the concentration in MCH. A reversible shift in the emission wavelength between green and red, which is caused by the degree of aggregation, could be triggered by the photochromic reaction. The different fluorescence colors derived from a monomeric or respective aggregated state of the PBI, depend on the configuration of the DAE unit. The fact that aggregation is favored for the open form was explained by an increase in the electronic density of the maleimide moiety upon ring closure, which suppressed aggregate formation and possibly due to geometrical changes.[57] Further examples for the interplay of a photochromic reaction and the aggregation behavior of PBI dyes **43o** and **44o**, published by the group of Sun[58] and Feringa,[59] respectively, were designed to study the influence of photochromic reactions on the aggregation behavior of PBI dyes.
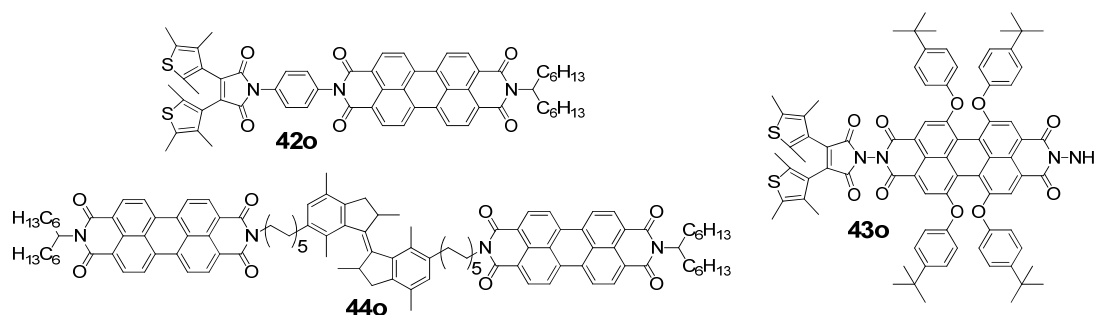
Figure 19. Examples for photochromic dyads, which enable triggering of aggregation behavior upon photoisomerization.[57-59]

In another paper by Fukaminato and Irie the bis(phenylethynyl)anthracene containing photochromic dyad **41o** was improved by replacing this unstable emitter unit by a bay-unsubstituted PBI (see compound **45o** in Figure 20) and further investigated by single-molecule detection techniques in polymer matrix.[30d] The fluorescence quantum yields for the pure isolated open form is 97% and for the respective closed form lower than 0.1%. The authors again utilized electron rich methoxy substituents at the central bond-forming carbon atoms to decreases the ring-opening quantum yield, which is considered necessary to clearly detect the photoswitching performance at the single-molecule level.[30d]
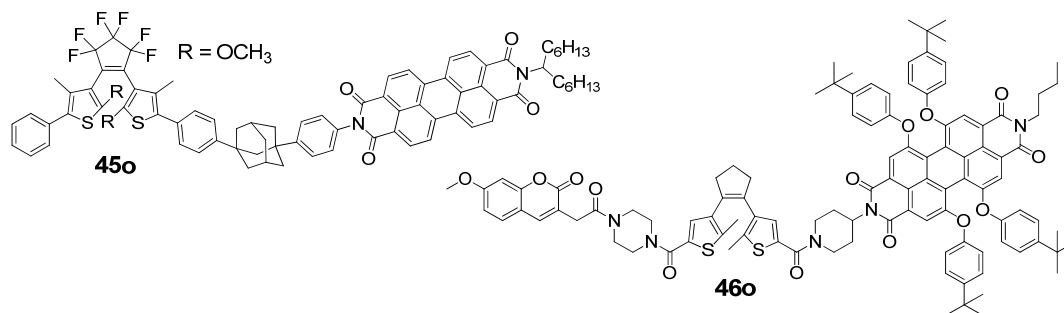
Figure 20. Further examples for fluorescence quenching by FRET in photochromic dyads **45o** and **46o** containing PBI and DAE units.[30d,e]

The group of Feringa synthesized a perylene bisimide-diarylethene-coumarin triad **46o** containing a highly fluorescent tetraaryloxy-substituted PBI and a DAE with fluorine-free bridge, which are known to be not photostable.[30e] In the open state of the DAE unit, an efficient energy transfer from the coumarin to the PBI takes place upon excitation at 312 nm. The PBI emission decreased by 60% in the photostationary state, which contains less than 70% of the closed form, due to energy transfer from the excited coumarin to the DAE unit and partial energy transfer from the excited PBI to the DAE unit. Besides the low photostability, the fact that excitation at 312 nm causes coumarin and PBI excitation as well as the photoisomerization from closed to open form of the DAE and *vice versa* are major drawbacks of the systems. It is also worth noting that this particular system was made for the investigation of energy-transfer processes, not for application as a non-destructive read-out memory device.

The read-out of a phosphorescence signal instead of fluorescence may circumvent the isomerizing overlap of emission band of the fluorophore and absorption band of the closed form of the DAE. Phosphorescence is generally more bathochromic than fluorescence and therefore, outside of the spectral region that is responsible for the photochromic reactions. Branda and coworker investigated the emission behavior of ruthenium-based metalloporphyrins **47o** that were axially coordinated to pyridine-substituted DAE (see Figure 21).[60]
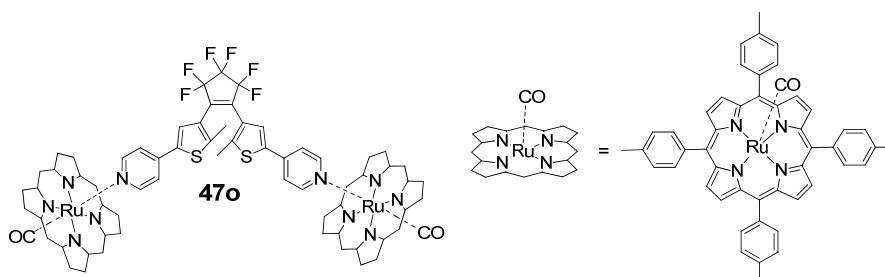

Figure 21. Photochromic triad **47o** containing a DAE connected to two metalloporphyrins.[60]

The open form of this supramolecular assembly showed high phosphorescence intensity (λ_{max} = 730 nm) upon excitation of the Soret band at 400–450 nm. Ring closure was performed upon

excitation at 380 nm, reducing the intensity of phosphorescence by one-third. The photochromic back reaction was induced in the region between 470–685 nm. Although, the DAE reveals very little absorption in the spectral region of the Soret band, excitation in this intensive band may induce photochromic reaction.

Emission quenching based on intramolecular photoinduced electron transfer (PET)[61] may circumvent the destructive read-out pathway, which is caused by the fluorescence quenching FRET and subsequent excitation of the ring-closed isomer. Some examples of electron-transfer switching with different photochromic units have been reported in the literature. An interesting system **48E/48Z** has been published by Tsuchiya where an electron-rich and an electron-poor porphyrin are connected by an azobenzene bridge allowing modulation of the donor-acceptor distance by photoinduced *cis-trans* isomerization, also denoted as *Z/E* isomerization.[62] Only in the *cis* isomeric form was electron transfer observed because of a markedly reduced distance between the porphyrin units (see Scheme 20). One major drawback, however, of azobenzene-based systems is the lack of thermal stability of the *cis* isomer. Nevertheless, azobenzene-based systems are convenient tools for facile tuning of the distance between two emissive chromophores and therefore, controlling the fluorescence intensity by PET. The same strategy was also applied in to systems containing a phosphorus(V) porphyrin[63] or a pyromellitic diimide and a zinc porphyrin.[64]
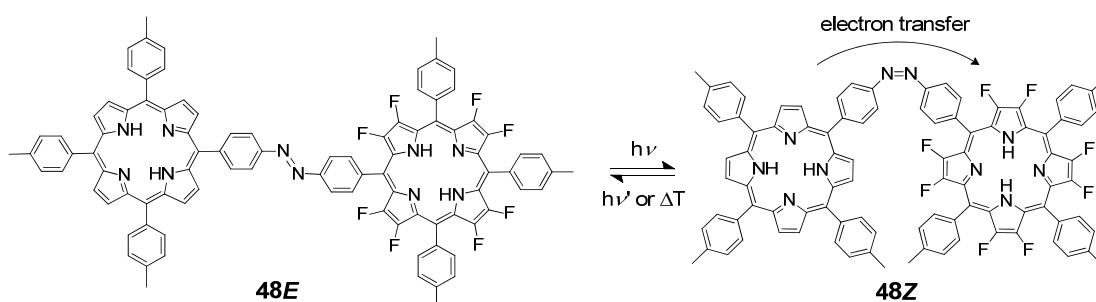

Scheme 20. Photochromic dyad **48E/48Z** containing an electron-rich and an electron-poor porphyrin unit linked by an azobenzene bridge.[62]

For triad **49o/49c**, composed of an anthracene donor, a DAE switch, and a pyridinium acceptor, Effenberger and coworkers showed already a decade ago that PET occurred from the excited anthracene donor to the pyridinium acceptor in the ring-open form of the DAE unit. Upon ring closure of the triad, a FRET process, from the excited anthracene donor to the DAE acceptor, outcompetes PET observed in the ring-open form (see Scheme 21).[65] Similar to other FRET-based photoswitches, energy transfer to the DAE resulted in destructive read-out owing to the disadvantageous excitation of the ring-closed form.
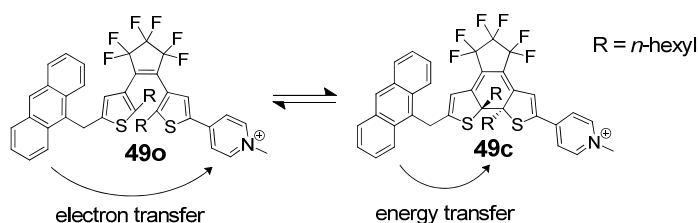
Scheme 21. Photochromic DAE for the switching between energy transfer and electron transfer pathways.[65a]

Such undesirable energy transfer pathways could be avoided by photoswitching of the redox potentials of photochromes as shown by the groups of Branda[66] and Gust[67] using fluorescent porphyrins as donors and phenoxynaphthacene quinone (see compounds **50trans**/**50ana** in Scheme 22) or dihydroindolizine (see compounds **51c**/**51o** in Scheme 22) as photochromic acceptor. While the dihydroindolizine/betaine-based system enables a fluorescence on/off ratio of 10 : 1,[67] no values were given for the phenoxynaphthacene system. However, these photochromic systems either exhibit poor photostability and thermal stability of both isomeric forms[67] or the thermodynamic discrimination of PET for only one isomer is not given.[66]
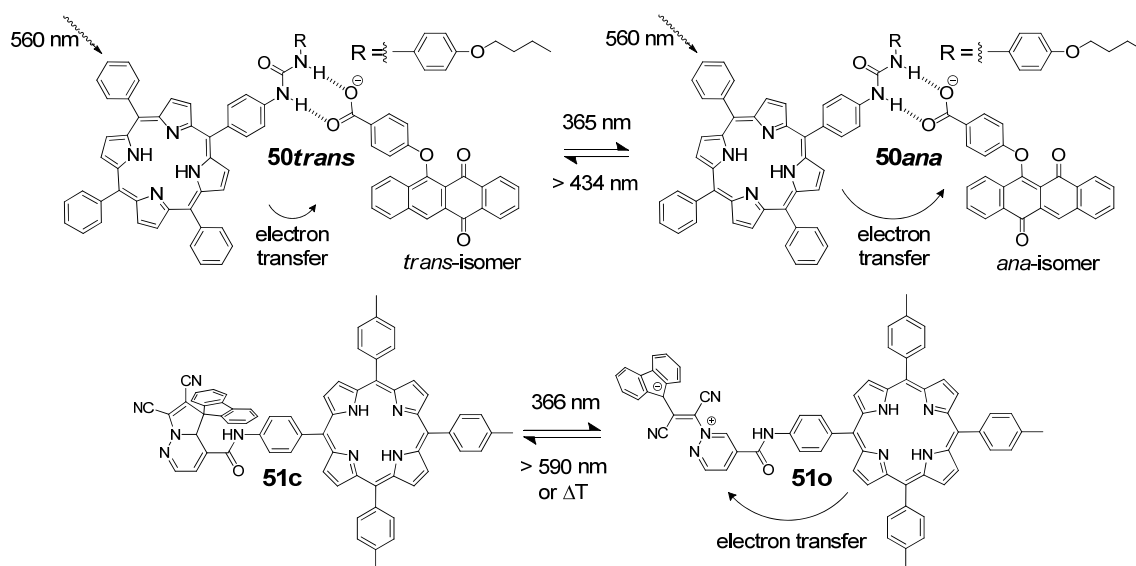

Scheme 22. Photochromic assembly **50trans**/**50ana** of a polycyclic quinone and a porphyrin unit connected by hydrogen bonds (upper row) and dyad **51c**/**51o** containing a spiropyran and a porphyrin unit (row below).[66-67]

Finally, the first convincing concept of fluorescence photoswitching by intramolecular PET based on dyads of photochromic DAE and fluorescent dyes was given in the preceding diploma work[68] for **52o** (Figure 22) and by the work of Odo *et al.*[69] for **53o** (Figure 22) according to the energy level diagram shown in Figure 23 that was suggested by Prof. Franco Scandola.
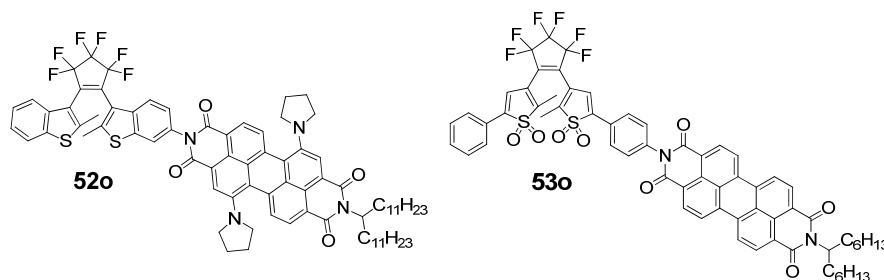
Figure 22. Photochromic dyads **52o** and **53o** for the light-induced switching of fluorescence.[68b,69]

The basic idea behind this concept is that the ring-open and ring-closed isomers of the photochromic DAE moiety possess different redox properties and that the electron transfer from the fluorescent dye is thermodynamically favorable only to one of the two DAE isomers, *i.e.* either to the ring-open or the ring-closed form. Due to the fact that several DAE derivatives also show electrochromic behavior (see Chapter 2.3), *i.e.* ring opening or ring closure, upon oxidation,[31a-c,32,34] which is undesired for such applications, the DAE unit of a photochromic donor-acceptor dyad should preferentially act as an electron acceptor. Nevertheless, also one example of a DAE exhibiting electrochromic behavior upon reduction has also been reported.[33] In an optimal case, electron transfer from a fluorescent dye to the DAE unit should be exergonic only for the DAE_C^-–Dye^+ but not for the DAE_O^-–Dye^+ charge-transfer (CT) state as schematically illustrated in Figure 23. Thus, upon excitation of the fluorescent dye, one isomeric state still emits, while a CT state is formed for the other one. For such dyads in contrast to former FRET systems the excitation of the fluorophore takes place at a lower energy than that required for both photochromic transformations (*i.e.* ring opening and ring closing) and accordingly can enable non-destructive read-out. Destructive FRET processes from the fluorophore to the DAE_O or the DAE_C is impossible for energetic reasons. For all PET processes the formation of the CT state (thermodynamics[53] and kinetics[52]) is governed by the polarity of the solvent. With an appropriately designed system and the right matrix, it would be possible to write, read, and erase optical memory without destructive read-out by using light sources of three different wavelengths.
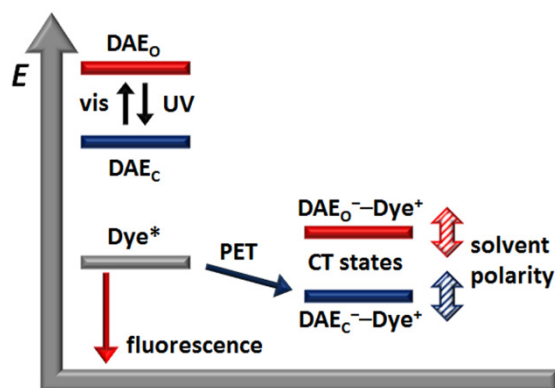
Figure 23. Schematic energy diagram for the fluorescent open form (red line) and the non-fluorescent closed form (blue line) of DAE–Dye conjugate suggested to us by Prof. Franco Scandola in 2006.[70]

Parallel to this PhD thesis the Japanese team of Fukaminato and Irie pursued related work on PET-dependent DAE–PBI dyads[71] (see **54o** and **55o** in Figure 24) following their initial work on a photochromic system composed of bay-unsubstituted PBI emitter and a DAE with oxidized sulfur atoms **53o/53c** (see Figure 22). Although bay-unsubstituted PBI dyes are pretty electron poor,[72] the PBI unit apparently serves as the electron donor in this dyad. Unfortunately, $\Delta G°$ values were not given for this system by the authors. The best on/off ratio of fluorescence quantum yields for both isomers was obtained in polar solvent ($\varepsilon_r \sim 20$), with a value of 76% for the open form and 60% for the closed form. The quantum yield for the open form, which is distinctly different to the 100% for bay-unsubstituted PBIs, suggests that PET is taking place for both isomers with a slightly better driving force for the closed form. More details on the thermodynamic driving force and the excited state dynamics were given for our first dyad **52o/52c**.

The photochromic system containing a dipyrrolidinyl-substituted PBI dye **52o/52c** revealed a slightly exergonic $\Delta G°$ value of –0.03 eV for the fluorescence quenching PET in the closed form, while the value is clearly positive (0.37 eV) for the open form.[68] This results in a distinct difference of emission intensity between open and closed form only in highly polar environment, *i.e.* acetone ($\varepsilon_r = 20.56$) or DMF ($\varepsilon_r = 36.71$). Transient species for the radical cation of the PBI moiety were clearly identified by ultrafast spectroscopy. This DAE–PBI dyad **52o/52c** has, however, the disadvantage of low fluorescence quantum yield ($\Phi_{fl} = 14\%$ in dichloromethane) and low photostability of the 1,7-dipyrrolidinyl-substituted PBI, leading to decomposition of this moiety upon continuing irradiation.
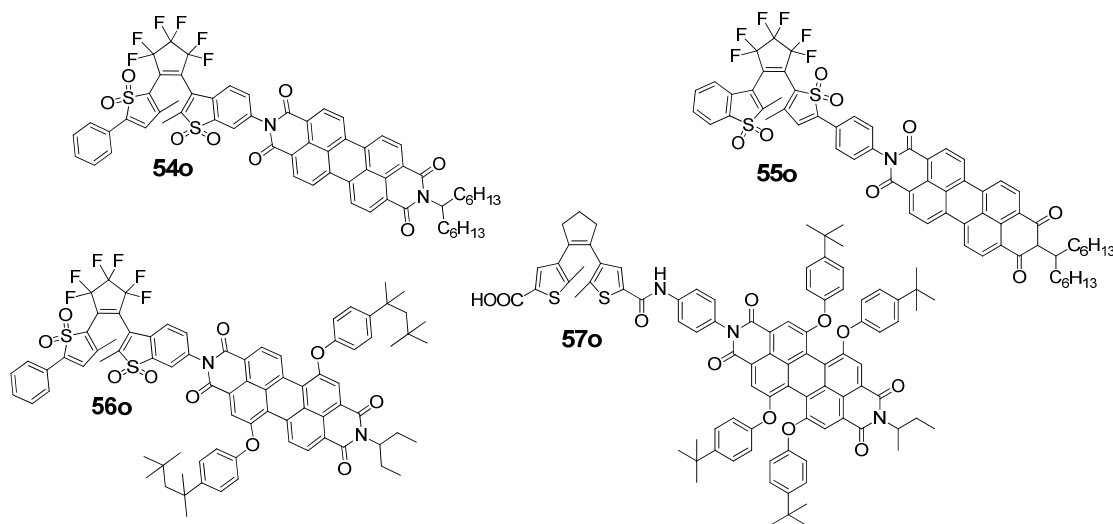
Figure 24. Recent examples for PBI containing photochromic dyads for fluorescence quenching by intramolecular PET.[71,73]

Subsequently, the on/off ratio of Odo's original system **53o/53c** (see Figure 22) was improved by a small modification of the switching unit.[71a,b] One thiophene subunit was connected in the 2- instead of the 3-position to the perfluorocyclopentene, which results in a $\Delta G°$ of 0.28 eV and

–0.15 eV for the open and closed form of system **54o**/**54c** (see Figure 24), respectively. The best on/off ratio was obtained in a 3 : 7 1,4-dioxane/methanol mixture with fluorescence quantum yields of 88% for the open and 12% for the closed form. The quantum yield of the open form of the dyad **54o** varies from 91% to 88% in the whole range of solvent polarities. This decrease of around 10% (bay-unsubstituted PBIs exhibit quantum yields near unity) was attributed by the authors to a triplet excitation and therefore, disadvantageous isomerization from the open to the closed form occurred. A further system **55o** was described within this publication,[71a] but no fluorescence data were provided.

A further improvement could be achieved by replacing the bay-unsubstituted PBI emitter by a 1,7-diaryloxy-substituted PBI.[71c] The additional aryloxy substituents shift the emission band from 510–610 nm for system **54o** to 530–650 nm for the new dyad **56o** (see Figure 24), which was enough to prevent unfavorable triplet formation. The respective $\Delta G°$ values were 0.05 eV for the ring-open and –0.37 eV for the ring-closed form in dichloromethane. The best on/off ratio was obtained in environments of medium polarity, *e.g.* 1,4-dioxane/methanol 7:3, revealing a fluorescence quantum yield of 62% for the open and 5.5% for the closed form. A drawback of this system is the decrease of emission intensity of the open form in highly polar solvents due to electron transfer processes from the electron rich aryloxy groups to the electron poor PBI core. Furthermore, the authors gave no data neither about photostability nor ring-opening and ring-closure quantum yields of their system.[71c]

The latest example of a tetraaryloxy-substituted PBI attached to a carboxy-substituted DAE **57o** was published by the group of Hernando in 2012 (see Figure 24).[73] The on/off ratio of fluorescence amounts around 9 : 1, *i.e.* around 90% for the open form and around 10% for the closed form, over the whole range of solvents from non-polar toluene ($\varepsilon_r = 2.38$) to polar acetonitrile ($\varepsilon_r = 37.5$). The $\Delta G°$ values in chloroform ($\varepsilon_r = 4.81$) for PET are –0.46 eV for the closed form and 0.22 eV for the open form. However, switching cycles between a PSS, which consists of mainly open form and another PSS with a ratio of 7 : 3 for **57c**/**57o**, revealed an actual on/off ratio of only 1 : 2.5. Furthermore, the 86% decrease of fluorescence intensity from open to closed form in toluene cannot be attributed only to a PET process, as an unfavorable energy transfer from PBI to DAE unit is also likely, due to a small overlap of the PBI emission band and the absorption band of the closed form of the DAE moiety

Figure 25 gives an overview of all dyads and triads composed of a photochromic DAE unit and an emissive PBI chromophore published to date (with the exception of our recently published systems[70,74] that will be discussed in detail in the following chapters). A photochromic triad **58o** composed of two PBI units and a central DAE switch, which acts as an organic optical transistor, was listed for the sake of completeness.[22] All of the current photoswitching systems **52o**, **53o**, **54o**, **56o**, and **57o** based on the concept of fluorescence quenching by PET suffer from certain disadvantages like low fluorescence quantum yield, photocyclization by triplet-state population, small driving force for fluorescence-quenching PET, or low photostability.[68-69,71] In light of these shortcomings, opportunities to improve the performance of such devices have been explored throughout the course of this doctoral work.
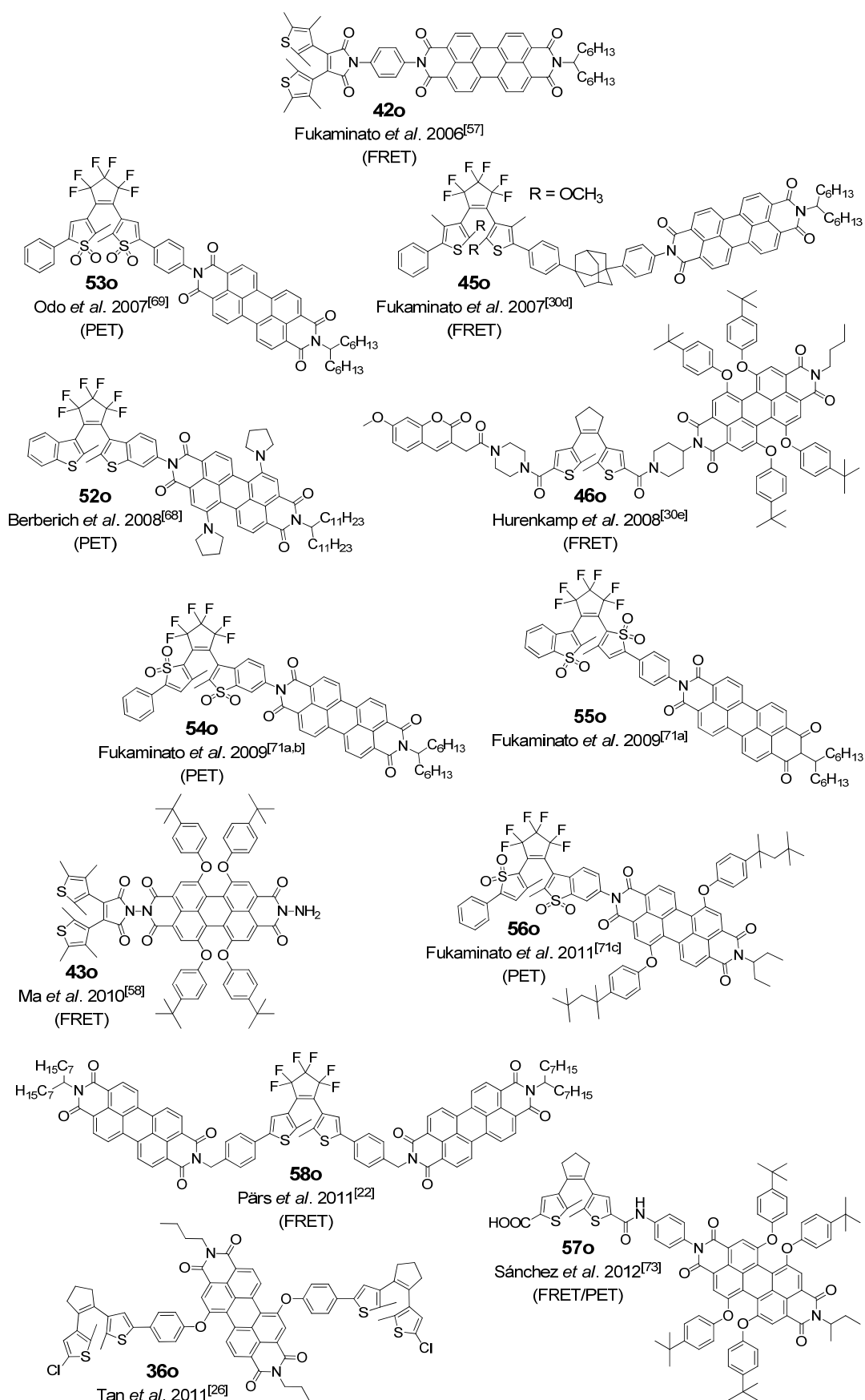
Figure 25. Chronological overview of all known perylene bisimide-diarylethene containing photochromic systems. The occurring fluorescence quenching processes by energy or electron transfer are denoted as (FRET) and (PET), respectively.

2.7   References

[1]   N. Hampp, *Chem. Rev.* **2000**, *100*, 1755-1776.

[2]   J. Fritsche, *C. R. Hebd. Seances Acad. Sci.* **1867**, *69*, 1035.

[3]   Y. Hirshberg, *C. R. Hebd. Seances Acad. Sci.* **1950**, *231*, 903-904.

[4]   a) H. Rau, *Angew. Chem. Int. Ed.* **1973**, *12*, 224-235; b) F. Hamon, F. Djedaini-Pilard, F. Barbot, C. Len, *Tetrahedron* **2009**, *65*, 10105-10123; c) R. Reuter, N. Hostettler, M. Neuburger, H. A. Wegner, *Chimia* **2010**, *64*, 180-183; d) M.-M. Russew, S. Hecht, *Adv. Mater.* **2010**, *22*, 3348-3360; e) A. A. Beharry, G. A. Woolley, *Chem. Soc. Rev.* **2011**, *40*, 4422-4437.

[5]   G. Berkovic, V. Krongauz, V. Weiss, *Chem. Rev.* **2000**, *100*, 1741-1754.

[6]   Y. Yokoyama, *Chem. Rev.* **2000**, *100*, 1717-1740.

[7]   a) M. Irie, *Chem. Rev.* **2000**, *100*, 1685-1716; b) H. Tian, S. Yang, *Chem. Soc. Rev.* **2004**, *33*, 85-97.

[8]   a) N. Koumura, R. W. J. Zijlstra, R. A. van Delden, N. Harada, B. L. Feringa, *Nature* **1999**, *401*, 152-155; b) M. Irie, T. Mrozek, J. Daub, A. Ajayaghosh, Y. Yokoyama, *Molecular Switches* (ed. Feringa, B. L.), Wiley-VCH, Weinheim, **2001**, pp. 37-121.

[9]   H. Tian, Y. Feng, *J. Mater. Chem.* **2008**, *18*, 1617-1622.

[10]   U. Al-Atar, R. Fernandes, B. Johnsen, D. Baillie, N. R. Branda, *J. Am. Chem. Soc.* **2009**, *131*, 15966-15967.

[11]   D. A. Parthenopoulos, P. M. Rentzepis, *Science* **1989**, *245*, 843-845.

[12]   M. Irie, M. Mohri, *J. Org. Chem.* **1988**, *53*, 803-808.

[13]   R. B. Woodward, R. Hoffmann, *The conversation of Orbital Symmetry*, Verlag Chemie/Academic Press, Weinheim, **1970**.

[14]   M. Walko, B. L. Feringa, *Chem. Commun.* **2007**, 1745-1747.

[15]   J. Ern, A. Bens, H. D. Martin, S. Mukamel, D. Schmid, S. Tretiak, E. Tsiper, C. Kryschi, *J. Lumin.* **2000**, *87–89*, 742-744.

[16]   Y.-C. Jeong, S. I. Yang, K.-H. Ahn, E. Kim, *Chem. Commun.* **2005**, 2503-2505.

[17]   J. Ern, A. T. Bens, H. D. Martin, S. Mukamel, D. Schmid, S. Tretiak, E. Tsiper, C. Kryschi, *Chem. Phys.* **1999**, *246*, 115-125.

[18]   T. A. Bens, D. Frewert, K. Kodatis, C. Kryschi, H.-D. Martin, H. P. Trommsdorff, *Eur. J. Org. Chem.* **1998**, 2333-2338.

[19]   a) S. Kawata, Y. Kawata, *Chem. Rev.* **2000**, *100*, 1777-1788; b) B. L. Feringa, *J. Org. Chem.* **2007**, *72*, 6635-6652; c) H. Tian, S. Wang, *Chem. Commun.* **2007**, 781-792; d) *Molecular Devices and Machines-Concepts and Perspectives for the Nanoworld* (eds. Balzani, V.; Credi, A.; Venturi, M.), Wiley-VCH, Weinheim, **2008**; e) C. Yun, J. You, J. Kim, J. Huh, E. Kim, *J. Photochem. Photobiol., C* **2009**, *10*, 111-129; f) U. Pischel, *Aust. J. Chem.* **2010**, *63*, 148-164; g) A. Bianco, S. Perissinotto, M. Garbugli, G. Lanzani, C. Bertarelli, *Laser & Photon. Rev.*

2011, *5*, 711-736; h) W. Zhu, Y. Yang, R. Métivier, Q. Zhang, R. Guillot, Y. Xie, H. Tian, K. Nakatani, *Angew. Chem. Int. Ed.* **2011**, *50*, 10986-10990; i) D. Gust, J. Andreasson, U. Pischel, T. A. Moore, A. L. Moore, *Chem. Commun.* **2012**, *48*, 1947-1957.

[20]   a) N. Katsonis, T. Kudernac, M. Walko, S. J. van der Molen, B. J. van Wees, B. L. Feringa, *Adv. Mater.* **2006**, *18*, 1397-1400; b) M. T. W. Milder, J. Areephong, B. L. Feringa, W. R. Browne, J. L. Herek, *Chem. Phys. Lett.* **2009**, *479*, 137-139.

[21]   P. Zacharias, M. C. Gather, A. Köhnen, N. Rehmann, K. Meerholz, *Angew. Chem. Int. Ed.* **2009**, *48*, 4038-4041.

[22]   M. Pärs, C. C. Hofmann, K. Willinger, P. Bauer, M. Thelakkat, J. Köhler, *Angew. Chem. Int. Ed.* **2011**, *50*, 11405-11408.

[23]   J. Piard, R. Metivier, M. Giraud, A. Leaustic, P. Yu, K. Nakatani, *New J. Chem.* **2009**, *33*, 1420-1426.

[24]   Z. Erno, I. Yildiz, B. Gorodetsky, F. M. Raymo, N. R. Branda, *Photochem. Photobiol. Sci.* **2010**, *9*, 249-253.

[25]   J. Andréasson, U. Pischel, S. D. Straight, T. A. Moore, A. L. Moore, D. Gust, *J. Am. Chem. Soc.* **2011**, *133*, 11641-11648.

[26]   W. Tan, X. Li, J. Zhang, H. Tian, *Dyes Pigm.* **2011**, *89*, 260-265.

[27]   a) J. Fölling, V. Belov, R. Kunetsky, R. Medda, A. Schönle, A. Egner, C. Eggeling, M. Bossi, S. W. Hell, *Angew. Chem. Int. Ed.* **2007**, *46*, 6266-6270; b) Y. Zou, T. Yi, S. Xiao, F. Li, C. Li, X. Gao, J. Wu, M. Yu, C. Huang, *J. Am. Chem. Soc.* **2008**, *130*, 15750-15751.

[28]   Y. Hirshberg, *J. Am. Chem. Soc.* **1956**, *78*, 2304-2312.

[29]   F.-K. Bruder, R. Hagen, T. Rölle, M.-S. Weiser, T. Fäcke, *Angew. Chem. Int. Ed.* **2011**, *50*, 4552-4573.

[30]   a) T. A. Golovkova, D. V. Kozlov, D. C. Neckers, *J. Org. Chem.* **2005**, *70*, 5545-5549; b) M. Bossi, V. Belov, S. Polyakova, S. W. Hell, *Angew. Chem. Int. Ed.* **2006**, *45*, 7462-7465; c) G. Jiang, S. Wang, W. Yuan, L. Jiang, Y. Song, H. Tian, D. Zhu, *Chem. Mater.* **2006**, *18*, 235-237; d) T. Fukaminato, T. Umemoto, Y. Iwata, S. Yokojima, M. Yoneyama, S. Nakamura, M. Irie, *J. Am. Chem. Soc.* **2007**, *129*, 5932-5938; e) J. H. Hurenkamp, J. J. D. de Jong, W. R. Browne, J. H. van Esch, B. L. Feringa, *Org. Biomol. Chem.* **2008**, *6*, 1268-1277; f) S. F. Yan, V. N. Belov, M. L. Bossi, S. W. Hell, *Eur. J. Org. Chem.* **2008**, 2531-2538; g) J. Fölling, S. Polyakova, V. Belov, A. van Blaaderen, M. L. Bossi, S. W. Hell, *Small* **2008**, *4*, 134-142; h) J. Cusido, E. Deniz, F. M. Raymo, *Eur. J. Org. Chem.* **2009**, 2031-2045; i) R. Métivier, S. Badré, R. Méallet-Renault, P. Yu, R. B. Pansu, K. Nakatani, *J. Phys. Chem. C* **2009**, *113*, 11916-11926; j) J. Kärnbratt, M. Hammarson, S. Li, H. L. Anderson, B. Albinsson, J. Andréasson, *Angew. Chem. Int. Ed.* **2010**, *49*, 1854-1857; k) B. Seefeldt, K. Altenhoner, O. Tosic, T. Geisler, M. Sauer, J. Mattay, *Photochem. Photobiol. Sci.* **2011**, *10*, 1488-1495; l) T. Fukaminato, *J. Photochem. Photobiol., C* **2011**, *12*, 177-208.

[31]   a) A. Peters, N. R. Branda, *Chem. Commun.* **2003**, 954-955; b) A. Peters, N. R. Branda, *J. Am. Chem. Soc.* **2003**, *125*, 3404-3405; c) Y. Moriyama, K. Matsuda, N. Tanifuji, S. Irie, M. Irie, *Org. Lett.* **2005**, *7*, 3315-3318; d) S. Lee, Y. You, K. Ohkubo, S. Fukuzumi, W. Nam, *Org. Lett.* **2012**, *14*, 2238-2241.

[32]   G. Guirado, C. Coudret, M. Hliwa, J.-P. Launay, *J. Phys. Chem. B* **2005**, *109*, 17445-17459.

[33]   B. Gorodetsky, H. D. Samachetty, R. L. Donkers, M. S. Workentin, N. R. Branda, *Angew. Chem. Int. Ed.* **2004**, *43*, 2812-2815.

[34]   a) W. R. Browne, J. J. D. de Jong, T. Kudernac, M. Walko, L. N. Lucas, K. Uchida, J. H. van Esch, B. L. Feringa, *Chem. Eur. J.* **2005**, *11*, 6414-6429; b) W. R. Browne, J. J. D. de Jong, T. Kudernac, M. Walko, L. N. Lucas, K. Uchida, J. H. van Esch, B. L. Feringa, *Chem. Eur. J.* **2005**, *11*, 6430-6441.

[35]   E. Orgiu, N. Crivillers, M. Herder, L. Grubert, M. Pätzel, J. Frisch, E. Pavlica, D. T. Duong, G. Bratina, A. Salleo, N. Koch, S. Hecht, P. Samorì, *Nat. Chem.* **2012**, *4*, 675-679.

[36]   K. Uchida, Y. Yamanoi, T. Yonezawa, H. Nishihara, *J. Am. Chem. Soc.* **2011**, *133*, 9239-9241.

[37]   F. Stellacci, C. Bertarelli, F. Toscano, M. C. Gallazzi, G. Zerbi, *Chem. Phys. Lett.* **1999**, *302*, 563-570.

[38]   E. Murguly, T. B. Norsten, N. R. Branda, *Angew. Chem. Int. Ed.* **2001**, *40*, 1752-1755.

[39]   S. H. Kawai, S. L. Gilat, R. Ponsinet, J.-M. Lehn, *Chem. Eur. J.* **1995**, *1*, 285-293.

[40]   a) G. M. Tsivgoulis, J.-M. Lehn, *Angew. Chem. Int. Ed.* **1995**, *34*, 1119-1122; b) G. M. Tsivgoulis, J.-M. Lehn, *Chem. Eur. J.* **1996**, *2*, 1399-1406.

[41]   Q. Luo, B. Chen, M. Wang, H. Tian, *Adv. Funct. Mater.* **2003**, *13*, 233-239.

[42]   H. Tian, B. Chen, H. Y. Tu, K. Müllen, *Adv. Mater.* **2002**, *14*, 918-923.

[43]   T. Saika, T. Iyoda, K. Honda, T. Shimidzu, *J. Chem. Soc., Chem. Commun.* **1992**, 591-592.

[44]   a) A. Fernández-Acebes, J.-M. Lehn, *Adv. Mater.* **1998**, *10*, 1519-1522; b) A. Fernández-Acebes, J.-M. Lehn, *Chem. Eur. J.* **1999**, *5*, 3285-3292.

[45]   T. van der Boom, R. T. Hayes, Y. Zhao, P. J. Bushard, E. A. Weiss, M. R. Wasielewski, *J. Am. Chem. Soc.* **2002**, *124*, 9582-9590.

[46]   A. S. Dvornikov, Y. Liang, C. S. Cruse, P. M. Rentzepis, *J. Phys. Chem. B* **2004**, *108*, 8652-8658.

[47]   S. H. Chen, H. M. P. Chen, Y. Geng, S. D. Jacobs, K. L. Marshall, T. N. Blanton, *Adv. Mater.* **2003**, *15*, 1061-1065.

[48]   S.-J. Lim, J. Seo, S. Y. Park, *J. Am. Chem. Soc.* **2006**, *128*, 14542-14547.

[49]   *Modern Molecular Photochemistry of Organic Molecules* (eds. Turro, N. J.; Ramamurthy, V.; Scaiano, J. C.), University Science Books, Sausalito (California), **2010**.

[50]   a) T. Förster, *Ann. Phys.* **1948**, *2*, 55-75; b) T. Förster, *Z. Naturforsch. A* **1949**, *4a*, 321-327.

[51]   D. L. Dexter, *J. Chem. Phys.* **1953**, *21*, 836-850.

[52]   R. A. Marcus, *Angew. Chem. Int. Ed.* **1993**, *32*, 1111-1121.

[53]   D. Rehm, A. Weller, *Ber. Bunsenges. Phys. Chem.* **1969**, *73*, 834-839.

[54]   A. Z. Weller, *Z. Phys. Chem.* **1982**, *133*, 93-98.

[55]   J. Walz, K. Ulrich, H. Port, H. C. Wolf, J. Wonner, F. Effenberger, *Chem. Phys. Lett.* **1993**, *213*, 321-324.

[56]   a) T. B. Norsten, N. R. Branda, *J. Am. Chem. Soc.* **2001**, *123*, 1784-1785; b) M. Irie, T. Fukaminato, T. Sasaki, N. Tamai, T. Kawai, *Nature* **2002**, *420*, 759-760; c) T. Fukaminato, T. Sasaki, T. Kawai, N. Tamai, M. Irie, *J. Am. Chem. Soc.* **2004**, *126*, 14843-14849.

[57]   T. Fukaminato, M. Irie, *Adv. Mater.* **2006**, *18*, 3225-3228.

[58]   L. Ma, Q. Wang, G. Lu, R. Chen, X. Sun, *Langmuir* **2010**, *26*, 6702-6707.

[59]   J. Wang, A. Kulago, W. R. Browne, B. L. Feringa, *J. Am. Chem. Soc.* **2010**, *132*, 4191-4196.

[60]   T. B. Norsten, N. R. Branda, *Adv. Mater.* **2001**, *13*, 347-349.

[61]   a) *Supramolecular Photochemistry* (eds. Balzani, V.; Scandola, F.), Ellis Horwood, New York, **1991**; b) *Fundamentals of Photoinduced Electron Transfer* (ed. Kavarnos, G. J.), VCH Publishers Inc, New York, **1993**; c) *Electron Transfer in Chemistry* (ed. Balzani, V.), Wiley-VCH, Weinheim, **2001**; d) N. Mataga, H. Chosrowjan, S. Taniguchi, *J. Photochem. Photobiol., C* **2005**, *6*, 37-79.

[62]   S. Tsuchiya, *J. Am. Chem. Soc.* **1999**, *121*, 48-53.

[63]   D. R. Reddy, B. G. Maiya, *Chem. Commun.* **2001**, 117-118.

[64]   J. Otsuki, A. Suka, K. Yamazaki, H. Abe, Y. Araki, O. Ito, *Chem. Commun.* **2004**, 1290-1291.

[65]   a) J. M. Endtner, F. Effenberger, A. Hartschuh, H. Port, *J. Am. Chem. Soc.* **2000**, *122*, 3037-3046; b) A. Hartschuh, I. B. Ramsteiner, H. Port, J. M. Endtner, F. Effenberger, *J. Lumin.* **2004**, *108*, 1-10.

[66]   A. J. Myles, N. R. Branda, *J. Am. Chem. Soc.* **2001**, *123*, 177-178.

[67]   Y. Terazono, G. Kodis, J. Andréasson, G. Jeong, A. Brune, T. Hartmann, H. Dürr, A. L. Moore, T. A. Moore, D. Gust, *J. Phys. Chem. B* **2004**, *108*, 1812-1814.

[68]   a) M. Berberich, Diploma Thesis, University of Würzburg, Würzburg (Germany), **2007**; b) M. Berberich, A.-M. Krause, M. Orlandi, F. Scandola, F. Würthner, *Angew. Chem. Int. Ed.* **2008**, *47*, 6616-6619.

[69]   Y. Odo, T. Fukaminato, M. Irie, *Chem. Lett.* **2007**, *36*, 240-241.

[70]   M. Berberich, F. Würthner, *Chem. Sci.* **2012**, *3*, 2771-2777.

[71]   a) T. Fukaminato, T. Doi, M. Tanaka, M. Irie, *J. Phys. Chem. C* **2009**, *113*, 11623-11627; b) T. Fukaminato, M. Tanaka, T. Doi, N. Tamaoki, T. Katayama, A. Mallick, Y. Ishibashi, H. Miyasaka, M. Irie, *Photochem. Photobiol. Sci.* **2010**, *9*, 181-187; c) T. Fukaminato, T. Doi, N. Tamaoki, K. Okuno, Y. Ishibashi, H. Miyasaka, M. Irie, *J. Am. Chem. Soc.* **2011**, *133*, 4984-4990.

[72]   F. Würthner, *Chem. Commun.* **2004**, 1564-1579.

[73]   R. S. Sánchez, R. Gras-Charles, J. L. Bourdelande, G. Guirado, J. Hernando, *J. Phys. Chem. C* **2012**, *116*, 7164-7172.

[74]   M. Berberich, M. Natali, P. Spenst, C. Chiorboli, F. Scandola, F. Würthner, *Chem. Eur. J.* **2012**, *18*, doi:10.1002/chem.201201484.

3   Energy-Level Tuning of Photochromic Switches

3.1   Variation of Electron-Acceptor Substituents

DAEs are appropriate units to regulate the electronic properties of a molecular system by the means of light. For the application in an electron-transfer system according to the above mentioned strategy (see Chapter 2.6), spectroscopic and electronic data of electron-poor DAE acceptor units are needed. Only a few publications by the groups of Feringa and Launay gave an overview on the effect of different substituents on the redox potentials of DAEs.[1] The spectroscopic and electronic properties of the switching unit have to comply exactly with those of the respective emitter units. Promising fluorophores are tetraaryloxy-substituted PBI and terrylene bisimide (TBI) dyes due to their outstanding photostability and high fluorescence quantum yields. 1,6,7,12-Tetraaryloxy-substituted PBI dyes possess an emission band between 550 and 750 nm and a first oxidation potential of about 0.78 V.[2] The respective 1,6,9,14-tetraaryloxy-substituted TBIs emit between 650 and 850 nm and have a first oxidation potential of 0.50 V.[3] Therefore, the requirements for an optimal DAE unit are an absorption band of the closed form, which is not overlapping with the emission band of the fluorophore, and in addition, is at shorter wavelengths. Furthermore, the first reduction potential of the closed form should have a value between –0.8 and –1.2 V, which means of course that a less negative value, *i.e.* easier to reduce, increases the driving force for the closed form, but also enables fluorescence quenching for the open form. This is because the respective first reduction value of the open form of the DAE is only around 0.3 to 0.6 V[1a] more negative than the closed form and the difference of both isomers in the Gibbs free energy, which could be calculated by the Rehm-Weller equation,[4] is not as high, *i.e.* approximately 0.3 to 0.5 eV. Due to the lack of published data on reduction and oxidation potentials of ring-open and ring-closed DAEs, and in particular electron-poor DAEs, references **1o** to **7o** and their respective closed forms **1c** to **7c** were synthesized and characterized (Figure 1).
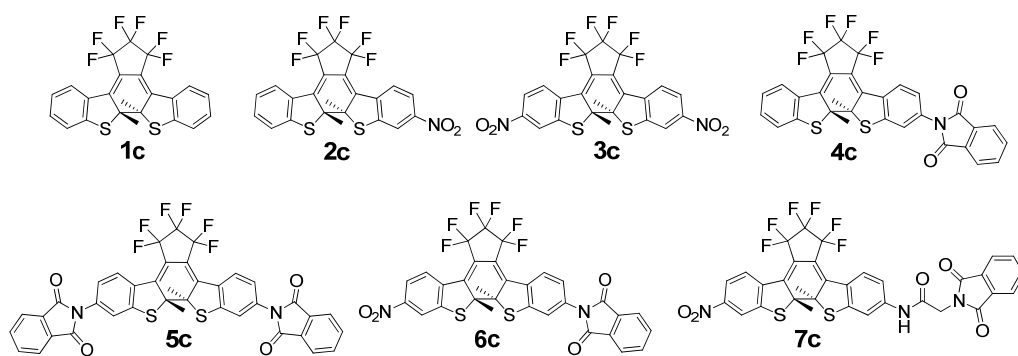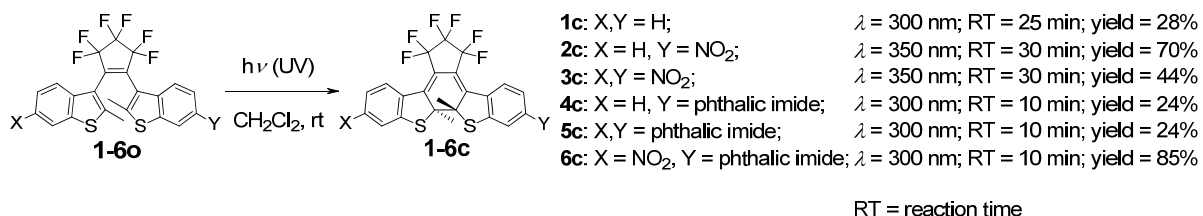

Figure 1. Literature known DAEs **1c**,[5] **2c**,[6] **3c**[7] and new DAEs **4c**,[8] **5c**, **6c**, and **7c**.

The increase of electron-acceptor capability should not be accompanied by a distinct bathochromic shift of the absorption band of the closed form of the DAE. Such a shift reduces the number of suitable fluorophores, which must have an emission band even more bathochromic then the closed form absorption band.

3.2   Synthesis

Although several diarylethenes are literature known, their closed forms were generally not separated and characterized. Therefore, the synthesis of several new reference DAEs and their closed forms are described. DAE **1o**, **2o**, and **3o** were synthesized according to literature procedures.[5-7] The synthesis and characterization of DAE **4o** and **5o** with phthalic imide groups was described in the preceding work[8-9] to this PhD thesis. The novel DAE **6o** with nitro and phthalic imide group will be described in detail in Chapter 4 of this PhD thesis.

The respective closed forms of reference DAEs **1c** to **6c** were isolated by irradiation of dichloromethane solutions of the open forms with UV light (300 or 350 nm) followed by column chromatography under exclusion of light (Scheme 1). The wide discrepancy of the yields (24% for **4c** and **5c** and 85% for **6c**) is not related to differing cyclization quantum yields, but rather for different reaction conditions such as the concentration and irradiation wavelength.

1c: X,Y = H; λ = 300 nm; RT = 25 min; yield = 28%
2c: X = H, Y = NO$_2$; λ = 350 nm; RT = 30 min; yield = 70%
3c: X,Y = NO$_2$; λ = 350 nm; RT = 30 min; yield = 44%
4c: X = H, Y = phthalic imide; λ = 300 nm; RT = 10 min; yield = 24%
5c: X,Y = phthalic imide; λ = 300 nm; RT = 10 min; yield = 24%
6c: X = NO$_2$, Y = phthalic imide; λ = 300 nm; RT = 10 min; yield = 85%

RT = reaction time

Scheme 1. Photochemical synthesis of closed form reference DAEs.

Based on the amino-nitro-substituted diarylethene **8** (see Chapter 4 for synthesis and characterization), a new reference compound **7o/7c** with an additional glycine linker between photochrome and phthalic imide residue was synthesized (see Scheme 2) to minimize possible unfavorable interactions between the DAE unit and the phthalic imide, which acts in this case as placeholder for the respective emitter unit. The procedure started with an amide coupling between the amino group of **8** and the carboxylic acid function of glycine with a BOC-protected amine. The protection group was cleaved with trifluoroacetic acid before subsequent condensation reaction of the deprotected DAE precursor **10** and phthalic anhydride. The closed form of reference DAE **7c** was obtained by irradiation of a solution of the open form **7o** with UV light (300 nm).
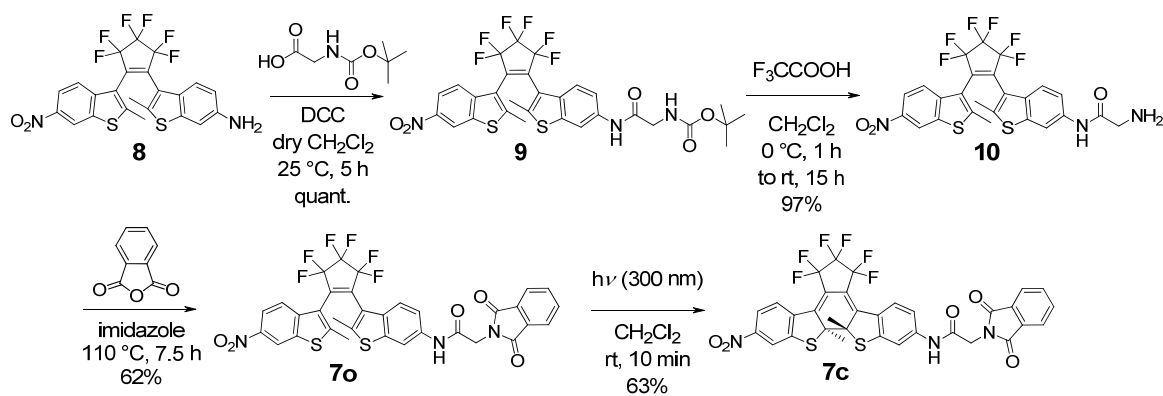
Scheme 2. Synthetic route to reference DAE **7o**/**7c** with glycine linker; DCC = *N*,*N'*-dicyclohexylcarbodiimide.
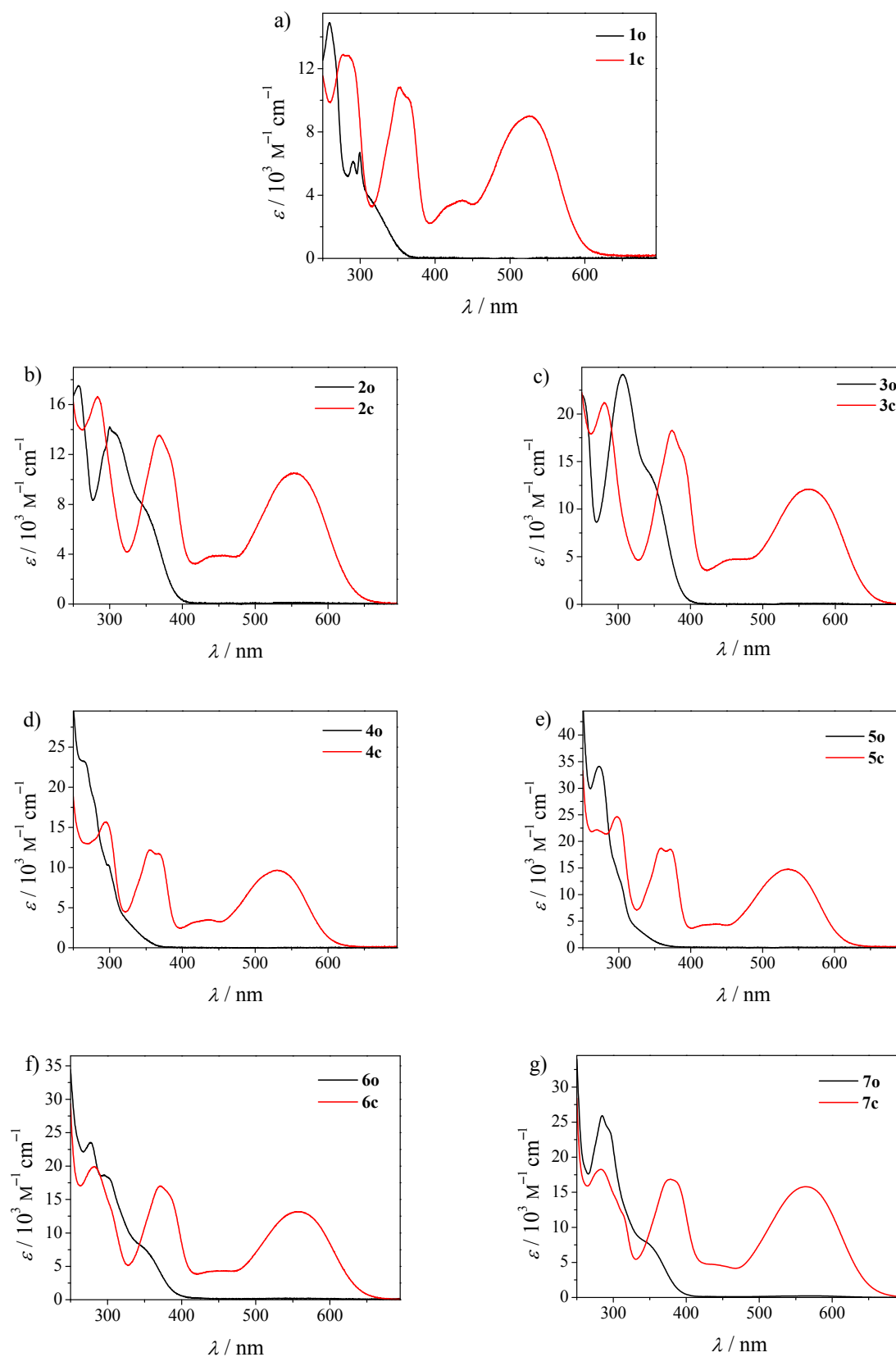
3.3 Absorption Data

It is particularly important that the absorption band of the closed form of the DAE does not overlap with the emission band of the fluorophore. The comparison of the absorption spectra of the closed forms **1c** to **7c** (Figure 2) revealed that the band in the visible range shifted more bathochromically with increasing number of nitro or imide electron-withdrawing groups attached to the benzo[*b*]thiophene of the DAE.
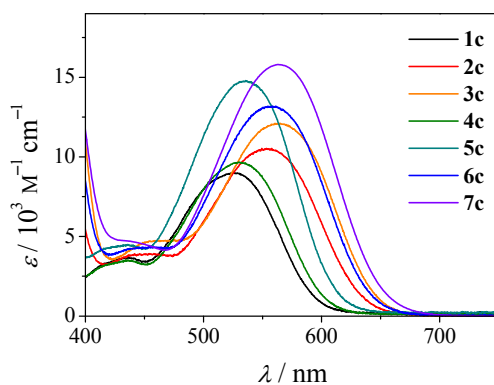
Figure 2. Section of UV/vis absorption spectra (range from 400 to 750 nm) of the closed form of reference DAEs **1c** to **7c** in dichloromethane (1×10^{-5} M) at 25 °C.

The wavelength maxima of DAE compounds **1c**–**7c** lie in a range of 38 nm between 525 nm (**1c**) and 563 nm (**3c**). The extinction at the maxima increases with the number of attached electron-withdrawing groups from 9000 $\text{M}^{-1}\,\text{cm}^{-1}$ for the unsubstituted **1c** to 15800 $\text{M}^{-1}\,\text{cm}^{-1}$ for **7c**. The absorption spectra of DAE **1o** to **7o** and their respective closed form **1c** to **7c** are depicted in Figure 3.

57

Figure 3. UV/vis absorption spectra of the open (black line) and closed form (red line) of reference DAEs (a) **1**, (b) **2**, (c) **3**, (d) **4**, (e) **5**, (f) **6**, and (g) **7** in dichloromethane (1×10^{-5} M) at 25 °C.

The complete absorption data of the DAEs **1o**/**1c** to **7o**/**7c** are listed in Table 1. None of these compounds showed fluorescence behavior.

Table 1. Optical properties of reference DAEs **1** to **7** in dichloromethane (1×10^{-5} M) at 25 °C.

	λ_{abs} [nm] (ε_{max} [M^{-1} cm^{-1}])
1o	259 (14900), 291 (6100), 300 (6700)
1c	278 (12900), 354 (10800), 437 (3700), 525 (9000)
2o	257 (17500), 300 (14200)
2c	283 (16700), 369 (13500), 553 (10500)
3o	307 (24200)
3c	281 (21200), 375 (18300), 563 (12100)
4o	265 (23300), 298 (10300)
4c	295 (15700), 355 (12200), 367 (11800), 530 (9700)
5o	273 (34100)
5c	297 (24600), 358 (18700), 372 (18500), 536 (14800)
6o	278 (23500), 295 (18700)
6c	282 (17100), 372 (14600), 558 (11300)
7o	285 (25900)
7c	283 (18300), 378 (16800), 563 (15800)

3.4   Cyclic Voltammetry

Cyclic voltammetric studies were performed of all DAEs **1o** to **7o** and their respective closed forms **1c** to **7c** in dichloromethane to obtain oxidation, and for the application as electron acceptor even more important, reduction potentials (Figure 4 for **1c**, **2o**/**2c** and **3o**/**3c** and Figure 5 for **4o**/**4c** to **7o**/**7c**). The open form of the unsubstituted diarylethene **1o** showed no half-wave within the voltage-range limited by the solvent.
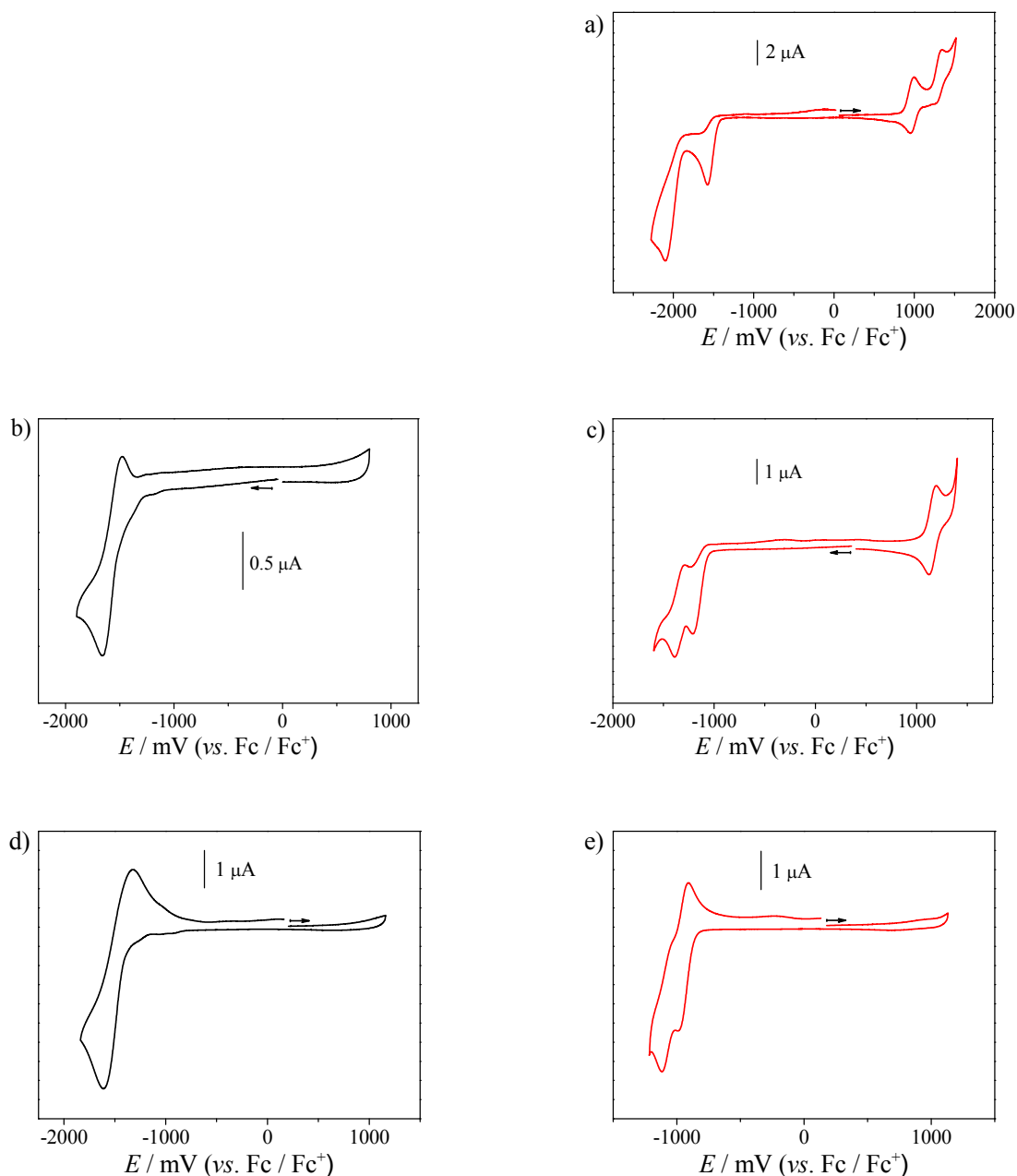
Figure 4. Cyclic voltammograms of open (black) and respective closed (red) form of DAE (a) **1c** (2.8×10^{-4} M), (b) **2o** (2.4×10^{-4} M), (c) **2c** (2.4×10^{-4} M), (d) **3o** (4.4×10^{-4} M), and (e) **3c** (3.5×10^{-4} M) in dichloromethane (supporting electrolyte TBAHFP (0.1 M), scan rate 100 mV s^{-1}). No potentials could be determined for the open form of reference DAE **1o** within the voltage-range limited by the solvent.
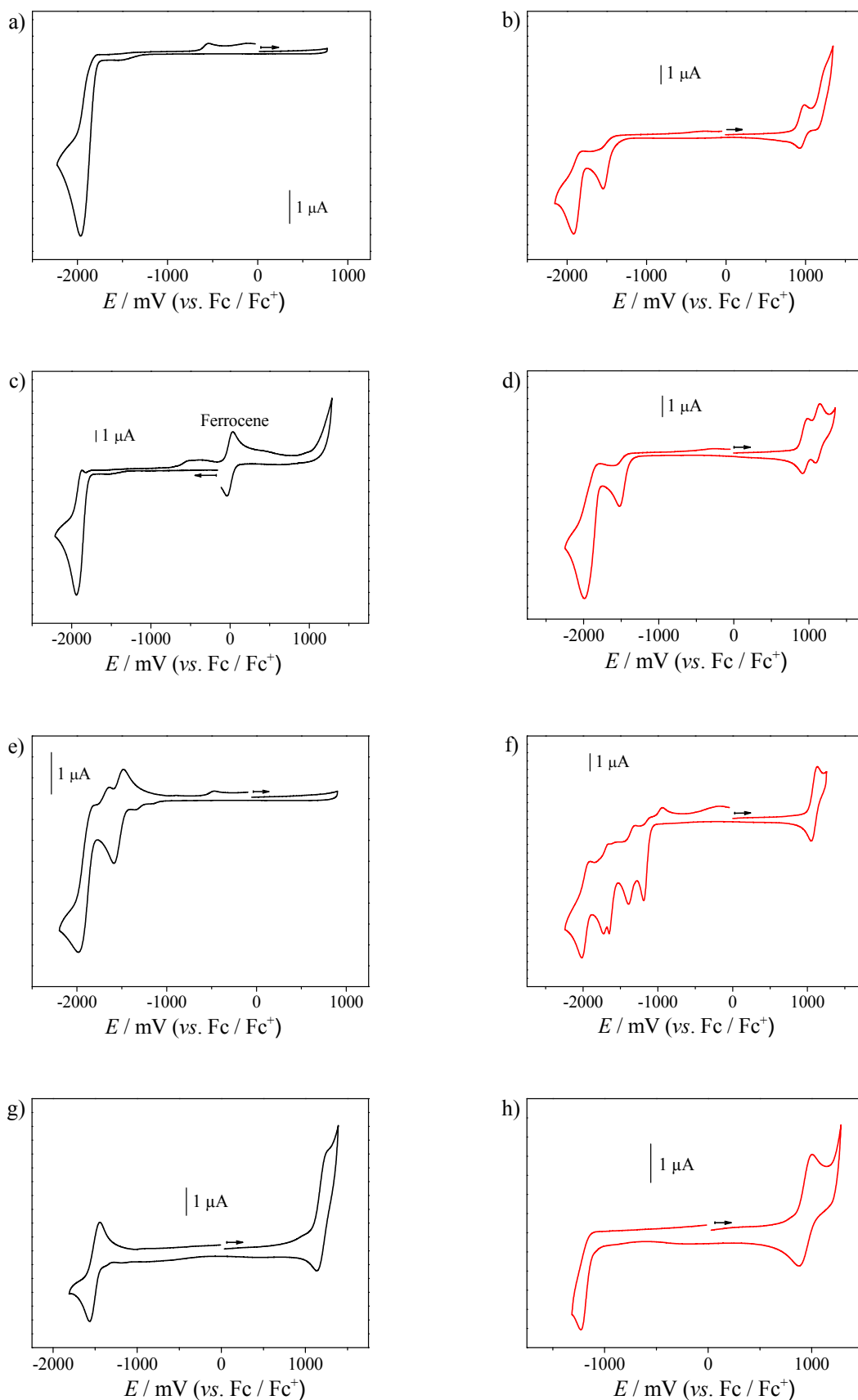
Figure 5. Cyclic voltammograms of DAE_O (black) and DAE_C (red) (a) **4o** (2.2×10^{-4} M), (b) **4c** (1.8×10^{-4} M), (c) **5o** (3.0×10^{-4} M), (d) **5c** (3.0×10^{-4} M), (e) **6o** (2.6×10^{-4} M), (f) **6c** (2.5×10^{-4} M), (g) **7o** (2.5×10^{-4} M), and (h) **7c** (2.6×10^{-4} M) in dichloromethane (supporting electrolyte TBAHFP (0.1 M), scan rate 100 mV s^{-1}).

Most of the reduction values were obtained only as irreversible peak potentials while the oxidation waves are consistently reversible. The largest difference between first reduction potential of open and closed form of the same DAE can be obtained for dinitro-substituted diarylethene **3o/3c** (0.55 V) Furthermore, this compound **3o/3c** is the most easily reduced. The addition of two nitro groups changes the first reduction potential of the electron acceptor unit, thus the closed form of the DAE, from −1.61 V for **1c** to −0.96 V for **3c**. The complete reduction and oxidation potentials are listed in Table 2.

Table 2. Half-wave potentials[a] of DAEs **1o/1c** to **7o/7c**.

	$E_{1/2}^{red}$ (V) (X^{3-}/X^{2-})	$E_{1/2}^{red}$ (V) (X^{2-}/X^{-})	$E_{1/2}^{red}$ (V) (X^{-}/X)	$E_{1/2}^{ox}$ (V) (X/X^{+})	$E_{1/2}^{ox}$ (V) (X^{+}/X^{2+})
1o	–	–	–	–	–
1c	–	−2.11[b]	−1.61[b]	0.95	1.34
2o	–	–	−1.56	–	–
2c	−1.66[b]	−1.40[b]	−1.21[b]	1.13	–
3o	–	–	−1.51	–	–
3c	–	−1.07	−0.96	–	–
4o	–	–	−1.96[b]	–	–
4c	–	−1.90[b]	−1.54[b]	0.95	–
5o	–	–	−1.94[b]	–	–
5c	–	−1.90[b]	−1.52	0.95	1.11
6o	–	−1.96[b]	−1.53	–	–
6c	−1.69[b]	−1.39[b]	−1.19[b]	1.34	–
7o	–	−1.90[b]	−1.51	1.27	–
7c	–	−1.41[b]	−1.20[b]	0.94	–

[a] All measurements were carried out in dry dichloromethane (10^{-4} M) using Fc/Fc$^+$ as internal standard and TBAHFP (0.1 M) as supporting electrolyte at a scan rate of 100 mV s^{-1}. [b] Peak potential of irreversible reduction.

3.5 Conclusions

In summary, electron withdrawing groups at the electron-accepting diarylethene core decrease the respective reduction potentials and therefore, increase the driving force for the electron transfer. The bathochromic shift of the absorption constrains the use of several emitters, due to the fact that the emission of the dye should not overlap with the absorption band of the closed form of the diarylethene. Therefore, only fluorescence dyes with an emissive band at wavelengths longer than 650 nm, *e.g.* tetraaryloxy-substituted terrylene bisimides, seem appropriate for the reference diarylethene with nitro and imide substituent like **6o/6c**.

3.6   Experimental Section

3.6.1   Materials and Methods

General: All solvents and reagents were purchased from commercial sources and used as received without further purification, unless otherwise stated. Column chromatography was performed using silica gel 60M (0.04–0.063 mm) from Macherey-Nagel. Melting points were determined on an Olympus BX41 polarization microscope and a Linkam TP 94 heating stage and are uncorrected. High resolution mass spectra (ESI) were recorded on an ESI micrOTOF Focus spectrometer from Bruker Daltonics. The APCI mass spectra were performed with micrOTOF Focus mass spectrometer (Bruker Daltonics, Bremen), equipped with an APCI ion source (Agilent G1947-60101). MALDI-TOF mass spectra were recorded on an Autoflex II spectrometer from Bruker Daltonics. The UV irradiation experiments were performed in a Rayonet Photoreactor RPR-100 (Southern New England Ultraviolet Company) with 16 UV lamps (24 W lamps with λ_{max} = 350 nm or 21 W lamps with λ_{max} = 300 nm).

NMR spectroscopy: ^{1}H and ^{13}C NMR spectra were recorded on Bruker Advance 400 or Bruker Advance DMX 600 spectrometer and calibrated to the residual solvent peak (CD$_2$Cl$_2$: 5.32 ppm for ^{1}H). The signals in ^{1}H NMR spectra for the respective open forms for parallel and *anti*-parallel isomers of photochromic DAE unit (Scheme 3) are indicated by "p" and "ap", respectively, and signal integrals of isomeric protons are normalized.
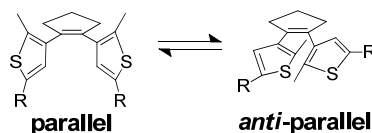
Scheme 3. Structures of parallel and *anti*-parallel isomers of photochromic DAE unit.

UV/vis absorption and fluorescence spectroscopy: For all spectroscopic measurements, spectroscopic grade solvents (Uvasol$^®$) from Merck (Hohenbrunn, Germany) were used. UV/vis spectra were recorded on a Perkin Elmer UV/vis spectrometer Lambda 35 in combination with a Perkin Elmer PTP–1+1 peltier system and a Lauda ecoline RE306/E300 refrigeration circulator.

Cyclic voltammetry: Cyclic voltammetry measurements were performed on a standard, commercial electrochemical analyzer (EC epsilon; BAS Instruments, UK) in a three electrode single-compartment cell under argon atmosphere. Dichloromethane (HPLC grade) was dried over calcium hydride under argon and degassed prior to use. The supporting electrolyte tetrabutylammonium hexafluorophosphate (TBAHFP) was synthesized according to literature,[10] recrystallized from ethanol/water and dried in high vacuum. The measurements were carried out under exclusion of air and moisture at a concentration of about 10^{-4} M with ferrocene as an internal standard for the calibration of the potential. Working electrode: Pt disc; reference electrode: Ag/AgCl; auxiliary electrode: Pt wire.

3.6.2　Synthesis and Characterization

1,2-Bis-(2-methylbenzo[b]thiophene-3-yl)-perfluorocyclopentene (1o)[5]

This DAE was synthesized according to the previously reported procedure in a yield of 71% (lit.: 75%).[5] Mp: 154–156 °C (from n-hexane; lit.: unknown).
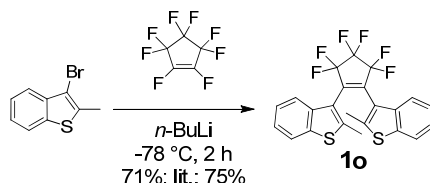
$C_{23}H_{14}F_6S_2$ (468.485)

^{1}H NMR (400 MHz, CDCl$_3$, TMS, 300 K): δ 7.62–7.72 (m, 2.6H), 7.53–7.62 (m, 1.4H), 7.26–7.39 (m, 2.6H), 7.14–7.20 (m, 1.4H), 2.49 (s, 2.1H), 2.21 (s, 3.9H).
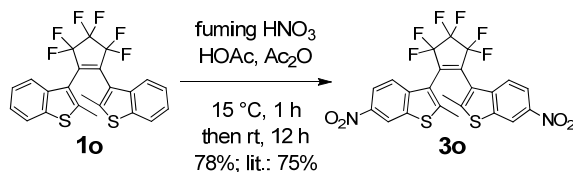
MS (MALDI, pos. mode, matrix DCTB 1:3 in CHCl$_3$): m/z: calcd for $C_{23}H_{14}F_6S_2$ 468.044: [M]$^+$; found: 468.007.

UV/vis (CH$_2$Cl$_2$): λ_{max}/nm (ε_{max}/M^{-1} cm^{-1}) = 259 (14900), 291 (6100), 300 (6700).

CV No values within the voltage-range limited by the solvent.

1-[2-Methyl-6-nitro-1-benzo[b]thiophen-3-yl)-2-(2'-methyl-1'-benzo[b]thiophen-3'-yl)-perfluoro-cyclopentene (2o)[8]

This DAE was synthesized according to the previously reported procedure.[8]
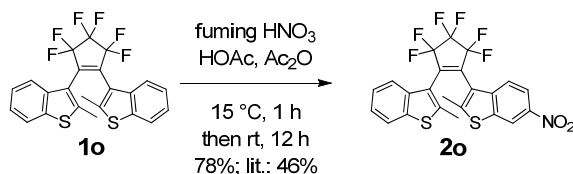
$C_{23}H_{13}F_6NO_2S_2$ (513.48)

UV/vis (CH$_2$Cl$_2$): λ_{max}/nm (ε_{max}/M^{-1} cm^{-1}) = 258 (17500), 300 (14200).

CV (CH$_2$Cl$_2$, 0.1 M TBAHFP, vs. Fc/Fc$^+$, scan rate 100 mV/s): $E_{1/2}^{red}$ (X/X$^-$) = −1.56 V.

1,2-Bis-(2-methyl-6-nitro-1-benzo[b]thiophene-3-yl)-perfluorocyclopentene (3o)[6]

This DAE was synthesized according to the previously reported procedure in a yield of 78% (lit.: 75%).[6] Mp: 216–218 °C (from n-hexane; lit.: 200–201 °C).[7]

$C_{23}H_{12}F_6N_2O_4S_2$ (558.480)

^{1}H NMR (400 MHz, CDCl$_3$, TMS, 300 K): δ 8.66 (d, ^4J(H,H) = 2.2 Hz, 1.3H), 8.57 (d, ^4J(H,H) = 1.6 Hz, 0.7H), 8.26 (dd, ^3J(H,H) = 8.9 Hz, ^4J(H,H) = 2.0 Hz, 1.3H), 8.09 (dd,

^3J(H,H) = 9.0 Hz, ^4J(H,H) = 1.8 Hz,   0.7H),   7.72   (d, ^3J(H,H) = 8.8 Hz,   1.3H),   7.60   (d, ^3J(H,H) = 8.8 Hz, 0.7H), 2.58 (s, 2.2H), 2.32 (s, 3.8H).

MS (MALDI, pos. mode, matrix DCTB 1:3 in CHCl$_3$): *m/z*: calcd for C$_{23}$H$_{12}$F$_6$N$_2$O$_4$S$_2$: 558.014 [M]$^+$, found: 558.044.

UV/vis (CH$_2$Cl$_2$): λ_{max}/nm (ε_{max}/M^{-1} cm^{-1}) = 307 (24200).

CV (CH$_2$Cl$_2$, 0.1 M TBAHFP, *vs.* Fc/Fc$^+$, scan rate 100 mV/s): $E_{1/2}^{red}$ (X/X$^-$) = −1.51 V.

Reference DAE 4o[8]

Synthetic details and characterization data for this reference DAE **4o** was previously reported.[8]
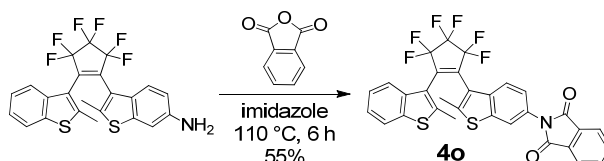
C$_{31}$H$_{17}$F$_6$NO$_2$S$_2$ (613.593)

UV/vis (CH$_2$Cl$_2$): λ_{max}/nm (ε_{max}/M^{-1} cm^{-1}) = 265 (23300), 298 (10300).

CV (CH$_2$Cl$_2$, 0.1 M TBAHFP, *vs.* Fc/Fc$^+$, scan rate 100 mV/s): E_{pp}^{red} (X/X$^-$) = −1.56 V.

Reference DAE 5o

This reference DAE **5o** was synthesized according to the procedure described for the synthesis of another reference DAE.[8] A mixture of 1,2-bis-(6-amino-2-methyl-1-benzo[*b*]thiophen-3-yl)-perfluorocyclopentene **11** (15.5 mg, 31.0 μmol), phthalic anhydride (36.8 mg, 248 μmol), and imidazole (500 mg) was heated to 105 °C under nitrogen atmosphere for 6 h. Ethanol (5 mL) was carefully poured in the hot solution. The reaction mixture was cooled to room temperature, and 20 mL dichloromethane and 10 mL 2 N HCl were added. The solution was extracted with dichloromethane (3 × 20 mL), dried over Na$_2$SO$_4$, and concentrated by rotary evaporation. The residue was purified by column chromatography on silica gel (dichloromethane), and dried at 10^{-3} mbar to yield 21.9 mg (28.8 μmol, 93%) of **5o** as a white solid. Mp: 346–348 °C (from dichloromethane).
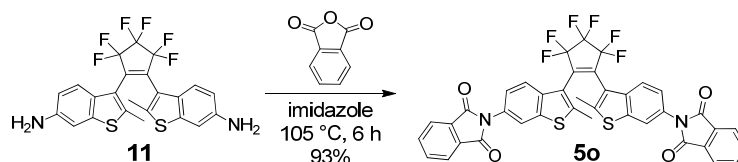
C$_{39}$H$_{20}$F$_6$N$_2$O$_4$S$_2$ (758.708)

^{1}H NMR (400 MHz, CD$_2$Cl$_2$, 300 K): δ 7.94–8.00 (m, 2.6H), 7.89–7.93 (m, 1.4H), 7.76–7.87 (m, 7.3H), 7.69 (d, ^3J(H,H) = 8.9 Hz, 0.7H), 7.50 (dd, ^3J(H,H) = 8.7 Hz, ^4J(H,H) = 1.9 Hz, 1.3H), 7.36 (dd, ^3J(H,H) = 8.6 Hz, ^4J(H,H) = 1.5 Hz, 0.7H), 2.57 (s, 2H), 2.31 (s, 4H).

HRMS (APCI, pos. mode, CHCl$_3$): *m/z*: calcd for C$_{39}$H$_{21}$F$_6$N$_2$O$_4$S$_2$: 759.0846 [M+H]$^+$; found: 759.0831.

UV/vis (CH$_2$Cl$_2$): λ_{max}/nm (ε/M^{-1} cm^{-1}) = 272 (34100).
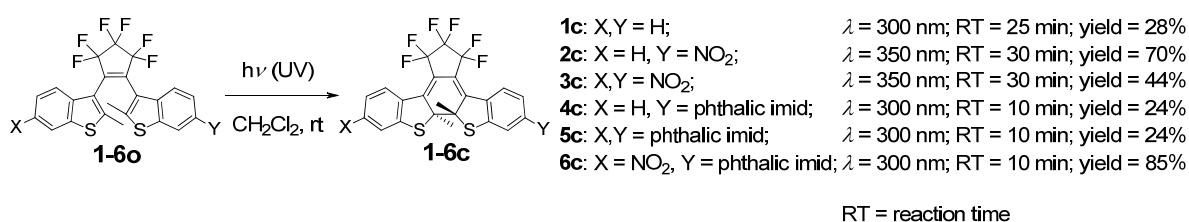
CV (CH$_2$Cl$_2$, 0.1 M TBAHFP, *vs.* Fc/Fc$^+$, scan rate 100 mV/s): E_{pp}^{red} (X/X$^-$) = −1.94 V.

Reference DAE 6o

The synthesis and characterization of reference DAE **6o** will be described in Chapter 4.7.2.

General procedure for light-induced ring closure of reference DAEs 1c–6c

These DAEs were irradiated according to the procedure previously reported for a reference DAE.[8] A solution of DAE (**1o-6o**) in dichloromethane was irradiated in a Rayonet photoreactor with UV light for a certain time under vigorous stirring. The solution was concentrated by rotary evaporation in the dark, and the precipitate was purified in the dark by column chromatography on silica gel and dried at 10^{-3} mbar to yield dark red solids.

1c: X,Y = H; λ = 300 nm; RT = 25 min; yield = 28%
2c: X = H, Y = NO$_2$; λ = 350 nm; RT = 30 min; yield = 70%
3c: X,Y = NO$_2$; λ = 350 nm; RT = 30 min; yield = 44%
4c: X = H, Y = phthalic imid; λ = 300 nm; RT = 10 min; yield = 24%
5c: X,Y = phthalic imid; λ = 300 nm; RT = 10 min; yield = 24%
6c: X = NO$_2$, Y = phthalic imid; λ = 300 nm; RT = 10 min; yield = 85%

RT = reaction time

Details for compounds 1c-6c

Closed form of 1,2-bis-(2-methylbenzo[*b*]thiophene-3-yl)-perfluorocyclopentene (1c)

A solution of **1o** (110 mg, 235 μmol) in 200 mL dichloromethane was irradiated with UV light (300 nm) for 25 minutes. The isomers were separated in the dark by column chromatography on silica gel (*n*-hexane) to yield 30.5 mg (65.1 μmol; 28%) of **1c**.

^{1}H NMR (600 MHz, CDCl$_3$, TMS, 300 K): δ 7.91 (d, ^3J(H,H) = 8.2 Hz, 2H), 7.29–7.33 (m, 2H), 7.25–7.28 (m, 2H), 7.14–7.18 (m, 2H), 2.02 (s, 6H).

HRMS (APCI, pos. mode, CHCl$_3$): *m/z*: calcd for C$_{23}$H$_{14}$F$_6$S$_2$: 468.0441 [M]$^+$; found: 468.0426.

UV/vis (CH$_2$Cl$_2$): λ_{max}/nm (ε_{max}/M^{-1} cm^{-1}) = 278 (12900), 354 (10800), 437 (3700), 526 (9000).

CV (CH$_2$Cl$_2$, 0.1 M TBAHFP, *vs.* Fc/Fc$^+$, scan rate 100 mV/s): E_{pp}^{red} (X$^-$/X^{2-}) = −2.11 V, E_{pp}^{red} (X/X$^-$) = −1.61 V, $E_{1/2}^{ox}$ (X$^+$/X) = 0.95 V, $E_{1/2}^{ox}$ (X^{2+}/X$^+$) = 1.34 V.

Closed form of 1-[2-methyl-6-nitro-1-benzo[*b*]thiophen-3-yl)-2-(2'-methyl-1'-benzo[*b*]thiophen-3'-yl)-perfluorocyclopentene (2c)

A solution of **2o** (120 mg, 234 μmol) in 500 mL dichloromethane was irradiated with UV light (350 nm) for 30 minutes. The isomers were separated in the dark by column chromatography on silica gel (dichloromethane/*n*-hexane 1:1 (v/v)) to yield 84.0 mg (164 μmol; 70%) of **2c**.

^{1}H NMR (600 MHz, CDCl$_3$, TMS, 300 K): δ 8.08 (d, ^4J(H,H) = 2.0 Hz, 1H), 7.93–8.01 (m, 3H), 7.34–7.39 (m, 1H), 7.29 (d, ^3J(H,H) = 7.9 Hz, 1H), 7.17–7.22 (m, 1H), 2.05 (s, 3H), 2.04 (s, 3H).

HRMS (APCI, neg. mode, acetonitrile): *m/z*: calcd for C$_{23}$H$_{12}$F$_6$NO$_2$S$_2$: 512.0213 [M–H]$^-$; found: 512.0220.

UV/vis (CH$_2$Cl$_2$): λ_{max}/nm (ε_{max}/M^{-1} cm^{-1}) = 283 (16700), 369 (13500), 553 (10500)

CV (CH_2Cl_2, 0.1 M TBAHFP, *vs.* Fc/Fc^+, scan rate 100 mV/s): E_{pp}^{red} (X^{2-}/X^{3-}) = -1.66 V, E_{pp}^{red} (X^-/X^{2-}) = -1.40 V, E_{pp}^{red} (X/X^-) = -1.21 V, $E_{1/2}^{ox}$ (X^+/X) = 1.13 V.

Closed form of 1,2-bis-(2-methyl-6-nitro-1-benzo[*b*]thiophene-3-yl)-perfluorocyclopentene (3c)

A solution of **3o** (415 mg, 743 μmol) in 600 mL dichloromethane was irradiated with UV light (350 nm) for 30 minutes. The isomers were separated in the dark by column chromatography on silica gel (dichloromethane/*n*-hexane 1:1 (v/v)) to yield 184 mg (329 μmol; 44%) of **3c**.

^{1}H NMR (600 MHz, $CDCl_3$, TMS, 300 K): δ 8.11 (d, $^4J(H,H)$ = 2.0 Hz, 2H), 8.05 (d, $^3J(H,H)$ = 9.0 Hz, 2H), 8.00 (dd, $^3J(H,H)$ = 8.8 Hz, $^4J(H,H)$ = 2.0 Hz, 2H), 2.08 (s, 6H).

HRMS (APCI, pos. mode, $CHCl_3$): *m*/*z*: calcd for $C_{23}H_{11}F_6N_2O_4S_2$: 557.0063 [M–H]$^-$; found: 557.0066.

UV/vis (CH_2Cl_2): λ_{max}/nm (ε_{max}/M^{-1} cm^{-1}) = 281 (21200), 375 (18300), 563 (12100).

CV (CH_2Cl_2, 0.1 M TBAHFP, *vs.* Fc/Fc^+, scan rate 100 mV/s): $E_{1/2}^{red}$ (X^-/X^{2-}) = -1.07 V, $E_{1/2}^{red}$ (X/X^-) = -0.96 V.

Closed form of reference DAE 4c[8]

Synthetic details and characterization data for this reference DAE **4c** was previously reported.[8]

UV/vis (CH_2Cl_2): λ_{max}/nm (ε_{max}/M^{-1} cm^{-1}) = 295 (15700), 355 (12200), 367 (11800), 530 (9700).

CV (CH_2Cl_2, 0.1 M TBAHFP, *vs.* Fc/Fc^+, scan rate 100 mV/s): E_{pp}^{red} (X^-/X^{2-}) = -1.90 V, $E_{1/2}^{red}$ (X/X^-) = -1.52 V, $E_{1/2}^{ox}$ (X^+/X) = 0.95 V, $E_{1/2}^{ox}$ (X^{2+}/X^+) = 1.11 V.

Closed form of reference DAE 5c

A solution of **5o** (117 mg, 154 μmol) in 200 mL dichloromethane was irradiated with UV light (300 nm) for 30 minutes. The isomers were separated in the dark by column chromatography on silica gel (dichloromethane/*n*-hexane 2:1 (v/v)) to yield 27.4 mg (36.1 μmol; 24%) of **5c**.

^{1}H NMR (600 MHz, $CDCl_3$, TMS): δ 8.03 (d, $^3J(H,H)$ = 8.6 Hz, 2H), 7.95–7.99 (m, 4H), 7.83–7.87 (m, 4H), 7.47 (d, $^4J(H,H)$ = 2.0 Hz, 2H), 7.34 (dd, $^3J(H,H)$ = 8.7 Hz, $^4J(H,H)$ = 2.0 Hz, 2H), 2.09 (s, 6H).

HRMS (APCI, pos. mode, $CHCl_3$): *m*/*z*: calcd for $C_{39}H_{21}F_6N_2O_4S_2$: 759.0847 [M+H]$^+$; found: 759.0851.

UV/vis (CH_2Cl_2): λ_{max}/nm (ε_{max}/M^{-1} cm^{-1}) = 270 (22200), 297 (24600), 358 (18700), 372 (18500), 438 (4500), 736 (14800).

CV (CH_2Cl_2, 0.1 M TBAHFP, *vs.* Fc/Fc^+, scan rate 100 mV/s): E_{pp}^{red} (X^{2-}/X^-) = -1.90 V, $E_{1/2}^{red}$ (X^-/X) = -1.52 V, $E_{1/2}^{ox}$ (X/X^+) = 0.95 V, $E_{1/2}^{ox}$ (X^+/X^{2+}) = 1.11 V.

Closed form of reference DAE 6c

The synthesis and characterization of reference DAE **6c** was described in Chapter 4.7.2.

Glycine-functionalized DAE with BOC-protecting group 9

This DAE derivative was synthesized according to the procedure previously reported for *N*-phenyl-*α*-[(*tert*-butoxycarbonyl)amino]acetamide.[11] A portion of 109 mg (206 μmol) of the amino-nitro-substituted DAE precursor **8**, 36 mg (206 μmol) BOC-protected glycine and 44 mg (212 μmol) DCC (*N,N'*-dicyclohexylcarbodiimide) were stirred in 2 mL dry dichloromethane at 25 °C for 5 h under an argon atmosphere. The suspension was cooled to 0 °C, the resulting precipitate was filtered off and washed with cold dichloromethane. The filtrate was washed with water, extracted with dichloromethane and the combined organic layers were evaporated under reduced pressure. The resulting residue was purified by column chromatography on silica gel (chloroform/ethyl acetate 9:1 (v/v)) to obtain a white solid (143 mg), which was still contaminated with some urea derivative residues.
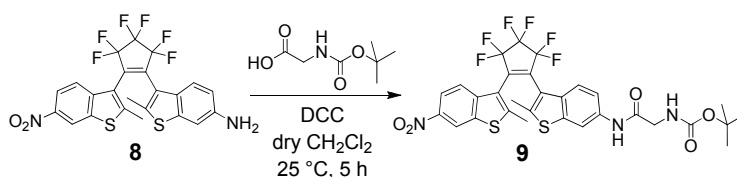

$C_{30}H_{25}F_6N_3O_5S_2$ (685.669)

^{1}H NMR (400 MHz, CD_2Cl_2, 300 K): δ 8.65 (s, 0.6H), 8.56 (s, 0.4H), 8.19–8.26 (m, 2.6H), 8.03 (d, ^3J(H,H) = 9.1 Hz, 0.4H), 7.74 (d, ^3J(H,H) = 8.9 Hz, 0.6H), 7.64 (d, ^3J(H,H) = 8.7 Hz, 0.4H), 7.56 (d, ^3J(H,H) = 7.8 Hz, 0.6H), 7.42 (d, ^3J(H,H) = 8.7 Hz, 0.4H), 7.31 (d, ^3J(H,H) = 8.8 Hz, 0.6H), 7.06 (d, ^3J(H,H) = 7.6 Hz, 0.4H), 5.22 (brs, 1H), 3.81–3.93 (m, 2H), 2.57 (s, 1.4H), 2.47 (s, 1.4H), 2.32 (s, 1.6H), 2.19 (s, 1.6H), 1.43–1.48 (m, 9H).

HRMS (ESI, pos. mode, acetonitrile/CHCl$_3$ 1:1): *m/z*: calcd for $C_{25}H_{17}F_6N_3O_3S_2$: 586.0693 [M–BOC]$^+$; found: 586.0687.

MS (MALDI, pos. mode, DCTB 1:3 in CHCl$_3$): *m/z*: calcd for $C_{30}H_{25}F_6N_3O_5S_2$ [M]$^+$ 685.114, found 685.132.

Glycine-functionalized DAE 10

This DAE precursor was synthesized according to the general procedure previously described for the synthesis of substituted 3-amino-*N*,3-diphenylpropanamide.[12] A portion of 130 mg of the impure glycine-functionalized DAE with BOC-protecting group **9** (still contaminated with urea-derivative) was solved in 1.5 mL trifluoric acid and 1.5 mL dichloromethane and stirred at 0 °C for 1 h. After warming to room temperature, the solution was stirred for further 15 h. The solution was neutralized with aqueous NaHCO$_3$ solution and extracted with dichloromethane. The combined organic layers were evaporated under reduced pressure and a white solid was isolated (92.2 mg; *ca*. 97%), which was still contaminated with some urea derivative residues.
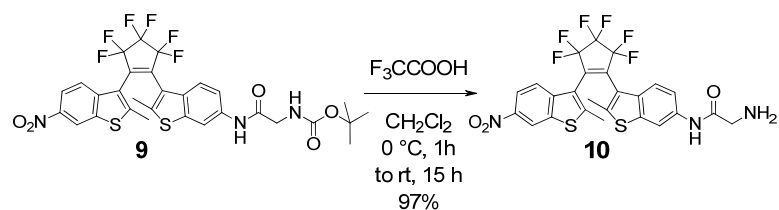
C$_{25}$H$_{17}$F$_6$N$_3$O$_3$S$_2$ (585.551)

^{1}H NMR (400 MHz, CD$_2$Cl$_2$, 300 K): δ 9.57 (s, 0.6H), 9.48 (s, 0.4H), 8.65 (s, 0.6H), 8.56 (s, 0.4H), 8.33 (s, 1H), 8.23 (dd, ^3J(H,H) = 8.9 Hz, ^4J(H,H) = 1.8 Hz, 0.6H), 8.05 (dd, ^3J(H,H) = 8.7 Hz, ^4J(H,H) = 1.5 Hz, 0.4H), 7.74 (d, ^3J(H,H) = 8.7 Hz, 0.6H), 7.65 (d, ^3J(H,H) = 8.9 Hz, 0.4H), 7.56 (d, ^3J(H,H) = 8.1 Hz, 0.6H), 7.37–7.46 (m, 1H), 7.13 (d, ^3J(H,H) = 8.7 Hz, 0.4H), 5.18 (brs, 1H), 3.45 (s, 1.2H), 3.40 (s, 0.8H), 2.57 (s, 1.4H), 2.47 (s, 1.4H), 2.32 (s, 1.6H), 2.19 (s, 1.6H).

HRMS (ESI, pos. mode, acetonitrile/CHCl$_3$ 1:1): *m/z*: calcd for C$_{25}$H$_{18}$F$_6$N$_3$O$_3$S$_2$: 586.0693 [M+H]$^+$; found: 586.0690.

MS (MALDI, pos. mode, DCTB 1:3 in CHCl$_3$): *m/z*: calcd for C$_{25}$H$_{18}$F$_6$N$_3$O$_3$S$_2$: 586.069 [M+H]$^+$; found: 586.057.

Reference DAE with glycine linker 7o

A mixture of 83.9 mg (*ca.* 143 µmol) of the slightly impure glycine-functionalized DAE **10** (still contaminated with urea-derivative), 63.7 mg (430 µmol) phthalic anhydride and 1 g imidazole were heated to 110 °C for 7.5 h under an argon atmosphere. Ethanol (5 mL) was added to the hot solution which was then cooled down to room temperature. Water was added to the solution, the mixture was extracted with dichloromethane and the combined organic layers were evaporated under reduced pressure. The resulting residue was purified by column chromatography on silica gel (dichloromethane/ethyl acetate 10:1 (v/v)) to obtain a white solid (63.7 mg; 89.0 µmol; *ca.* 62%).
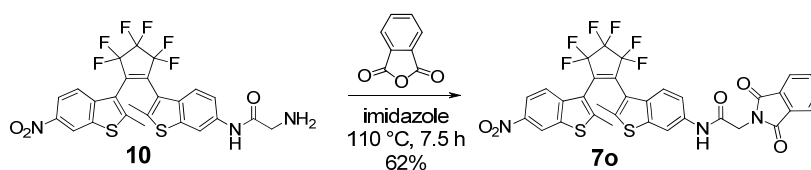
C$_{33}$H$_{19}$F$_6$N$_3$O$_5$S$_2$ (715.655)

^{1}H NMR (400 MHz, CD$_2$Cl$_2$, 300 K): δ 8.64 (s, 0.6H), 8.55 (s, 0.4H), 8.22 (d, ^3J(H,H) = 8.9 Hz, 0.6H), 8.16 (s, 1H), 8.05 (d, ^3J(H,H) = 8.7 Hz, 0.4H), 7.68–7.92 (m, 5.6H), 7.64 (d, ^3J(H,H) = 8.9 Hz, 0.4H), 7.55 (d, ^3J(H,H) = 9.1 Hz, 0.6H), 7.41 (d, ^3J(H,H) = 8.4 Hz, 0.4H), 7.32 (d, ^3J(H,H) = 8.5 Hz, 0.6H), 7.06 (d, ^3J(H,H) = 8.5 Hz, 0.4H), 4.49 (s, 1.2H), 4.44 (s, 0.8H), 2.55 (s, 1.4H), 2.46 (s, 1.4H), 2.30 (s, 1.6H), 2.19 (s, 1.6H).

HRMS (ESI, pos. mode, acetonitrile/CHCl$_3$ 1:1): *m/z*: calcd for C$_{33}$H$_{20}$F$_6$N$_3$O$_5$S$_2$: 716.0748 [M+H]$^+$; found: 716.0747.

MS (MALDI, neg. mode, DCTB 1:3 in CHCl$_3$): *m/z*: calcd for C$_{33}$H$_{19}$F$_6$N$_3$O$_5$S$_2$ 715.067 [M]$^-$; found: 715.059.

UV/vis (CH$_2$Cl$_2$): λ_{max}/nm (ε_{max}/M^{-1} cm^{-1}) = 285 (25900).

CV (CH$_2$Cl$_2$, 0.1 M TBAHFP, *vs.* Fc/Fc$^+$, scan rate 100 mV/s): E_{pp}^{red} (X$^-$/X^{2-}) = −1.90 V, $E_{1/2}^{red}$ (X/X$^-$) = −1.51 V, $E_{1/2}^{ox}$ (X/X$^+$) = 1.27 V.

Closed form of reference DAE with glycine linker 7c

This reference DAE was synthesized according to the procedure described for the synthesis of the closed form of another reference DAE.[8] A solution of 54.1 mg (75.6 µmol) **7o** in 300 mL dichloromethane was irradiated in a Rayonet photoreactor with UV light (300 nm) for 10 min under vigorous stirring. The solution was concentrated by rotary evaporation in the dark and the resultant precipitate was purified in the dark by column chromatography on silica gel (dichloromethane/*n*-hexane 7:1 (v/v)), dried at 10^{-3} mbar to yield 33.9 mg (47.4 µmol, 63%) of a dark red solid.
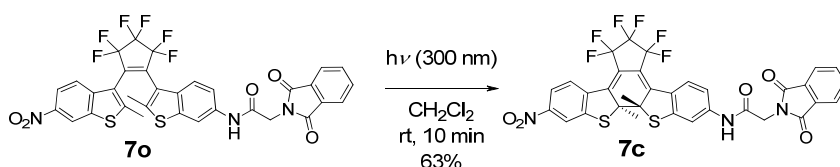
C$_{33}$H$_{19}$F$_6$N$_3$O$_5$S$_2$ (715.655)

^{1}H NMR (600 MHz, CD$_2$Cl$_2$, 300 K): δ 8.07 (d, ^4J(H,H) = 2.1 Hz, 1H), 7.97 (d, ^3J(H,H) = 9.0 Hz, 1H), 7.94 (dd, ^3J(H,H) = 8.8 Hz, ^4J(H,H) = 2.0 Hz, 1H), 7.89–7.92 (m, 2H), 7.88 (d, ^3J(H,H) = 8.7 Hz, 1H), 7.85 (brs, 1H), 7.82 (d, ^4J(H,H) = 2.0 Hz, 1H), 7.79–7.82 (m, 2H), 7.13 (dd, ^3J(H,H) = 8.9 Hz, ^4J(H,H) = 2.1 Hz, 1H), 4.50 (s, 2H), 2.03 (s, 3H), 2.02 (s, 3H).

HR-MS (ESI, pos. mode, acetonitrile/ CHCl$_3$ 1:1): *m/z*: calcd for C$_{33}$H$_{19}$F$_6$N$_3$NaO$_5$S$_2$: 738.0568 [M+Na]$^+$; found: 738.0562.

UV/vis (CH$_2$Cl$_2$): λ_{max}/nm (ε_{max}/M^{-1} cm^{-1}) = 283 (18300), 378 (16800), 563 (15800).

CV (CH$_2$Cl$_2$, 0.1 M TBAHFP, *vs.* Fc/Fc$^+$, scan rate 100 mV/s): $E_{1/2}^{red}$ (X$^-$/X^{2-}) = −1.41 V, $E_{1/2}^{red}$ (X/X$^-$) = −1.20 V, $E_{1/2}^{ox}$ (X/X$^+$) = 0.94 V.

3.7   References

[1]   a) W. R. Browne, J. J. D. de Jong, T. Kudernac, M. Walko, L. N. Lucas, K. Uchida, J. H. van Esch, B. L. Feringa, *Chem. Eur. J.* **2005**, *11*, 6430-6441; b) G. Guirado, C. Coudret, M. Hliwa, J.-P. Launay, *J. Phys. Chem. B* **2005**, *109*, 17445-17459.

[2]   M. Berberich, M. Natali, P. Spenst, C. Chiorboli, F. Scandola, F. Würthner, *Chem. Eur. J.* **2012**, *18*, doi:10.1002/chem.201201484.

[3]   M. Berberich, F. Würthner, *Chem. Sci.* **2012**, *3*, 2771-2777.

[4]   A. Z. Weller, *Z. Phys. Chem.* **1982**, *133*, 93-98.

[5]   M. Hanazawa, R. Sumiya, Y. Horikawa, M. Irie, *J. Chem. Soc., Chem. Commun.* **1992**, 206-207.

[6]   E. Kim, M. Kim, K. Kim, *Tetrahedron* **2006**, *62*, 6814-6821.

[7]   S. Kobatake, M. Yamada, T. Yamada, M. Irie, *J. Am. Chem. Soc.* **1999**, *121*, 8450-8456.

[8]   M. Berberich, A.-M. Krause, M. Orlandi, F. Scandola, F. Würthner, *Angew. Chem. Int. Ed.* **2008**, *47*, 6616-6619.

[9]   M. Berberich, Diploma Thesis, University of Würzburg, Würzburg (Germany), **2007**.

[10]   A. J. Fry, *Laboratory Techniques in Electroanalytical Chemistry* (eds. P. T. Kessing, W. R. Heinemann), 2nd ed., Marcel Dekker Ltd, New York, **1996**, p. 481.

[11]   A. Jeganathan, S. K. Richardson, R. S. Mani, B. E. Haley, D. S. Watt, *J. Org. Chem.* **1986**, *51*, 5362-5367.

[12]   V. Kumar, M. Jaggi, A. T. Singh, A. Madaan, V. Sanna, P. Singh, P. K. Sharma, R. Irchhaiya, A. C. Burman, *Eur. J. Med. Chem.* **2009**, *44*, 3356-3362.

4   Terrylene Bisimide-Diarylethene Containing Photochromic System[a]
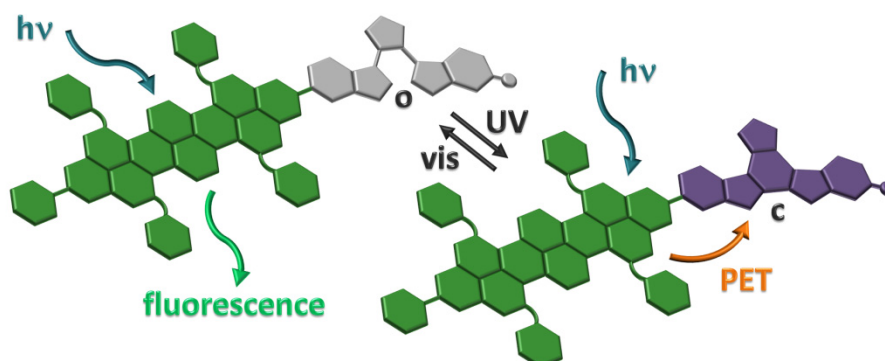
4.1   Introduction

In our previous work (see Chapter 2.6),[1] the principle of fluorescence quenching by photoinduced electron transfer has been demonstrated for photochromic dyad **1o**/**1c** composed of a DAE derivative and a fluorescent 1,7-dipyrrolidinyl-substituted PBI dye (Scheme 1). However, this photochromic system **1o**/**1c** suffers from low photostability of the 1,7-dipyrrolidinyl-substituted PBI emitter unit, which decomposes upon continuing irradiation. In addition, this PBI possesses a low fluorescence quantum yield of only 15% in dichloromethane.[1b] Therefore, a more photostable fluorophore emitting in the same spectral region above 650 nm (clearly separated from DAE absorptions at 550 nm) exhibiting high fluorescence quantum yields was desired. 1,6,9,14-Tetraaryloxy-substituted terrylene bisimide (TBI) **4** (Scheme 1) was chosen as a suitable fluorophore that fulfills these requirements.
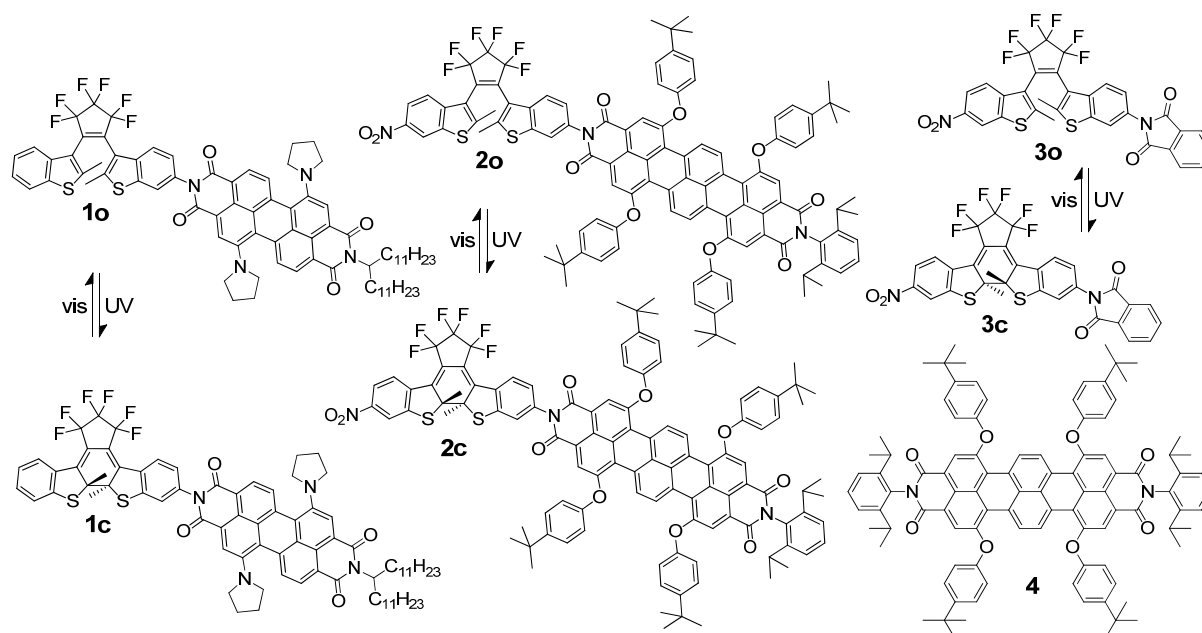
Scheme 1. Photochromic dyads **1o**/**1c** and **2o**/**2c**, and reference compounds **3o**/**3c** and **4**.


TBI dyes have attracted increasing interest as functional materials over the last decade due to their excellent optical and redox properties, and high photostability.[2] Appropriate tailoring of the TBI derivatives by functionalization at the imide positions, altering the substituents at the bay or *ortho*-positions of the aromatic core afforded chromophores with desirable optical and electronic properties.[3] The simplicity of structural variations by common synthetic methods facilitates spectral and electronic fine-tuning of TBI dyes over a wide range, which makes them attractive as electron donors or acceptors, and thus popular building blocks for photophysical investigations.[4] TBI dyes have found use as emitters for single-molecule spectroscopy, in supramolecular arrays and dendrimeric scaffolds as light-harvesting and energy cascade systems and for protein tagging and labeling.[2,5] Furthermore, appropriate substituents at TBI dyes allow spectroscopic investigations in aqueous medium,[6] or the formation of liquid crystals,[7] nanoparticles[8] and quantum dot-dye hybrids.[9] While TBIs have recently been tested for organic field effect transistors (OFET)[10] and photovoltaic applications,[11] no conjugates composed of TBI dye and photochromic switches have been reported in the literature to date.

The work in the following chapter presents the first photochromic system **2o/2c** based on a tetraaryloxy-substituted terrylene bisimide (TBI **4**) as photostable, electron-rich emissive moiety and a DAE photoswitch (Scheme 1). Three DAE–TBI systems have been synthesized and investigated, *i.e.* dyad **2o/2c**, a similar dyad without the additional nitro group at the DAE unit, and a third dyad with a glycine linker between DAE and TBI unit (see Appendix). Notably, the system without the additional nitro group was the first one to synthesize, but no fluorescence quenching upon isomerization could be observed. To comply with the PET switching mechanism schematically illustrated in Figure 23 in Chapter 2.6, the change of the oxidation potential of the emitter unit (*i.e.* tetraaryloxy-substituted TBI in **2** instead of dipyrrolidinyl-substituted PBI in dyad **1**) required a modified DAE photochrome with a stronger electron-acceptor character. Therefore, an additional electron-withdrawing nitro group was attached to the DAE unit of **2** and an appropriate reference DAE **3o/3c** with phthalic imide residue was synthesized and characterized. The third system with glycine linker between emissive and photochromic units was synthesized to reduce possible interactions between TBI and DAE. However, the additional system provides no improvement, and therefore, Chapter 4 focuses on the well-functioning system **2o/2c**. The synthesis and characterization of the two additional new systems are described in the Appendix.

4.2   Synthesis of Photochromic System and Reference Diarylethene

The synthesis of TBI relies on the coupling of a perylene imide with a naphthalene imide, which can be achieved under either basic or Pd-catalyzed conditions. Both possibilities start with the literature known cleavage of one anhydride function of perylene-3,4:9,10-tetracarboxylic acid bisanhydride (**5**) and simultaneously imidization of the remaining anhydride function with 2,6-diisopropylaniline (see route 1 in Scheme 2).[12] Perylene imide **6** was subsequently brominated at the 9-position of the

perylene core.[13] The corresponding boron ester **8** was obtained by a Pd-catalyzed reaction of the perylene imide **7** and bis(pinacolato)diboron. These mild conditions tolerate functional groups such as cyano, esters, ketones, and nitro substituents, in contrast to the conventional method with a lithiation step.[5c] Unfortunately, this literature known reaction was problematic in regard to the purification. The boron ester was not stable on silica gel and the yield decreased dramatically, while the isolated material also contained the homocoupled product. Concerning the purification step, the authors are not self-consistent. The group of Müllen described a separation of the homocoupling product by column chromatography in 2004,[5c] while the same group stated that purification by column chromatography leads to low yields due to sticking of the product **8** on silica gel in 2007.[14]
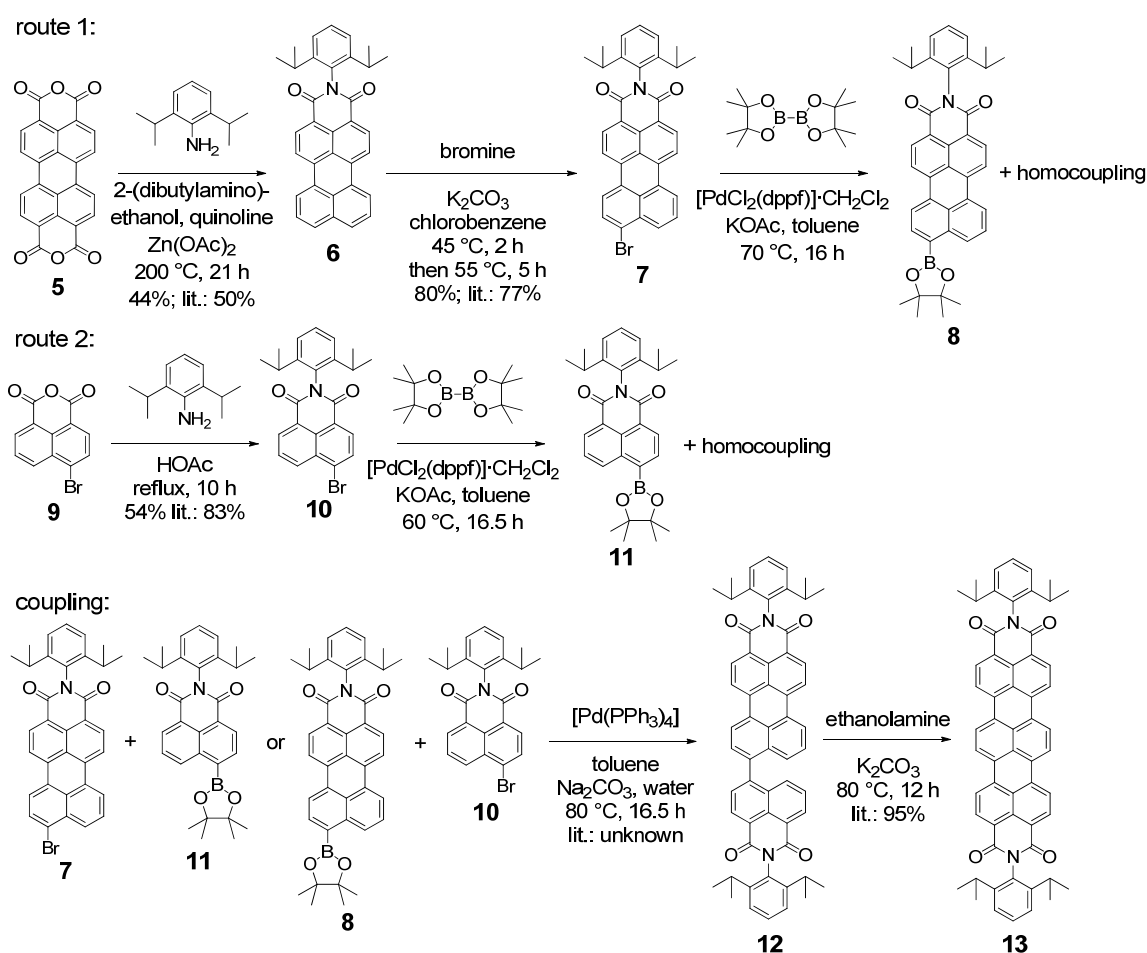

Scheme 2. Alternative syntheses of unsubstituted terrylene bisimide **13**.

The preparation of the respective boron esters of the naphthalene imide **11** (see route 2 in Scheme 2), which was made from bromo-substituted naphthalene imide **10**,[15] caused the same problems of formation of homocoupling product, which could not be separated, and low yields due to retention of the boron ester **11** on silica gel. Therefore, the crude product mixture was used for the next step, a Pd-catalyzed Suzuki coupling of the boron ester **11** or **8** and the respective rylene **7** or **10** (bottom row in Scheme 2).[16] The blue bay-unsubstituted TBI **13** was formed by heating of the

terrylene precursor **12** under basic conditions.[16] Purification and complete separation of homocoupling product was successful at this step, but led to an overall low yield.

A second procedure for TBIs, bypassing the unfavorable boron ester, was described by Sakamoto *et al.* as the so called "green route" to rylene dyes, but has actually a lower reported yield then the Pd-catalyzed synthetic route.[17] For this fusion of two rylene imides, the authors postulated the formation of a base complex reagent of potassium *tert*-butoxide and 1,5-diazabicyclo[4.3.0]non-5-ene (DBN) in diglyme. This reactive species abstracts a proton from the 4-position of the naphthalene imide which furthermore reacts as an aryl anion at a second rylene imide by nucleophilic addition.[17]

Although F. Nolde *et al.*[16] reported a yield of 42% by applying this procedure for the synthesis of the unsubstituted terrylene bisimide dye **13** (Scheme 3), the best received yield during this thesis was 29%. However, this could not be consistently reproduced with obtained yields usually in the range of 0–10%, and larger quantities of perylene bisimide as main product and even a small fraction of quaterrylene bisimide were isolated. Consequently, neither the palladium-catalyzed nor the base-promoted fusion was a convincing procedure for the synthesis of terrylene bisimides. Nevertheless, according to the procedure by Sakamoto *et al.*, the precursor for the bromo-substituted TBI **14**, *i.e.* bay-unsubstituted TBI **13** was synthesized from perylene bisanhydride **5** and naphthalene anhydride **15** in three steps (Scheme 3) using the "green route".[12,15-17]
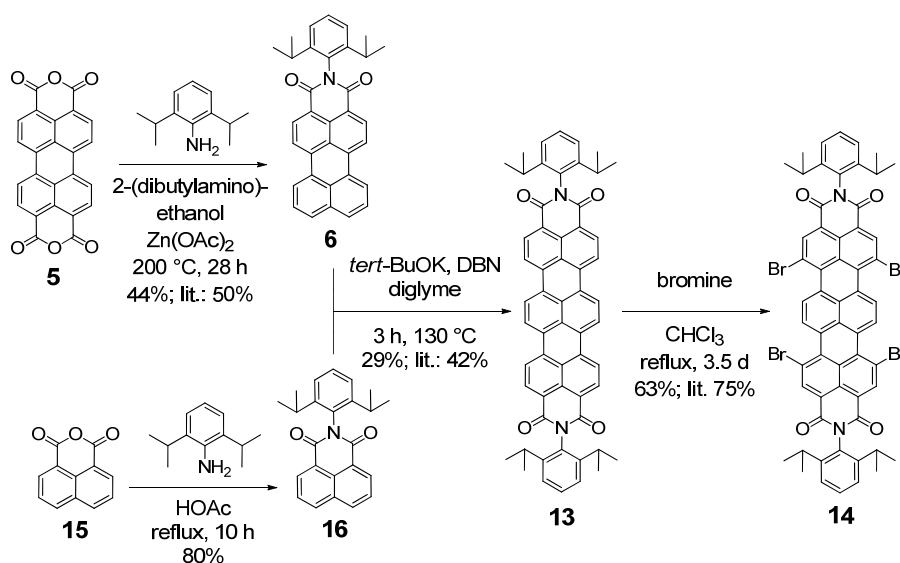

Scheme 3. Synthesis of tetrabromo-substituted terrylene bisimide **14**; DBN = 1,5-diazabicyclo[4.3.0]non-5-ene.[5c,12,15-17]

The unsubstituted TBI **13** was furthermore brominated to receive the literature known bromo-substituted TBI **14**.[5c] In contrast to this literature procedure, the reaction time needed to be extended to 80 hours and additional portions of bromine (5 eq.) were added eight times in order for the reaction to run to completion.

Next, the bromine atoms in terrylene bisimide **14** were substituted by 4-*tert*-butylphenol in dry *N*-methyl-2-pyrrolidone (NMP) to get the so far literature-unknown tetraaryloxy-substituted terrylene bisimide **4** as a dark green solid,[16] and alkaline hydrolysis of the latter afforded the emissive building block tetraaryloxy-substituted terrylene anhydride imide **17** (Scheme 4).[18]

The precursor for the photochromic unit **18**, *i.e.* 1,2-bis(2-methylbenzo[*b*]thiophen-3-yl)perfluorocyclopentene, which was first reported in 1992 by the group of Irie, was initially obtained in a four steps synthesis,[19] but since 2008 was obtained from a commercial source. In order to increase the driving force for the electron transfer to facilitate fluorescence quenching of the emitter unit particularly in a less polar environment, an additional electron-withdrawing nitro group was attached to the diarylethene on the opposite side to the fluorescent dye compared to the DAE moiety of **1o** (Scheme 1).[1b] Therefore, diarylethene **18** was firstly nitrated twice using fuming nitric acid (Scheme 4).[20] New conditions for the following selective reduction of only one nitro group had to be applied, due to the fact that the published conditions for the reduction of nitro-groups attached to diarylethenes with sodium borohydride in methanol did not work selectively on only one group.[21] The selective reduction of only one of the nitro-groups of diarylethene **19** based on the preliminary work of Idox[22] and the elaborated condition of Lemenovskii *et al.*[23] with sodium hydrosulfide hydrate as the reducing agent in a methanol/toluene mixture resulted in the literature-unknown amino-substituted DAE **20** as a pale beige solid.
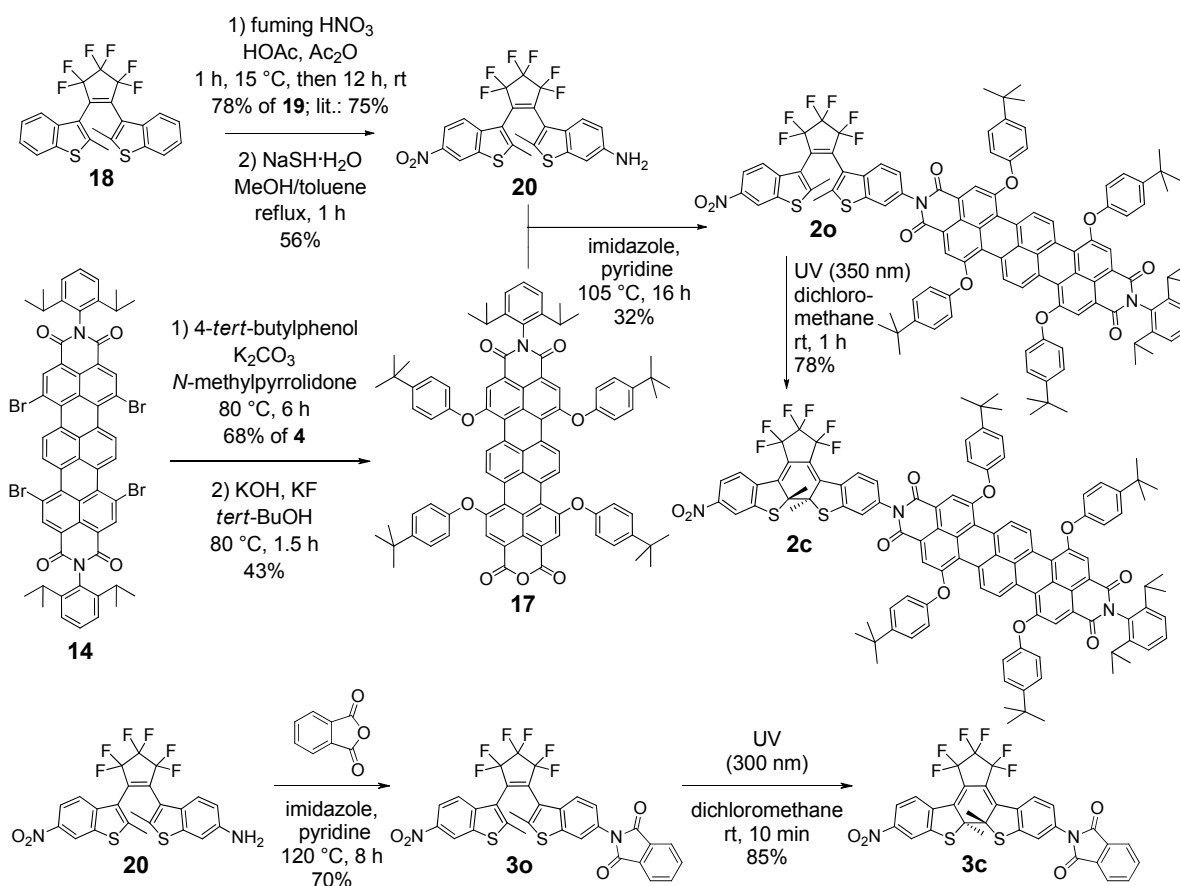

Scheme 4. Synthesis of the open and closed form of dyad **2o** and **2c**, and photochromic references **3o** and **3c**.

In the final step, the condensation reaction of terrylene anhydride imide **17** with the amino-function containing DAE **20** in a mixture of imidazole and pyridine afforded the target photochromic dyad **2o** as a dark green solid in 32% yield.

The isomerization of dyad **2o** into its ring-closed form **2c** was performed in a Rayonet photoreactor RPR-100 by irradiation of a dichloromethane solution of **2o** with UV light ($\lambda_{max} = 350$ nm) in 78% yield. Furthermore, the photochromic reference compound **3o** with a phthalic imide residue, instead of the fluorescent terrylene bisimide dye, was synthesized by a condensation reaction of DAE **6** with phthalic anhydride in 70% yield according to a previously published procedure.[1b] The closed form of this reference diarylethene **3c** was obtained by irradiation of a dichloromethane solution in a Rayonet photoreactor RPR-100 as a dark magenta solid in 85% yield. All new compounds, including the target dyad **2o/2c** as well as references **3o/3c** and **4** were characterized by ^{1}H and ^{13}C NMR spectroscopy and high-resolution mass spectrometry. The synthetic details and the characterization data of all new compounds are provided in the experimental section (see Chapter 4.7.2).

4.3   Absorption and Emission Spectroscopy

Absorption spectra of the naphthalene imide **16** and perylene imide **6** precursors as well as unsubstituted **13**, bromo-substituted **14** and aryloxy-substituted TBI **4** were measured in dichloromethane (Figure 1).
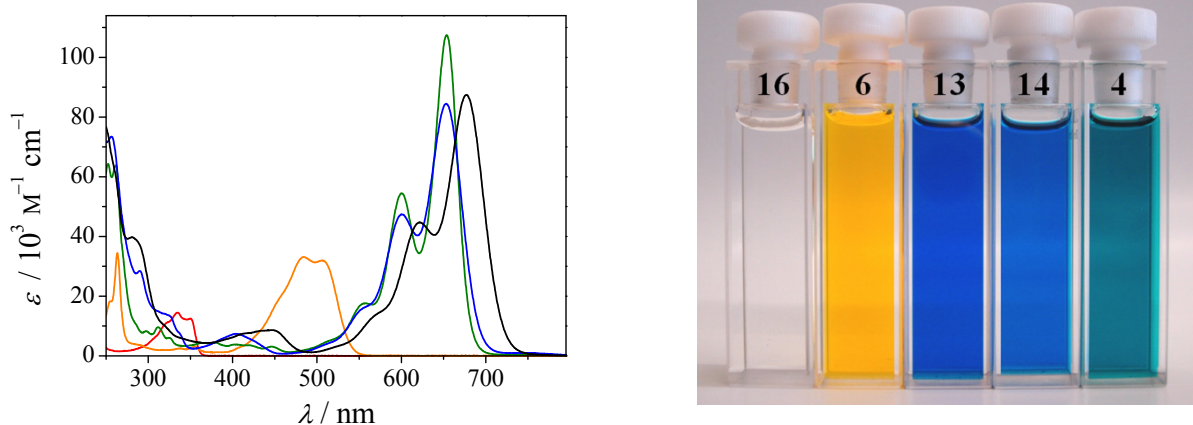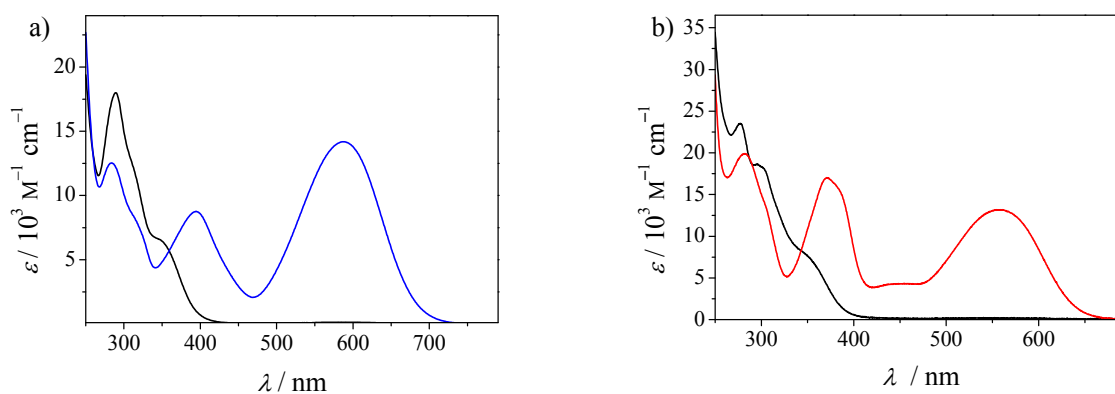

Figure 1. Left panel: UV/vis absorption spectra of naphthalene imide **16** (red line), perylene imide **6** (orange line), unsubstituted TBI **13** (green line), tetrabromo-substituted TBI **14** (blue line), and tetraaryloxy-substituted TBI **4** (black line) in dichloromethane (1×10^{-5} M) at 25 °C; right panel: Photograph of solutions of **16**, **6**, **13**, **14**, and **4** (from left to right) in dichloromethane (1×10^{-4} M) under ambient laboratory light.

While naphthalene imide **16** shows absorption in the UV region between 300 and 370 nm, the respective perylene imide **6** has a broad absorption between 400 and 550 nm. The bay-unsubstituted terrylene bisimide **13** with 2,6-diisopropylphenyl-substituents absorbs in the visible region between 500 and 700 nm with a maximum at 654 nm and a distinctly higher extinction coefficient than its

rylene imide precursors. Bromination of the terrylene core has no influence on the absorption range (λ_{max} = 653 nm) but leads to a lower extinction coefficient, whereas substitution of the four bromines by electron-rich 4-*tert*-butylphenoxy substituents leads to a bathochromic shift of the absorption by 24 nm and an intense absorption between 550 and 730 nm with a maximum at 677 nm.

The colorless open form of precursor DAE **20**, which contains an amino and a nitro group, can be switched into its blue colored closed form by UV irradiation (λ_{max} = 365 nm) in dichloromethane (Figure 2a). The open form of the reference diarylethene with phthalic imide residue (**3o**) absorbs only in the UV area below 400 nm, whereas the respective ring-closed isomer **3c** exhibits two additional bands, one in the UV area with a maximum at 372 nm and a broad one in the visible region with a maximum at 558 nm (Figure 2b).


Figure 2. UV/vis absorption spectra of (a) DAE precursor **20** before irradiation (black line) and the photostationary state (PSS) after irradiation with UV light (365 nm; blue line) in dichloromethane (1×10^{-5} M) for 11 min at 25 °C and (b) open form (black line) and closed form (red line) of reference photochrome **3o/3c** in dichloromethane (1×10^{-5} M) at 25 °C.

The absorption spectra of both forms of the photochromic dyad **2o** and **2c** and the TBI reference **4**, and the respective emission spectra are shown in Figure 3. The open form of photochromic dyad **2o** (DAE$_O$–TBI; Figure 3a) has almost identical absorption bands in the visible region (> 400 nm) compared to those of reference dye **4** (TBI; Figure 3c). However, dyad **2o** exhibits a more pronounced absorption in the UV area. The closed form of dyad **2c** (DAE$_C$–TBI; Figure 3b) shows additional bands between 350 and 400 nm as well as between 500 and 650 nm, which correspond to the absorption of the closed DAE moiety. The absorption of the terrylene bisimide moiety of dyad **2c**, which can be ascribed to the $S_1 \leftarrow S_0$ transition, increased slightly and shifted bathochromically to a maximum at 683 nm (see differential spectra Figure 4) compared to that of **2o** and reference **4**, which is in accordance with our previous observation for DAE–PBI dyad **1c**.[1b]
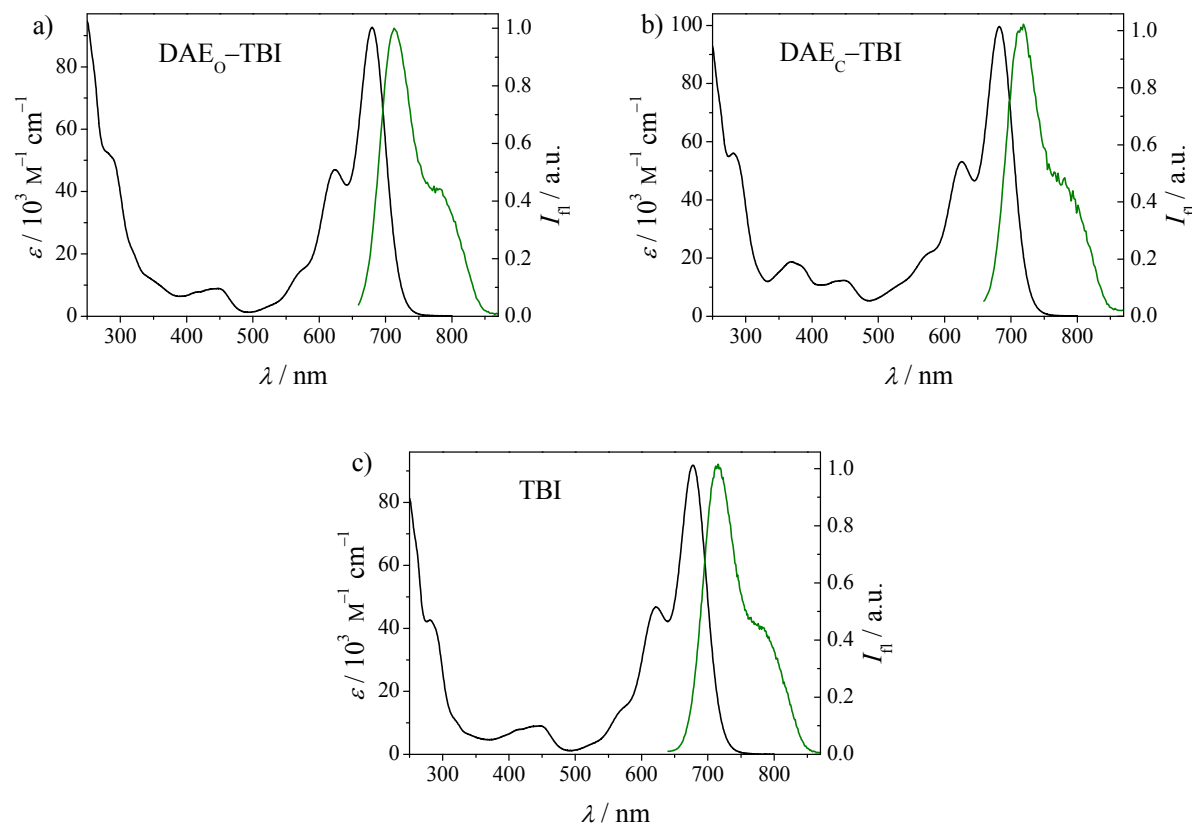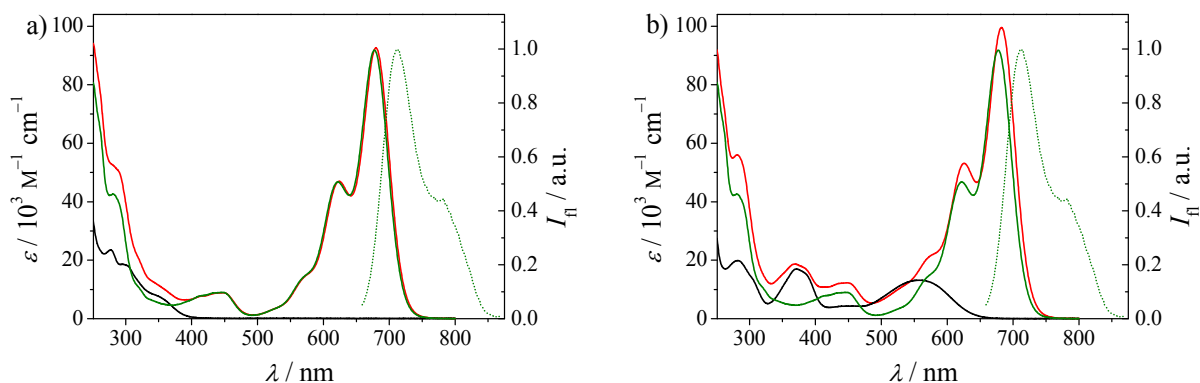
Figure 3. UV/vis absorption (black line) and normalized fluorescence emission spectrum (green line; λ_{ex} = 650 nm for (a) and (b) and λ_{ex} = 615 nm for (c)) of (a) **2o**, (b) **2c** and (c) **4** in dichloromethane (1×10^{-5} M).
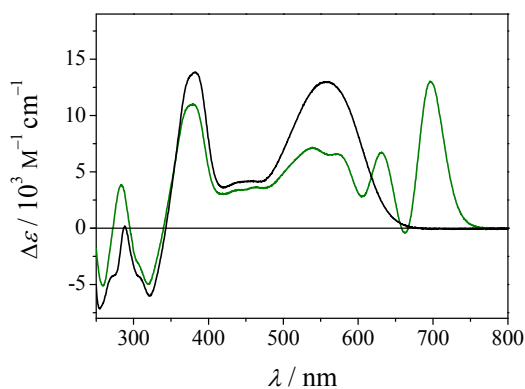
Figure 4. UV/vis absorption differential spectra of the photochromic dyads **2o** and **2c** (spectrum of **2c** minus spectrum of **2o**; green line) and reference photochromes **3o** and **3c** (spectrum of **3c** minus spectrum of **3o**; black line) in dichloromethane (1×10^{-5} M) at 25 °C.

With the aid of this superposition of spectra (Figure 5a), it is clearly obvious, that the open form spectrum **2o** corresponds to an addition of the spectra of the open form DAE **3o** and TBI **4** with little differences in the UV area due to absorption of additional phthalic imide group of **3o**. Accordingly, the spectrum of closed form **2c** approximately sums the spectra of closed form DAE **3c** and TBI **4** with the already mentioned higher extinction of the TBI band (Figure 5b). Furthermore, the emission band of

TBI **4** does not overlap with the band of the closed form of reference DAE **3c**, which avoids additional FRET processes. The absorption and fluorescence data of **2o/2c**, **3o/3c** and **4** and its precursors are summarized in Table 1.

Figure 5. Comparison of UV/vis absorption spectra of (a) open form dyad **2o** (red line) and its individual units, reference photochrome **3o** (black line) and reference TBI **4** (green line); and (b) closed form dyad **2c** (red line) and its individual units, reference photochrome **3c** (black line) and reference TBI **4** (green line) in dichloromethane (1×10^{-5} M) at 25 °C; the green dotted line reveals the emission spectrum of TBI **4** (λ_{ex} = 651 nm) in dichloromethane.

Table 1. Optical properties of terrylene bisimide **4** and precursors **16**, **6**, **13**, **14**, dyad system **2o/2c**, and reference photochromes **3o** and **3c** in dichloromethane (1×10^{-5} M) at 25 °C.

	λ_{abs} [nm] (ε_{max} [M^{-1} cm^{-1}])	λ_{em} [nm][a]	Φ_{fl} [%][a]
16	334 (14500), 351 (12500)	[b]	[b]
6	264 (33400), 484 (33100), 506 (32000)	[b]	[b]
13	312 (9600), 557 (17600), 601 (54500), 654 (107500)	[b]	[b]
14	290 (28500), 404 (7400), 601 (47400), 653 (84400)	[b]	[b]
4	280 (42600), 448 (9000), 623 (46800), 677 (91800)	715	28
2o	447 (8900), 624 (47000), 680 (92600)	713	29
2c	281 (56000), 369 (18700), 447 (12300), 626 (53100), 683 (99600)	719	10
3o	278 (23500), 295 (18700)	–	–
3c	282 (17100), 372 (14600), 558 (11300)	–	–

[a] Excitation wavelength 647–655 nm. [b] Value not determined.

The fluorescence quantum yields of the two isomers **2o** and **2c** were measured in several solvents with different polarity and compared with the respective value of the reference terrylene bisimide **4** (Table 2). The fluorescence quantum yield of TBI **4** decreases with increasing solvent polarity from 58% in tetrachloromethane (ε_r = 2.24) down to 9% in dimethyl sulfoxide (ε_r = 46.45). The observed

parallel decrease in fluorescence of reference TBI **4** and open form dyad **2o** in strongly polar solvents is indicative of a charge-transfer process from the electron-rich aryloxy-substituents in the bay positions to the electron-poor terrylene bisimide core.[24] The quantum yields of the open form **2o** correspond perfectly to those of the reference TBI **4** in the whole range of solvents, from nonpolar tetrachloromethane up to the most polar solvent used in this study, *i.e.* dimethyl sulfoxide. Accordingly, no additional fluorescence quenching channel arises for the TBI fluorophore in open form DAE **2o**. The distinct lower value of open form **2o** (23%) in chloroform compared to reference **4** (33%) is an exception from this general trend. In contrast, for the closed form DAE **2c** the emission of TBI is strongly quenched even in fairly nonpolar solvents. Thus, the fluorescence intensity in tetrachloromethane is lowered by half from 60% for **2o** to 34% for **2c**, while the extent of quenching is increased up to three-fourths in 1,2-dichloroethane (23% to 6%) and dimethyl sulfoxide (8% to 2%) (Table 2). The fluorescence quantum yields of **2o** and **2c** (Φ_{fl}) divided by the quantum yield of reference terrylene bisimide **4** (Φ_{fl}^{ref}) are shown as a function of the dielectric constants of solvents in Figure 6.

Table 2. Fluorescence quantum yields of **2o**, **2c** and reference dye **4** in different solvents.

solvent	ε_r^a	Φ_{fl} [%]		
		2o	**2c**	**4**
tetrachloromethane	2.24	60	34	58
1,4-dioxane	2.21	40	23	41
chloroform	4.89	23	15	33
ethyl acetate	6.02	32	10	31
dichloromethane	8.93	29	10	28
1,2-dichloroethane	10.36	23	6	23
acetone	20.56	16	5	18
dimethyl sulfoxide	46.45	8	2	9

^a Solvent polarity values are taken from ref.[25]

As the fluorescence intensity of both **2o** and **2c** is very weak in highly polar solvents like dimethyl sulfoxide, solvents or polymeric matrices of intermediate polarity, where fluorescence quantum yields of **2o** and **2c** are about 30% and 10%, respectively, would be most suitable for real-world applications. More pronounced fluorescence quenching of the closed form **2c** with increasing solvent polarity is in accordance with a preferential PET from TBI dye to the closed form photochrome as depicted in Figure 23 in Chapter 2.6. Moreover, the quenching ratio for **2o/2c** is markedly improved, particularly in less polar environment, compared to that for the previously reported photochromic system **1o/1c**.[1b]
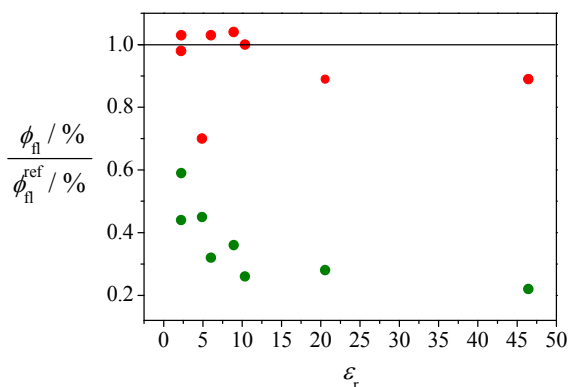
Figure 6. Fluorescence quantum yields of **2o** and **2c** (Φ_{fl}) divided by the quantum yield of reference terrylene bisimide **4** (Φ_{fl}^{ref}) as a function of dielectric constants of solvents; open form **2o** (●), closed form **2c** (●).

4.4   Cyclic Voltammetry and Driving Force Calculation

For an estimation of the driving force for the PET in the present photochromic system, the first oxidation potential of the terrylene bisimide dye moiety and the first reduction potentials of both isomers of the photochromic diarylethene moiety are required. Therefore, we performed cyclic voltammetry measurements of the compounds **2o**, **2c**, and **4** as well as the references **3o** and **3c** in dichloromethane. The oxidation and reduction potentials of these compounds are collected in Table 3 and the cyclic voltammograms are depicted in Figure 7.

Table 3. Half-wave potentials of **2o** and **2c**, TBI **4** and reference photochromes **3o** and **3c**.[a]

	$E_{1/2}^{red}$ [V]	$E_{1/2}^{ox}$ [V]
4	−1.15	0.50, 0.83
2o	−1.12, −1.57	0.52, 0.81
2c	−1.12, −1.38, −1.90[b]	0.52, 0.80
3o	−1.53, −1.96[b]	−
3c	−1.19[b], −1.39[b], −1.69[b]	1.14

[a] The values that belong to the DAE unit are shown in black, those attributed to the TBI unit in green, and the overlapped value of DAE and TBI units in red. All measurements were carried out in dry dichloromethane (10⁻⁴ M) using Fc/Fc⁺ as an internal standard and TBAHFP (0.1 M) as supporting electrolyte at a scan rate of 100 mV s⁻¹. [b] Peak potential of irreversible reduction.
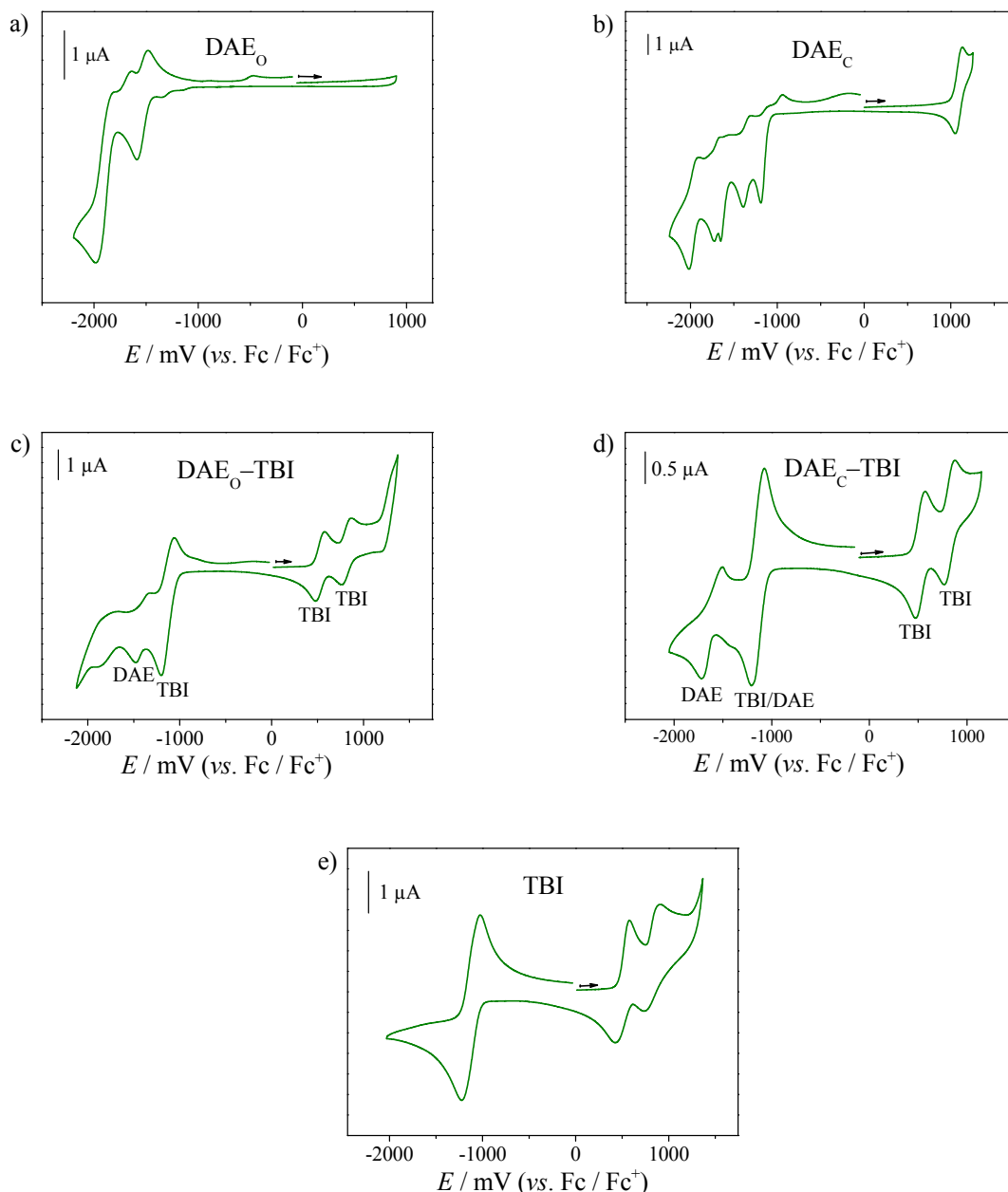
Figure 7. Cyclic voltammograms of compound (a) **3o** (2.64×10^{-4} M), (b) **3c** (2.54×10^{-4} M), (c) **2o** (2.29×10^{-4} M), (d) **2c** (2.78×10^{-4} M), and (e) **4** (2.72×10^{-4} M) in dichloromethane: supporting electrolyte TBAHFP (0.1 M), scan rate 100 mV s^{-1}.

For the open and closed form dyad **2o** and **2c**, a first oxidation was observed at 0.52 V, which is very close to the first oxidation potential of the reference dye **4** (see Table 3 and Figure 7c-e). These results demonstrate that the DAE and TBI units are electronically decoupled in dyads **2o** and **2c**. The first reduction potential of the open form of the reference diarylethene **3o** was observed at −1.53 V and it is considerably increased to −1.19 V for the closed isomer **3c** (Figure 7a,b). Unfortunately, the first reduction wave for the closed form of photochromic unit in **2c** is overlapped with the two-electron reduction wave of its TBI unit, while the subsequent reduction wave at −1.38 V is clearly visible.

83

Therefore, for the estimation of the driving force, the first reduction potential of the reference DAE **3c** (–1.19 V) is used. The significant difference of 0.34 V between the first reduction potential of photochromic ring-closed DAE (–1.19 V) and the respective reduction potential (–1.53 V) of ring-open DAE is the prerequisite for the desired fluorescence switching mechanism by PET. With the $E_{ox}(D)$ and $E_{red}(A)$ values of the first oxidation potential of the donor terrylene bisimide and first reduction potentials of the acceptor DAE unit in **2o** and **2c** as well as E_{00} value for the spectroscopic excited state energy of terrylene bisimide, the driving force for electron transfer can be calculated according to the Rehm-Weller equation (1), where R_{CC} is the distance between the center of the donor and acceptor units.[26]

$$\Delta G° = e\left[E_{ox}(D) - E_{red}(A)\right] - E_{00} - \frac{e^2}{4\pi\varepsilon_0\varepsilon_S R_{CC}} - \frac{e^2}{8\pi\varepsilon_0}\left(\frac{1}{r^+} + \frac{1}{r^-}\right)\left(\frac{1}{\varepsilon_{ref}} - \frac{1}{\varepsilon_S}\right) \tag{1}$$

Since all of our measurements were performed in the same solvent, *i.e.* dichloromethane ($\varepsilon_S = \varepsilon_{ref}$), no estimations for the effective ionic radii of the donor radical cation r^+ and acceptor radical anion r^- are needed and thus the solvent related fourth term in the Rehm-Weller equation can be neglected for this particular case.

The oxidation potential of the donor TBI unit is 0.52 V and the reduction potentials of the acceptor units in **2o** and **2c** (DAE_O and DAE_C) are –1.57 V and –1.19 V, respectively. The excited state energy E_{00} for the TBI dye moiety of dyad **2** can be calculated from its absorption maximum at around 680 nm and the emission maximum at around 715 nm, providing a value of 1.78 eV for the open and 1.77 eV for the closed form. From optimized geometries of **2o** and **2c** structures (on force field level: MM3*, MacroModel 9.8), donor-acceptor distances of 1.40 nm and 1.49 nm, respectively, were estimated (Figure 8).
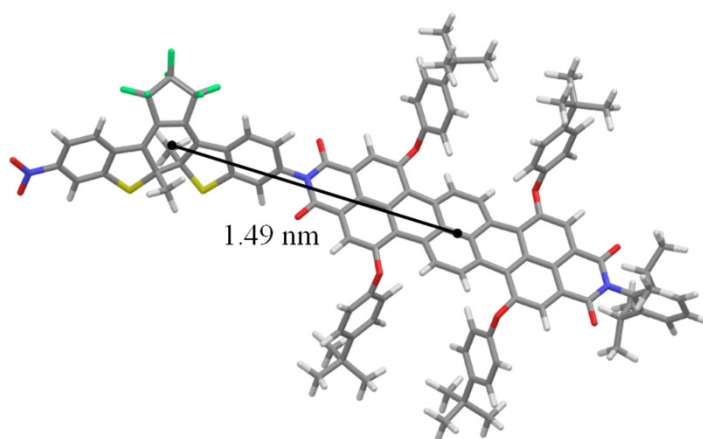
Figure 8. Geometry optimized structure of **2c** on force field level (MM3*, MacroModel 9.8).

By using these values in Rehm-Weller equation, the standard Gibbs free energy ($\Delta G°$) for the formation of intramolecular charge-separated state by an electron transfer process is estimated to be

0.16 eV for the open form **2o** and –0.24 eV for the closed form **2c**. These energy values imply that, in dichloromethane ($\varepsilon_r = 8.93$), the electron-transfer process is thermodynamically feasible only for the closed form. In more polar solvents, such as dimethyl sulfoxide ($\varepsilon_r = 46.45$), the CT state should be more stable and thus PET becomes more facile also for **2c** ($DAE_C^- - TBI^+$) in polar solvents (see Table 2).

## 4.5   Photoswitching and Read-out Behavior

Photocyclization and photocycloreversion quantum yields of the present system **2o/2c** and reference **3o/3c** were determined to elucidate the influence of TBI fluorophore on the photochromic transformation. The cyclization quantum yield of dyad **2o** (0.23) at 311 nm decreased significantly compared to that for reference DAE **3o** (0.59), while the effect of the attached fluorophore for the respective cycloreversion is rather small with quantum yields of 0.12 and 0.17 for **2c** and **3c** at 517 nm, respectively (Table 4). The absorption of the TBI unit is nearly identical to the absorption of the photochromic unit at 311 nm, while the TBI unit absorbs only around one fourth of the DAE absorption at 517 nm (Figure 5). Apparently, these different absorption ratios at 311 and 517 nm account for the observed changes in the quantum yields for the ring-opening and ring-closure reactions which suggests that for neither photoexcited DAE_O nor for photoexcited DAE_C additional DAE deactivation channels (such as FRET to TBI) become competitive to the ultrafast DAE photoswitching reactions.[27]

Table 4 Photocyclization ($\Phi_{O \to C}$) and photocycloreversion ($\Phi_{C \to O}$) quantum yields of **2o/2c** and references **3o/3c**.[a]

	$\Phi_{O \to C}$	$\Phi_{C \to O}$
2o	0.23	–
2c	–	0.12
3o	0.59	–
3c	–	0.17

[a] Quantum yields were determined in ethyl acetate at 25 °C by using 1,2-bis-(2-methylbenzo[*b*]thiophene-3-yl)-perfluorocyclopentene ($\Phi_{O \to C}$ = 0.31 at 311 nm and $\Phi_{C \to O}$ = 0.28 at 517 nm in ethyl acetate)[28] as a reference.

The stability of both photochromic isomers was examined by repeating switching cycles, which were performed by alternating irradiation of a dichloromethane solution of **2c** with conventional light sources, *i.e.* UV (365 nm) and visible light (see Figure 9).
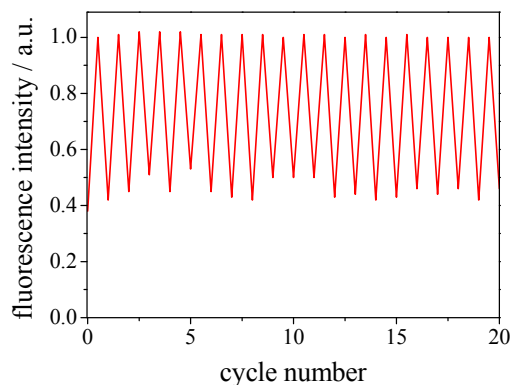
Figure 9. Switching cycles of **2c** in dichloromethane upon alternating irradiation with UV (365 nm) and visible light.

Even after twenty cycles, the emission intensity, which can be switched between a high emissive state (around 84% open form and 16% closed form) and a less emissive state (around 11% open form and 89% closed form) equating to around 40% of the intensity of the higher emissive state, remained unchanged and thus no decomposition occurred.

In addition to the switching cycles, enduring ionization by increasing voltage showed no decomposition. Thus, spectroelectrochemistry studies of the reference terrylene bisimide **4** with increasing positive voltage up to complete conversion to the TBI radical cation, and of the closed form of the reference diarylethene **3c** with increasing negative voltage up to the complete conversion to the DAE radical anion, showed no evidence for competing decomposition processes (Figure 10a and 10b).
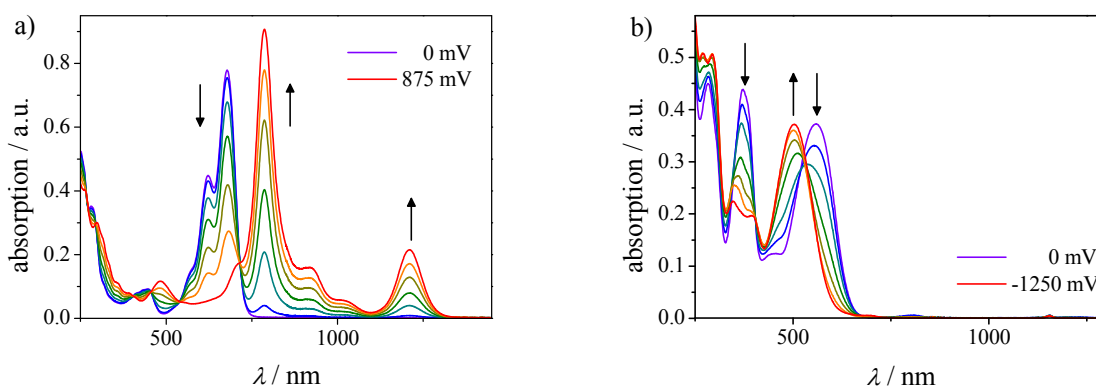
Figure 10. (a) Absorption spectra of reference TBI **4** with increasing positive voltage (indicated by the arrows) in dichloromethane (5.8×10^{-4} M, 0.1 M TBAHFP). The violet line represents the neutral dye (0 mV) and the red line the radical cation of **4** (875 mV); (b) absorption spectra of the closed form of the reference photochrome **3c** with increasing negative voltage (indicated by the arrows) in dichloromethane (1.1×10^{-3} M, 0.1 M TBAHFP). The violet line represents the neutral dye (0 mV) and the red line the radical anion of **3c** (–1250 mV).

86

The non-destructive read-out capability was tested by enduring excitation of the fluorophore unit of **2o** and **2c** with a light intensity of 4.3 mW/cm² at 720 nm in chloroform, dichloromethane, and ethyl acetate (see Figure 11). While the emission intensity for the open form **2o** remained virtually constant in chloroform, a negligible change of 3% of the fluorescence intensity in chloroform over one hour of continuous excitation was observed for **2c** (see Figure 11a and b).
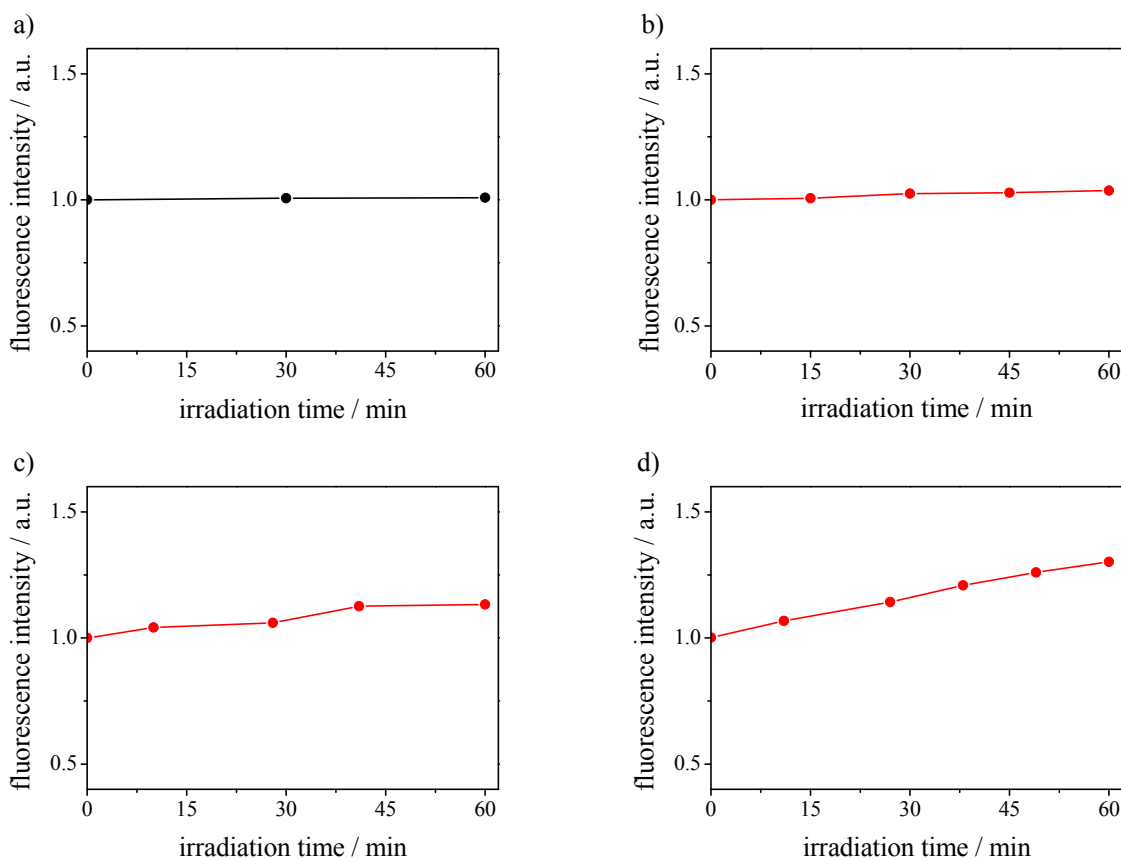
Figure 11. Time-dependent fluorescence intensity of **2o** (a) and **2c** (b) in chloroform, **2c** in dichloromethane (c), and **2c** in ethyl acetate (d) at 750 nm upon continuous excitation at 720 nm (±10 nm FWHM) with a 75 W Xenon short arc lamp (4.3 mW/cm²) for 60 min (cut-off filter at 640 nm); FWHM = full width half maximum.

Surprisingly, the same studies for **2c** in other solvents like dichloromethane and ethyl acetate revealed a more significant increase of the fluorescence intensity. While the emission of **2c** increased by 10% over 1 hour in dichloromethane, the rise is considerably higher in ethyl acetate with a value of 30% in the same time range (see Figure 11c and d). Therefore, the disadvantageous fluorescence increase for **2c** upon selective excitation of the TBI unit, which is insignificant in chloroform, is enhanced in ethyl acetate and non-destructive read-out capability is not given in such environment.

Further fluorescence spectroscopy studies were carried out to get more insight into the observed increasing fluorescence intensity of **2c**. Thus, the emission of reference TBI **4** and dyads **2o** and **2c** were analyzed at a wavelength, where only the TBI unit emits (λ_{ana} = 725 nm), by excitation over the whole spectral region from 250 nm to 850 nm in dichloromethane (Figure 12).
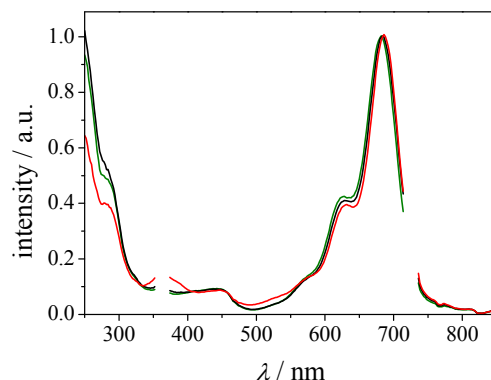
Figure 12. Excitation spectrum of the TBI emission in dyad **2c** (red line) compared with those of reference TBI **4** (green line) and open form **2o** (black line) in dichloromethane (monitoring wavelength 725 nm).

While the spectra of open form **2o** and reference TBI **4** are almost identical, the closed form **2c** exhibits additional weak bands at around 360 nm and 520 nm, which can be attributed to an energy transfer from the closed form of the DAE moiety to the TBI unit. This process might compete with the switching of the DAE unit into the open form. If originating from a Dexter-type coupling,[29] this process could be related to the steady increase of the fluorescence intensity for the closed form **2c** upon excitation of the TBI unit in dichloromethane and ethyl acetate (Figure 11c and d), which might be circumvented by incorporating a non-conjugated spacer between DAE and TBI units (see Appendix 8.2).

4.6   Conclusions

In conclusion, a novel photochromic system **2o**/**2c**[30] based on an excellent terrylene bisimide emitter allows tuning of fluorescence by photochromic switching between the two isomers of a properly adjusted DAE unit in a wide range of solvents with different polarity. The efficient emission quenching of the closed form **2c** is attributed to a photoinduced electron transfer as this process is exergonic with a significantly negative Gibbs free energy value of –0.24 eV. Dyad **2** represents a prototype photochromic switch for a non-destructive read-out optical memory system in carefully selected environments. Owing to its outstanding photostability, photochromic system **2o**/**2c** should be of particular interest for ultrafast and single-molecule spectroscopy studies as well as superresolution fluorescence imaging.[31]

4.7   Experimental Section

4.7.1   Materials and Methods

General: All solvents and reagents were purchased from commercial sources and used as received without further purification, unless otherwise stated. 1,2-Bis(2-methyl-6-nitro-benzo[b]thiophen-3-yl)-perfluorocyclopentene (**19**) was prepared according to literature procedure.[20b] N,N'-Bis(2,6-diiso-propylphenyl)-1,6,9,14-tetrabromoterrylene-3,4:11,12-tetracarboxylic acid bisimide (**14**) was prepared from perylene-3,4:9,10-tetracarboxylic acid bisanhydride according to a published sequence of four steps with a slight modification of the bromination step (see Synthesis and Characterization).[5c,12,16] Column chromatography was performed using silica gel 60M (0.04–0.063 mm) from Macherey-Nagel. Melting points were determined on an Olympus BX41 polarization microscope and a Linkam TP 94 heating stage and are uncorrected. High resolution mass spectra (ESI) were recorded on an ESI micrOTOF Focus spectrometer from Bruker Daltonics. MALDI-TOF mass spectra were recorded on an Autoflex II spectrometer from Bruker Daltonics. The UV irradiation experiments were performed in a Rayonet Photoreactor RPR-100 (Southern New England Ultraviolet Company) with 16 UV lamps (24 W lamps with $\lambda_{max} = 350$ nm or 21 W lamps with $\lambda_{max} = 300$ nm). A L42 filter (L42_.SP - 08.08.03 - 0.1 mm cuvette) and a R64 filter (R64_.SP – 08.08.03 – 0.1 mm cuvette) from JASCO Corporation were used for filtering irradiation below 420 nm or 640 nm, respectively.

NMR spectroscopy: ^{1}H and ^{13}C NMR spectra were recorded on Bruker Advance 400 or Bruker Advance DMX 600 spectrometer and calibrated to the residual solvent peak (CD$_2$Cl$_2$: 5.32 ppm for ^{1}H and 53.84 ppm for ^{13}C; CDCl$_3$: 7.26 ppm for ^{1}H). The signals in ^{1}H NMR spectra of **2o**, **3o** and **20** for parallel and *anti*-parallel isomers of photochromic DAE unit (Scheme 6) are indicated by "p" and "ap", respectively, and signal integrals of isomeric protons are normalized.
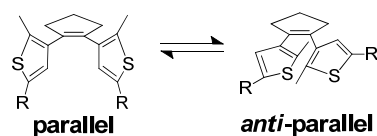
Scheme 6. Structures of parallel and *anti*-parallel isomers of photochromic DAE unit.

UV/vis absorption and fluorescence spectroscopy: For all spectroscopic measurements, spectroscopic grade solvents (Uvasol®) from Merck (Hohenbrunn, Germany) were used. UV/vis spectra were recorded on a Perkin Elmer UV/vis spectrometer Lambda 35 in combination with a Perkin Elmer PTP–1+1 peltier system and a Lauda ecoline RE306/E300 refrigeration circulator. Fluorescence spectra as well as excitation spectra were recorded with a PTI QM-4/2003 using conventional quartz cells (light path 1 cm). All fluorescence measurements were performed under aerobic conditions and fluorescence spectra are corrected against photomultiplier and lamp intensity. The fluorescence quantum yields were determined as the average value for five different excitation

wavelengths using Rhodamine 800 as reference ($\Phi_{fl} = 0.21$ in ethanol) by applying the high dilution method (abs.: <0.05).[32]

Cyclic voltammetry: Cyclic voltammetry measurements were performed on a standard, commercial electrochemical analyzer (EC epsilon; BAS Instruments, UK) in a three electrode single-compartment cell under argon atmosphere. Dichloromethane (HPLC grade) was dried over calcium hydride under argon and degassed prior to use. The supporting electrolyte tetrabutylammonium hexafluorophosphate (TBAHFP) was synthesized according to literature,[33] recrystallized from ethanol/water and dried in high vacuum. The measurements were carried out under exclusion of air and moisture at a concentration of about 10^{-4} M with ferrocene as an internal standard for the calibration of the potential. Working electrode: Pt disc; reference electrode: Ag/AgCl; auxiliary electrode: Pt wire.

Spectroelectrochemistry: Spectroelectrochemistry measurements were performed in a specially designed sample compartment consisting of a cylindrical quartz cell, a platinum disc (ø 6 mm), a gold-covered metal (V2A) plate as the auxiliary electrode and a Ag/AgCl pseudo-reference electrode. All spectra were recorded in reflection mode and the optical path length was varied by adjusting the vertical position of the working electrode with a micrometer screw. The potential applied was varied in steps of 25 or 50 mV with a potentiostat (EG & G Princeton Applied research Model 283). A JASCO V-670 spectrometer was used for recording UV/vis/NIR absorption spectra. The compounds were checked for reversibility of the spectra.

4.7.2   Synthesis and Characterization

***N,N'*-Bis(2,6-diisopropylphenyl)-1,6,9,14-tetrabromoterrylene-3,4:11,12-tetracarboxylic   acid bisimide (14)[5c]**

The compound was synthesized according to the procedure with a distinct differing reaction time and quantity of added bromine.[5c] *N,N'*-Bis(2,6-diisopropylphenyl)terrylene-3,4:11,12-tetracarboxylic acid bisimide (**13**) (367 mg, 439 µmol) was dissolved in 20 mL chloroform and 0.11 mL (351 mg; 2.20 mmol; 5 eq.) bromine were added. The reaction mixture was heated to reflux for 12 h with exclusion of light. After that time, only the once, twice and triply brominated TBI could be detected in the mixture. Therefore, additional bromine was added eight times (each with 0.1 mL, 311 mg; 1.95 mmol) over a period of 80 h. After cooling to ambient temperature, saturated $Na_2S_2O_3$ solution was added and the mixture was extracted with dichloromethane. The combined organic layers were dried over sodium sulfate and concentrated by rotary evaporation. The crude product was purified by column chromatography on silica gel (dichloromethane) to yield a dark blue solid (317 mg; 275 µmol; 63%; Lit.: 75%).[5c] Mp: > 400 °C (from dichloromethane; lit.: > 300 °C).[5c]

13   **14**
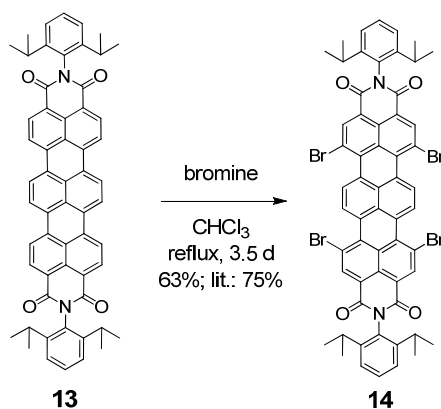
C$_{58}$H$_{42}$Br$_4$N$_2$O$_4$ (1150.600)

^{1}H NMR (400 MHz, CDCl$_3$, 300 K): δ 9.55 (s, 4H), 9.01 (s, 4H), 7.52 (t, ^3J(H,H) = 7.8 Hz, 2H), 7.37 (t, ^3J(H,H) = 7.8 Hz, 4H), 2.74 (sept, ^3J(H,H) = 6.8 Hz, 4H), 1.20 (d, ^3J(H,H) = 6.9 Hz, 24H).

**MS** (MALDI, pos. mode, matrix DCTB 1:3 in CHCl$_3$): *m/z*: calcd for C$_{58}$H$_{42}$Br$_4$N$_2$O$_4$: 1145.988 [M]$^+$; found: 1145.974.

UV/vis (CHCl$_3$): λ_{max}/nm (ε_{max}/M^{-1} cm^{-1}) = 290 (28500), 404 (7400), 601 (47400), 653 (84400).

CV (CH$_2$Cl$_2$, 0.1 M TBAHFP, *vs.* Fc/Fc$^+$): $E_{1/2}^{red}$ (X$^-$/X^{2-}) = –0.93 V, $E_{1/2}^{red}$ (X/X$^-$) = –0.86 V, $E_{1/2}^{ox}$ (X$^+$/X) = 0.98 V.

N,N'-Bis(2,6-diisopropylphenyl)-1,6,9,14-tetra(4-*tert*-butylphenoxy)terrylene-3,4:11,12-tetra-carboxylic acid bisimide (4)

This compound was synthesized according to the procedure reported for N,N'-(2,6-diisopropylphenyl)-1,6,9,14-tetra[4-(1,1,3,3-tetra-methylbutyl)-phenoxy]terrylene-3,4:11,12-tetracarboxylic acid bisimide.[16] A mixture of 277 mg (241 µmol) N,N'-bis(2,6-diisopropylphenyl)-1,6,9,14-tetrabromoterrylene-3,4:11,12-tetracarboxylic acid bisimide (**14**), 312 mg (2.08 mmol; 8 equiv.) dried 4-*tert*-butylphenol and 180 mg (1.30 µmol, 5 equiv.) dried potassium carbonate in 20 mL dried *N*-methyl-2-pyrrolidone (NMP) was heated at 80 °C under argon and exclusion of ambient light for 6 h. After cooling down to room temperature, diluted aqueous hydrochloric acid (50 mL) was added and the resultant precipitate was separated by filtration. The crude product was purified by column chromatography on silica gel (dichloromethane/*n*-hexane (2/1, v/v)) to yield 234 mg (164 µmol; 68%) of a dark green solid. Mp: 350–351 °C (from dichloromethane).
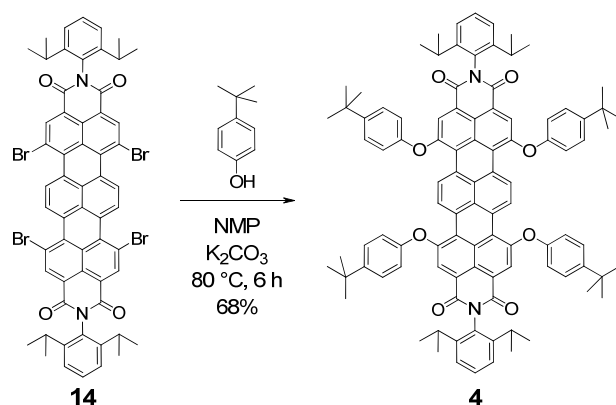
$C_{98}H_{94}N_2O_8$ (1427.850)

¹H NMR (400 MHz, CD_2Cl_2, 300 K): δ 9.54 (s, 4H), 8.24 (s, 4H), 7.44–7.50 (m, 10H), 7.31 (d, ^3J(H,H) = 7.8 Hz, 4H), 7.12–7.17 (m, 8H), 2.70 (sept, ^3J(H,H) = 6.8 Hz, 4H), 1.34 (s, 36H), 1.11 (d, ^3J(H,H) = 6.8 Hz, 24H).

¹³C NMR (100 MHz, CD_2Cl_2, 300 K): δ 163.62, 155.21, 153.78, 148.17, 146.44, 131.60, 131.52, 129.93, 129.81, 129.46, 129.27, 127.70, 126.57, 124.42, 123.87, 123.28, 122.47, 119.22, 34.80, 31.61, 29.46, 24.13.

HRMS (ESI, pos. mode, acetonitrile/$CHCl_3$ 1:1): m/z: calcd for $C_{98}H_{95}N_2O_8$: 1427.7087 $[M+H]^+$; found: 1427.7083.

UV/vis (CH_2Cl_2): λ_{max}/nm (ε/M^{-1} cm^{-1}) = 280 (42600), 448 (9000), 623 (46800), 677 (91800).

Fluorescence (CH_2Cl_2): λ_{max} = 715 nm (λ_{ex} = 615 nm), Φ_{fl} = 0.28.

CV (CH_2Cl_2, 0.1 M TBAHFP, $vs.$ Fc/Fc$^+$): $E_{1/2}^{red}$ (X/X$^-$) = −1.15 V, $E_{1/2}^{ox}$ (X/X$^+$) = 0.50 V, $E_{1/2}^{ox}$ (X$^+$/X^{2+}) = 0.83 V.

N-(2,6-Diisopropylphenyl)-1,6,9,14-tetra(4-tert-butylphenoxy)terrylene-3,4:11,12-tetra-carboxylic acid-3,4-anhydride-11,12-imide (17)

This compound was synthesized according to the procedure reported for N-(2,6-diisopropylphenyl)-1,6,9,14-tetra-[4-(1,1,3,3-tetramethylbutyl)-phenoxy]terrylene-3,4:11,12-tetracarboxylic acid-3,4-an-hydride-11,12-imide.[18] A solution of N,N'-bis(2,6-diisopropylphenyl)-1,6,9,14-tetra(4-tert-butyl-phenoxy)terrylene-3,4:11,12-tetracarboxylic acid bisimide (**4**; 150 mg, 105 μmol) in 7 mL $tert$-butanol was heated to 80 °C under an argon atmosphere and subsequently a solution of potassium hydroxide (294 mg, 5.24 mmol) and potassium fluoride (304 mg, 5.23 mmol) in 16 mL hot $tert$-butanol was added to the reaction mixture. After heating for 45 min, 29 mL of 50% acetic acid were added to the hot mixture and stirred for additional 1 h. The reaction mixture was cooled down to room temperature and extracted with dichloromethane (3 × 20 mL), and the combined organic layers were dried over Na_2SO_4 and concentrated by rotary evaporation. The resultant green residue was purified by column chromatography on silica gel (CH_2Cl_2/n-hexane/acetic acid (160/40/1, v/v/v)) and the isolated product was dried at 10^{-3} mbar to yield 66.3 mg (52.3 μmol, 50%) of **8** as a dark green solid. Mp: > 400 °C (from dichloromethane).
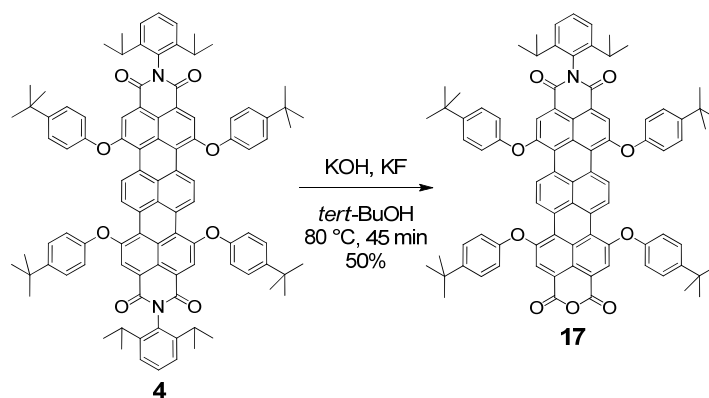
C$_{86}$H$_{77}$NO$_9$ (1268.574)

^{1}H NMR (400 MHz, CD$_2$Cl$_2$, 300 K): δ 9.49 (s, 4H), 8.21 (s, 2H), 8.12 (s, 2H), 7.43–7.50 (m, 9H), 7.30 (d, ^3J(H,H) = 7.8 Hz, 2H), 7.10–7.16 (m, 8H), 2.70 (sept, ^3J(H,H) = 7.0 Hz, 2H), 1.36 (s, 18H), 1.34 (s, 18H), 1.10 (d, ^3J(H,H) = 6.8 Hz, 12H).

^{13}C NMR (100 MHz, CD$_2$Cl$_2$, 300 K): δ 163.53, 159.90, 155.55, 155.21, 153.48, 153.37, 148.54, 148.41, 146.53, 131.51, 131.31, 131.19, 129.79, 129.69, 129.42, 128.96, 128.72, 127.80, 127.76, 127.07, 125.75, 124.39, 124.29, 123.44, 122.84, 119.60, 119.55, 117.44, 34.85, 34.84, 31.64, 31.62, 29.37, 24.15.

HRMS (ESI, pos. mode, acetonitrile/CHCl$_3$ 1:1): m/z: calcd for C$_{86}$H$_{78}$NO$_9$: 1268.5676 [M+H]$^+$; found: 1268.5671.

MS (MALDI, pos. mode, matrix DCTB 1:1 in CHCl$_3$): m/z: calcd for C$_{86}$H$_{77}$NO$_9$: 1267.560 [M]$^+$; found: 1267.548.

UV/vis (CH$_2$Cl$_2$): λ_{max}/nm (ε/M^{-1} cm^{-1}) = 445 (11500), 624 (50200), 679 (100100).

1-(6-Amino-2-methyl-1-benzo[*b*]thiophen-3-yl)-2-(2'-methyl-6'-nitro-1'-benzo[*b*]thiophen-3'-yl)-perfluorocyclopentene (20)

This compound was synthesized according to the procedure described for 4-amino-4'-nitrobiphenyl.[23] A solution of 1,2-bis-(2-methyl-6-nitro-benzo[*b*]thiophen-3-yl)-perfluorocyclopentene (**19**) (240 mg, 430 μmol) in 2.4 mL dry toluene and 4 mL dry methanol was heated under reflux and a solution of dried sodium hydrosulfide hydrate (121 mg, 1.64 mmol) in 9 mL dry methanol was added drop wise under an argon atmosphere. The reaction mixture was heated at the boiling point of the solvent mixture under stirring for additional 40 min. After cooling down to ambient temperature, 15 mL water and 5 mL brine were added to the reaction mixture and extracted with diethyl ether (5 × 15 mL). The combined layers were dried over Na$_2$SO$_4$ and the solvent was removed under vacuum. The crude product was purified by column chromatography on silica gel (*n*-hexane/ethyl acetate (3/1, v/v)) and dried at 10^{-3} mbar to yield 127 mg (241 μmol; 56%) of a brownish solid.
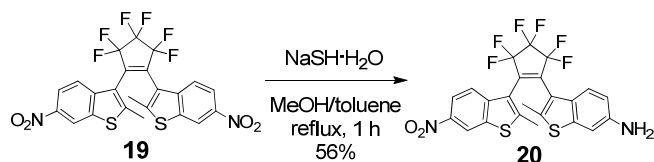
C$_{23}$H$_{14}$F$_6$NO$_2$S$_2$ (528.499)

^{1}H NMR (400 MHz, CD$_2$Cl$_2$, 300 K): δ 8.64 (s, 0.6H, ap), 8.57 (s, 0.4H, p), 8.22 (d, ^3J(H,H) = 8.8 Hz, 0.6H ap), 8.06 (d, ^3J(H,H) = 9.3 Hz, 0.4H, p), 7.74 (d, ^3J(H,H) = 9.2 Hz, 0.6H, ap), 7.64 (d, ^3J(H,H) = 8.9 Hz, 0.4H, p), 7.38 (d, ^3J(H,H) = 8.2 Hz, 0.6H, ap), 7.26 (d, ^3J(H,H) = 8.6 Hz, 0.4H, p), 6.95 (s, 0.6H, ap), 6.86 (s, 0.4H, p), 6.76 (d, ^3J(H,H) = 8.3 Hz, 0.6H, ap), 6.58 (d, ^3J(H,H) = 8.5 Hz, 0.4H, p), 3.84 (brs, 1.2H, ap), 3.75 (brs, 0.8H, p), 2.57 (s, 1.4H, p), 2.40 (s, 1.4H, p), 2.33 (s, 1.6H, ap), 2.13 (s, 1.6H, ap).

HRMS (ESI, pos. mode, acetonitrile/CHCl$_3$ 1:1): m/z: calcd for C$_{23}$H$_{14}$F$_6$NO$_2$S$_2$: 528.0400 [M]$^+$; found: 528.0396.

UV/vis (CH$_2$Cl$_2$): λ_{max}/nm (ε/M^{-1} cm^{-1}) = 289 (18000).

Photochromic dyad 2o

This compound was synthesized according to a similar procedure previously reported for a 1,7-dipyrrolidinyl-perylene bisimide-diarylethene conjugate.[1b] A mixture of 1-(6-amino-2-methyl-1-benzo[*b*]thiophen-3-yl)-2-(2'-methyl-6'-nitro-1'-benzo[*b*]thiophen-3'-yl)-perfluorocyclopentene (**20**) (77.0 mg, 146 μmol), *N*-(2,6-diisopropylphenyl)-1,6,9,14-tetra(4-*tert*-butylphenoxy)terrylene-3,4:11,12-tetracarboxylic acid-3,4-anhydride-11,12-imide (**17**; 104 mg, 81.6 μmol), 1.5 mL pyridine and 1.5 g imidazole was heated to 105 °C under an argon atmosphere for 8 h. Ethanol (5 mL) was carefully poured into the hot solution. The reaction mixture was then cooled down to room temperature and 20 mL dichloromethane and 10 mL aqueous HCl solution (2 N) were added. The layers were separated and the aqueous layer was extracted with dichloromethane (3 × 20 mL), dried over Na$_2$SO$_4$, and concentrated by rotary evaporation. The residue was purified by column chromatography on silica gel (CH$_2$Cl$_2$/*n*-hexane/acetic acid (350/150/1, v/v/v)) and the isolated product was dried at 10^{-3} mbar to yield 53.0 mg (29.8 μmol, 37%) of **2o** as a green solid. Mp: 278–279 °C (from dichloromethane).
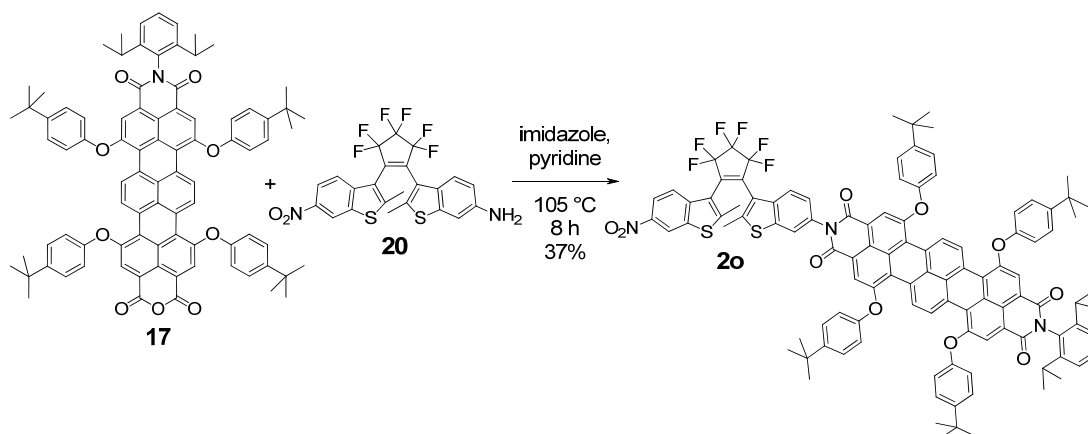
$C_{109}H_{89}F_6N_3O_{10}S_2$ (1779.057)

^{1}H NMR (400 MHz, CD_2Cl_2, 300 K): δ 9.47–9.54 (m, 4H), 8.65 (d, ^4J(H,H) = 2.1 Hz, 0.7H, ap), 8.58 (d, ^4J(H,H) = 1.6 Hz, 0.3H, p), 8.06–8.26 (m, 5H), 7.56–7.77 (m, 3H), 7.42–7.49 (m, 9H), 7.27–7.33 (m, 2.6H), 7.08–7.15 (m, 8.4H), 2.69 (sept, ^3J(H,H) = 6.9 Hz, 2H), 2.58 (s, 1H, p), 2.56 (s, 1H, p), 2.33 (s, 2H, ap), 2.26 (s, 2H, ap), 1.34 (s, 36H), 1.08 (d, ^3J(H,H) = 6.7 Hz, 12H).

HRMS (ESI, pos. mode, acetonitrile/$CHCl_3$ 3:1): m/z: calcd for $C_{109}H_{89}F_6N_3O_{10}S_2$: 1777.5891 $[M]^+$; found: 1777.5885.

MS (MALDI, pos. mode, matrix DCTB 1:1 in $CHCl_3$): m/z: calcd for $C_{109}H_{90}F_6N_3O_{10}S_2$: 1778.597 $[M+H]^+$; found: 1778.575.

UV/vis (CH_2Cl_2): λ_{max}/nm (ε/M^{-1} cm^{-1}) = 447 (8900), 624 (47000), 680 (92600).

Fluorescence (CH_2Cl_2): λ_{max} = 713 nm (λ_{ex} = 651 nm), Φ_{fl} = 0.29.

CV (CH_2Cl_2, 0.1 M TBAHFP, $vs.$ Fc/Fc$^+$): $E_{1/2}^{red}$ (X^-/X^{2-}) = −1.57 V, $E_{1/2}^{red}$ (X/X^-) = −1.12 V, $E_{1/2}^{ox}$ (X/X^+) = 0.52 V, $E_{1/2}^{ox}$ (X^+/X^{2+}) = 0.81 V.

Closed form photochromic dyad 2c

This compound was synthesized according to the procedure reported for the closed form of a 1,7-dipyrrolidinylperylene bisimide-diarylethene conjugate.[1b] A solution of the open form of dyad **2o** (50.0 mg, 28.1 μmol) in 250 mL dichloromethane was irradiated in a Rayonet photoreactor RPR-100 with UV light (350 nm) for 1 h under vigorous stirring. The solution was concentrated by rotary evaporation in the dark and the resultant precipitate was purified in the dark by column chromatography on silica gel (acetone/n-hexane (1/4, v/v)) and the isolated product was dried at 10^{-3} mbar to yield 38.8 mg (21.4 μmol; 78%) of **2c** as a dark green solid.
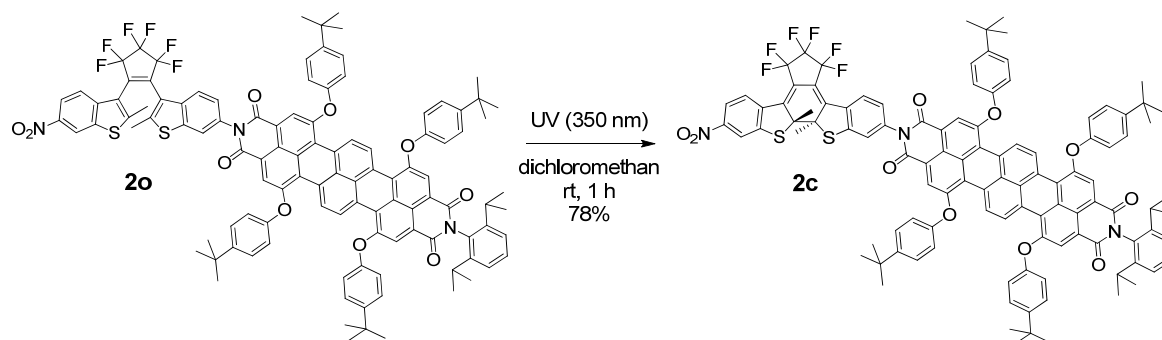
$C_{109}H_{89}F_6N_3O_{10}S_2$ (1779.057)

^{1}H NMR (600 MHz, CD_2Cl_2, 300 K): δ 9.43–9.49 (m, 4H), 8.21 (s, 2H), 8.13 (s, 2H), 8.09 (d, ^4J(H,H) = 2.2 Hz, 1H), 8.04 (d, ^3J(H,H) = 8.5 Hz, 1H), 8.01 (d, ^3J(H,H) = 8.9 Hz, 1H), 7.96 (dd, ^3J(H,H) = 8.9 Hz, ^4J(H,H) = 2.1 Hz, 1H), 7.41–7.48 (m, 9H), 7.30 (d, ^3J(H,H) = 7.9 Hz, 2H), 7.25 (d, ^4J(H,H) = 1.9 Hz, 1H), 7.09–7.13 (m, 9H), 2.69 (sept, ^3J(H,H) = 6.9 Hz, 2H), 2.10 (s, 3H), 2.08 (s, 3H), 1.34 (s, 18H), 1.33 (s, 18H),1.08 (d, ^3J(H,H) = 6.9 Hz, 12H).

HRMS (ESI, pos. mode, acetonitrile/$CHCl_3$ 3:1): m/z: calcd for $C_{109}H_{89}F_6N_3O_{10}S_2$: 1777.5891 $[M]^+$; found: 1777.5903.

UV/vis (CH_2Cl_2): λ_{max}/nm (ε/M^{-1} cm^{-1}) = 281 (56000), 369 (18700), 447 (12300), 626 (53100), 683 (99600).

Fluorescence (CH_2Cl_2): λ_{max} = 719 nm (λ_{ex} = 651 nm), Φ_{fl} = 0.10.

CV (CH_2Cl_2, 0.1 M TBAHFP, *vs.* Fc/Fc$^+$): E_{pp}^{red} (X^{2-}/X^{3-}) = –1.90 V, $E_{1/2}^{red}$ (X^-/X^{2-}) = –1.38 V, $E_{1/2}^{red}$ (X/X^-) = –1.12 V, $E_{1/2}^{ox}$ (X/X^+) = 0.52 V, $E_{1/2}^{ox}$ (X^+/X^{2+}) = 0.80 V.

Reference diarylethene 3o

The compound was synthesized according to the procedure described previously for the open form of another reference compound with phthalic imide residue.[1b] A solution of 1-(6-amino-2-methyl-1-benzo[*b*]thiophen-3-yl)-2-(2'-methyl-6'-nitro-1'-benzo[*b*]thiophen-3'-yl)-perfluorocyclopentene (**20**) (89.1 mg, 169 μmol), phthalic anhydride (50.4 mg, 340 μmol) in 1 mL pyridine and 1.0 g imidazole was heated to 120 °C under argon atmosphere for 8 h. The reaction mixture was cooled down to ambient temperature and 25 mL aqueous HCl solution (2 N) was added. The solution was extracted with dichloromethane (4 × 20 mL), combined organic layers were dried over Na_2SO_4, and the solvent was removed by rotary evaporation. The residue was purified by column chromatography on silica gel (*n*-hexane/ethyl acetate (3/1, v/v)), and dried at 10^{-3} mbar to yield 78.0 mg (118 μmol, 70%) of **3o** as a yellowish solid. Mp: 142–144 °C (from dichloromethane).
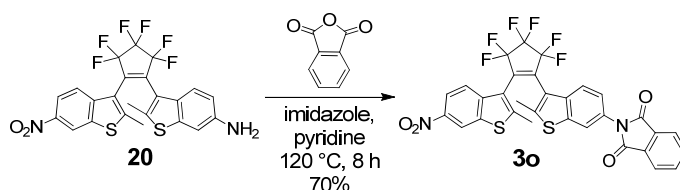
$C_{31}H_{16}F_6N_2O_4S_2$ (658.603)

^{1}H NMR (400 MHz, CD$_2$Cl$_2$, 300 K): δ 8.65 (d, ^4J(H,H) = 1.9 Hz, 0.6H, ap), 8.57 (d, ^4J(H,H) = 1.9 Hz, 0.4H, p), 8.25 (dd, ^3J(H,H) = 8.9 Hz, ^4J(H,H) = 2.1 Hz, 0.6H, ap), 8.09 (dd, ^3J(H,H) = 8.9 Hz, ^4J(H,H) = 2.0 Hz, 0.4H, p), 7.88–7.97 (m, 2H), 7.73–7.86 (m, 4H), 7.70 (d, ^3J(H,H) = 8.5 Hz, 0.6H, ap), 7.60 (d, ^3J(H,H) = 8.4 Hz, 0.4H, p), 7.49 (dd, ^3J(H,H) = 8.7 Hz, ^4J(H,H) = 1.8 Hz, 0.6H, ap), 7.31 (dd, ^3J(H,H) = 8.6 Hz, ^4J(H,H) = 1.8 Hz, 0.4H, p), 2.58 (s, 1.2H, p), 2.55 (s, 1.2H, p), 2.37 (s, 1.8H, ap), 2.26 (s, 1.8H, ap).

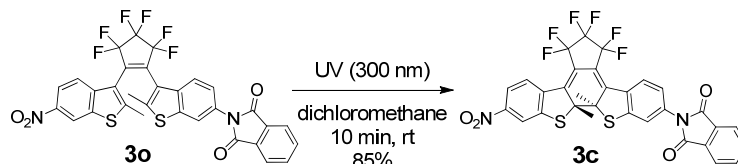**HRMS** (ESI, pos. mode, acetonitrile/CHCl$_3$ 1:1): m/z: calcd for C$_{31}$H$_{17}$F$_6$N$_2$O$_4$S$_2$: 659.0533 [M+H]$^+$; found: 659.0529.

UV/vis (CH$_2$Cl$_2$): λ_{max}/nm (ε/M^{-1} cm^{-1}) = 278 (23500), 295 (18700).

CV (CH$_2$Cl$_2$, 0.1 M TBAHFP, *vs*. Fc/Fc$^+$): E_{pp}^{red} (X$^-$/X^{2-}) = −1.96 V, $E_{1/2}^{red}$ (X/X$^-$) = −1.53 V.

Closed form of reference diarylethene 3c

The compound was synthesized according to the procedure described previously for the closed form of another reference compound with phthalic imide residue.[1b] A solution of **3o** (49.6 mg, 75.3 μmol) in 200 mL dichloromethane was irradiated in a Rayonet photoreactor RPR-100 with UV light (300 nm) for 10 min under vigorous stirring. The solution was concentrated by rotary evaporation in the dark and the resultant precipitate was purified in the dark by column chromatography on silica gel (*n*-hexane/dichloromethane (1/1, v/v)) and the isolated product was dried at 10^{-3} mbar to yield 42.0 mg (63.8 μmol; 85%) of **3c** as a deep magenta solid.

C$_{31}$H$_{16}$F$_6$N$_2$O$_4$S$_2$ (658.603)

^{1}H NMR (600 MHz, CD$_2$Cl$_2$, 300 K): δ 8.10 (dd, ^4J(H,H) = 2.2 Hz, ^5J(H,H) = 0.4 Hz, 1H), 8.06 (d, ^3J(H,H) = 8.6 Hz, 1H), 8.01 (d, ^3J(H,H) = 8.6 Hz, 1H), 7.95–7.99 (m, 3H), 7.83–7.87 (m, 2H), 7.51 (dd, ^4J(H,H) = 2.0 Hz, ^5J(H,H) = 0.3 Hz, 1H), 7.38 (dd, ^3J(H,H) = 8.7 Hz, ^4J(H,H) = 2.0 Hz, 1H), 2.10 (s, 3H), 2.08 (s, 3H).

HRMS (ESI, pos. mode, acetonitrile/CHCl$_3$ 1:1): m/z: calcd for C$_{31}$H$_{16}$F$_6$N$_2$O$_4$S$_2$: 658.0455 [M]$^+$; found: 658.0451.

MS (MALDI, pos. mode, matrix DCTB 1:3 in CHCl$_3$): m/z: calcd for C$_{31}$H$_{16}$F$_6$N$_2$O$_4$S$_2$: 658.046 [M]$^+$; found: 658.038.

UV/vis (CH$_2$Cl$_2$): λ_{max}/nm (ε/M^{-1} cm^{-1}) = 282 (17100), 372 (14600), 558 (11300).

CV (CH$_2$Cl$_2$, 0.1 M TBAHFP, *vs*. Fc/Fc$^+$): $E_{1/2}^{red}$ (X^{4-}/X^{5-}) = −1.95 V, E_{pp}^{red} (X^{3-}/X^{4-}) = −1.74 V, E_{pp}^{red} (X^{2-}/X^{3-}) = −1.69 V, E_{pp}^{red} (X$^-$/X^{2-}) = −1.39 V, E_{pp}^{red} (X/X$^-$) = −1.19 V, $E_{1/2}^{ox}$ (X/X$^+$) = 1.14 V.

4.8   References

[1]   a) M. Berberich, Diploma Thesis, University of Würzburg, Würzburg (Germany), **2007**; b) M. Berberich, A.-M. Krause, M. Orlandi, F. Scandola, F. Würthner, *Angew. Chem. Int. Ed.* **2008**, *47*, 6616-6619.

[2]   T. Weil, T. Vosch, J. Hofkens, K. Peneva, K. Müllen, *Angew. Chem. Int. Ed.* **2010**, *49*, 9068-9093.

[3]   a) H. Langhals, S. Poxleitner, *Eur. J. Org. Chem.* **2008**, 797-800; b) Y. Avlasevich, C. Li, K. Müllen, *J. Mater. Chem.* **2010**, *20*, 3814-3826; c) J. E. Bullock, M. T. Vagnini, C. Ramanan, D. T. Co, T. M. Wilson, J. W. Dicke, T. J. Marks, M. R. Wasielewski, *J. Phys. Chem. B* **2010**, *114*, 1794-1802; d) Q. Bai, B. Gao, Q. Ai, Y. Wu, X. Ba, *Org. Lett.* **2011**, *13*, 6484-6487.

[4]   a) R. Métivier, F. Nolde, K. Müllen, T. Basché, *Phys. Rev. Lett.* **2007**, *98*, 047802; b) M. Haase, C. G. Hübner, F. Nolde, K. Müllen, T. Basché, *Phys. Chem. Chem. Phys.* **2011**, *13*, 1776-1785.

[5]   a) T. Weil, E. Reuther, K. Müllen, *Angew. Chem. Int. Ed.* **2002**, *41*, 1900-1904; b) M. Cotlet, R. Gronheid, S. Habuchi, A. Stefan, A. Barbafina, K. Müllen, J. Hofkens, F. C. De Schryver, *J. Am. Chem. Soc.* **2003**, *125*, 13609-13617; c) T. Weil, E. Reuther, C. Beer, K. Müllen, *Chem. Eur. J.* **2004**, *10*, 1398-1414; d) J. Kirstein, B. Platschek, C. Jung, R. Brown, T. Bein, C. Bräuchle, *Nat. Mater.* **2007**, *6*, 303-310; e) C. Jung, J. Kirstein, B. Platschek, T. Bein, M. Budde, I. Frank, K. Müllen, J. Michaelis, C. Bräuchle, *J. Am. Chem. Soc.* **2008**, *130*, 1638-1648.

[6]   a) C. Jung, B. K. Müller, D. C. Lamb, F. Nolde, K. Müllen, C. Bräuchle, *J. Am. Chem. Soc.* **2006**, *128*, 5283-5291; b) K. Peneva, G. Mihov, F. Nolde, S. Rocha, J.-i. Hotta, K. Braeckmans, J. Hofkens, H. Uji-i, A. Herrmann, K. Müllen, *Angew. Chem. Int. Ed.* **2008**, *47*, 3372-3375; c) C. Jung, N. Ruthardt, R. Lewis, J. Michaelis, B. Sodeik, F. Nolde, K. Peneva, K. Müllen, C. Bräuchle, *ChemPhysChem* **2009**, *10*, 180-190; d) M. Davies, C. Jung, P. Wallis, T. Schnitzler, C. Li, K. Müllen, C. Bräuchle, *ChemPhysChem* **2011**, *12*, 1588-1595.

[7]   a) W. Pisula, M. Kastler, D. Wasserfallen, J. W. F. Robertson, F. Nolde, C. Kohl, K. Müllen, *Angew. Chem. Int. Ed.* **2006**, *45*, 819-823; b) F. Nolde, W. Pisula, S. Müller, C. Kohl, K. Müllen, *Chem. Mater.* **2006**, *18*, 3715-3725.

[8]   T. L. Andrew, T. M. Swager, *Macromolecules* **2011**, *44*, 2276-2281.

[9]   T. Ren, P. K. Mandal, W. Erker, Z. Liu, Y. Avlasevich, L. Puhl, K. Müllen, T. Basché, *J. Am. Chem. Soc.* **2008**, *130*, 17242-17243.

[10]   C. Liu, Z. Liu, H. T. Lemke, H. N. Tsao, R. C. G. Naber, Y. Li, K. Banger, K. Müllen, M. M. Nielsen, H. Sirringhaus, *Chem. Mater.* **2010**, *22*, 2120-2124.

[11]   J. Gorenflot, A. Sperlich, A. Baumann, D. Rauh, A. Vasilev, C. Li, M. Baumgarten, C. Deibel, V. Dyakonov, *Synth. Met.* **2012**, *161*, 2669-2676.

[12]   M. Könemann, P. Blaschka, H. Reichelt (BASF AG) DE 10 2004 054 303 A1, **2006**.

[13]   H. Langhals, L. Feiler (Ciba Specialty Chemicals Holding Inc) EP 0657 436 B1, **2001**.

[14]   Y. Avlasevich, K. Müllen, *J. Org. Chem.* **2007**, *72*, 10243-10246.

[15]   S. N. Naik, A. M. Dhalla, Y. B. Chauhan (Cantorcolburn LCP-GE Plastics-Smith) US 2007/117887 A1, **2007**.

[16]   F. Nolde, J. Qu, C. Kohl, N. G. Pschirer, E. Reuther, K. Müllen, *Chem. Eur. J.* **2005**, *11*, 3959-3967.

[17]   T. Sakamoto, C. Pac, *J. Org. Chem.* **2001**, *66*, 94-98.

[18]   N. G. Pschirer, J. Qu, M. Könemann (BASF AG) DE 10 2005 021 362 A1, **2006**.

[19]   M. Hanazawa, R. Sumiya, Y. Horikawa, M. Irie, *J. Chem. Soc., Chem. Commun.* **1992**, 206-207.

[20]   a) E. Kim, M. Kim, K. Kim, *Tetrahedron* **2006**, *62*, 6814-6821; b) S. Kobatake, M. Yamada, T. Yamada, M. Irie, *J. Am. Chem. Soc.* **1999**, *121*, 8450-8456.

[21]   M. Takeshita, M. Yamada, N. Kato, M. Irie, *J. Chem. Soc., Perkin Trans. 2* **2000**, 619-622.

[22]   J. P. Idoux, *J. Chem. Soc. C* **1970**, 435-437.

[23]   D. A. Lemenovskii, M. V. Makarov, V. P. Dyadchenko, A. E. Bruce, M. R. M. Bruce, S. A. Larkin, B. B. Averkiev, M. Starikova, M. Y. Antipin, *Russ. Chem. Bull. Int. Ed.* **2003**, *52*, 607-615.

[24]   a) P. Osswald, F. Würthner, *Chem. Eur. J.* **2007**, *13*, 7395-7409; b) E. Fron, G. Schweitzer, P. Osswald, F. Würthner, P. Marsal, D. Beljonne, K. Müllen, F. C. De Schryver, M. Van der Auweraer, *Photochem. Photobiol. Sci.* **2008**, *7*, 1509-1521.

[25]   C. Reichardt, *Solvents and Solvent Effects in Organic Chemistry*, 3rd ed., Wiley-VCH, Weinheim, **2003**.

[26]   A. Z. Weller, *Z. Phys. Chem.* **1982**, *133*, 93-98.

[27]   N. Tamai, H. Miyasaka, *Chem. Rev.* **2000**, *100*, 1875-1890.

[28]   K. Matsuda, M. Irie, *Tetrahedron Lett.* **2000**, *41*, 2577-2580.

[29]   D. L. Dexter, *J. Chem. Phys.* **1953**, *21*, 836-850.

[30]   M. Berberich, F. Würthner, *Chem. Sci.* **2012**, *3*, 2771-2777.

[31]   M. Heilemann, P. Dedecker, J. Hofkens, M. Sauer, *Laser & Photon. Rev.* **2009**, *3*, 180-202.

[32]   a) R. Gvishi, R. Reisfeld, Z. Burshstein, *Chem. Phys. Lett.* **1993**, *213*, 338-344; b) *Principles of Fluorescence Spectroscopy* (ed. J. R. Lakowitz), 2nd ed., Kluwer Academic/Plenum, New York, **1999**, pp. 52-55.

[33]   A. J. Fry, *Laboratory Techniques in Electroanalytical Chemistry* (eds. P. T. Kessing, W. R. Heinemann), 2nd ed., Marcel Dekker Ltd, New York, **1996**, p. 481.

5   Perylene Bisimide-Diarylethene Containing Photochromic Dyad[b]
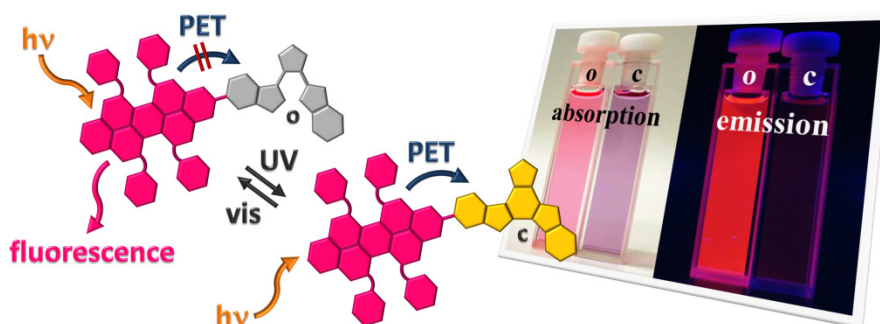
5.1   Introduction

While fluorophores with emission between 650 and 850 nm and a photochrome with absorption of the closed, colored form between 500 and 600 nm were used for our previous work[1] (compound **1o** in Scheme 1) and the terrylene bisimide system (see Chapter 4),[2] the use of aryloxy-substituted PBI dyes, which emit between 550 and 750 nm requires a distinct hypsochromic shift of the absorption of the closed form of the switching unit. 1,6,7,12-Tetraaryloxy-substituted PBI dyes are well-known for their outstanding photostability and fluorescence quantum yields close to 100 % and should therefore be suitable as emitter unit for an improved photochromic system.[3] However, their oxidation potential is higher, thus a DAE derivative with stronger electron acceptor character was needed to achieve the required driving force for PET, besides the desired optical changes.
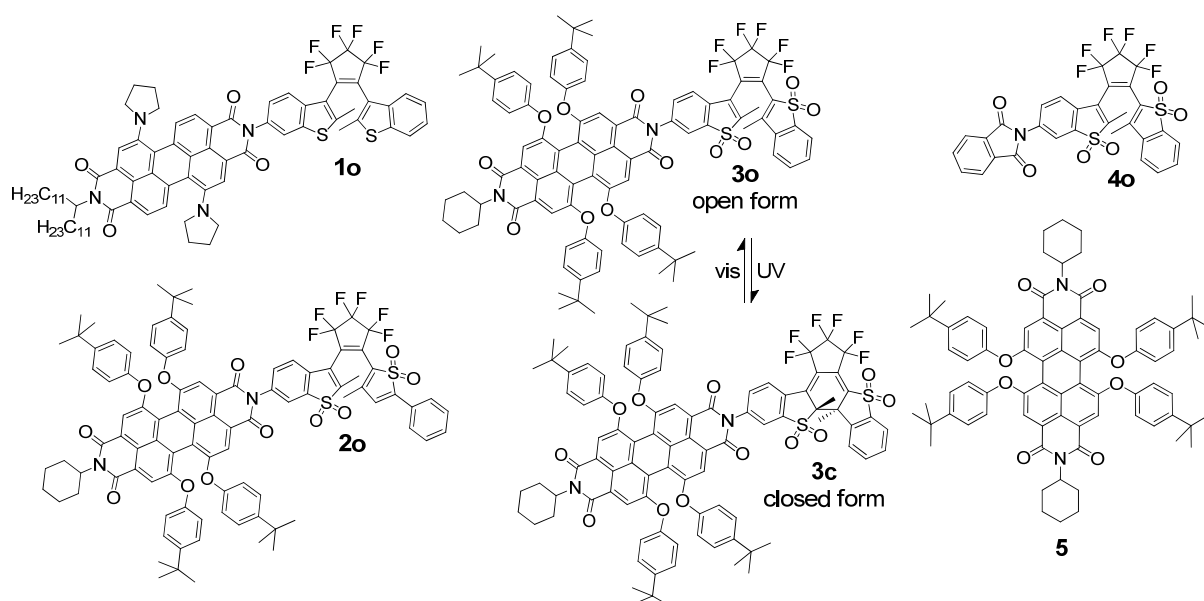
**Scheme 1.** Photochromic dyad **1o**,[1] **2o**,[4] and **3o/3c**, and reference compounds **4o** and **5**.

PBI chromophores are attractive as electron donors or acceptors and their optical and redox properties can easily be tuned over a wide range by judicious alteration of substituents at the bay areas (1,6,7,12-positions).[3b,c,3e,5] These desirable properties have made especially 1,7-di- and 1,6,7,12-tetraaryloxy-substituted PBIs popular building blocks for the spectroscopic investigation of energy or electron-transfer processes in artificial light-harvesting arrays that are self-assembled in solution or on surfaces.[6]

In a first step, dyad **2o** (Scheme 1) that contains an unsymmetrically substituted DAE derivative bearing a benzo[*b*]thiophene 1,1-dioxide and a phenylthiophene 1,1-dioxide subunit was synthesized. This DAE derivate was also used previously by the Irie group in their photochromic dyad,[4,7] however, such 3-methyl-5-phenyl-thiophene units were reported to have low stability upon irradiation.[8] Unfortunately, in dyad **2o** this photochromic DAE unit is shown to be unstable under irradiation with visible light (see Chapter 4.3), and thus photoswitching properties of dyad **2o** could not be explored. Therefore, dyad **3o/3c** containing a highly stable DAE photoswitch, with two benzo[*b*]thiophene 1,1-dioxide units substituted, where the ring-closed isomer is a considerably better electron acceptor than the ring-open isomer, and a highly fluorescent tetraaryloxy-substituted PBI chromophore with a matched oxidation potential to facilitate electron transfer to the ring-closed DAE was synthesized. Furthermore, reference DAE **4o** and reference PBI **5** were synthesized and characterized for a complete investigation and comparison of the new photochromic system **3o/3c**.

5.2   Synthesis of Target Compound and Reference Molecules

The synthesis of reference PBI **5** and the tetraaryloxy-substituted perylene anhydride imide **6** as the emissive part of the dyad systems **2** and **3** started with a condensation reaction[c] of tetrachloro-substituted perylene bisanhydride **7** with cyclohexylamine in imidazole (Scheme 2).[9]
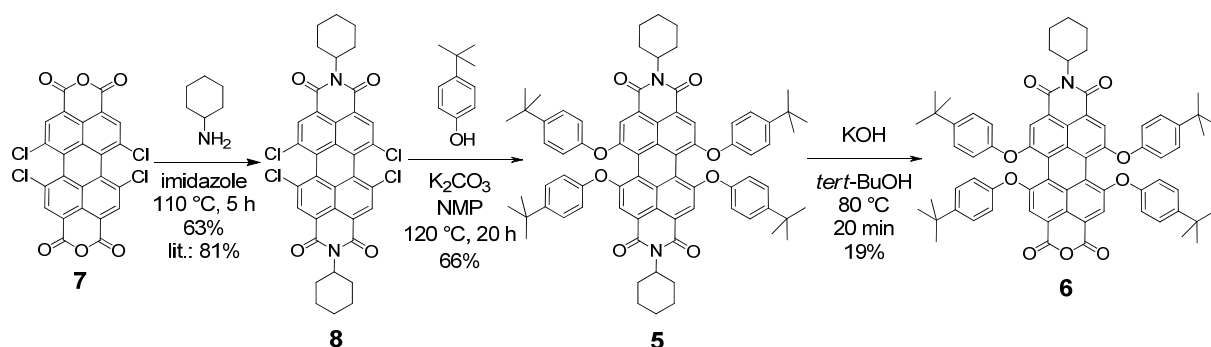
Scheme 2. Synthesis of tetraphenoxy-substituted perylene anhydride imide **6**; NMP = *N*-methyl-2-pyrrolidone.

The chlorine atoms of the poorly soluble PBI **8** were subsequently replaced by 4-*tert*-butylphenoxy groups under basic conditions in dry *N*-methyl-2-pyrrolidone to receive reference PBI **5** in a yield of 66%. One of the imides of PBI **5** was converted to an anhydride in an alkaline hydrolysis resulting in

---

[c] Procedure known for this compound with other conditions and without purification by chromatography.

perylene anhydride imide **6** in a poor yield of only 19%, while the bisimide and the bisanhydride were also isolated.

The synthesis of the part of the photochromic precursor with an amino group, which is same for compounds **2o** and **3o**, started with the reaction of perfluorocyclopentene and the lithiated 3-bromo-2-methylbenzo[*b*]thiophene[10] (**9**). 2-Methylbenzo[*b*]thiophen-3-yl-perfluorocyclopentene (**10**) was synthesized according to the procedure described for its constitutional isomer 3-methylbenzo[*b*]thiophen-2-yl-perfluorocyclopentene in which the lithiated benzo[*b*]thiophene was added to a solution of the volatile perfluorocyclopentene in THF to favor the reaction of only one aromatic moiety with the bridging unit (Scheme 3).[11]
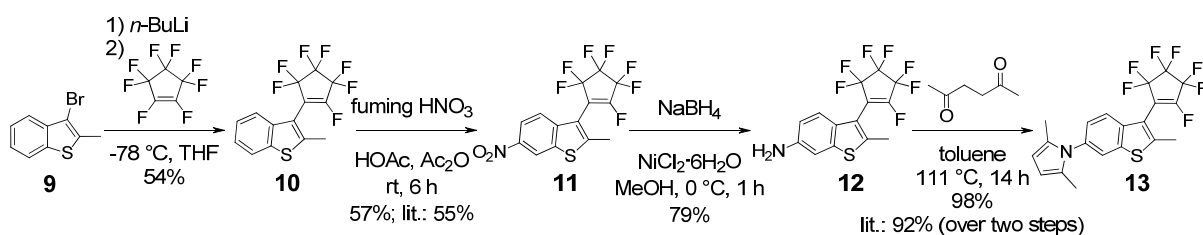
Scheme 3. Synthesis of diarylethene precursor **13** according to literature procedure.[4,11]

The following nitration with fuming nitric acid, reduction of the resulting nitro function using sodium borohydride and protection of the aromatic amino-group with hexane-2,5-dione forming a pyrrole as protective group by Paal-Knorr synthesis gave the precursor **13** according to the literature.[4]

Two possible routes for the synthesis of the second thiophene moiety **14** for the literature known DAE unit of dyad **2o** are depicted in Scheme 4.
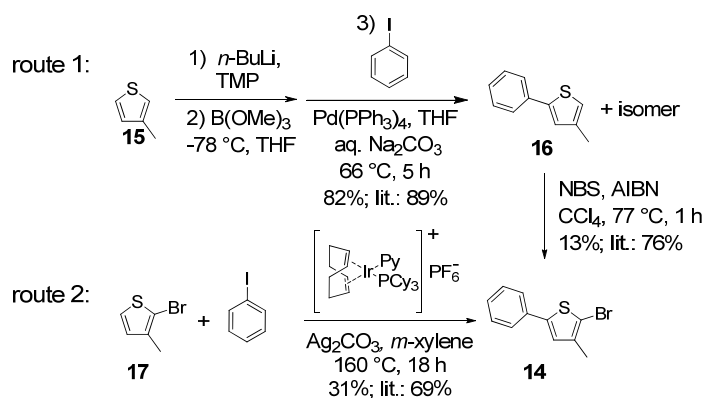
Scheme 4. Two paths for the synthesis of 2-bromo-3-methyl-5-phenylthiophene **14**; AIBN = azobisisobutyronitrile, Cy = cyclohexyl, NBS = *N*-bromosuccinimide, Py = pyridinyl, TMP = 2,2,6,6-tetra-methylpiperidine.

On the one hand, the synthesis of 2-bromo-3-methyl-5-phenylthiophene (**14**) can be initiated by the lithiation of 3-methylthiophene (**15**) in 5-position by the help of sterically demanding 2,2,6,6-tetra-methylpiperidine. A borate ester of the thiophene was formed by adding trimethyl borate, which was

in situ coupled with iodobenzene by a Pd-catalyzed Suzuki-Miyaura reaction. 3-Methyl-5-phenyl-thiophene (**16**) and its isomer 3-methyl-2-phenylthiophene could not be separated by column chromatography.[12] The subsequent bromination with *N*-bromosuccinimide gave the isomer-free 2-bromo-3-methyl-5-phenylthiophene (**14**) in a poor yield of only 13% (lit.: 76%).[13] A direct iridium-catalyzed coupling of iodobenzene and 2-bromo-3-methyl-thiophene (**17**) gave the product **14** in a yield of 31% (lit.: 69%).[14]

2-Bromo-3-methyl-5-phenylthiophene (**14**) was lithiated and a solution of the second building block **13** was gradually added forming the photochromic precursor with pyrrole-protected amino group **18**, which was finally cleaved under basic conditions (Scheme 5).[4]
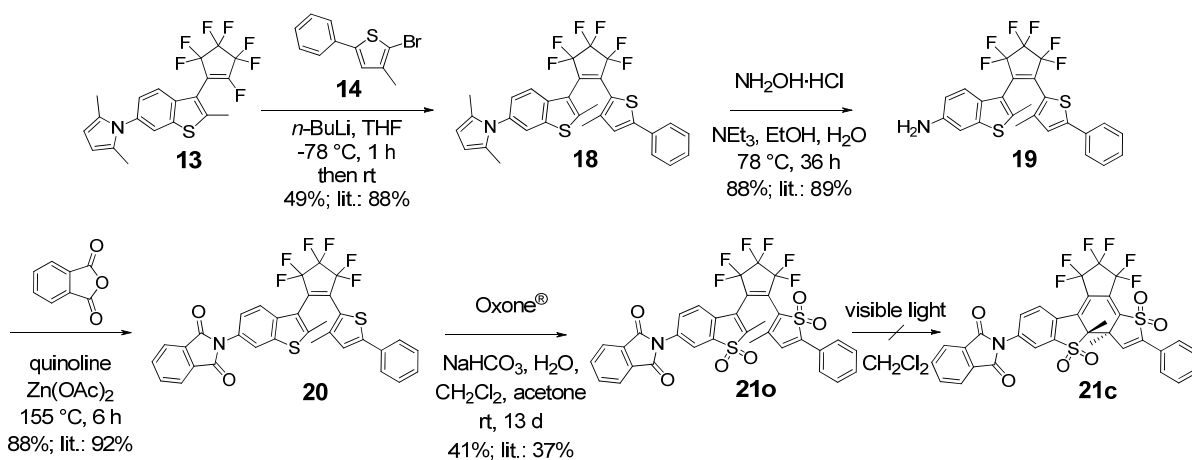

Scheme 5. Synthesis of DAE precursor **19** according to literature procedure[4] and reference DAE **21o**; Oxone® = $2KHSO_5 \cdot KHSO_4 \cdot K_2SO_4$, THF = tetrahydrofuran.

The amino-group of the diarylethene **19** and phthalic anhydride were subsequently condensed and the sulfur atoms of the precursor **20** were oxidized in a concluding step using Oxone® ($2KHSO_5 \cdot KHSO_4 \cdot K_2SO_4$) in a water-dichloromethane-acetone solvent mixture according to a literature procedure reported for the oxidation of a similar benzo[*b*]thiophene compound.[15] The mild and neutral oxidation reagent Oxone® was used in preference to acidic *m*CPBA,[16] to avoid the formation of side products.

In contrast to the majority of diarylethenes, whose ring closure is induced upon irradiation with UV light, visible light must be used for compound **21o**.[4] Surprisingly, irradiation of a solution of reference compound **21o** in dichloromethane leads only to a small proportion of the closed form in the mixture of both forms (see spectroscopic part in Chapter 4.3), which is in accordance with the literature.[4]

For the synthesis of the new photochromic unit with two benzo[*b*]thiophene residues, the pyrrole-protected precursor **13**[4] was reacted with lithiated 2-bromo-3-methylbenzo[*b*]thiophene (**22**) to afford photochromic precursor **23** in 54% yield (Scheme 6).
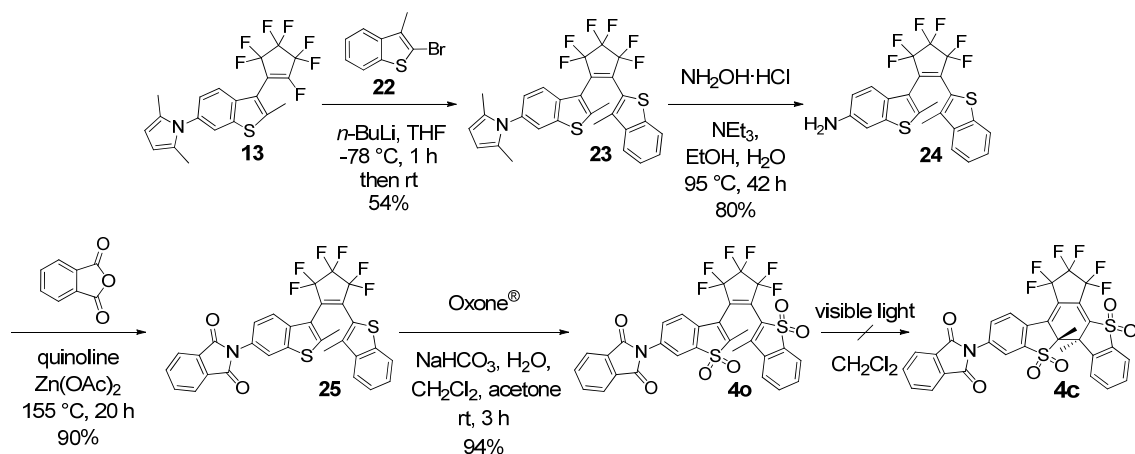
Scheme 6. Synthesis of reference photochrome **4o**; Oxone® = 2KHSO$_5$•KHSO$_4$•K$_2$SO$_4$, THF = tetrahydrofuran.

The pyrrole-protected amino group in **23** was deprotected by treatment with hydroxylamine under basic conditions to obtain compound **24**, which was further used for the synthesis of reference diarylethene **4o** and the target dyad **3o**. The condensation reaction of **24** with phthalic anhydride to the photochrome **25** and subsequent oxidation of the sulfur atoms in **25** with Oxone® (2KHSO$_5$•KHSO$_4$•K$_2$SO$_4$) afforded the reference DAE **4o** in very high yield. This time, the ring closure was initiated upon irradiation of the open form **4o** with UV light, which is common practice for most diarylethenes,[17] but once again did not lead to a distinct accumulation of closed form isomer **4c** (see spectroscopic part in Chapter 4.3), which could not be separated from the open form.

The synthetic route to photochromic system **2o** started with the imidization of perylene anhydride imide **6** with the literature known amino group containing photochrome **19** in imidazole and gave the condensation product **26** in 73% yield (left branch in Scheme 7). Compound **26** was then oxidized with Oxone® yielding the unstable dyad **2o** in only 11%, which decomposed continuously during the purification step by column chromatography. It was not possible to isolate pure closed form **2c** after irradiation of a dichloromethane solution of **2o** because of its low stability under ambient conditions.

The condensation of the new amino group containing photochrome **24** with perylene anhydride imide **6** in imidazole afforded the dyad precursor **27** in 69% yield and the subsequent oxidation of the latter with Oxone® yielded the target open-form dyad **3o** in 67% yield (right branch in Scheme 7). UV irradiation (350 nm) of ring-open isomer **3o** in dichloromethane leads to the formation of ring-closed isomer **3c**. The closed form **3c** (69%) could be easily separated from the remaining open form (28%) by column chromatography with silica gel under exclusion of light. The synthetic details and the characterization data of all new compounds are given in the Experimental Section (see Chapter 5.7.2).
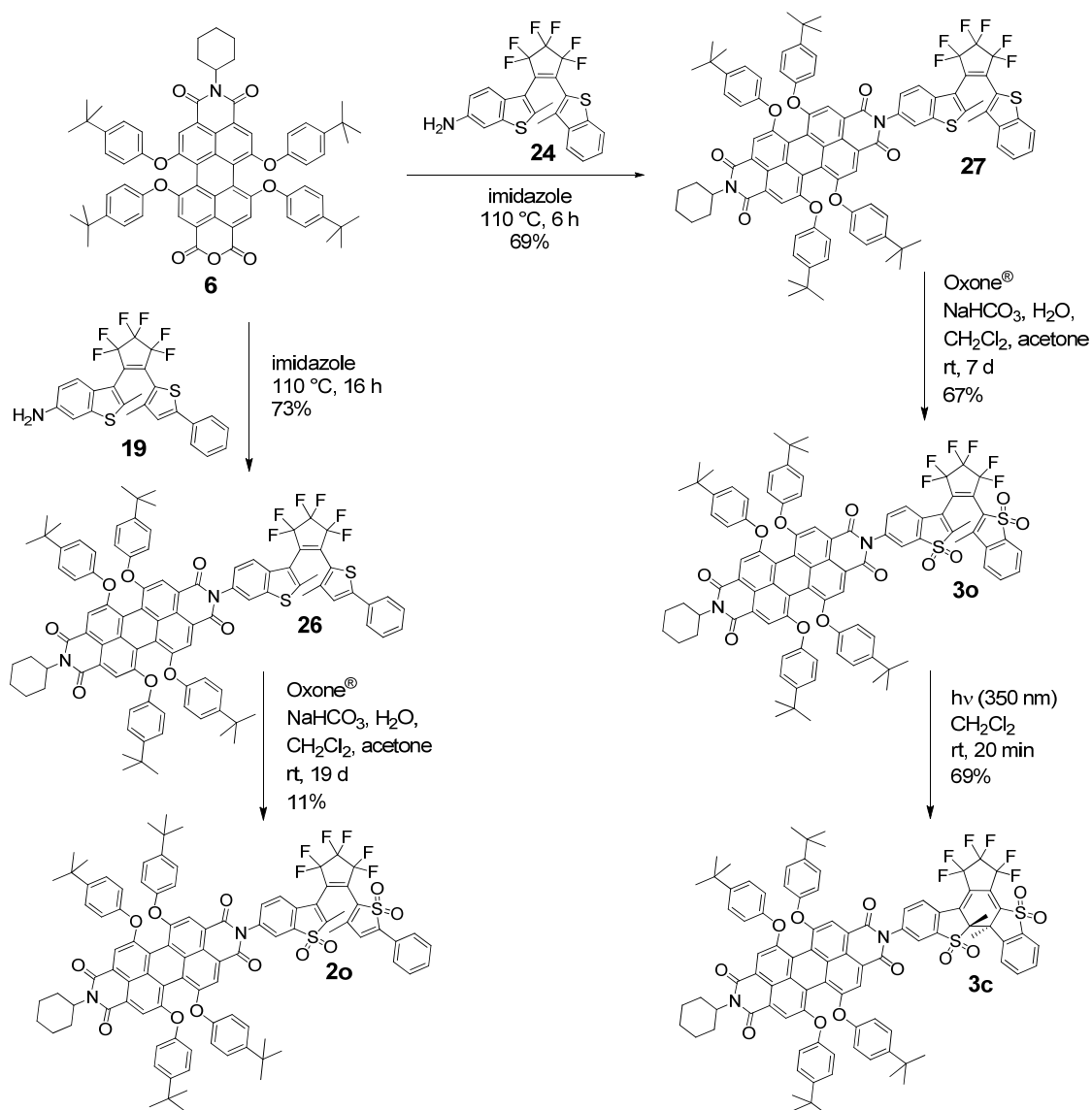
Scheme 7. Synthesis of photochromic dyads **2o** and **3o/3c**; Oxone$^{®}$ = 2KHSO$_5$•KHSO$_4$•K$_2$SO$_4$.

5.3   Absorption and Emission Spectroscopy

UV/vis investigations of dyad **2o** that bears a benzo[*b*]thiophene 1,1-dioxide and a phenyl-thiophene 1,1-dioxide group at the photochromic moiety were performed (Figure 1). The absorption spectrum of **2o** in dichloromethane in the visible region is very similar to that of reference PBI dye **5**. An additional band, compared to PBI **5**, is observed at 369 nm that can be attributed to the open form of the photochromic moiety of this dyad. Upon irradiation with visible light (> 400 nm) for 80 min (see Figure 1a), this band increases owing to the more pronounced absorption of the closed form of this DAE in this wavelength range resulting in a 53 : 47 ratio of **2o** and **2c** according to ^{1}H NMR analysis.
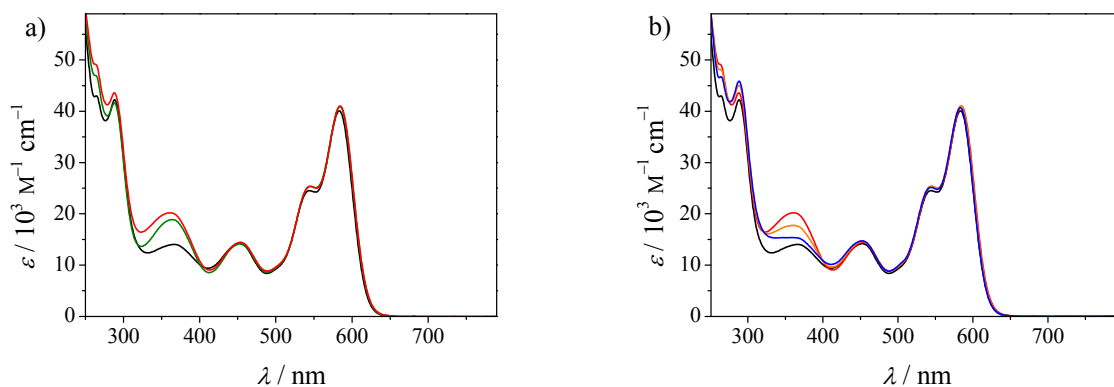
Figure 1. (a) UV/vis absorption spectra of dyad **2o** (black line), the same solution upon irradiation with visible light (> 400 nm) (green line) and the irradiated solution after 15 h in the dark (red line); (b) UV/vis absorption spectra of dyad **2o** (black line), the same solution upon irradiation with visible light (> 400 nm) stored for 15 h in the dark (red line) and after irradiation with UV light (365 nm) for 4 min (orange line) and 14 min (blue line). Studies were performed with a dichloromethane solution of **2o** (1×10^{-5} M) at 25 °C.

This visible-light irradiated solution of **2o** in dichloromethane was stored for 15 h in the dark, and during this time, absorption in the UV region increased further with a hypsochromic shift of the maximum at 365 nm. Fukaminato used UV light of 365 nm to open the ring-closed form of this photochromic unit.[4] Using the same wavelength, the spectrum of **2o** was not fully recovered (see Figure 1b). The observation clearly indicates that UV light irradiation of ring-closed dyad **2c** did not exclusively lead to its ring-open form **2o**, or another photostationary state composed of **2o** and **2c**, and thus the spectral changes observed in the region between 300 and 400 nm upon irradiation with UV light are instead due to decomposition of dyad **2o**. Therefore, no further investigations were performed with dyad **2o** and studies to prove the stability of system **3o**/**3c** were initially carried out.

Unlike dyad **2o**, the ring closure of dyad **3o** takes place upon irradiation with UV light, and the closed form **3c** can be reopened by visible light (> 400 nm), which is a common behavior for diarylethenes.[17] Switching cycles of **3o** in dichloromethane show the increased photostability of this photochromic dyad compared to our previous systems **1o**/**1c**[1] and **2o**/**2c** (Figure 2). The emission intensity can be switched between a high (around 80% open form and 20% closed form) and a less emissive state (around 25% open form and 75% closed form) with approximately 38% of the intensity of the higher emissive state. Even after ten cycles, the emission returns to the original value and no decomposition occurs.
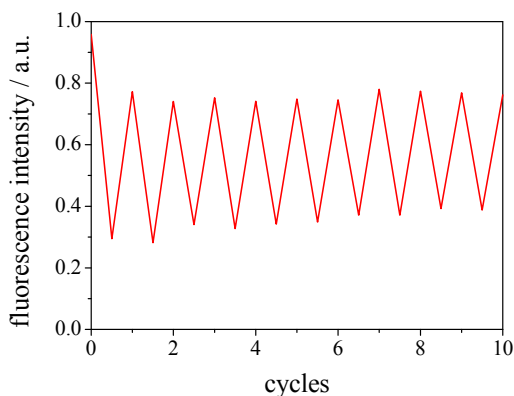
Figure 2. Switching cycles of **3o** recorded by means of the fluorescence intensity at 650 nm in dichloromethane upon alternating irradiation with UV light at 320 nm (±10 nm FWHM; xenon arc lamp, 150 W) and visible light (cut-off filter at 395 nm; xenon arc lamp, 175 W); FWHM = full width half maximum.[d]
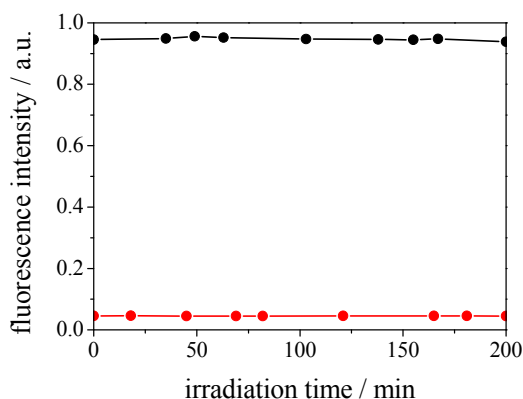

Figure 3. Fluorescence intensity at 650 nm of **3o** (black dots) and **3c** (red dots) in dichloromethane upon continuing excitation with monochromatic light at 600 nm (±10 nm FWHM; xenon short arc lamp, 75 W, 6.9 mW/cm^2); FWHM = full width half maximum.

The non-destructive read-out capability was shown by enduring excitation of the fluorophore unit of **3o** and **3c** at 600 nm in dichloromethane (Figure 3). The emission intensity of **3o** and **3c** remained constant over the time range of more than 3 h of intense irradiation of the PBI fluorophore at 600 nm. This observation evidences that excitation of the PBI unit does not lead to decomposition or an unfavorable ring-closure process of **3o** or a just as disadvantageous ring opening of **3c**.

Absorption spectra of **3o**, **3c**, and reference PBI dye **5** were measured in dichloromethane (Figure 4). The absorption maximum is bathochromically shifted by about 10 nm for both ring-open (**3o**) and ring-closed (**3c**) dyads compared to PBI **5** and the closed form exhibits a noticeable higher extinction, which is in accordance with our previous observation (see Figure 5a–d for single absorption and emission spectra of **2o**, **3o**, **3c**, and **5**).[1] The emission maximum of PBI chromophore ($\lambda_{em} = 604$ nm) is likewise bathochromically shifted by 10 nm for **3o** and **3c** (see Table 1).

---

[d] These measurements were performed in the group of Prof. F. Scandola at the University of Ferrara.
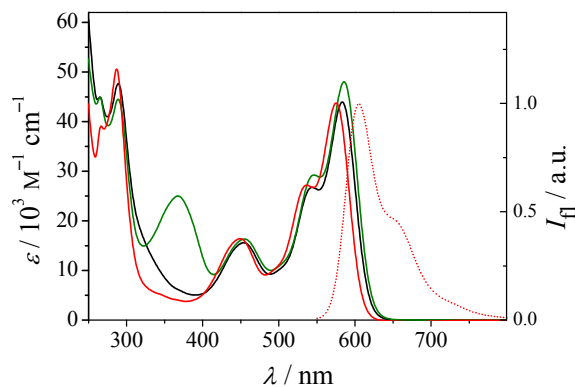
Figure 4. UV/vis absorption spectra of dyads **3o** (black line) and **3c** (green line) and reference PBI dye **5** (red line) in dichloromethane (1×10^{-5} M) at 25 °C and fluorescence emission spectrum of reference **5** (red dotted line; λ_{ex} = 530 nm) in dichloromethane.
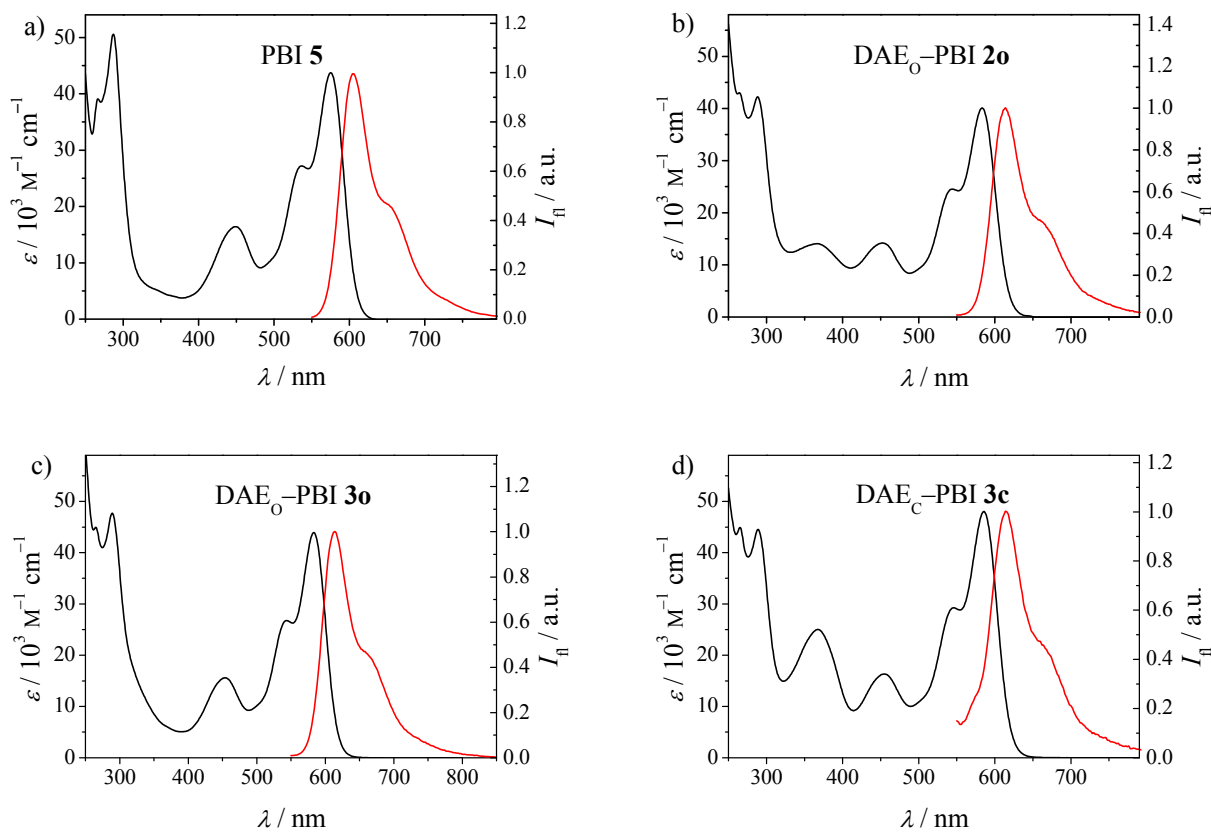

Figure 5. UV/vis absorption (black line, 10^{-5} M) and fluorescence emission (red line, λ_{ex} = 530 nm) spectra of (a) reference PBI **5**, (b) dyad **2o**, (c) open form dyad **3o** and (d) closed form dyad **3c** in dichloromethane at 25 °C.

108

Table 1. Optical properties of dyads **3o** and **3c**, reference compounds **5** and **4o** in dichloromethane (1×10^{-5} M) at 25 °C.

compound	λ_{abs} [nm] (ε_{max} [M^{-1} cm^{-1}])	λ_{em} [nm][a]	Φ_{fl} [%][a]
3o	265 (44900), 289 (47800), 455 (15600), 544 (26800), 582 (43900)	614	95
3c	265 (44900), 289 (44500), 368 (25000), 445 (16300), 546 (29200), 586 (48000)	614	5
5	267 (39100), 287 (50600), 450 (16400), 537 (27200), 575 (43700)	604	96
4o	304 (7800), 318 (7800)	–	–

[a] Excitation wavelength 520–540 nm.

The closed form **3c** exhibits a broad absorption band with a maximum at 368 nm that extends into the visible range and can be assigned to the diarylethene moiety. The absorption spectrum of the open form of reference diarylethene **4o** in dichloromethane shows absorption only in the UV range while ring closure revealed a new band between 350 and 430 nm (Figure 6). The ring closure of the compound with benzo[*b*]thiophene moiety **4o** can be obtained upon irradiation with UV light, while the ring closure of the literature-known reference DAE **21o** with one phenylthiophene and one benzo[*b*]thiophene unit is induced upon irradiation with visible light, which is relatively unusually for diarylethenes.
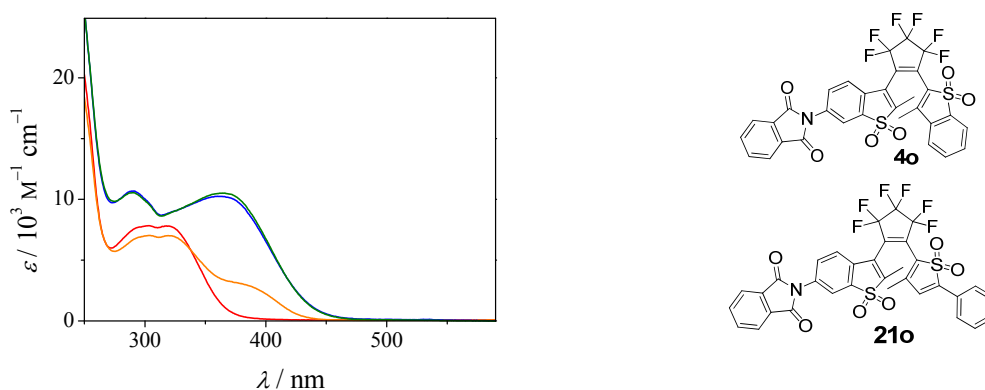
Figure 6. UV/vis absorption spectra of reference diarylethene **4o** with benzo[*b*]thiophene moiety (red line), **21o** with phenylthiophene moiety (blue line) and the respective photostationary states upon irradiation with UV light (254 nm; 2 min) for **4o** (orange line) and visible light (> 400 nm; cut-off filter at 400 nm; 55 min) in the case of **21o** (green line) in dichloromethane (1×10^{-5} M) at 25 °C.

Surprisingly, irradiation of a solution of **4o** in dichloromethane with UV light (254 nm) leads to a poor conversion to the closed form **4c**, a behavior that totally differs from that of open-form dyad **3o**, which converts nearly completely to the ring-closed form **3c** upon UV (350 nm) irradiation. These

observations reveal that PBI chromophore has a different impact on the photochromic behavior of diarylethene moiety than phthalic imide in the reference system **4**. Irradiation of the literature known photochromic reference **21o** with visible light (> 400 nm) led to an even worse conversion to the closed form of only 6% in the photostationary state.[4]

Although the open and closed form dyads **3o** and **3c** have similar absorption behavior in the visible region, dichloromethane solutions of these dyads exhibit distinctly different colors (Figure 7). The solution of the open form appears pink, while that of the closed form appears violet. Under UV light (365 nm), the solution of **3o** is bright red emissive and, in contrast, that of **3c** is barely visible red emissive. In accordance with these coloristic attributes, the fluorescence quantum yields of open form **3o** (95%) and closed form (5%) in dichloromethane are strikingly different.
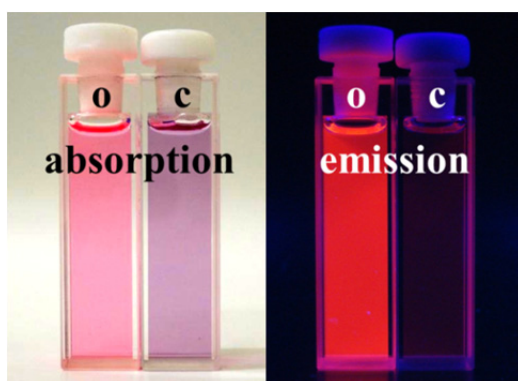
Figure 7. Photographs of solutions of **3o** and **3c** in dichloromethane (1×10^{-5} M) under ambient laboratory light (left) and under UV light (365 nm; right).

The fluorescence quantum yields of **3o** and **3c** were determined in several solvents of different polarity from tetrachloromethane ($\varepsilon_r = 2.24$) to dimethyl formamide ($\varepsilon_r = 36.71$) and divided by the respective value of reference PBI **5** to explore whether the fluorescence quenching behavior of these dyads is dependent on the solvent polarity as expected for a PET quenching mechanism. The fluorescence quantum yields of **3o**, **3c**, and PBI **5** in different solvents are listed in Table 2 and the values of Φ_{fl} (%)/Φ_{fl}^{ref} (%) as a function of solvent polarities are shown in Figure 8.

The open form dyad **3o** shows a fluorescence quantum yield of almost unity in solvents of low or intermediate polarity such as tetrachloromethane ($\varepsilon_r = 2.24$) and dichloromethane ($\varepsilon_r = 8.93$). With increasing solvent polarity, the quantum yield is decreased ultimately to 67% in dimethyl formamide ($\varepsilon_r = 36.71$). Notably, the quantum yield of reference dye **5** is decreased as well from nearly unity in non-polar environments to 87% in dimethyl formamide. For similar PBI dyes this behavior has been attributed to charge transfer from the aryloxy-substituents to the electron-poor PBI.[18]

Table 2 Fluorescence quantum yields of **3o**, **3c** and reference dye **5** in different solvents.

solvent	ε_r [a]	Φ_{fl} [%]		
		3o	**3c**	**5**
tetrachloromethane	2.24	95 ± 0.8	99 ± 1.8	96 ± 2.5
di-*n*-butyl ether	3.08	95 ± 2.1	91 ± 1.5	95 ± 2.7
chloroform	4.89	97 ± 2.5	11 ± 0.3	96 [19]
dichloromethane	8.93	95 ± 1.1	5 ± 0.3	96 ± 1.1
1,2-dichloroethane	10.36	89 ± 1.5	4 ± 0.1	96 ± 1.2
acetone	20.56	74 ± 1.7	2 ± 0.1	88 ± 4.0
DMF [b]	36.71	67 ± 2.9	3 ± 0.3	87 ± 2.9

[a] Solvent polarity values are taken from ref.[20]

[b] DMF = *N,N*-dimethylformamide
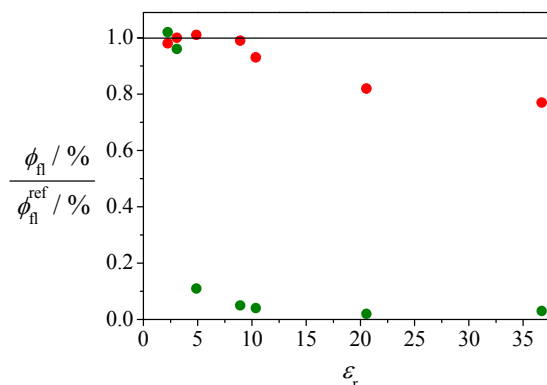
Figure 8. Fluorescence quantum yields of **3o** and **3c** (Φ_{fl}) divided by the quantum yield of reference PBI **5** (Φ_{fl}^{ref}) as a function of dielectric constants of solvents; open form (●), closed form (●).

A far more pronounced solvent dependency is observed for closed form **3c**. This isomer exhibits a fluorescence quantum yield of unity in tetrachloromethane that is already dramatically decreased to 11% in chloroform ($\varepsilon_r = 4.89$). In more polar solvents such as acetone ($\varepsilon_r = 20.56$) fluorescence of **3c** is negligible. This tremendous on/off ratio of fluorescence is a great advantage of our new photochromic dyad **3** compared to other known PET-based photochromic optical data storage systems. The observed increased luminescence quenching of **3c** with increasing solvent polarity is indicative of a favored PET process, whereas a FRET-based process would not show such solvent polarity dependence for fluorescence.

## 5.4 Cyclic Voltammetry and Driving Force Calculation

To calculate the driving force for the PET process of dyad **3o/3c**, the first oxidation potential of the PBI electron donor in dyad **3** and the first reduction potential of the DAE electron acceptor are

required. Thus, the redox potentials of open and closed form dyads **3o** and **3c**, as well as reference PBI **5** and DAE **4o**, were measured by cyclic voltammetry. The electrochemical data are collected in Table 3 and the cyclic voltammograms are shown in Figures 9a-d.

Table 3. Half-wave potentials of **3o** and **3c** and reference compounds **4o** and **5**.[a]

	$E_{1/2}^{red}$ [V]	$E_{1/2}^{ox}$ [V]
4o	−1.37[b], −1.62[b], −1.92[b]	−
3o	−1.24[b], −1.41[b], −1.83[b]	0.84, > 1.10[c]
3c	−0.97, −1.17, −1.32, −1.76[b]	0.89, > 1.20[c]
5	−1.27, −1.41	0.78, > 1.10[c]

[a] All values that are attributed to the DAE unit are shown in black, those attributed to the PBI subunit are shown in red, overlapping values of DAE and PBI subunits in blue. All measurements were carried out in dry dichloromethane (10^{-4} M) using Fc/Fc$^+$ as internal standard and TBAHFP (0.1 M) as supporting electrolyte at a scan rate of 100 mV s^{-1}. [b] Peak potential of irreversible reduction. [c] Potential at the edge of the solvent range.
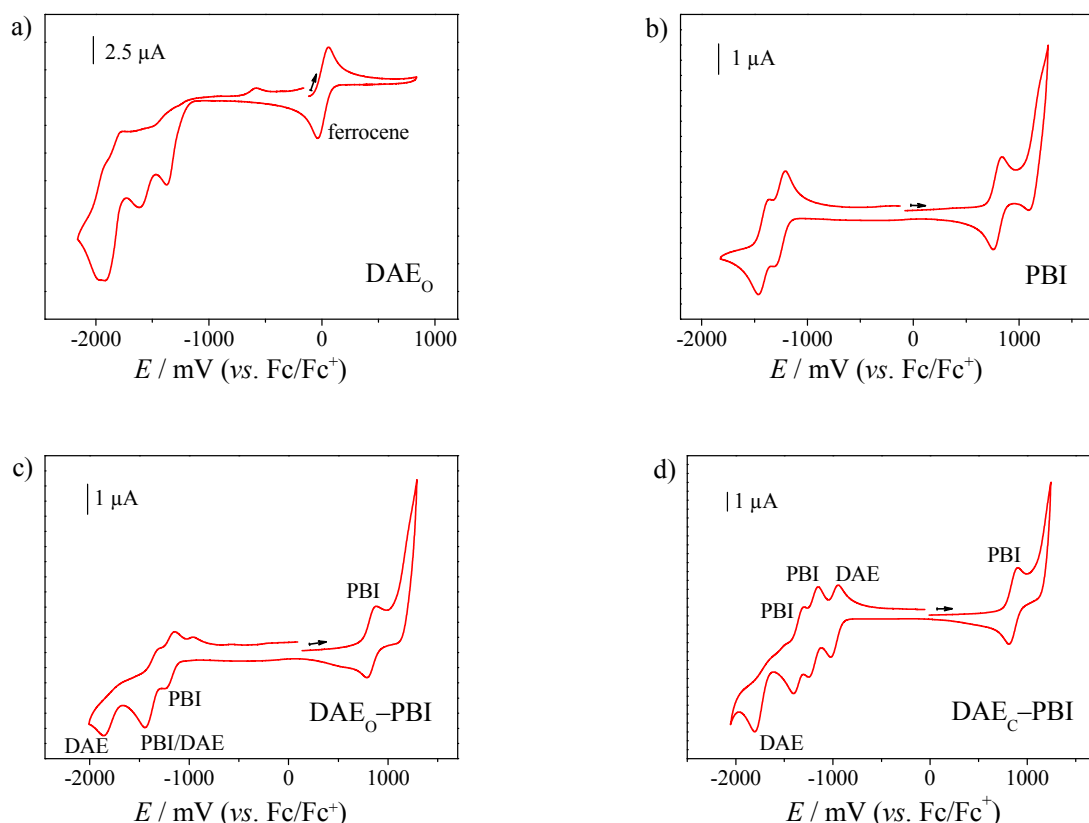
Figure 9. Cyclic voltammograms of compound (a) **4o** (2.2×10^{-4} M), (b) **5** (5.4×10^{-4} M), (c) **3o** (1.3×10^{-4} M) and (d) **3c** (3.5×10^{-4} M) in dichloromethane (supporting electrolyte TBAHFP (0.1 M), scan rate 100 mV s^{-1}).

According to the data shown in Table 3, an oxidation potential between 0.8 and 0.9 V is observed for the PBI unit for all compounds, irrespective of the attachment of an open or closed form DAE or a

cyclohexane unit at the imide nitrogens. Likewise, the first reduction potential of the PBI unit is found in a narrow range between –1.17 and –1.27 V. Importantly, the first reduction potential of ring-closed **3c** at –0.97 V is significantly less negative than that of ring open **3o**, as well as reference **4o**, and is accordingly attributable to the closed DAE subunit. Unfortunately, the reduction waves of the open DAE and PBI moieties overlap in the cyclic voltammogram of open form **3o** at a value of about –1.41 V. Thus, for the first reduction potential of open form, we used the value of –1.37 V observed for reference DAE **4o**. The pronounced difference of 0.40 V between the first reduction potentials of the open and closed form of photoswitch **3** indicates that the driving force for an electron transfer process should be much more favorable for **3c** than for **3o** in dichloromethane or other polar solvents. This is in accordance with the observed strong fluorescence quenching for **3c** in such solvents (see Table 2). Thus, based on the cyclic voltammetry analysis the electron transfer from PBI donor to diarylethene acceptor should be thermodynamically favored for the closed form over the open form.

To quantify the thermodynamic driving force for the photoinduced electron transfer process of photochromic dyad **3**, the Rehm-Weller equation was applied (Equation (1)).[21]

$$\Delta G^{\circ} = e[E_{ox}(D) - E_{red}(A)] - E_{00} - \frac{e^2}{4\pi\varepsilon_0\varepsilon_S R_{CC}} - \frac{e^2}{8\pi\varepsilon_0}\left(\frac{1}{r^+} + \frac{1}{r^-}\right)\left(\frac{1}{\varepsilon_{ref}} - \frac{1}{\varepsilon_S}\right) \qquad (1)$$

The variables of Rehm-Weller equation are described in Chapter 2.5. Since dichloromethane was used in cyclic voltammetry and spectroscopy studies, the solvent related fourth term in the Rehm-Weller equation can be neglected for dyad **3** for this particular environment. The reduction potentials of the DAE acceptor units in open and closed form are –1.37 V and –0.97 V, respectively, while the oxidation potentials of the PBI unit in both forms are 0.84 V and 0.89 V. The excited state energy E_{00} was calculated from the average value of the measured absorption maximum at 585 nm and emission maximum at 614 nm of the PBI moiety in dyad **3**, resulting in a value of 2.07 eV for both open and closed forms. From the optimized structures of **3o** and **3c** at force field level MM3* (MacroModel 9.8) center to center distances R_{CC} between donor and acceptor units of **3o** and **3c** are estimated as 1.27 nm, respectively (Figure 10).
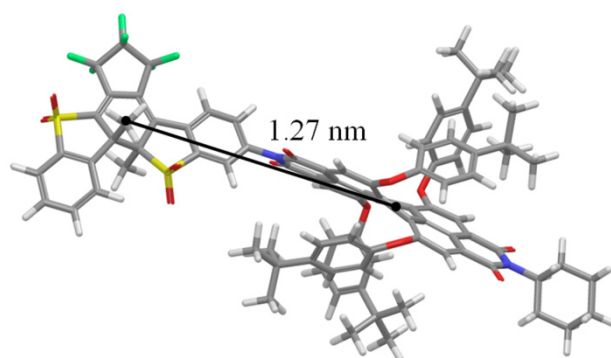
Figure 10. Geometry optimized structure of **3o** on force field level (MM3*, MacroModel 9.8).

By applying these values in Equation (1), the Gibbs free energy ($\Delta G°$) for the formation of an intramolecular charge-separated state in covalently bound donor-acceptor system **3o/3c** was calculated to be +0.01 eV for the open **3o** and –0.34 eV for the closed form **3c**. These values imply that in moderately polar solvents like dichloromethane electron transfer is thermodynamically highly favorable for the ring-closed form and hence the formation of PBI$^{•+}$–DAE$_C$$^{•–}$ charge-transfer state, while electron transfer should be disfavorable in ring-open form under similar conditions. In less polar solvents like tetrachloromethane, the formation of a charge-transfer state is expected to be energetically uphill for both open and closed forms and thus the fluorescence should not be significantly quenched, which is indeed experimentally observed. In contrast, highly polar solvents like dimethyl formamide should stabilize the charge-transfer states and thus fluorescence quenching is expected even for the open form, which is also in accordance with our observations (see Table 2).

5.5   Photophysical Studies[e]

To get insight into the fluorescence quenching process of photoswitch **3**, the fluorescence lifetimes of the open-ring (**3o**) and closed-ring (**3c**) isomers, as well as reference fluorophore PBI **5**, were determined in dichloromethane and acetone by the time-correlated single-photon counting (TC-SPC) technique.

As a short summary, the data reveal that the lifetime of **3o** (6.5 ns) is almost identical to that of the reference PBI **5** (6.6 ns) in dichloromethane, while a small (*ca*. 20 %) decrease for **3o** (5.3 ns) compared to the value for **5** (6.9 ns) is observed in acetone. This behavior, paralleled by the fluorescence quantum yield data shown in Table 2, can be explained by considering that photoinduced electron transfer with no driving force in dichloromethane may become slightly exergonic in the more polar acetone, providing a slow deactivation process for the PBI excited state of **3o**. Overall, the similar behavior of **3o** and **5** indicates the absence of any major quenching of the PBI excited state by the appended open form of the photochromic DAE unit. By contrast, the lifetime of closed form **3c** is drastically decreased in both solvents compared to those of **3o** and PBI **5**, revealing that the excited state of PBI unit is efficiently quenched in the closed form. In both solvents, the lifetimes of the closed form **3c** are too short (< 0.25 ns) for an accurate determination by single-photon counting technique.

To access the shorter timescale and to explore the mechanism for fluorescence quenching of **3c**, ultrafast transient absorption spectroscopy measurements of **3c** and, for comparison, of **3o** and reference PBI **5** were performed by using a femtosecond pump-probe setup (technical details described elsewhere)[43] and selective excitation of the PBI unit at its lowest singlet excited state with pump light of 550 nm. The transient behavior observed for the open form **3o** in dichloromethane is very similar to that exhibited by the reference dye **5**. This very similar transient spectral behavior of
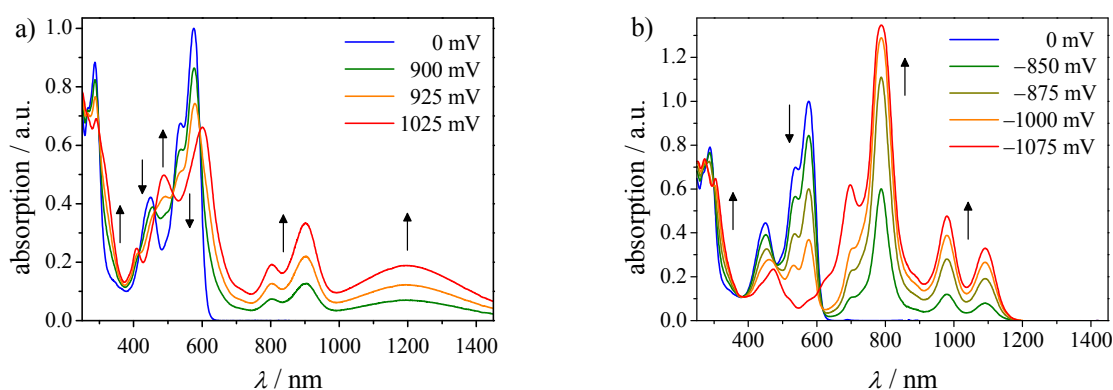
---

[e] The photophysical studies were performed in the group of Prof. Franco Scandola at the Università di Ferrara. They are documented in detail in a recent publication[8] and will be summarized in the following Chapter 5.5.

dyad **3o** and reference PBI **5** confirms the conclusion inferred from the emission measurements that little, if any, intercomponent quenching of the fluorophoric unit takes place in the open form **3o**.

The transient spectral changes of the closed form **3c** in dichloromethane exhibit a biphasic spectral behavior entirely different from that observed for the open form **3o** and reference **5**. In the early time window (*ca*. 1–35 ps), besides the features associated to the PBI excited state, the evident formation of a positive absorption centered at 510 nm can be observed, while in the subsequent time window (*ca*. 35–600 ps) the transient spectrum undergoes a clean decay to the baseline. This biphasic behavior can be assigned to the following sequence of charge separation (Equation (2)) and charge recombination steps (Equation (3)):

$$^{1}*\text{PBI–DAE}_C \rightarrow \text{PBI}^{\bullet+}\text{–DAE}_C^{\bullet-} \qquad (2)$$

$$\text{PBI}^{\bullet+}\text{–DAE}_C^{\bullet-} \rightarrow \text{PBI–DAE}_C \qquad (3)$$

This assignment is supported by the spectroelectrochemical (SEC) data upon increasing positive voltage of a dichloromethane solution of reference PBI **5** (Figure 11a). The alteration of voltage caused a decrease of the absorption maxima of the neutral form at 287 nm, 450 nm, and 576 nm while new maxima of the radical cation at 601 nm, 902 nm, and a broad absorption band between 1000 and 1450 nm with a maximum at 1194 nm appeared. These studies revealed that a one-electron oxidation of this chromophore is accompanied by bleaching in the region of the absorption maximum at 576 nm and by positive absorbance changes at both shorter (characteristic maximum at 486 nm) and longer wavelengths.[22]

Figure 11. Absorption spectra of reference PBI **5** with (a) increasing positive voltage (indicated by the arrows) in dichloromethane (5.8×10^{-4} M; 0.1 M TBAHFP): The blue line represents the neutral dye (0 mV) and the red line the radical cation of **5** (1025 mV); and (b) increasing negative voltage (indicated by the arrows) in dichloromethane (6.4×10^{-4} M; 0.1 M TBAHFP): The blue line represents the neutral dye (0 mV) and the red line the radical anion of **5** (–1075 mV).

These SEC studies permit an easy interpretation of the transient spectral changes: The formation of the charge-separated state from the PBI excited state is signaled by the build-up of the absorption

maximum at 510 nm (formation of oxidized PBI). The decay of the charge-separated state by charge recombination mirrors the spectral changes observed in the spectroelectrochemical oxidation of reference PBI **5**.

Likewise, increasing negative voltage was applied to obtain the spectrum of the radical anion in order to exclude the possibility that PBI **5** acts as an electron acceptor unit in the respective photochromic dyad (see Figure 11b). New maxima at 789 nm, 979 nm, and 1091 nm occurred while the absorption band of the neutral form between 400 and 650 nm vanished almost completely. Comparison of the electrochemically generated radical cation and radical anion absorption spectra of PBI **5** to the ultrafast transient absorption spectra helps to define the species observed.

Ultrafast spectroscopy measurements for the closed form **3c** showed similar biphasic qualitative behavior when performed in dichloromethane and in acetone. The kinetic analysis in acetone ($\varepsilon_r = 20.56$), which was monitored at the wavelength of PBI$^{\bullet+}$ absorption maximum, revealed shorter time constants for charge separation and even for recombination than in dichloromethane ($\varepsilon_r = 8.93$). The acceleration of the photoinduced electron transfer in the more polar solvent complies with our expectations for a process in the Marcus normal region as a consequence of the increased driving force (by *ca*. 0.1 eV, estimated from a Weller-type[21,23] calculation), whilst the simultaneous slight acceleration of the charge recombination points to a process in the Marcus inverted region. The observed solvent effect on quenching rate is in accordance with the strong fluorescence quenching of **3c** in polar solvents (Table 2).

For the purpose of comparison, ultrafast spectroscopy experiments were also performed with the closed dyad **3c** by excitation at 400 nm. At this wavelength, light is absorbed by both molecular components of the dyad in an approximate 30 : 70 ratio of PBI/DAE (Figure 4). The transient spectral behavior is practically the same as observed upon excitation at 550 nm, with clear evidence for photoinduced charge separation and recombination. However, the intensity of the transient signals was much larger than expected from the fraction of light absorbed by the PBI unit. Thus, a sizeable fraction of the light absorbed by the ring-closed DAE$_C$ unit apparently contributes to the photophysical response from PBI unit. This suggests the occurrence of excitation energy transfer as shown in Equation (4).

$$PBI-^1{*}DAE_C \rightarrow {}^1{*}PBI-DAE_C \qquad (4)$$

This hypothesis can be verified by measuring the excitation spectrum of the weak PBI emission of **3c** (Figure 12a). Besides the two PBI bands at 590 and 450 nm, a clear feature is observed at 365 nm, where the closed form of the DAE unit has its absorption maximum. The lower intensity of this feature in the excitation (Figure 12a) relative to the absorption spectrum (Figure 4) indicates that energy transfer is only partially (*ca*. 50 %) efficient, implying a competition between the energy-transfer process and other photoprocesses taking place in the excited state of the ring-closed DAE$_C$ unit. The main photoprocess expected from the excited state of the ring-closed DAE$_C$ unit is the photochemical ring opening to DAE$_O$ (Equation (5)):

$$PBI-^1*DAE_C \rightarrow PBI-DAE_O \qquad (5)$$

Such processes are generally known to be ultrafast (typically ps),[24] proceeding *via* conical intersections between the excited state and the ground state.[25] The observed energy transfer process competes in the excited state with ring opening and is relevant to the efficiency of photochemical switching in **3c**.
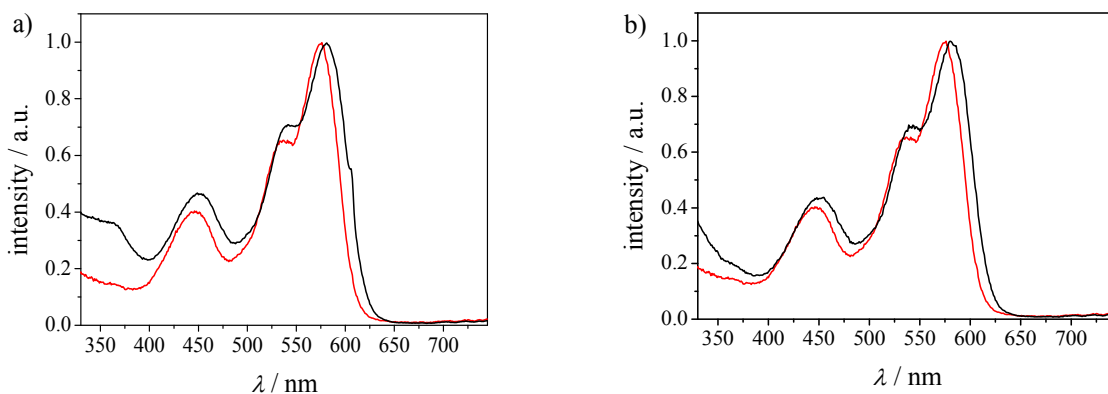
Figure 12. (a) Excitation spectrum of the PBI emission in dyad **3c** (green line), as compared with reference PBI **5** (red line), and (b) excitation spectrum of the PBI emission in dyad **3o** (black line), as compared with reference PBI **5** (red line). The feature at $\lambda < 350$ nm for compound **3o** is attributed to absorption of DAE_O (measurements in dichloromethane; monitoring wavelength: $\lambda_{ana} = 610$ nm).[f]

The photophysical/photochemical behavior of the **3c** and **3o** dyads discussed above is summarized in the energy level diagram of Figure 13. In this diagram, the energy-transfer process (Equation (4)) has been assumed to take place *via* FRET to the second singlet excited state of the PBI unit (maximum absorption at 445 nm), which is expected to give a better spectral overlap than the lower energy one. The triplet state of the DAE unit is not considered to be involved in the photophysical behavior. Its energy is unknown but, based on comparisons with related systems,[7b] is expected to be out of reach of the lowest PBI excited singlet state. The energy transfer process from DAE_O excited state to the PBI fluorophore is similar to that of the closed form DAE_C (Figure 13). The presence of such process is suggested by excitation spectra of the PBI fluorescence in **3o** with a small feature at *ca*. 335 nm (Figure 12b).

[f] These measurements were performed in the group of Prof. F. Scandola at the University of Ferrara.
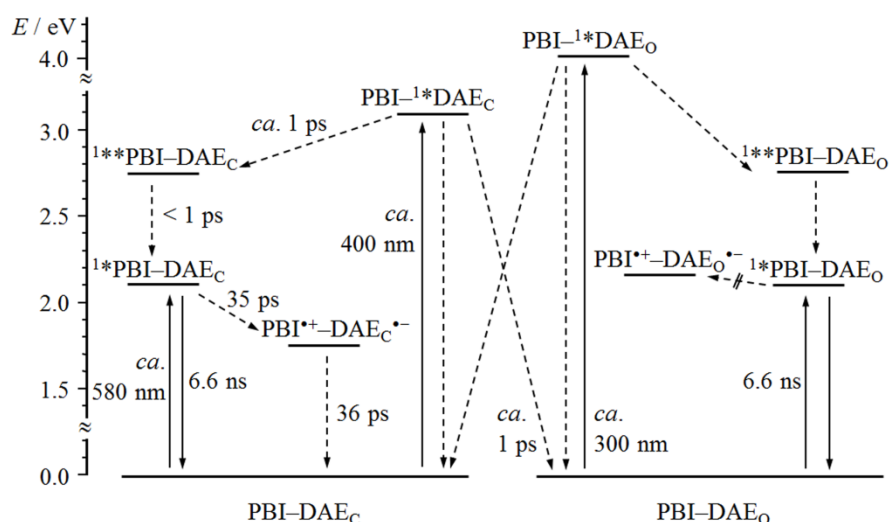
Figure 13. Energy level diagram and photophysical/chemical processes of dyad system **3o/3c** in dichloromethane.[26]

5.6   Conclusions

The newly developed photochromic dyad **3o/3c** composed of a highly photostable and emissive tetraaryloxy-substituted perylene bisimide (PBI) chromophore ($\Phi_{fl} \sim 100\%$) and a hitherto unknown diarylethene (DAE) photochrome, can be reversibly switched by UV irradiation of the open form **3o** and visible light irradiation of closed form **3c** without significant decomposition.[26] A complete characterization of the photoswitching mechanism of the system **3o/3c** has been achieved by ultrafast spectroscopic techniques. From the viewpoint of a fluorescent switch with non-destructive read-out, as sketched in Chapter 2.6, the excited-state behavior of **3o** and **3c** is quite satisfactory and all the main features sought for have been experimentally verified. These are: (i) a pronounced difference in fluorescence quenching efficiency of the PBI excited state by the open and closed forms of the DAE unit, and (ii) an efficient electron transfer quenching mechanism. As compared to previous reports on related perylene bisimide-diarylethene systems,[1,4,7,27] the experimental evidence for an electron-transfer mechanism is very definite in the present case, with well distinguished charge-separation and charge-recombination steps. Also, from a practical point of view, the determined fluorescence on/off ratio of up to 19 : 1 in dichloromethane (37 : 1 in acetone) for **3o/3c** and of 3 : 1 for the photo-stationary states at 320/395 nm in dichloromethane facilitates excellent discriminability between two states (see Figure 8). Thus, this novel photochromic system satisfies the necessary requirements for non-destructive read-out in a write/read/erase fluorescent memory device.

5.7   Experimental Section

5.7.1   Materials and Methods

General: All solvents and reagents were purchased from commercial sources and used as received without further purification, unless otherwise stated. 2-Fluoro-1-{2'-methyl-6-(2,5-dimethyl-pyrrol-1-yl)-benzo[*b*]thiophen-3-yl}perfluorocyclopentene (**13**) was prepared according to literature procedure.[4] 1,6,7,12-Tetrachloroperylene-3,4:9,10-tetracarboxylic acid bisanhydride (**7**) was kindly provided by BASF SE, Ludwigshafen, Germany. Column chromatography was performed using silica gel 60M (0.04–0.063 mm) from Macherey-Nagel.

Melting points were determined on an Olympus BX41 polarization microscope and a Linkam TP 94 heating stage and are uncorrected. ^{1}H and ^{13}C NMR spectra were recorded on Bruker Advance 400 or Bruker Advance DMX 600 and calibrated to the residual solvent peak. High-resolution mass spectra (ESI) were recorded on an ESI micrOTOF Focus from Bruker Daltonics. MALDI-TOF mass spectra were recorded on an Autoflex II from Bruker Daltonics. The UV irradiation was performed by a Rayonet photoreactor RPR-100 (Southern New England Ultraviolet Company) with 16 UV lamps (24 W lamps with λ_{max} = 350 nm). A L42 filter from JASCO Corporation (L42_.SP - 08.08.03 - 0.1 mm cuvette) was used for filtering irradiation below 400 nm.

UV/vis absorption and fluorescence spectroscopy: For all spectroscopic measurements, spectroscopic grade solvents (Uvasol®) from Merck (Hohenbrunn, Germany) were used. UV/vis spectra were recorded on a Perkin Elmer UV/vis spectrometer Lambda 35 in combination with a Perkin Elmer PTP–1+1 peltier system and a Lauda ecoline RE306/E300 refrigeration circulator. Fluorescence spectra were recorded with a PTI QM-4/2003 using conventional quartz cells (light path: 1 cm). All fluorescence measurements were performed under aerobic conditions and fluorescence spectra are corrected against photomultiplier and lamp intensity. The fluorescence quantum yields were determined as the average value for five different excitation wavelengths using *N,N'*-bis-(2,6-diisopropylphenyl)-1,6,7,12-tetraphenoxyperylene-3,4:9,10-tetracarboxylic acid bisimide as reference (Φ_{fl} = 0.96 in chloroform) by applying the high dilution method (abs.: < 0.05).[19,28]

Cyclic voltammetry: Cyclic voltammetry was performed on a standard commercial electrochemical analyzer (EC epsilon; BAS Instruments, UK) in a three electrode single-compartment cell under argon. Dichloromethane (HPLC grade) was dried over calcium hydride under argon and degassed prior to use. The supporting electrolyte tetrabutylammonium hexafluorophosphate (TBAHFP) was synthesized according to literature,[29] recrystallized from ethanol/water and dried in high vacuum. The measurements were carried out under exclusion of air and moisture at a concentration of about 10^{-4} M with ferrocene as internal standard for the calibration of the potential. Working electrode: Pt disc; reference electrode: Ag/AgCl; auxiliary electrode: Pt wire.

Spectroelectrochemistry: Spectroelectrochemistry measurements were performed in a specially designed sample compartment consisting of a cylindrical quartz cell, a platinum disc (ø 6 mm), a gold-

covered metal (V2A) plate as the auxiliary electrode and a Ag/AgCl pseudo-reference electrode. All spectra were recorded in reflection mode and the optical path length was varied by adjusting the vertical position of the working electrode with a micrometer screw. The potential applied was varied in steps of 25 or 50 mV with a potentiostat EG & G Princeton Applied research Model 283. A JASCO V-670 spectrometer was used for UV/vis/NIR absorption spectrum. The compounds were checked for reversibility of the spectra.

5.7.2   Synthesis and Characterization

Reference Diarylethene 21o

The oxidation of precursor **20** to DAE **21o** was performed according to a general procedure described for thiophene derivatives.[15] A portion of 277 mg (451 µmol) Oxone® ($2KHSO_5 \cdot KHSO_4 \cdot K_2SO_4$) was added carefully to a heterogeneous mixture of 49.5 mg (77.4 µmol) of DAE **20**, 169 mg sodium bicarbonate in 2.8 mL water, 2.3 mL acetone, and 2.5 mL dichloromethane. The mixture was stirred vigorously for 13 d at room temperature, and then extracted with dichloromethane (3 × 20 mL). The mixture was extracted with dichloromethane, the combined organic layers were dried over sodium sulfate and evaporated under reduced pressure. The resulting residue was purified by column chromatography on silica gel (dichloromethane) to obtain a yellow solid (22.5 mg, 32.0 µmol, 41%; lit.: 37%).[4]
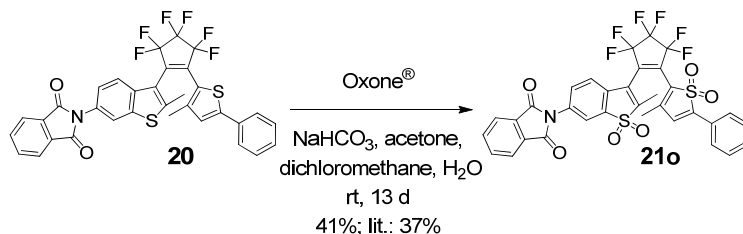
$C_{33}H_{19}F_6NO_6S_2$ (703.641)

^{1}H NMR (400 MHz, CD_2Cl_2, 300 K): δ 8.01 (d, ^4J(H,H) = 1.6, 1H), 7.94–7.99 (m, 2H), 7.83–7.87 (m, 2H), 7.75 (dd, ^3J(H,H) = 8.3, ^4J(H,H) = 2.0 Hz, 1H), 7.53–7.57 (m, 2H), 7.29–7.41 (m, 4H), 7.16 (s, 1H), 2.20 (s, 3H), 2.16 (s, 3H).

HRMS (ESI, pos. mode, acetonitrile/CHCl$_3$ 1:1): m/z: calcd for $C_{33}H_{20}F_6NO_6S_2$: 704.0636 [M+H]$^+$; found: 704.0629.

MS (MALDI, neg. mode, DCTB 1:3 in chloroform): m/z: calcd for $C_{33}H_{19}F_6NO_6S_2$: 703.056 [M]$^-$; found: 703.076.

UV/vis (CH_2Cl_2): λ_{max}/nm (ε_{max}/M^{-1} cm^{-1}) = 291 (10700), 364 (10200).

1-(3-Methyl-benzo[*b*]thiophen-2-yl)-2-{2-methyl-6-{2,5-dimethyl-pyrrol-1-yl}-benzo[*b*]thiophen-3-yl}perfluorocyclopentene (23)

This compound was synthesized according to the procedure reported for 1-(3-methyl-

5-phenylthiophen-2-yl)-2-{2-methyl-6-{2,5-dimethylpyrrole-1-yl)-benzo[*b*]thiophen-3-yl}perfluoro-cyclopentene that contains one phenylthiophene group.[4] A portion of 55 mg (242 μmol) 2-bromo-3-methylbenzo[*b*]thiophene (**22**) was dissolved in 5 mL dry THF and cooled to –78 °C. *n*-Butyllithium (0.10 mL, 250 μ mol; 2.5 M in *n*-hexane) was added dropwise to the solution and stirred for 30 min at –78 °C. Subsequently, 102 mg (235 μmol) 2-fluoro-1-{2'-methyl-6-(2,5-dimethyl-pyrrol-1-yl)-benzo[*b*]thiophen-3-yl}perfluorocyclopentene (**13**) in 2.5 mL dry THF was added dropwise to the reaction mixture and stirred for an additional hour at –78 °C and 15 min at ambient temperature. The reaction mixture was quenched with diluted hydrochloric acid and then extracted with diethyl ether (4 × 15 mL). The combined organic layers were dried over sodium sulfate and evaporated under reduced pressure. The crude product was purified by column chromatography on silica gel (*n*-hexane/ethyl acetate 19:1 (v/v)) to yield a pale brownish solid (70.1 mg; 125 μmol; 54%).
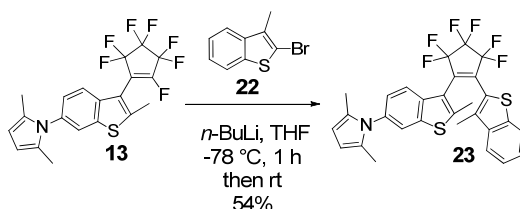

$C_{29}H_{21}F_6NS_2$ (561.604)

^{1}H NMR (400 MHz, CD$_2$Cl$_2$, 300 K): δ 7.76–7.80 (m, 1H), 7.61–7.67 (m, 2H), 7.57 (d, ^4J(H,H) = 1.4 Hz, 1H), 7.34–7.41 (m, 2H), 7.17 (dd, ^3J(H,H) = 8.5 Hz, ^4J(H,H) = 1.9 Hz, 1H), 5.84 (s, 2H), 2.42 (s, 3H), 2.10 (s, 3H), 1.97 (s, 6H).

HRMS (ESI, pos. mode, acetonitrile/CHCl$_3$ 1:1): *m/z*: calcd for $C_{23}H_{16}F_6NS_2$: 484.0628 [M–"protecting group"+H]$^+$; found: 484.0619.

MS (MALDI, pos. mode, matrix DCTB 1:3 in CHCl$_3$): *m/z*: calcd for $C_{29}H_{22}F_6NS_2$: 561.102 [M+H]$^+$; found: 561.100.

1-(3-Methyl-benzo[*b*]thiophen-2-yl)-2-(2-methyl-6-amino-benzo[*b*]thiophen-3-yl)perfluorocyclopentene (24)

This compound was synthesized according to the procedure reported for 1-(3-methyl-5-phenylthiophen-2-yl)-2-(2-methyl-6-amino-benzo[*b*]thiophen-3-yl)perfluorocyclopentene.[4] A mixture of 64.0 mg (114 μmol) 1-(3-methyl-benzo[*b*]thiophen-2-yl)-2-{2-methyl-6-{2,5-dimethyl-pyrrol-1-yl)-benzo[*b*]thiophen-3-yl}perfluorocyclopentene (**23**), 161 mg (2.32 mmol) hydroxyl-ammonium chloride, 0.17 mL triethylamine, 3 mL ethanol and 0.6 mL water was stirred for 42 h at 95 °C. Water was added to the solution, which was extracted with ethyl acetate (3 × 20 mL). The combined organic layers were dried over sodium sulfate and evaporated under reduced pressure. The crude product was purified by column chromatography on silica gel (ethyl acetate/*n*-hexane 7:3 (v/v)) to yield an orange solid (51.1 mg; 91.0 μmol; 80%).
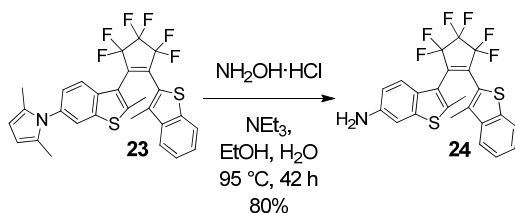
C$_{23}$H$_{15}$F$_6$NS$_2$ (483.492)

^{1}H NMR (400 MHz, CD$_2$Cl$_2$, 300 K): δ 7.74–7.79 (m, 1H), 7.60–7.65 (m, 1H), 7.34–7.40 (m, 2H), 7.31 (dd, ^3J(H,H) = 8.6, ^4J(H,H) = 1.8 Hz, 1H), 6.98 (d, ^4J(H,H) = 1.7 Hz, 1H), 6.72 (dd, ^3J(H,H) = 8.6, ^4J(H,H) = 2.2 Hz, 1H), 3.81 (brs, 2H), 2.29 (s, 3H), 2.09 (s, 3H).

HRMS (ESI, pos. mode, acetonitrile/CHCl$_3$ 1:1): m/z: calcd for C$_{23}$H$_{16}$F$_6$NS$_2$: 484.0628 [M+H]$^+$; found: 484.0624.

MS (MALDI, pos. mode, matrix DCTB 1:3 in CHCl$_3$): m/z: calcd for C$_{23}$H$_{15}$F$_6$NS$_2$: 483.055 [M]$^+$; found: 483.057.

Diarylethene derivative 25

Compound **25** was synthesized according to the procedure reported for a similar photochromic reference diarylethene.[4] A mixture of 62.0 mg (128 μmol) 1-(3-methyl-benzo[b]thiophen-2-yl)-2-(2-methyl-6-amino-benzo[b]thiophen-3-yl)perfluorocyclopentene (**24**), 38.0 mg (256 μmol) phthalic anhydride, 6.5 mL dry quinoline and 6.9 mg zinc acetate was heated to 155 °C for 20 h under an argon atmosphere. Hydrochloric acid (1 N) was added to the solution, and the mixture was extracted with dichloromethane (3 × 20 mL). The combined organic layers were evaporated under reduced pressure. The resulting residue was purified by column chromatography on silica gel (n-hexane/ethyl acetate 3:1 (v/v)) to obtain a yellowish solid (71.0 mg, 116 μmol, 90%). Mp: 202–204 °C (from dichloromethane).
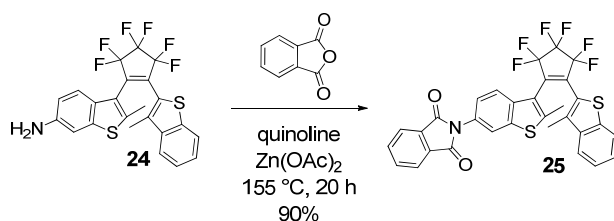
C$_{31}$H$_{17}$F$_6$NO$_2$S$_2$ (613.593)

^{1}H NMR (400 MHz, CD$_2$Cl$_2$, 300 K): δ 7.93–7.98 (m, 2H), 7.85–7.87 (m, 1H), 7.81–7.85 (m, 2H), 7.75–7.80 (m, 1H), 7.70 (dd, ^3J(H,H) = 8.6 Hz, ^4J(H,H) = 1.7 Hz, 1H), 7.63–7.67 (m, 1H), 7.45 (dd, ^3J(H,H) = 8.6 Hz, ^4J(H,H) = 1.9 Hz, 1H), 7.35–7.41 (m, 2H), 2.42 (s, 3H), 2.17 (s, 3H).

HRMS (ESI, pos. mode, acetonitrile/CHCl$_3$ 1:1): m/z: calcd for C$_{31}$H$_{18}$F$_6$NO$_2$S$_2$: 614.0683 [M+H]$^+$; found: 614.0675.

MS (MALDI, pos. mode, matrix DCTB 1:3 in CHCl$_3$): m/z: calcd for C$_{31}$H$_{17}$F$_6$NO$_2$S$_2$: 613.061 [M]$^+$; found: 613.058.

Reference diarylethene 4o

The oxidation of precursor **25** to diarylethene **4o** was performed according to a general procedure described for benzo[*b*]thiophene derivatives.[15] A portion of 920 mg Oxone® (2KHSO$_5$•KHSO$_4$•K$_2$SO$_4$) was added carefully to a heterogeneous mixture of 142 mg (231 μmol) of diarylethene **25**, 563 mg sodium bicarbonate in 9.2 mL water, 7.5 mL acetone and 8.3 mL dichloromethane. The mixture was stirred vigorously for 3 h at room temperature and then extracted with dichloromethane (3 × 20 mL). The combined organic layers were dried over sodium sulfate and evaporated under reduced pressure. The resulting residue was purified by column chromatography on silica gel (chloroform/methanol 99.5/0.5 (v/v)) to obtain a yellow solid (147 mg; 216 μmol; 94%). Mp: 179–181 °C (from dichloromethane).
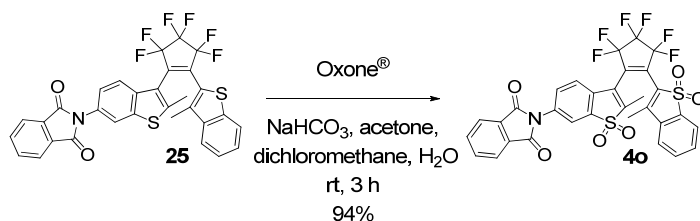
$C_{31}H_{17}F_6NO_6S_2$ (677.590)

^{1}H NMR (400 MHz, CD$_2$Cl$_2$, 300 K): δ 7.95–8.00 (m, 3H), 7.83–7.88 (m, 2H), 7.80 (dd, ^3J(H,H) = 8.3 Hz, ^4J(H,H) = 2.0 Hz, 1H), 7.70–7.75 (m, 1H), 7.61–7.68 (m, 2H), 7.52–7.56 (m, 1H), 7.37–7.41 (m, 1H), 2.28 (s, 3H), 2.25 (s, 3H).

HRMS (ESI, pos. mode, acetonitrile/CHCl$_3$ 1:1): *m/z*: calcd for $C_{31}H_{18}F_6NO_6S_2$: 678.0479 [M+H]$^+$; found: 678.0476.

MS (MALDI, pos. mode, matrix DCTB 1:3 in CHCl$_3$): *m/z*: calcd for $C_{31}H_{17}F_6NNaO_6S_2$: 700.030 [M+Na]$^+$; found: 700.038.

UV/vis (CH$_2$Cl$_2$): λ_{max}/nm (ε_{max}/M^{-1} cm^{-1}) = 303 (7800), 318 (7800).

CV (CH$_2$Cl$_2$, 0.1 M TBAHFP, *vs*. Fc/Fc$^+$, scan rate 100 mV/s): E_{pp}^{red} (X^{2-}/X^{3-}) = −1.92 V, E_{pp}^{red} (X$^-$/X^{2-}) = −1.62 V, E_{pp}^{red} (X/X$^-$) = −1.37 V.

N,N'-Dicyclohexyl-1,6,7,12-tetrachloroperylene-3,4:9,10-tetracarboxylic acid bisimide (8)

This perylene bisimide was synthesized according to the procedure previously reported for N,N'-di(1-undecyldodecyl)-1,7-dipyrrolidinylperylene-3,4:9,10-tetracarboxylic acid bisimide.[1] A mixture of 1,6,7,12-tetrachloroperylene-3,4:9,10-tetracarboxylic acid bisanhydride (**7**) (1.50 g, 2.83 mmol), cyclohexylamine (561 mg, 5.20 mmol), and imidazole (8.00 g) was heated to 110 °C under an argon gas atmosphere for 5 h. Ethanol (14 mL) was carefully added into the hot solution. The reaction mixture was then cooled down to room temperature, and 100 mL dichloromethane and 40 mL 2 N HCl were added. The layers were separated and the aqueous solution was extracted with dichloromethane (2 × 20 mL), dried over Na$_2$SO$_4$, and concentrated by rotary evaporation. The resulting residue was purified by column chromatography on silica gel (dichloromethane) and dried at

50 °C/10^{-3} mbar to yield 1.23 g (1.78 mmol; 63%) of **8** as an orange solid. Mp: *ca.* 360 °C subl. (from dichloromethane).
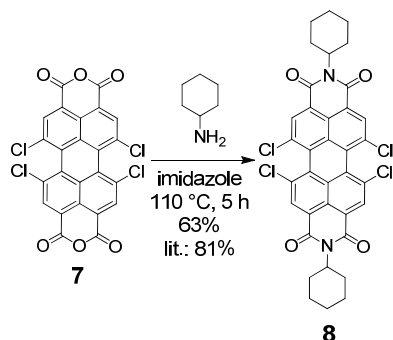

C$_{36}$H$_{26}$Cl$_4$N$_2$O$_4$ (692.415)

^{1}H NMR (400 MHz, CDCl$_3$, 300 K): δ 8.64 (s, 4H), 5.02–5.06 (m, 2H), 2.49–2.58 (m, 4H), 1.91–1.94 (m, 4H), 1.74–1.76 (m, 6H), 1.46–1.49 (m, 6H).

MS (MALDI, neg. mode, matrix DCTB 1:3 in CHCl$_3$): *m/z*: calcd for C$_{36}$H$_{26}$Cl$_4$N$_2$O$_4$: 692.065 [M]$^-$; found: 692.084.

N,N'-Dicyclohexyl-1,6,7,12-tetra(4-*tert*-butylphenoxy)-perylene-3,4:9,10-tetracarboxylic   acid bisimide (5)

N,N'-Dicyclohexyl-1,6,7,12-tetrachloroperylene-3,4:9,10-tetracarboxylic acid bisimide (**8**) (1.00 g, 1.44 mmol) was reacted under nitrogen at 120 °C with 4-*tert*-butylphenol (1.10 g, 7.32 mmol) in 27 mL dry *N*-methyl-2-pyrrolidone (NMP) in the presence of K$_2$CO$_3$ (853 mg, 6.17 mmol) for 20 h. After cooling to room temperature, the reaction mixture was acidified with 2 N HCl (20 mL) and the precipitate was filtered and successively washed with methanol and distilled water. The raw product was purified by column chromatography on silica gel (CH$_2$Cl$_2$/*n*-hexane (1/1, v/v)), and dried at 30 °C/10^{-3} mbar to yield 1.09 g (0.95 mmol, 66%) of **5** as a red solid. Mp: 372 °C decomp. (from dichloromethane).
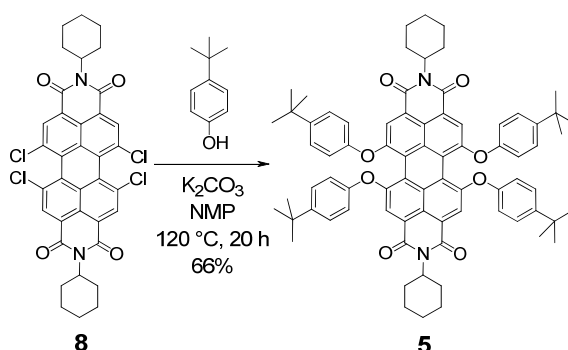
C$_{76}$H$_{78}$N$_2$O$_8$ (1147.441)

^{1}H NMR (400 MHz, CD$_2$Cl$_2$, 300 K): δ 8.09 (s, 4H), 7.26–7.31 (m, 8H), 6.79–6.86 (m, 8H), 4.85–5.33 (m, 2H), 2.38–2.49 (m, 4H), 1.78–1.86 (m, 4H), 1.61–1.69 (m, 6H), 1.32–1.44 (m, 6H), 1.31 (s, 36H).

^{13}C NMR (100 MHz, CD$_2$Cl$_2$, 300 K): δ 163.96, 156.14, 153.71, 147.64, 133.23, 126.99, 123.57,

120.79, 120.28, 119.98, 119.54, 34.68, 31.63, 29.49, 26.96, 25.93.

HRMS (ESI, pos. mode, acetonitrile/CHCl$_3$ 1:1): m/z: calcd for C$_{76}$H$_{78}$N$_2$NaO$_8$: 1169.5656 [M+Na]$^+$; found: 1169.5668.

MS (MALDI, pos. mode, matrix DCTB 1:3 in CHCl$_3$): m/z: calcd for C$_{75}$H$_{78}$N$_2$O$_8$: 1146.576 [M]$^+$; found: 1146.575.

UV/vis (CH$_2$Cl$_2$): λ_{max}/nm (ε_{max}/M^{-1} cm^{-1}) = 267 (39100), 287 (50600), 450 (16400), 537 (27200), 575 (43700).

Fluorescence (CH$_2$Cl$_2$): λ_{max} = 604 nm (λ_{ex} = 530 nm), Φ_{fl} = 0.96.

CV (CH$_2$Cl$_2$, 0.1 M TBAHFP, $vs.$ Fc/Fc$^+$, scan rate 100 mV/s): $E_{1/2}^{red}$ (X$^-$/X^{2-}) = –1.41 V, $E_{1/2}^{red}$ (X/X$^-$) = –1.27 V; $E_{1/2}^{ox}$ (X/X$^+$) = 0.78 V, $E_{1/2}^{ox}$ (X$^+$/X^{2+}) > 1.10 V.

N-Cyclohexyl-1,6,7,12-tetra(4-$tert$-butylphenoxy)-perylene-3,4:9,10-tetracarboxylic-3,4-anhydride-9,10-imide (6)

This perylene derivative was synthesized according to the previously reported procedure for N-1-undecyldodecyl-1,7-dipyrrolidinylperylene-3,4:9,10-tetracarboxylic acid-3,4-anhydride-9,10-imide.[1] N,N'-Dicyclohexyl-1,6,7,12-tetra(4-$tert$-butylphenoxy)-perylene-3,4:9,10-tetracarboxylic acid bisimide (**5**) (364 mg, 320 μmol) and 42 mL $tert$-butanol were brought to reflux under a nitrogen atmosphere. KOH (99.0 mg, 1.76 mmol) was dissolved in 27 mL hot $tert$-butanol and given to the reaction solution. After heating for 20 min, 30 mL of 2 N HCl were carefully added to the mixture, which was then extracted with dichloromethane (2 × 20 mL), dried over Na$_2$SO$_4$, and concentrated by rotary evaporation. The resulting residue was purified by column chromatography on silica gel (CH$_2$Cl$_2$/n-hexane (1/1, v/v)) and dried at 10^{-3} mbar to yield 64.0 mg (59.6 μmol; 19%) of **6** as a red solid. Mp: 376–378 °C (from dichloromethane).
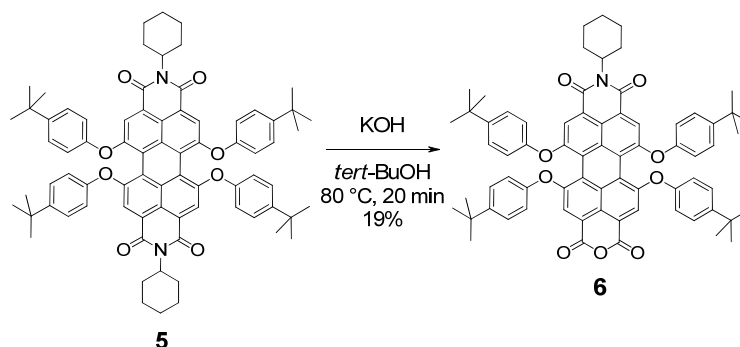
C$_{70}$H$_{67}$NO$_9$ (1066.282)

^{1}H NMR (400 MHz, CD$_2$Cl$_2$, 300 K): δ 8.15 (s, 2H), 8.12 (s, 2H), 7.25–7.31 (m, 8H), 6.81–6.87 (m, 8H), 4.85–4.95 (m, 1H), 2.36–2.49 (m, 2H), 1.80–1.88 (m, 2H), 1.63–1.72 (m, 3H), 1.35–1.46 (m, 3H), 1.31 (s, 18H), 1.30 (s, 18H).

^{13}C NMR (100 MHz, CD$_2$Cl$_2$, 300 K): δ 163.83, 160.44, 156.92, 156.05, 153.44, 153.31, 148.12, 147.99, 133.56, 133.53, 127.19, 127.10, 124.29, 122.78, 122.20, 122.01, 120.09, 119.99, 119.78, 119.66, 119.61, 118.37, 34.72, 32.01, 31.62, 31.60, 29.49, 26.94, 25.91, 23.07, 14.28.

HRMS (ESI, pos. mode, acetonitrile/CHCl$_3$ 1:1): m/z: calcd for C$_{70}$H$_{67}$NNaO$_9$: 1169.5656 [M+Na]$^+$; found: 1169.5668.

MS (MALDI, pos. mode, matrix DCTB 1:3 in CHCl$_3$): m/z: 1065.479 [M]$^+$ (calcd for C$_{70}$H$_{67}$NO$_9$ 1065.482).

UV/vis (CH$_2$Cl$_2$): λ_{max}/nm (ε_{max}/M^{-1} cm^{-1}) = 270 (27200), 290 (37300), 451 (13500), 542 (20500), 580 (33500).

Perylene bisimide-diarylethene dyad 26

This dyad was synthesized according to the previously reported procedure described for a photochromic dyad bearing pyrrolidinyl-substituted perylene bisimide unit.[1] A mixture of 60.0 mg (118 μmol) 1-(3-methyl-5-phenylthiophen-2-yl)-2-(2-methyl-6-amino-benzo[*b*]thiophen-3-yl)per-fluorocyclopentene (**19**), 127 mg (119 μmol) *N*-cyclohexyl-1,6,7,12-tetra(4-*tert*-butylphenoxy)-perylene-3,4:9,10-tetracarboxylic-3,4-anhydride-9,10-imide (**6**) and 2.6 g imidazole was heated to 110 °C for 16 h under an argon atmosphere. Ethanol (15 mL) was added to the hot solution, 20 mL of 2 N hydrochloric acid was added to the mixture at room temperature and then extracted with dichloromethane (3 × 20 mL). The combined organic layers were evaporated under reduced pressure. The resulting residue was purified by column chromatography on silica gel (dichloromethane/*n*-hexane/acetic acid 500:500:3 (v/v/v)) to obtain a red solid (134 mg, 86.0 μmol, 73%). Mp: 273–275 °C (from dichloromethane).
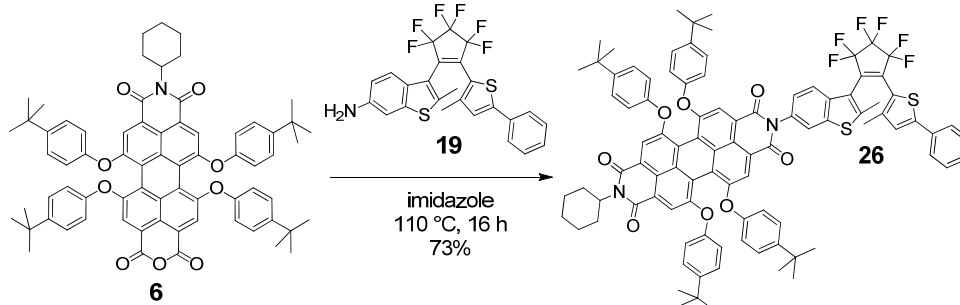
C$_{95}$H$_{82}$F$_6$N$_2$O$_8$S$_2$ (1557.797)

^{1}H NMR (400 MHz, CD$_2$Cl$_2$, 300 K): δ 8.17 (s, 2H), 8.12(s, 2H), 7.69 (dd, ^4J(H,H) = 1.9 Hz, ^5J(H,H) = 0.5 Hz, 1H), 7.63 (dd, ^3J(H,H) = 8.5 Hz, ^4J(H,H) = 1.2 Hz, 1H), 7.47–7.51 (m, 2H), 7.21–7.36 (m, 12H), 7.04 (s, 1H) 6.83–6.86 (m, 8H), 4.86–4.91 (m, 1H), 2.39–2.49 (m, 2H), 2.40 (s, 3H), 1.95 (s, 3H), 1.83–1.86 (m, 2H), 1.67–1.69 (m, 3H), 1.38–1.44 (m, 3H), 1.31 (s, 18H), 1.28 (s, 18H).

HRMS (ESI, pos. mode, acetonitrile/CHCl$_3$ 1:1): m/z: calcd for C$_{95}$H$_{83}$F$_6$N$_2$O$_8$S$_2$: 1557.5492 [M+H]$^+$; found: 1557.5486.

UV/vis (CH$_2$Cl$_2$): λ_{max}/nm (ε_{max}/M^{-1} cm^{-1}) = 267 (61000), 287 (61000), 348 (21200), 452 (17300), 541 (30200), 580 (48800).

Oxidation of precursor dyad 26 to 2o

The oxidation of **26** with Oxone$^®$ was conducted to the a general procedure reported for

benzo[*b*]thiophene derivatives.[15] A portion of 156 mg (254 µmol) Oxone$^®$ (2KHSO$_5$•KHSO$_4$•K$_2$SO$_4$) was added carefully to a heterogeneous mixture of 62.9 mg (40.4 µmol) of perylene bisimide-diarylethene dyad **26**, 95.5 mg sodium bicarbonate in 1.6 mL water, 1.3 mL acetone, and 1.4 mL dichloromethane. The mixture was stirred vigorously for 19 d at room temperature. Additional portions of 156 mg (254 µmol) Oxone$^®$ (2KHSO$_5$•KHSO$_4$•K$_2$SO$_4$) were added twice to the solution after 7 and 14 days. Water was added to the mixture, which was then extracted with dichloromethane (3 × 20 mL). The combined organic layers were dried over sodium sulfate and evaporated under reduced pressure. The resulting residue was purified by column chromatography on silica gel (dichloromethane) to obtain a red solid (7.50 mg; 4.62 µmol; 11%).

C$_{95}$H$_{82}$F$_6$N$_2$O$_{12}$S$_2$ (1621.837)

^{1}H NMR (400 MHz, CD$_2$Cl$_2$, 300 K): δ 8.18 (s, 2H), 8.12 (s, 2H), 7.67–7.70 (m, 3H), 7.53 (dd, ^3J(H,H) = 8.2 Hz, ^4J(H,H) = 1.9 Hz, 1H), 7.43–7.49 (m, 3H), 7.35 (d, ^3J(H,H) = 7.9 Hz, 1H), 7.26–7.32 (m, 8H), 6.83–6.87 (m, 8H), 6.79 (s, 1H), 4.86–4.96 (m, 1H), 2.36–2.48 (m, 2H), 2.25 (s, 3H), 2.12 (s, 3H), 1.80–1.86 (m, 2H), 1.64–1.71 (m, 3H), 1.32–1.43 (m, 3H), 1.31 (s, 18H), 1.28 (s, 18H).
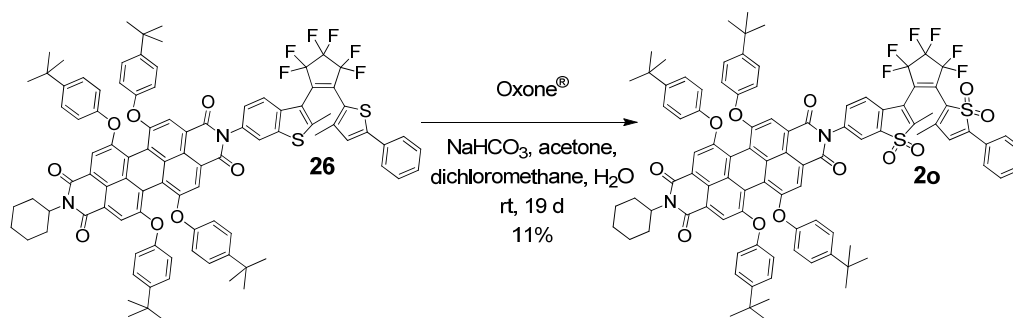
HRMS (ESI, pos. mode, acetonitrile/CHCl$_3$ 1:1): *m/z*: calcd for C$_{95}$H$_{83}$F$_6$N$_2$O$_{12}$S$_2$: 1621.5289 [M+H]$^+$; found: 1621.5298.

MS (MALDI, pos. mode, matrix DCTB 1:3 in CHCl$_3$): *m/z*: calcd for C$_{95}$H$_{82}$F$_6$N$_2$O$_{12}$S$_2$: 1620.521 [M]$^+$; found: 1620.510.

UV/vis (CH$_2$Cl$_2$): λ_{max}/nm (ε_{max}/M^{-1} cm^{-1}) = 265 (42400), 288 (42200), 369 (12300), 454 (14400), 583 (40000).

Fluorescence (CH$_2$Cl$_2$): λ_{max} = 614 nm (λ_{ex} = 530 nm), Φ_{fl} = 0.82.

Perylene bisimide-diarylethene dyad 27

This dyad was synthesized according to the previously reported procedure for a photochromic dyad bearing pyrrolidinyl-substituted perylene bisimide.[1] A mixture of 41.4 mg (85.6 µmol) 1-(3-methyl-benzo[*b*]thiophen-2-yl)-2-(2-methyl-6-amino-benzo[*b*]thiophen-3-yl)perfluorocyclopentene **(24)**, 91.3 mg (85.6 µmol) *N*-cyclohexyl-1,6,7,12-tetra(4-*tert*-butylphenoxy)-perylene-3,4:9,10-tetra-carboxylic-3,4-anhydride-9,10-imide **(6)**, and 2.0 g imidazole was heated to 110 °C for 6 h under an argon atmosphere. Ethanol (5 mL) was added to the hot solution and 20 mL of 2 N hydrochloric acid was added to the mixture at room temperature, which was then extracted with dichloromethane

(3 × 15 mL). The combined organic layers were evaporated under reduced pressure. The resulting residue was purified by column chromatography on silica gel (dichloromethane/*n*-hexane/acetic acid 500:500:3 (v/v/v)) to obtain a red solid (91.1 mg, 59.5 μmol, 69%). Mp: 288–290 °C (from dichloromethane).
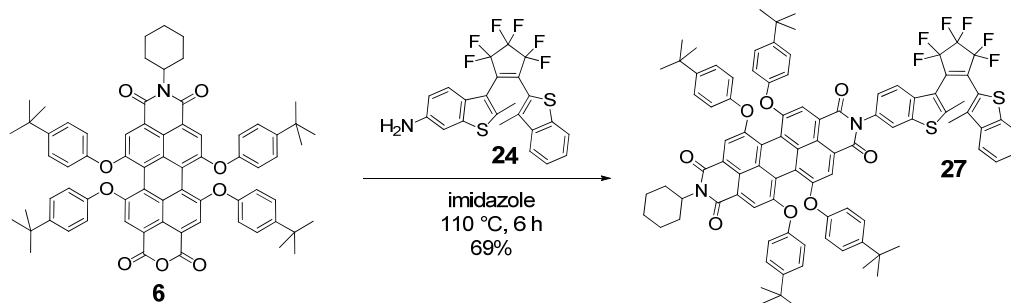
$C_{93}H_{80}F_6N_2O_8S_2$ (1531.759)

^{1}H NMR (400 MHz, CD_2Cl_2, 300 K): δ 8.18 (s, 2H), 8.12 (s, 2H), 7.75–7.80 (m, 1H), 7.62–7.71 (m, 3H), 7.34–7.39 (m, 2H), 7.23–7.30 (m, 9H), 6.85 (d, ^3J(H,H) = 9.6 Hz, 8H), 4.86–4.91 (m, 1H), 2.37–2.49 (m, 2H), 2.40 (s, 3H), 2.14 (s, 3H), 1.90–1.94 (m, 2H), 1.83–1.86 (m, 3H), 1.34–1.45 (m, 3H), 1.31 (s, 18H), 1.28 (s, 18H).

HRMS (ESI, pos. mode, acetonitrile/CHCl$_3$ 1:1): *m/z*: calcd for $C_{93}H_{81}F_6N_2O_8S_2$: 1531.5336 [M+H]$^+$; found: 1531.5338.

MS (MALDI, neg. mode, matrix DCTB 1:1 in CHCl$_3$): *m/z*: calcd for $C_{93}H_{80}F_6N_2O_8S_2$: 1530.526 [M]$^-$; found: 1530.553.

UV/vis (CH_2Cl_2): λ_{max}/nm (ε_{max}/M^{-1} cm^{-1}) = 266 (62200), 287 (54500), 452 (16600), 539 (29100), 579 (47300).

Oxidation of dyad 13 to open form dyad 3o

The oxidation was conducted according to a general procedure reported for benzo[*b*]thiophene derivatives.[15] A portion of 152 mg (247 μmol) Oxone$^®$ (2KHSO$_5$•KHSO$_4$•K$_2$SO$_4$) was added carefully to a heterogeneous mixture of 34.1 mg (21.8 μmol) of dyad **27** and 93.1 mg of sodium bicarbonate in 1.5 mL water, 1.3 mL acetone and 1.4 mL dichloromethane. The mixture was stirred vigorously for 7 d at room temperature. Water was added to the mixture and then extracted with dichloromethane (3 × 15 mL). The combined organic layers were dried over sodium sulfate and evaporated under reduced pressure. The resulting residue was purified by column chromatography on silica gel (dichloromethane) to obtain a red solid (23.5 mg; 14.7 μmol; 67%). Mp: 286–287 °C (from dioxane).
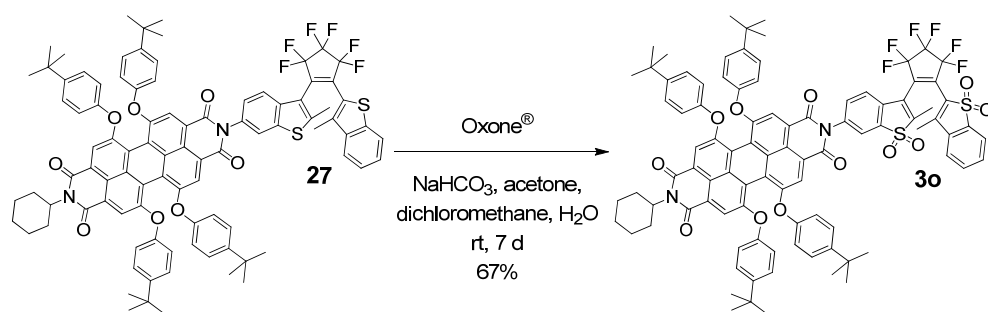
$C_{93}H_{80}F_6N_2O_{12}S_2$ (1595.757)

^{1}H NMR (400 MHz, CD_2Cl_2, 300 K): δ 8.18 (s, 2H), 8.12 (s, 2H), 7.69–7.73 (m, 1H), 7.59–7.68 (m, 3H), 7.50–7.54 (m, 2H), 7.35–7.38 (m, 1H), 7.25–7.31 (m, 8H), 6.85 (d, ^3J(H,H) = 8.0 Hz, 8H), 4.86–4.91 (m, 1H), 2.38–2.48 (m, 2H), 2.25 (s, 3H), 2.24 (s, 3H), 1.80–1.88 (m, 2H), 1.63–1.71 (m, 3H), 1.34–1.45 (m, 3H), 1.31 (s, 18H), 1.28 (s, 18H).

HRMS (ESI, pos. mode, acetonitrile/$CHCl_3$ 1:1): m/z: calcd for $C_{93}H_{81}F_6N_2O_{12}S_2$: 1595.5133 [M+H]$^+$; found: 1595.5141.

MS (MALDI, pos. mode, matrix DCTB 1:3 in $CHCl_3$): m/z: calcd for $C_{93}H_{80}F_6N_2O_{12}S_2$: 1594.513 [M]$^+$; found: 1594.506.

UV/vis (CH_2Cl_2): λ_{max}/nm (ε_{max}/M^{-1} cm^{-1}) = 265 (44900), 289 (47800), 455 (15600), 544 (26800), 582 (43900).

Fluorescence (CH_2Cl_2): λ_{max} = 614 nm (λ_{ex} = 530 nm), Φ_{fl} = 0.95.

CV (CH_2Cl_2, 0.1 M TBAHFP, vs. Fc/Fc$^+$, scan rate 100 mV/s): E_{pp}^{red} (X^{2-}/X^{3-}) = –1.83 V, E_{pp}^{red} (X$^-$/X^{2-}) = –1.41 V, E_{pp}^{red} (X/X$^-$) = –1.24 V; $E_{1/2}^{ox}$ (X/X$^+$) = 0.84 V, $E_{1/2}^{ox}$ (X$^+$/X^{2+}) > 1.10 V.

Photolytic conversion of open form dyad 3o to closed form 3c

The compound was synthesized according to the procedure described for the closed form of a 1,7-dipyrrolidinylperylene bisimide-diarylethene conjugate.[1] A solution of the open form **3o** (35.2 mg, 22.1 μmol) in 200 mL dichloromethane was irradiated in a Rayonet photoreactor with UV light (350 nm) for 20 min under vigorous stirring. The solution was concentrated by rotary evaporation in the dark, the resulting precipitate was purified in the dark by column chromatography on silica gel (acetone/n-hexane (1/4 (v/v)), and dried at 10^{-3} mbar to yield 24.1 mg (15.1 μmol; 69%) of **3c** as a dark red solid. About 9.9 mg (6.2 μmol; 28%) of the open form was reisolated.
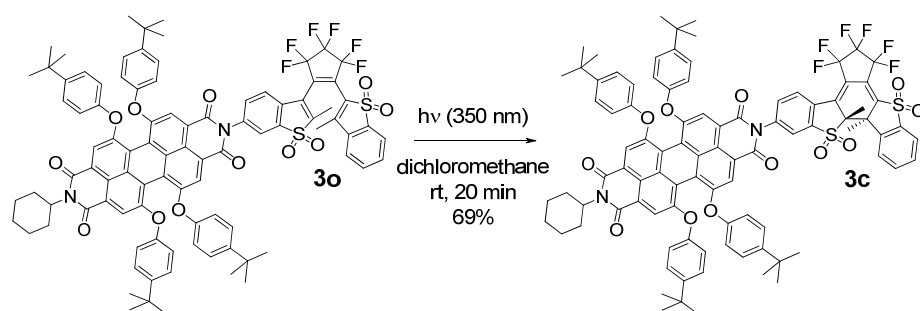
$C_{93}H_{80}F_6N_2O_{12}S_2$ (1595.757)

¹H NMR (600 MHz, CD$_2$Cl$_2$, 300 K): δ 8.39 (d, ^3J(H,H) = 7.7 Hz, 1H), 8.23 (s, 2H), 8.12 (s, 2H), 8.02 (d, ^3J(H,H) = 8.0 Hz, 1H), 7.98 (d, ^4J(H,H) = 1.9 Hz, 1H), 7.89 (d, ^3J(H,H) = 9.7 Hz, 1H), 7.83–7.89 (m, 2H), 7.25–7.31 (m, 8H), 6.83–6.88 (m, 8H), 4.90 (tt, ^3J(H,H) = 12.2 Hz, ^4J(H,H) = 3.6 Hz, 1H), 2.39–2.46 (m, 2H), 1.90 (s, 3H), 1.82–1.86 (m, 2H), 1.66–1.69 (m, 3H), 1.35–1.43 (m, 3H), 1.31 (s, 18H), 1.28 (s, 18H), 1.24 (s, 3H).

HRMS (ESI, pos. mode, acetonitrile/CHCl$_3$ 1:1): m/z: calcd for C$_{93}$H$_{80}$F$_6$N$_2$O$_{12}$S$_2$: 1595.5133 [M]$^+$; found: 1595.5122.

UV/vis (CH$_2$Cl$_2$): λ_{max}/nm (ε/M^{-1} cm^{-1}) = 265 (44900), 289 (44500), 368 (25000), 445 (16300), 546 (29200), 586 (48000).

Fluorescence (CH$_2$Cl$_2$): λ_{max} = 614 nm (λ_{ex} = 530 nm), Φ_{fl} = 0.05.

CV (CH$_2$Cl$_2$, 0.1 M TBAHFP, $vs.$ Fc/Fc$^+$, scan rate 100 mV/s): E_{pp}^{red} (X^{3-}/X^{4-}) = –1.76 V, $E_{1/2}^{red}$ (X^{2-}/X^{3-}) = –1.32 V, $E_{1/2}^{red}$ (X$^-$/X^{2-}) = –1.17 V, $E_{1/2}^{red}$ (X/X$^-$) = –0.97 V; $E_{1/2}^{ox}$ (X/X$^+$) = 0.89 V, $E_{1/2}^{ox}$ (X$^+$/X^{2+}) > 1.20 V.

5.8   References

[1]   M. Berberich, A.-M. Krause, M. Orlandi, F. Scandola, F. Würthner, *Angew. Chem. Int. Ed.* **2008**, *47*, 6616-6619.

[2]   M. Berberich, F. Würthner, *Chem. Sci.* **2012**, *3*, 2771-2777.

[3]   a) G. Seybold, G. Wagenblast, *Dyes Pigm.* **1989**, *11*, 303-317; b) H. Langhals, *Heterocycles* **1995**, *40*, 477-500; c) F. Würthner, *Chem. Commun.* **2004**, 1564-1579; d) T. Weil, T. Vosch, J. Hofkens, K. Peneva, K. Müllen, *Angew. Chem. Int. Ed.* **2010**, *49*, 9068-9093; e) C. Huang, S. Barlow, S. R. Marder, *J. Org. Chem.* **2011**, *76*, 2386-2407.

[4]   T. Fukaminato, M. Tanaka, T. Doi, N. Tamaoki, T. Katayama, A. Mallick, Y. Ishibashi, H. Miyasaka, M. Irie, *Photochem. Photobiol. Sci.* **2010**, *9*, 181-187.

[5]   a) Y. Avlasevich, C. Li, K. Müllen, *J. Mater. Chem.* **2010**, *20*, 3814-3826; b) X. Zhan, A. Facchetti, S. Barlow, T. J. Marks, M. A. Ratner, M. R. Wasielewski, S. R. Marder, *Adv. Mater.* **2011**, *23*, 268-284.

[6]   a) A. Marcos Ramos, S. C. J. Meskers, E. H. A. Beckers, R. B. Prince, L. Brunsveld, R. A. J. Janssen, *J. Am. Chem. Soc.* **2004**, *126*, 9630-9644; b) M. R. Wasielewski, *J. Org. Chem.* **2006**, *71*, 5051-5066; c) E. E. Neuteboom, S. C. J. Meskers, E. H. A. Beckers, S. Chopin, R. A. J. Janssen, *J. Phys. Chem. A* **2006**, *110*, 12363-12371; d) J. Baggerman, D. C. Jagesar, R. A. L. Vallée, J. Hofkens, F. C. De Schryver, F. Schelhase, F. Vögtle, A. M. Brouwer, *Chem. Eur. J.* **2007**, *13*, 1291-1299; e) E. Fron, R. Pilot, G. Schweitzer, J. Qu, A. Herrmann, K. Müllen, J. Hofkens, M. Van der Auweraer, F. C. De Schryver, *Photochem. Photobiol. Sci.* **2008**, *7*, 597-604; f) M. R. Wasielewski, *Acc. Chem. Res.* **2009**, *42*, 1910-1921; g) T. Vosch, E. Fron, J.-i. Hotta, A. Deres, H. Uji-i, A. Idrissi, J. Yang, D. Kim, L. Puhl, A. Haeuseler, K. Müllen, F. C. De Schryver, M. Sliwa, J. Hofkens, *J. Phys. Chem. C* **2009**, *113*, 11773-11782; h) M. Wolffs,

N. Delsuc, D. Veldman, N. V. Anh, R. M. Williams, S. C. J. Meskers, R. A. J. Janssen, I. Huc, A. P. H. J. Schenning, *J. Am. Chem. Soc.* **2009**, *131*, 4819-4829; i) R. K. Dubey, A. Efimov, H. Lemmetyinen, *Chem. Mater.* **2010**, *23*, 778-788; j) J. R. Siekierzycka, C. Hippius, F. Würthner, R. M. Williams, A. M. Brouwer, *J. Am. Chem. Soc.* **2010**, *132*, 1240-1242; k) L. Flamigni, B. Ventura, A. Barbieri, H. Langhals, F. Wetzel, K. Fuchs, A. Walter, *Chem. Eur. J.* **2010**, *16*, 13406-13416; l) Á. J. Jiménez, B. Grimm, V. L. Gunderson, M. T. Vagnini, S. Krick Calderon, M. S. Rodríguez-Morgade, M. R. Wasielewski, D. M. Guldi, T. Torres, *Chem. Eur. J.* **2011**, *17*, 5024-5032.

[7]   a) T. Fukaminato, T. Doi, M. Tanaka, M. Irie, *J. Phys. Chem. C* **2009**, *113*, 11623-11627; b) T. Fukaminato, T. Doi, N. Tamaoki, K. Okuno, Y. Ishibashi, H. Miyasaka, M. Irie, *J. Am. Chem. Soc.* **2011**, *133*, 4984-4990.

[8]   M. Irie, T. Lifka, K. Uchida, S. Kobatake, Y. Shindo, *Chem. Commun.* **1999**, 747-750.

[9]   S. Mathew, M. R. Johnston, *Chem. Eur. J.* **2009**, *15*, 248-253.

[10]   a) W. K. Anderson, E. J. LaVoie, J. C. Bottaro, *J. Chem. Soc., Perkin Trans. 1* **1976**, 1-4; b) W. H. Cherry, J. T. Craig, Q. N. Porter, *Aust. J. Chem.* **1979**, *32*, 133-143.

[11]   F. Sun, F. Zhang, H. Guo, X. Zhou, R. Wang, F. Zhao, *Tetrahedron* **2003**, *59*, 7615-7621.

[12]   K. Uchida, T. Matsuoka, S. Kobatake, T. Yamaguchi, M. Irie, *Tetrahedron* **2001**, *57*, 4559-4565.

[13]   E. Campaigne, R. L. White, *J. Heterocycl. Chem.* **1988**, *25*, 367-373.

[14]   B. Join, T. Yamamoto, K. Itami, *Angew. Chem. Int. Ed.* **2009**, *48*, 3644-3647.

[15]   D. Enders, G. Del Signore, *Heterocycles* **2004**, *64*, 101-120.

[16]   W. Adam, C.-G. Zhao, C. R. Saha-Möller, K. Jakka, *Oxidation of Organic Compounds by Dioxiranes*, John Wiley & Sons, Inc., Hoboken (New Jersey), **2009**.

[17]   M. Irie, *Chem. Rev.* **2000**, *100*, 1685-1716.

[18]   E. Fron, G. Schweitzer, P. Osswald, F. Würthner, P. Marsal, D. Beljonne, K. Müllen, F. C. De Schryver, M. Van der Auweraer, *Photochem. Photobiol. Sci.* **2008**, *7*, 1509-1521.

[19]   R. Gvishi, R. Reisfeld, Z. Burshstein, *Chem. Phys. Lett.* **1993**, *213*, 338-344.

[20]   C. Reichardt, *Solvents and Solvent Effects in Organic Chemistry*, 3rd ed., Wiley-VCH, Weinheim, **2003**.

[21]   A. Z. Weller, *Z. Phys. Chem.* **1982**, *133*, 93-98.

[22]   F. Würthner, A. Sautter, D. Schmid, P. J. A. Weber, *Chem. Eur. J.* **2001**, *7*, 894-902.

[23]   D. Rehm, A. Weller, *Ber. Bunsenges. Phys. Chem.* **1969**, *73*, 834-839.

[24]   N. Tamai, H. Miyasaka, *Chem. Rev.* **2000**, *100*, 1875-1890.

[25]   M. Boggio-Pasqua, M. Ravaglia, M. J. Bearpark, M. Garavelli, M. A. Robb, *J. Phys. Chem. A* **2003**, *107*, 11139-11152.

[26]   M. Berberich, M. Natali, P. Spenst, C. Chiorboli, F. Scandola, F. Würthner, *Chem. Eur. J.* **2012**, *18*, doi:10.1002/chem.201201484.

[27]   Y. Odo, T. Fukaminato, M. Irie, *Chem. Lett.* **2007**, *36*, 240-241.

[28]   *Principles of Fluorescence Spectroscopy* (ed. J. R. Lakowitz), 2nd ed., Kluwer Academic/Plenum, New York, **1999**, pp. 52-55.

[29]   A. J. Fry, *Laboratory Techniques in Electroanalytical Chemistry* (eds. P. T. Kessing, W. R. Heinemann), 2nd ed., Marcel Dekker Ltd, New York, **1996**, p. 481.

6 Comparison of Known and New Rylene Bisimide-Diarylethene Dyads

In this chapter the properties of the two new photochromic systems described in Chapter 4 and 5 (compound **7**, **8**, and **9** in Figure 1) will be compared to those of earlier reported dyad compounds **1** to **6** that are shown in Figure 1 in chronological order.
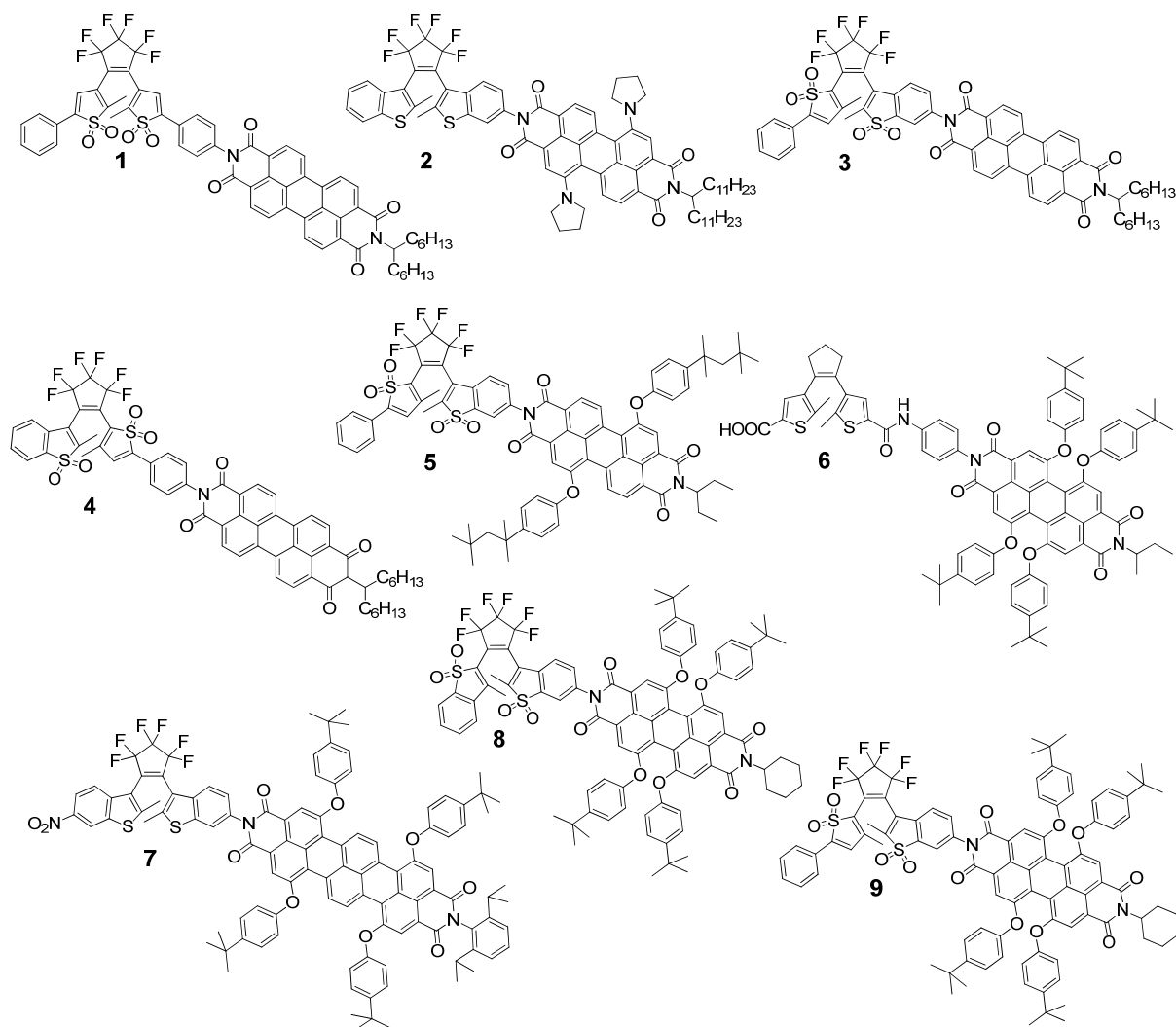
Figure 1. Overview of the literature known photochromic systems **1** to **6** and the new systems **7**, **8**, and **9**.

Reported by Odo in 2007, photochromic compound **1** introduced for the first time the basic idea for fluorescence quenching by PET in a PBI–DAE system.[1] The use of an unsubstituted PBI provided high fluorescence values, but the driving force for the fluorescence quenching PET was low due to its disadvantageous low redox potentials. Therefore, a poor fluorescence on/off ratio between 76% for the pure open form and 60% of the respective pure closed form was achieved even in the most polar environment ($\varepsilon_r = 37.5$) (see Table 1). However, the absorption band of the closed form of the DAE moiety does not overlap the emission band of the fluorophoric unit, which is a prerequisite to prevent

disadvantageous FRET processes (see Table 2). Furthermore, the authors provide no additional data, neither about repeated switching cycles as stability test nor driving forces for the electron transfer or photoisomerization quantum yields (see Table 3).

Table 1. Comparison of fluorescence quantum yields (Φ_{fl}) reported for seven photochromic systems (**1** to **3** and **5** to **8**) for solvents or solvent mixtures with different permittivities (Φ_{fl} (open) / Φ_{fl} (closed) ratios larger than eight are highlighted with bold characters).

compound	Φ_{fl} (open) / Φ_{fl} (closed) non-polar range ($\varepsilon_r = 2.2\text{–}2.3$)[a]	Φ_{fl} (open) / Φ_{fl} (closed) medium-polar range ($\varepsilon_r = 8.9\text{–}10.4$)	Φ_{fl} (open) / Φ_{fl} (closed) polar range ($\varepsilon_r = 20.5\text{–}37.5$)[b]
1[1]	1.00 / 1.00	1.00 / 0.97	0.76 / 0.60
2[2]	0.39 / 0.40	0.14 / 0.12	**0.08 / 0.01**
3[3]	0.91 / 0.82	0.90 / 0.50	0.88 / 0.12
5[4]	0.91 / 0.84	**0.68 / 0.07**	**0.34 / 0.02**
6[5]	**0.96 / 0.10**[c]	**0.90 / 0.10**[c]	**0.79 / 0.07**[c]
7[6]	0.60 / 0.34	0.29 / 0.10	0.08 / 0.02
8[7]	0.95 / 0.99	**0.95 / 0.05**	**0.67 / 0.03**

[a] Solvents or solvent mixtures with lowest polarity, which was used in the respective publication.
[b] Most polar solvents or solvent mixtures used in the respective publication. [c] Fluorescence quenching due to disadvantageous FRET process.

Table 2. Comparison of the absorption bands of the closed forms of the DAE moieties to the emission bands of the respective fluorophores of photochromic systems **1** to **8**, and number of repeated switching cycles, which were performed as stability test.

compound	absorption range of closed form of DAE moiety (nm)	emission range of fluorescent moiety (nm)	stability test: number of repeated switching cycles
1[1]	350–490	510–610	[a]
2[2]	320–620	650–850	[a]
3[3,8]	300–430	510–610	10
4[8]	310–470	510–610	[a]
5[4]	300–430	530–650	[a]
6[5]	330–630[b]	550–770[b]	3
7[6]	320–640	650–850	20
8[7]	330–410	550–770	10

[a] These values were not determined. [b] The emission band of fluorophore overlaps the absorption band of closed form of the DAE moiety, which leads to an unfavorable FRET process.

Dyad **2**, published by us in 2008,[2] provided good on/off fluorescence ratios in polar solvents (see Table 1). In addition, a detailed description of the concept of fluorescence quenching by intramolecular PET in a PBI–DAE photochromic system was given, supported by the clear observation of the PBI charge-transfer state by ultrafast transient absorption spectroscopy. However, the low fluorescence quantum yield of the dipyrrolidinyl-substituted PBI (see Table 1), the low driving force for PET (see Table 3), and the low photostability upon UV irradiation are serious disadvantages of this system.

Table 3. Comparison of driving forces ($\Delta G°$), on/off ratios of emission in the PSS, and ring-closure ($\Phi_{O\to C}$) and ring-opening ($\Phi_{C\to O}$) quantum yields reported for photochromic systems **1** to **8**.

compound	driving forces $\Delta G°$ (open) / $\Delta G°$ (closed) (in CH$_2$Cl$_2$: ε_r = 8.93)	emission on/off ratios of both PSS (ε_r of solvent)	ring-closure quantum yields $\Phi_{O\to C}$ (λ_{ex})	ring-opening quantum yields $\Phi_{C\to O}$ (λ_{ex})
1[1]	a	a	a	a
2[2]	0.37 eV / –0.03 eV	a	0.017 (350 nm)	a
3[3,8]	0.28 eV / –0.15 eV	4.8 : 1 (ε_r = 17.4)	0.0135 (410 nm)^c 0.0012 (522 nm)^c	0.014 (365 nm)
4[8]	a	a	0.015 (410 nm) 0.016 (522 nm)	0.26 (313 nm)
5[4]	0.05 eV / –0.37 eV	3 : 1 (ε_r = 17.4)	a	a
6[5]	–0.04 eV / –0.71 eV^b	2.5 : 1 (ε_r = 10.63)	0.13 (254 nm)	0.06 (532 nm)
7[6]	0.16 eV / –0.24 eV	2.5 : 1 (ε_r = 8.93)	0.23 (311 nm)	0.12 (517 nm)
8[7]	0.01 eV / –0.34 eV	3 : 1 (ε_r = 8.93)	a	a

^{a} These values were not determined. ^{b} These energy values were calculated for 1,2-dichloroethane (ε_r = 10.63) as solvent. ^{c} The wavelength dependence suggests that the photocyclization of dyad **3** at 410 and 522 nm proceeds *via* different reaction pathways.[8]

Further developments of these first two systems were published by Fukaminato *et al.* in 2009 and 2010 (see compound **3** in Figure 1).[3,8] Changing the connectivity of one thiophene from the 3- to the 2-position shifted the absorption of the closed DAE unit to the UV (see Table 2), and increased the driving force compared to their former photochromic dyad (see Table 3). The poor fluorescence on/off ratio of 91% to 82% in non-polar solvent mixtures (as in the former systems **1** and **2**) became much better in a highly polar environment (ε_r = 23.48) with values of 88% for the open form and 12% for the closed form. Dyad **3** possesses the best on/off ratio of emission (4.8 : 1) in the PSS of all investigated systems (see Table 3). However, even in a non-polar environment, the PBI fluorescence was quenched by 10% in **3o** which was attributed to a disadvantageous triplet-state population leading to photocyclization and therefore destructive read-out.[3,8] The distinct wavelength dependence suggests that the photocyclization of dyad **3** at 410 (0.0135) and 522 nm (0.0012) proceeds *via*

different reaction pathways.[8] A similar photochromic dyad **4** (see Figure 1), published alongside compound **3**,[8] could not be compared to the other systems, due to the fact that insufficient data was provided by the authors.

In 2011, Fukaminato *et al.* published a photochromic system **5** with the DAE moiety of compound **3** and a highly emissive diaryloxy-substituted PBI.[4] Dyad **5** showed switching of fluorescence even on the single-molecular level. The new PBI possessed a lower oxidation potential, which led to an enhanced driving force for PET (see Table 3). Therefore, this dyad demonstrated a good fluorescence on/off ratio even in the modest polarity range ($\varepsilon_r = 9.82$) with values of 68% for the pure open form and 7% for the pure closed form (see Table 1). Disadvantageous fluorescence quenching for the open form increases with increasing polarity of the solvent polarity to give a value of 34% in solvents with the highest permittivity ($\varepsilon_r = 20.46$). The authors gave no information on photostability and cyclization or cycloreversion quantum yields, which leads to the presumption that similar stability problems to those discussed in Chapter 5 for the related compound **9** bearing four aryloxy substituents at the PBI may have been encountered.

Most recently, Sánchez *et al.* published a photochromic dyad **6** composed of a highly fluorescent tetraaryloxy-substituted PBI and described the possibility of emission quenching by intramolecular PET.[5] A very good fluorescence on/off ratio in non-polar solvent ($\varepsilon_r = 2.38$) was observed, with 96% to 10% for the open and closed forms, respectively. Increasing polarity once again led to a decrease in fluorescence quantum yield. However, the remarkably high on/off ratio in non-polar environments should be attributed to a fluorescence quenching FRET process due to the overlap of the emission band of the PBI unit and the absorption band of the closed form of the DAE moiety (see Table 2).[5] This FRET is the main reason for the quenching over the whole range of solvent polarity and leads to disadvantageous destructive read-out.

Besides these PBI-based systems, the novel terrylene bisimide photochromic system **7** (see Chapter 4) exhibited high photostability of photochromic and emissive units and good switchability between open and closed form (see Table 2).[6] However, the TBI fluorescence quantum yield is far from unity even in non-polar solvents (60% in tetrachloromethane; $\varepsilon_r = 2.24$) and decreased distinctly with increasing solvent polarity (8% in DMSO; $\varepsilon_r = 46.45$). Therefore, the ideal environment for this system should be of medium polarity ($\varepsilon_r = 8.93$) although the fluorescence on/off ratio of 29% for the open form and 10% of the closed form is only modest (see Table 1). In contrast to most other photochromic systems in Figure 1, dyad **7** revealed a distinctly lower fluorescence quantum yield in non-polar solvents for the closed than for the open form. This observation cannot be explained at the present time.

Finally, the novel system **8** (see Chapter 5), which contains a tetraaryloxy-substituted PBI and a novel DAE moiety, revealed a superior fluorescence on/off ratio in solvents of medium polarity ($\varepsilon_r = 8.93$), illustrated by quantum yields of 95% for the open form and only 5% for the closed form (see Table 1).[7] The simultaneously synthesized system **9** with a different photochromic unit lacks in

photostability and was not further investigated. In a highly polar environment ($\varepsilon_r = 36.71$), the fluorescence of the open form of **8o** (67%) is clearly quenched compared to the reference PBI (87%), which is attributed to an increasing driving force for intramolecular PET also for the open form with increasing solvent polarity. The detailed photophysical studies by ultrafast techniques and repeating switching cycles revealed an unfavorably low ring-opening quantum yield of the photochromic unit, but due to the convincing on/off ratio (see Table 3) and the enhanced photostability (see Table 2), this system shows nevertheless great promise for further studies for non-destructive read-out in write/read/erase fluorescent memory devices.

References

[1]   Y. Odo, T. Fukaminato, M. Irie, *Chem. Lett.* **2007**, *36*, 240-241.

[2]   M. Berberich, A.-M. Krause, M. Orlandi, F. Scandola, F. Würthner, *Angew. Chem. Int. Ed.* **2008**, *47*, 6616-6619.

[3]   T. Fukaminato, M. Tanaka, T. Doi, N. Tamaoki, T. Katayama, A. Mallick, Y. Ishibashi, H. Miyasaka, M. Irie, *Photochem. Photobiol. Sci.* **2010**, *9*, 181-187.

[4]   T. Fukaminato, T. Doi, N. Tamaoki, K. Okuno, Y. Ishibashi, H. Miyasaka, M. Irie, *J. Am. Chem. Soc.* **2011**, *133*, 4984-4990.

[5]   R. S. Sánchez, R. Gras-Charles, J. L. Bourdelande, G. Guirado, J. Hernando, *J. Phys. Chem. C* **2012**, *116*, 7164-7172.

[6]   M. Berberich, F. Würthner, *Chem. Sci.* **2012**, *3*, 2771-2777.

[7]   M. Berberich, M. Natali, P. Spenst, C. Chiorboli, F. Scandola, F. Würthner, *Chem. Eur. J.* **2012**, *18*, doi:10.1002/chem.201201484.

[8]   T. Fukaminato, T. Doi, M. Tanaka, M. Irie, *J. Phys. Chem. C* **2009**, *113*, 11623-11627.

7   Summary

7.1   Summary in English

The possibility of information storage on a molecular level possesses an extremely high data storage capacity. Switchable organic molecules, which reversibly change properties like absorption and emission behavior, oxidation/reduction potentials, dielectric constants, refractive indices and geometrical structures upon irradiation with light of two different wavelengths, offer the cornerstone for such an application. Photochromic diarylethenes (DAEs) are of particular interest as they provide highly desirable thermal bistability in both ring-open (denoted as DAE_O) and ring-closed (denoted as DAE_C) forms.

For organic memories (OMEM) applications of such photochromic systems, it is important that the emission of the dye unit can be turned on and off repeatedly by isomerization. With an additional third light source of a different wavelength, the respective fluorescent or non-fluorescent state can be obtained as "read-out" signal resulting in a binary emissive "1" and non-emissive "0" code. While direct excitation of the photochrome during the read-out of the emission signal can lead to unfavorable isomerization, several systems were designed containing a photochromic unit and an attached fluorophore.

Several dyads composed of an emissive dye and a photochromic DAE were reported to control the fluorescence of the dye upon isomerization of the photochrome by Förster resonance energy transfer (FRET) (left panel of Figure 1).
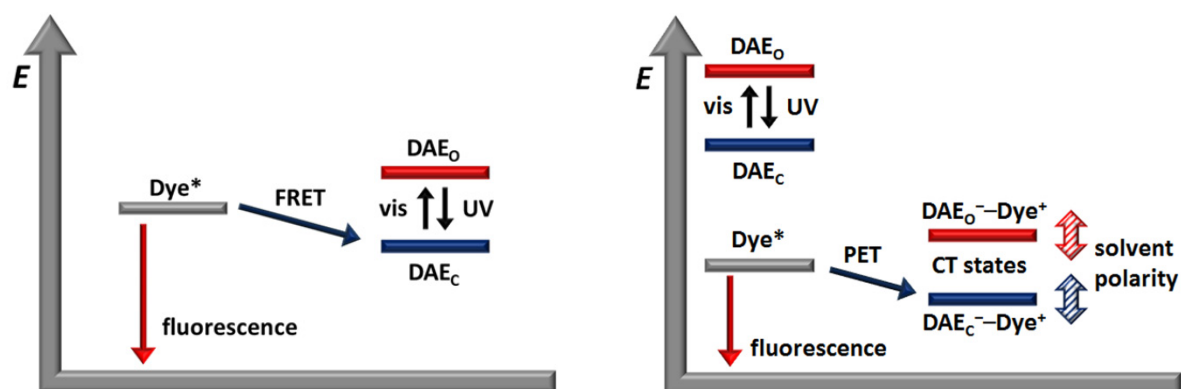

Figure 1. Schematic illustration of energy diagram for the fluorescent open form (red line) and the non-fluorescent closed form (blue line) of a photochromic system revealing fluorescence quenching by a FRET process (left panel) and a PET process (right panel).

Only the closed form of the DAE unit is able to quench the fluorescence of the dye by overlapping of the emission band of the fluorophore with the absorption band of only this isomer of the photochrome. One detrimental effect of the intramolecular fluorescence quenching by FRET is the

concomitant excitation of the ring-closed form of the photochromic dyad during the read-out process, resulting in undesirable ring opening. For this reason, such dyads are very sensitive to the light intensity of the read-out beam.

This unfavorable photoinduced cycloreversion can be circumvented by applying the concept of fluorescence photoswitching by intramolecular photoinduced electron transfer (PET). The basic idea behind this concept is that the ring-open and ring-closed isomers of the photochromic DAE moiety possess different redox properties and the electron transfer from the fluorescent dye is thermodynamically favorable for only one of the two DAE isomers, *i.e.* either to the ring-open or the ring-closed form (right panel in Figure 1). In an optimal case, electron transfer from a fluorescent dye to the DAE unit should be exergonic only for the $DAE_C^- \text{-Dye}^+$ but not for $DAE_O^- \text{-Dye}^+$ charge transfer (CT) state.

The objective of this thesis was the improvement of dyad **1o/1c** (Scheme 1) composed of a DAE derivative and a fluorescent 1,7-dipyrrolidinyl-substituted perylene bisimide dye, which suffered from a rather poorly photostable dye with low fluorescence quantum yields.
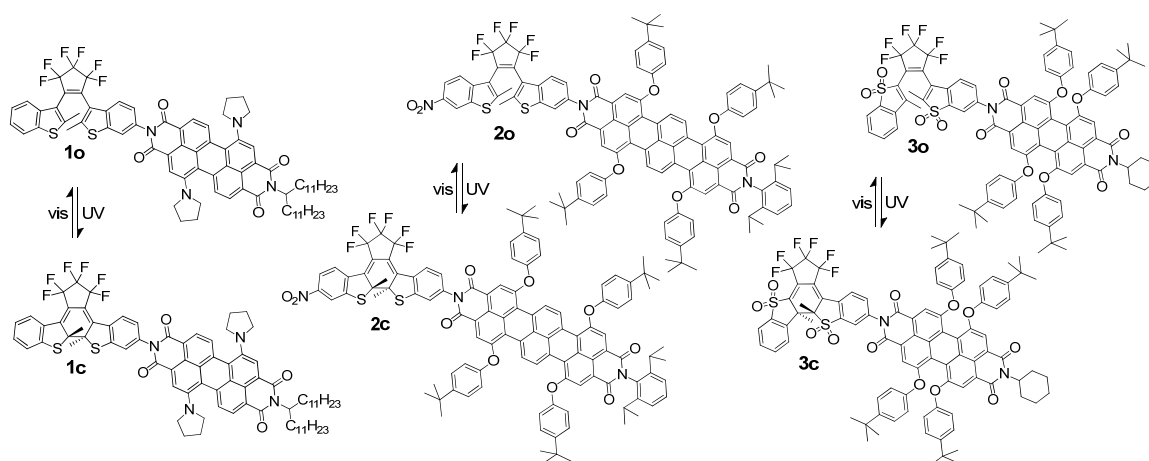

Scheme 1. Previous photochromic dyad **1o/1c** and new systems **2o/2c** and **3o/3c**.

Towards this goal, two appropriate systems **2o/2c** and **3o/3c** were designed and synthesized, and their properties were studied by absorption and emission spectroscopy, cyclic voltammetry, spectroelectrochemistry, and in the case of **3o/3c** the electron-transfer processes were investigated in detail by ultrafast techniques. The content of this thesis is summarized below:

In the introductory Chapter 2, photochromism and diarylethenes as a particular class of photochromic compounds were described. A literature survey explained the development of photochromic compounds for photoinduced electron transfer (PET) applications and gave an overview of photochromic systems containing a DAE unit and a fluorescent perylene bisimide (PBI) dye. Although several photochromic systems were published, each of them suffer from certain disadvantages, such as low fluorescence quantum yield, photocyclization by triplet excitation, small driving force for fluorescence-quenching PET, or low photostability.

Chapter 3 compares three literature known and four new DAEs, which are synthesized within this work for the first time. The spectroscopic and electronic properties of these DAEs were investigated and their suitability as electron-acceptor unit for the above introduced concept was assessed. The particular emphasis was on preparing DAEs with electron-withdrawing groups because photochromic units, which are easy to reduce, are needed for this application. A further criterion is that the absorption band of the closed form of the DAEs should not be shifted to longer wavelengths due to the electron-withdrawing groups.

Chapter 4 describes the first photochromic systems composed of an emitting terrylene bisimide (TBI) dye and a photochromic DAE switch. This was achieved by a ten-step synthetic route (Scheme 2) and new compounds were characterized in detail. In particular, the procedure for the selective reduction of only one nitro group of DAE precursor **12** using sodium hydrosulfide is worth emphasizing.
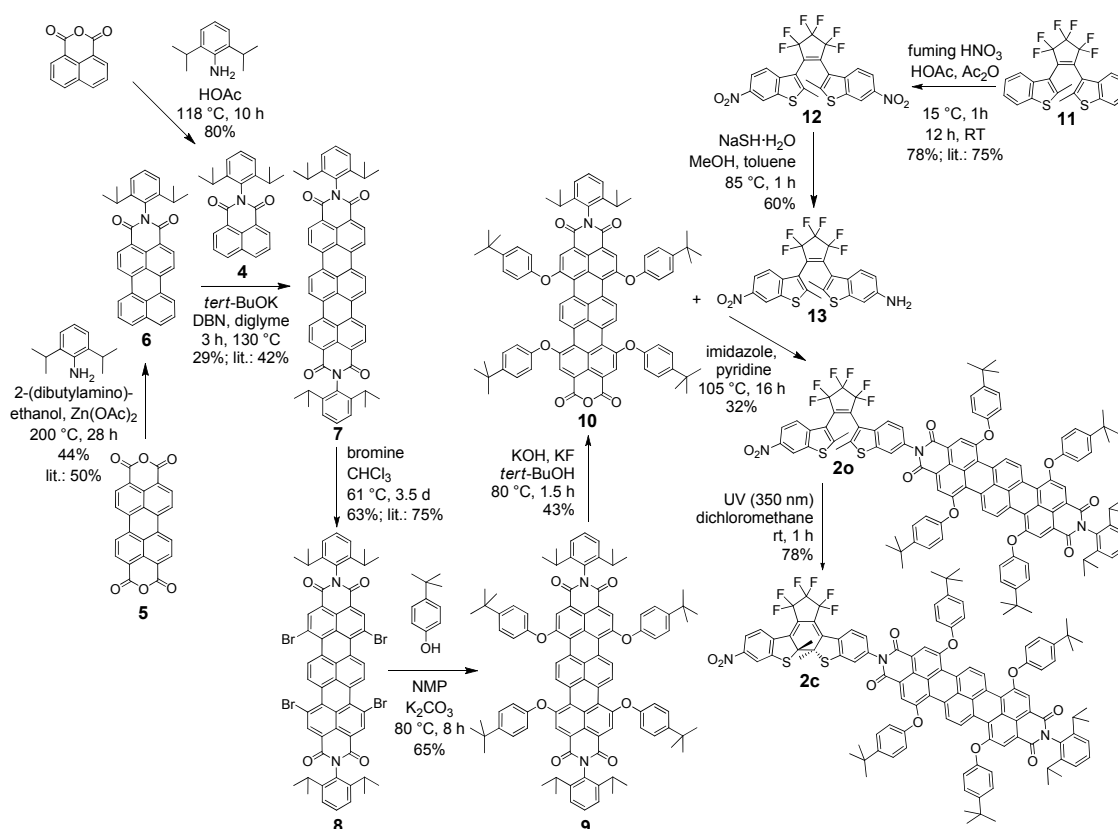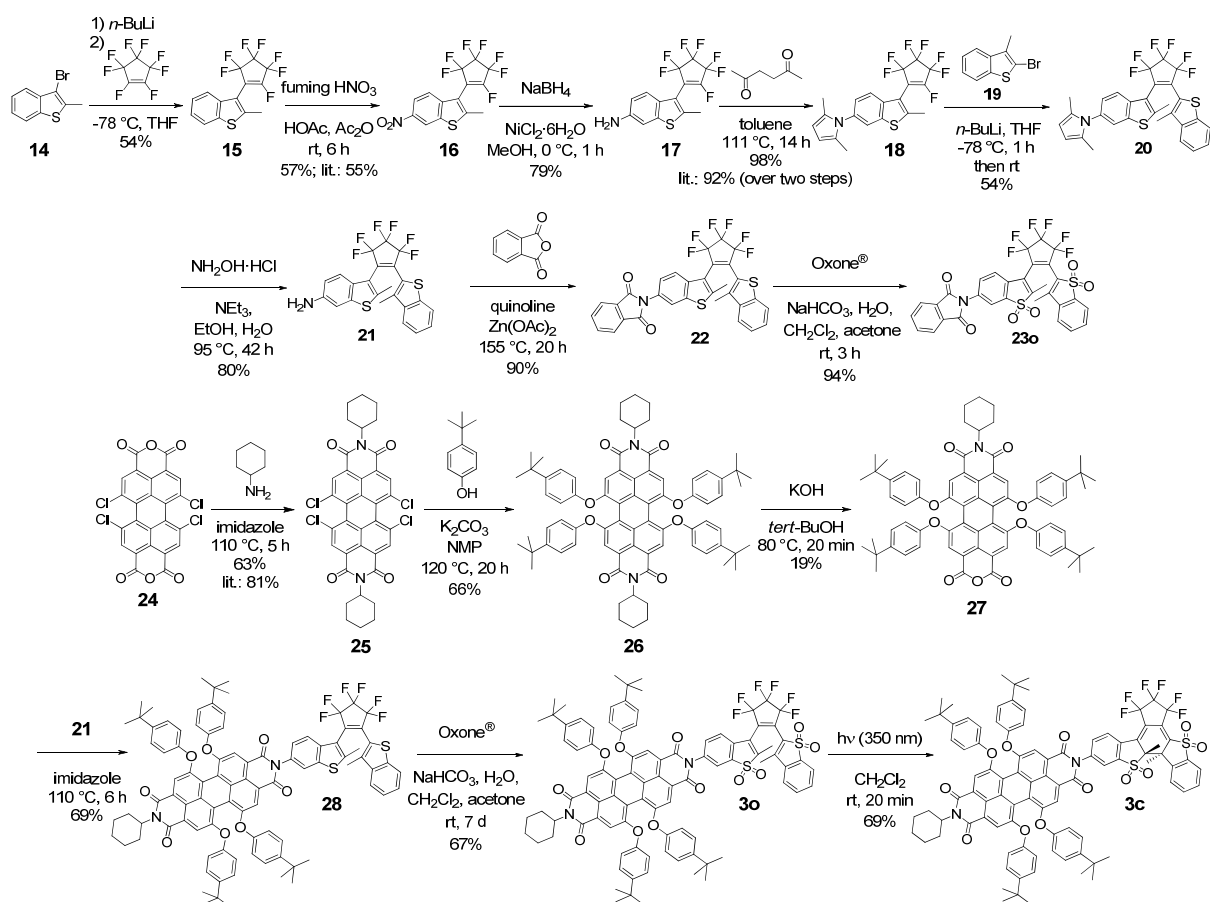

Scheme 2. Complete synthetic route of photochromic system **2o/2c**. DBN = 1,5-diazabicyclo[4.3.0]non-5-ene, NMP = *N*-methyl-2-pyrrolidone.

Switching between both states of the DAE unit by irradiation with UV and visible light led to a significant difference in fluorescence quantum yields of TBI unit of open **2o** and closed form **2c**. The fluorescence quantum yields were determined in a range of solvents from non-polar tetrachloromethane ($\varepsilon_r = 2.24$) to highly polar dimethyl sulfoxide ($\varepsilon_r = 46.45$). For practical purposes, this system performs optimally in solvents or polymeric matrices of intermediate polarity, where

fluorescence quantum yields of **2o** and **2c** are clearly distinguishable, *i.e.* about 30% and 10%, respectively. In highly polar solvents, the fluorescence quantum yields tend to be too low for sensitive detection.

Cyclic voltammetry measurements have shown that the reduction potentials of the open and closed form of the DAE moiety of this photochromic system differ significantly, thus the electron transfer from excited TBI donor takes places only to the closed form of DAE acceptor. The driving force for the emission quenching by PET has been estimated by the Rehm-Weller equation, providing a $\Delta G°$ value of –0.24 eV for the closed form, while this value is positive (0.16 eV) for the open form. The photostability of the present system has been proven by repeating switching cycles performed by alternating irradiation with UV and visible light.

In Chapter 5 the photochromic unit was optimized by oxidation of the sulfur atoms to thiophene 1,1-dioxide groups. This oxidation is accompanied by a hypsochromic shift of the absorption of the closed form of the DAE unit to the UV region and therefore, a broader range of dyes fluorescing in the *visible* range can be used. The complete fourteen-step synthetic route for photochromic system **3o**/**3c** and reference molecules **23o** and **26** is depicted in Scheme 3. Particularly notable is the use of the mild and neutral oxidation reagent Oxone® ($2KHSO_5 \cdot KHSO_4 \cdot K_2SO_4$). *meta*-Chloroperoxybenzoic acid (*m*CPBA) is often used for the oxidation of sulfur atoms in diarylethene compounds, but using Oxone® reduced the formation of side products observed by *m*CPBA oxidation. Thereby, the concluding oxidation steps possessed high to excellent yields for **3o** and **23o**.

Scheme 3. Complete synthetic route of photochromic system **3o/3c** and reference DAE **23o**. NMP = *N*-methyl-2-pyrrolidone, Oxone® = (2KHSO$_5$•KHSO$_4$•K$_2$SO$_4$).

Solvent-dependent fluorescence studies revealed that the emission of ring-closed form **3c** is drastically quenched in solvents of medium (*e.g.* chloroform: ε_r = 4.89) to high polarities (*e.g.* acetone: ε_r = 20.56), while the emission of the ring-open form **3o** is quenched only slightly with increasing solvent polarity (see Figure 2). Although the open and closed form dyads **3o** and **3c** have similar absorption behavior in the visible region, dichloromethane solutions of these dyads exhibit distinctly different colors due to their substantially different fluorescence intensity (see Figure 2): *i.e.* the solution of the open form appears pink, while that of the closed form appears violet. Under UV light (365 nm), the solution of **3o** is brightly emissive and, in contrast, that of **3c** is barely emissive. In accordance with these coloristic attributes, the fluorescence quantum yields of open form **3o** (95%) and closed form (5%) in dichloromethane are strikingly different.
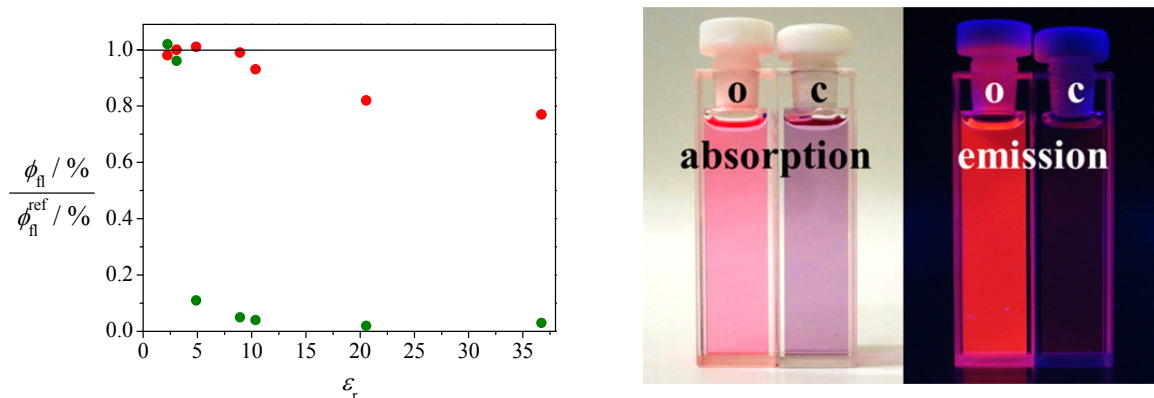
Figure 2. Left panel: Fluorescence quantum yields of **3o** and **3c** (Φ_{fl}) divided by the quantum yield of reference PBI **26** (Φ_{fl}^{ref}) as a function of the dielectric constants of solvents (ε_r); open form (●), closed form (●). Right panel: photographs of solutions of **3o** and **3c** in dichloromethane (1×10^{-5} M) under ambient laboratory light (left) and under UV light (365 nm; right).

The strong fluorescence quenching of **3c** is attributed to a photoinduced electron transfer (PET) process from the excited PBI unit to ring-closed DAE moiety as this process is thermodynamically highly favorable with a Gibbs free energy value of –0.34 eV in dichloromethane. The electron-transfer mechanism for the fluorescence quenching of ring-closed **3c** is substantiated by ultrafast transient measurements in dichloromethane and acetone, revealing stabilization of charge-separated states of **3c** in these solvents. The results reported in this chapter show that the new photochromic dyad **3** has potential for non-destructive optical information storage.

Chapter 6 provides a clear comparison of recent perylene bisimide-diarylethene photochromic systems and the two new systems **2o/2c** and **3o/3c** (see Scheme 1) in respect to their fluorescence quenching behavior in media of different polarities.

In conclusion, the present thesis enhances the strategy of non-destructive fluorescence read-out in rylene bisimide-diarylethene containing photochromic systems. The diploma work compound **1o/1c** (see Scheme 1) with its unfavorable low photostability and low fluorescence quantum yield was replaced by two novel, photostable systems, which were investigated in detail. Thus, these novel photochromic systems satisfy the necessary requirements for non-destructive read-out in write/read/erase fluorescent memory devices and should be of particular interest for single-molecule spectroscopy.

7.2   Zusammenfassung (Summary in German)

Die Möglichkeit, einzelne Moleküle zur Datenspeicherung zu nutzen, stellt eine extrem hohe Datendichte in Aussicht. Schaltbare organische Moleküle, deren Eigenschaften wie beispielsweise Absorptions- und Emissionsverhalten, Oxidations- und Reduktionspotential, Dielektrizitätskonstante, Brechungsindex und geometrische Struktur reversibel durch Bestrahlung mit Licht zweier unterschiedlicher Wellenlängen verändert werden können, stellen einen wichtigen Grundstein für solche Anwendungen dar. Besonders die photochromen Diarylethene (DAE) sind mit ihrer thermischen Stabilität beider Isomere, der ringoffenen Form (bezeichnet als DAE_O) und der ringgeschlossenen Form (bezeichnet als DAE_C), von hohem Interesse.

Für den Einsatz solcher photochromer Systeme als mögliche Datenspeichermedien (OMEM = organic memory) ist es notwendig, die Emission des Farbstoffs wiederholt ein- bzw. ausschalten zu können, indem die photochrome Einheit mit Licht zweier unterschiedlicher Wellenlängen isomerisiert wird. Durch Zuhilfenahme einer zusätzlichen dritten Lichtquelle mit einer dazu unterschiedlichen Wellenlänge ist es nun möglich, den fluoreszierenden bzw. nicht fluoreszierenden Zustand als binäre Auslesesignale „1" (fluoreszent) oder „0" (nicht fluoreszent) zu erhalten. Weil das direkte Anregen der photochromen Einheit während des Auslesens des Emissionssignals zur unerwünschten Isomerisierung führen kann, wurden mehrere Moleküle konzipiert, die aus einer photochromen Einheit und einem daran gebundenen Fluorophor aufgebaut sind.

Einige Publikationen behandeln Dyaden, die aus einem fluoreszierenden Farbstoff und einem photochromen DAE aufgebaut sind und mit deren Hilfe man durch Isomerisierung der photochromen Einheit die Fluoreszenzintensität mittels Förster-Resonanzenergietransfer (FRET) kontrollieren kann (siehe linke Seite von Abbildung 1).
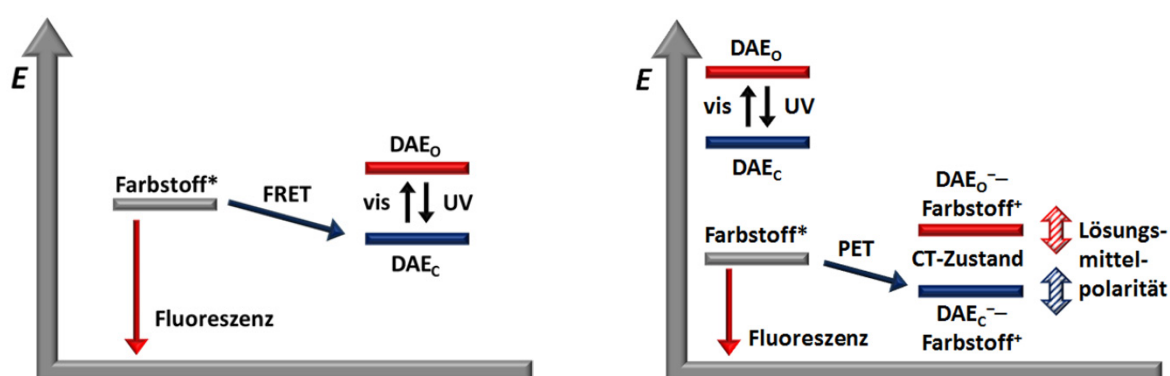
Abbildung 1. Schematische Darstellung des Energiediagramms der fluoreszierenden, offenen Form (rote Linie) und der nicht fluoreszierenden, geschlossenen Form (blaue Linie) eines photochromen Systems, dessen Fluoreszenzlöschung auf einem FRET Prozess (linke Abbildung) bzw. einem PET Prozess (rechte Abbildung) beruht.

Dabei kann nur die ringgeschlossene Form der DAE-Einheit die Fluoreszenz löschen, da nur bei ihr die Möglichkeit besteht, dass die Emissionsbande des Farbstoffs mit der Absorptionsbande der

photochromen Einheit überlappt. Ein nachteiliger Effekt der intramolekularen Fluoreszenzlöschung durch FRET ist die gleichzeitige Anregung der ringgeschlossenen Form des Photoschalters während des Ausleseprozesses, was zur unerwünschten Ringöffnung führen kann. Aus diesem Grund sind solche Dyaden sehr empfindlich bezüglich der Lichtintensität des Auslesestrahls.

Diese durch Licht induzierte Zykloreversion kann verhindert werden, indem man das Konzept des Photoschaltens der Fluoreszenz durch intramolekularen lichtinduzierten Eletronentransfer (PET = photoinduced electron transfer) anwendet. Die Grundidee dieses Konzeptes ist, dass die ringoffene und die ringgeschlossene Form der photochromen DAE-Einheit unterschiedliche Redoxpotentiale besitzen und dabei der Elektronentransfer nur zu einer der beiden DAE-Isomere, also entweder der ringoffenen oder der ringgeschlossenen Form, thermodynamisch begünstigt ist (siehe rechte Seite von Abbildung 1). Im optimalen Fall sollte der Elektronentransfer vom fluoreszierenden Farbstoff zur DAE-Einheit nur für den ladungsgetrennten Zustand (CT state = charge-transfer state) DAE_C^-– $Farbstoff^+$ und nicht für DAE_O^-–$Farbstoff^+$ exergon sein.

Die Zielsetzung dieser Doktorarbeit war die Weiterentwicklung der Dyade **1o**/**1c** (Abbildung 1), welche aus einem DAE-Derivat und einem fluoreszierenden 1,7-dipyrrolidinylsubstituierten Perylenbisimidfarbstoff aufgebaut ist, wobei letzterer weder eine große Lichtstabilität noch eine hohe Fluoreszenzquantenausbeute aufwies.
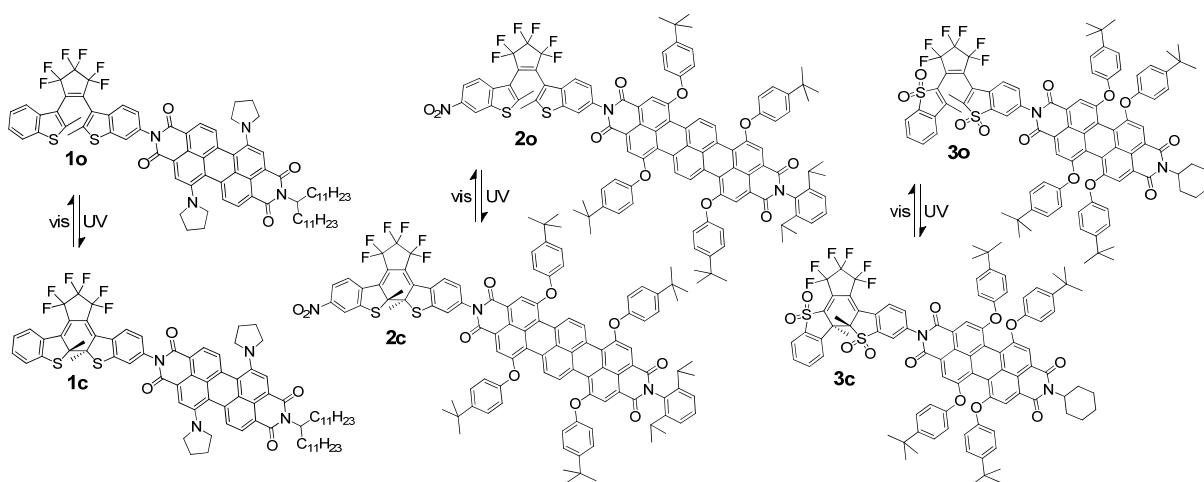
Abbildung 2. Photochrome Vorläuferverbindung **1o**/**1c** und die neuen Systeme **2o**/**2c** und **3o**/**3c**.

Um dieses Ziel zu erreichen, wurden die zwei geeigneten Systeme **2o**/**2c** und **3o**/**3c** entwickelt und dargestellt und ihre Eigenschaften mittels Absorptions- und Emissionsspektroskopie, Cyclovoltammetrie und Spektroelektrochemie untersucht. Im Falle von **3o**/**3c** wurde der Elektronentransferprozess darüber hinaus mittels Ultrakurzzeitspektroskopie studiert. Der Inhalt der Arbeit ist im Folgenden zusammengefasst:

Im einleitenden Kapitel 2 wurden Photochromismus und Diarylethene als besondere Vertreter der photochromen Verbindungen vorgestellt. Mit Hilfe einer Literaturübersicht wurde die Entwicklung photochromer Moleküle für lichtinduzierte Elektronentransferanwendungen dargelegt und im

Weiteren alle bekannten photochromen Systeme, die aus einer DAE-Einheit und einem fluoreszierenden Perylenbisimidfarbstoff aufgebaut sind, aufgezeigt. Obwohl mehrere photochrome Systeme bekannt sind, weisen alle deutliche Nachteile wie geringe Fluoreszenzquantenausbeuten, Ringschluss durch Triplettanregung, zu geringe Triebkraft für den fluoreszenzlöschenden Elektronentransfer oder geringe Lichtstabilität auf.

In Kapitel 3 werden drei literaturbekannte sowie vier im Rahmen dieser Arbeit erstmals synthetisierte DAEs vorgestellt, ihre spektroskopischen und elektronischen Eigenschaften untersucht und ihre Tauglichkeit als Elektronenakzeptoreinheit nach dem hier vorgestellten Konzept beurteilt. Der Schwerpunkt wurde dabei auf DAEs mit elektronenziehenden Gruppen gelegt, da für die hier beschriebene Anwendung leicht reduzierbare photochrome Einheiten mit einer Absorptionsbande der geschlossenen Form im nicht zu langwelligen Bereich des sichtbaren Spektrums gesucht werden.

In Kapitel 4 wird, mit Hilfe der Daten aus Kapitel 3, die allererste photochrome Verbindung vorgestellt, die aus einem fluoreszierenden Terrylenbisimidfarbstoff (TBI) und einem DAE-Schalter aufgebaut ist. Die zehnstufige Synthese wurde nachvollziehbar dargelegt und alle bislang unbekannten Verbindungen genau charakterisiert (Abbildung 3). Besonders erwähnenswert bei dieser Synthese ist die selektive Reduktion nur einer der beiden Nitrofunktionen der DAE-Zwischenstufe **12** unter Verwendung von Natriumhydrogensulfid.

Abbildung 3. Vollständigerer Syntheseweg zum photochromen System **2o/2c**. DBN = 1,5-Diaza-bicyclo[4.3.0]non-5-en, Diglyme = Bis(2-methoxyethyl)ether, NMP = *N*-Methyl-2-pyrrolidon.

Schalten zwischen beiden Isomeren der DAE-Einheit mit UV- bzw. sichtbarem Licht führt zu einer deutlichen Veränderung der Fluoreszenzquantenausbeute der TBI-Einheit für die offene Form **2o** und die geschlossene Form **2c**. Die Quantenausbeute der beiden Formen **2o** und **2c** wurde in Abhängigkeit von der Lösungsmittelpolarität bestimmt, wobei ein Bereich von sehr unpolarem Tetrachlormethan ($\varepsilon_r = 2.24$) bis zu stark polarem Dimethylsulfoxid ($\varepsilon_r = 46.45$) abgedeckt wurde. Für die praktische Anwendung bieten sich Lösungsmittel oder Polymermatrizes von mittlerer Polarität an, da hierbei die Fluoreszenzquantenausbeuten von **2o** und **2c** bei 30% bzw. 10% bereits deutlich unterscheidbar sind. In hochpolaren Lösungsmitteln sind die Fluoreszenzquantenausbeuten dann insgesamt zu niedrig für eine empfindliche Detektion.

Cyclovoltammetrische Messungen zeigten, dass sich die Reduktionspotentiale der offenen und geschlossenen Form der DAE-Einheit des photochromen Systems deutlich unterscheiden, sodass der Elektronentransfer von dem angeregten TBI-Donor nur zur geschlossenen Form des DAE-Akzeptors stattfinden kann. Die Triebkraft für den fluoreszenzlöschenden PET wurde mit Hilfe der Rehm-Weller-Gleichung berechnet, wobei man einen $\Delta G°$-Wert von -0.24 eV für die geschlossene und 0.16 eV für die offene Form erhielt. Die Lichtstabilität des dargebotenen Systems wurde belegt, indem wiederholte Schaltzyklen durch abwechselnde Belichtung mit UV- und sichtbarem Licht aufgenommen wurden.

In Kapitel 5 wurde die photochrome Einheit durch Oxidation der Schwefelatome zu Thiophen-1,1-dioxidgruppen optimiert. Diese Oxidation wird begleitet von einer hypsochromen Verschiebung der Absorptionsbande der geschlossenen Form der Diaryletheneinheit, wodurch eine breitere Palette von Farbstoffen, die im *sichtbaren* Bereich fluoreszieren, nutzbar wird. Die komplette vierzehnstufige Synthese des Systems **3o**/**3c** sowie der Referenzen **23o** und **26** ist in Abbildung 4 zusammengefasst. Besonders zu erwähnen ist hierbei der Gebrauch des milden Oxidationsmittels Oxone[®] ($2KHSO_5 \cdot KHSO_4 \cdot K_2SO_4$) anstelle von *meta*-Chlorperbenzoesäure (*m*CPBA), die oft für die Oxidation von Schwefelatomen von DAE-Verbindungen verwendet wird. Die Oxidation von DAE-Derivaten mit schwefelhaltigen Heterozyklen mit dem sauren *m*CPBA kann allerdings zur vermehrten Nebenproduktbildung führen. Mit Oxone[®] wies der abschließende Oxidationsschritt für **3o** und **23o** exzellente Ausbeuten auf.
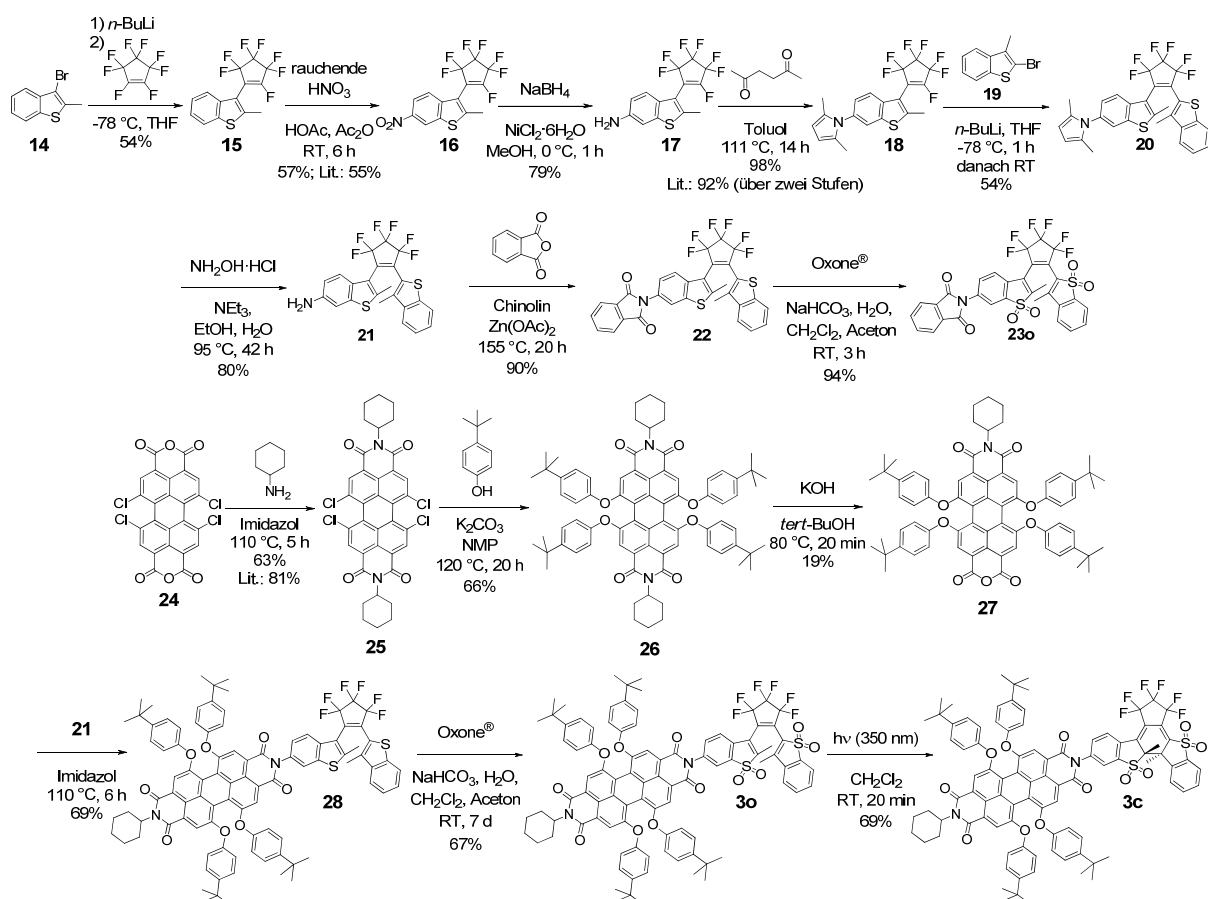
Abbildung 4. Vollständiger Syntheseweg für das photochrome System **3o/3c**. NMP = *N*-Methyl-2-pyrrolidon, Oxone$^{®}$ = (2KHSO$_5$•KHSO$_4$•K$_2$SO$_4$).

Lösungsmittelabhängige Fluoreszenzstudien zeigten, dass die Emission der ringgeschlossenen Form **3c** drastisch in Lösungsmitteln von mittlerer (z. B. Chloroform; $\varepsilon_r = 4.89$) bis hoher (z. B. Aceton; $\varepsilon_r = 20.56$) Polarität reduziert wird, während die Emission der ringoffenen Form **3o** nur in stärker polaren Lösungsmitteln allmählich abnimmt (siehe Abbildung 5). Obwohl die offene und geschlossene Form der Dyade **3o** und **3c** sehr ähnliche Absorptionsverhalten im sichtbaren Bereich des Spektrums aufweisen, zeigen Dichlormethanlösungen dieser zwei Isomere aufgrund ihrer sehr unterschiedlichen Fluoreszenzintensitäten auch deutlich unterschiedliche Farben (siehe Abbildung 5): die Lösung der offenen Form erscheint pink, für die geschlossene Form beobachtet man eine violette Farbe. Unter UV-Licht (365 nm) emittiert die Lösung von **3o** strahlend rot, wohingegen als deutlicher Kontrast die nur sehr schwache Emission von **3c** sichtbar ist. Begleitet von diesen Merkmalen zeigen die Fluoreszenzquantenausbeuten der ringoffenen Form **3o** mit 95% und der ringgeschlossenen Form **3c** mit 5% in Dichlormethan einen beachtlichen Unterschied.
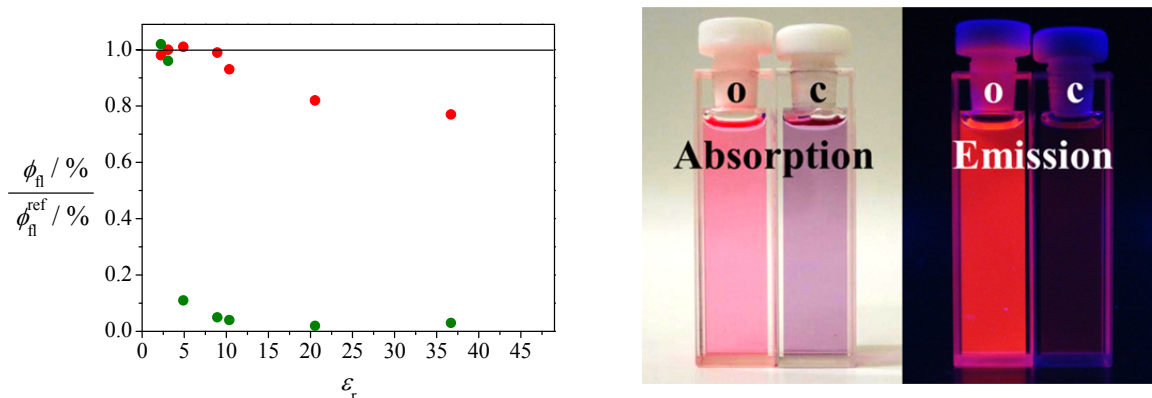
Abbildung 5. Linke Seite: Fluoreszenzquantenausbeuten von **3o** und **3c** (Φ_{fl}) geteilt durch die Quantenausbeute des Vergleichsfarbstoffs PBI **26** (Φ_{fl}^{ref}) als Funktion der Dielektrizitätskonstante ε_r des jeweiligen Lösungsmittels; offene Form **3o** (●), geschlossene Form **3c** (●); rechte Seite: Fotographien von Dichlormethanlösungen (1×10^{-5} M) von **3o** und **3c** bei normaler Raumbeleuchtung (Absorption) und unter UV-Licht (365 nm; Emission).

Die starke Fluoreszenzlöschung von **3c** konnte auf einen lichtinduzierten Elektronentransfer vom angeregten PBI-Farbstoff zur ringgeschlossenen DAE-Einheit zurückgeführt werden, der eine thermodynamische Triebkraft von –0.34 eV für die Gibbs-Energie in Dichlormethan aufweist. Der Elektronentransfermechanismus für die Fluoreszenzlöschung der geschlossenen Form **3o** wurde durch ultrakurzzeitspektroskopische Untersuchungen in Dichlormethan und Aceton belegt, wobei eine Stabilisierung des ladungsgetrennten Zustandes in **3c** in diesen Lösungsmitteln nachgewiesen wurde. Die in diesem Kapitel aufgeführten Ergebnisse zeigen, dass die photochrome Dyade **3** Anwendungspotential für das nicht-destruktive Auslesen in einem auf Schreib-, Lese- und Löschvorgängen basierenden fluoreszierenden Datenspeicher besitzt.

In Kapitel 6 wurden die bisher veröffentlichten photochromen Systeme bestehend aus Perylenbisimidfarbstoffen und Diaryethenen mit den zwei neuen, in dieser Arbeit vorgestellten Verbindungen **2o/2c** und **3o/3c** (Abbildung 2) in Bezug auf ihr Fluoreszenzlöschverhalten in unterschiedlich polaren Medien verglichen.

Zusammenfassend zeigt diese Doktorarbeit deutlich verbesserte aus Rylenbisimiden und Diarylethenen aufgebaute, photochrome Systeme für das nicht-destruktive Auslesen von Fluoreszenz. Die aus der Diplomarbeit stammende Verbindung **1o/1c** (Abbildung 2) mit ihrer geringen Lichtstabilität und niedrigen Fluoreszenzquantenausbeuten wurde dabei durch zwei neue, lichtstabile Systeme ersetzt und intensive Untersuchen durchgeführt. Auf diese Weise war es möglich, neue photochrome Systeme darzustellen, die die notwendigen Anforderungen für ein nicht-destruktives Auslesen in einem auf Schreiben, Auslesen und Löschen basierenden fluoreszierenden Datenspeicher erfüllen und darüber hinaus für einzelmolekülspektroskopische Untersuchungen von Interesse sein sollten.

Appendix

Supplements for Chapter 4 – Two Additional Terrylene Bisimide Dyad Systems

The development of the photochromic TBI containing system **1o** (see Figure 1), which was described in detail in Chapter 4, started with the synthesis and preliminary studies of a similar dyad **2o** (see Figure 1) without the additional nitro group at the DAE moiety. The approximate driving force for this dyad **2o/2c** can be obtained by replacing the reduction potentials of the photochromic system in Chapter 4.4 by the published values of the photochromic unit without the additional nitro group.[1] Thus, one receives two positive values for the driving force, *i.e.* +0.55 eV for the open form **2o** and +0.11 eV for the closed form **2c**, which makes fluorescence quenching by PET thermodynamically unfavorable, at least in dichloromethane and less polar environments. With the help of this system **2o/2c**, it was possible to prove that PET, and not other processes, causes fluorescence quenching for system **1o/1c**.
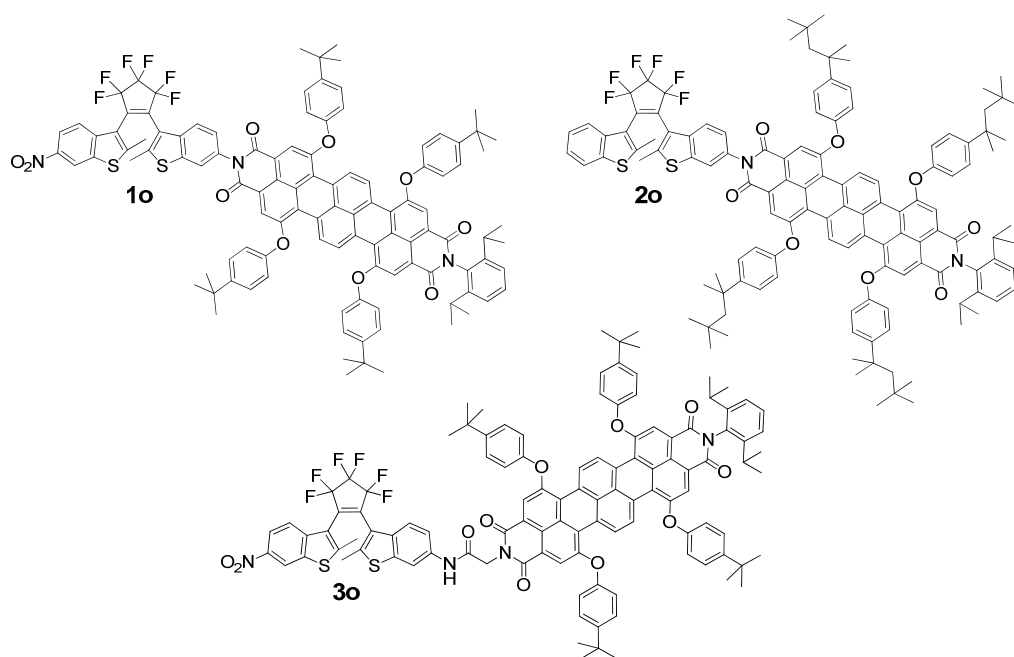
Figure 1. Photochromic terrylene bisimide systems **1o**, **2o**, and **3o**.

The terrylene bisimide containing photochromic system **1o** (see Figure 1) showed disadvantageous ring opening during selective excitation of the TBI unit of the closed form of the dyad in dichloromethane and ethyl acetate (see Chapter 4.5). Therefore, non-destructive fluorescence read-out was not possible in these media. The feasibility of such an interaction between DAE unit and a rylene bisimide dye because of the direct linkage should be very low, due to nodes at the imide nitrogens of both frontier orbitals, *i.e.* HOMO (highest occupied molecular orbital) and LUMO (lowest unoccupied

molecular orbital).[2] Furthermore, destructive FRET processes from the fluorophore to DAE$_O$ and DAE$_C$ are both impossible for energetic reasons (see Chapter 2.6).

The following section describes the synthesis and introductory spectroscopic studies of a photochromic system **3o** (see Figure 1) with an additional glycine linker between photochrome and fluorophore in order to avoid the direct linkage between both aromatic systems. A respective reference DAE with phthalic imide residue instead of the emitter was described in Chapter 3.2. The driving force for the fluorescence quenching PET for the closed form of the new dyad should not be distinctly influenced by the glycine linker, as the first reduction potential of the closed form of a reference DAE with glycine linker (see Chapter 3.4) with a value of −1.20 V matches the value of a reference DAE without this linker (see Chapter 4.4). However, the slightly larger distance between acceptor and donor unit may influence the thermodynamics and kinetics of the photoinduced electron transfer.

Synthesis

Terrylene anhydride imide **4** with 4-(1,1,3,3-tetramethylbutyl)-phenoxy substituents was reacted with 1-(6-amino-2-methyl-1-benzo[*b*]thiophen-3-yl)-2-(2'-methyl-1'-benzo[*b*]thiophen-3'-yl)-perfluoro-cyclopentene[1] (**5**) in a condensation reaction yielding in 80% of the open form of dyad **2o** (see Scheme 1). The ring closure was likewise performed in a Rayonet photoreactor using UV light (350 nm). The dark green product **2c** was obtained in 51% yield.
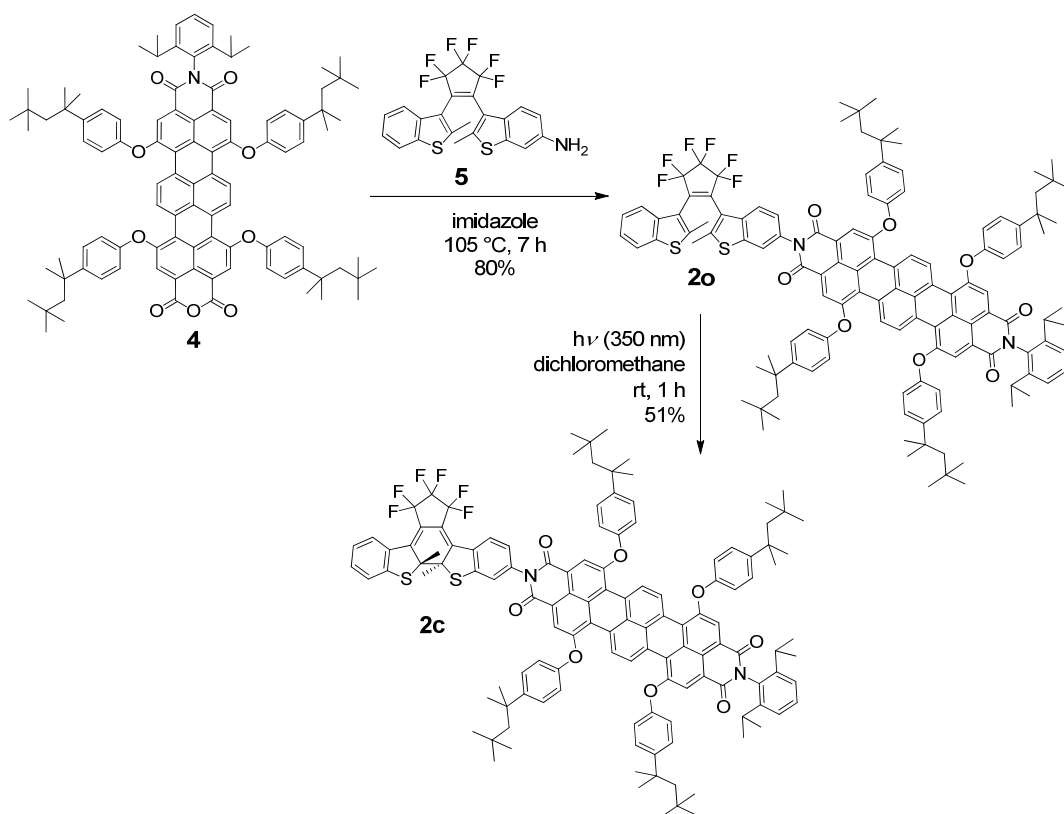
Scheme 1. Synthetic route for photochromic system **2o**/**2c** without the additional nitro group at the DAE unit.

Terrylene anhydride imide **6** (see Chapter 4.2 for synthetic details) and glycine-functionalized DAE **7** (see Chapter 3.2) were reacted in a condensation reaction to yield photochromic dyad **1o** in a yield of 33% (Scheme 2). The closed form of dyad **3c** was obtained in 75% yield by irradiation of a dichloromethane solution of the open form **3o** with UV light (350 nm) in a Rayonet photoreactor and subsequent separation of both isomers by column chromatography under exclusion of light. The synthetic details and the characterization data of **2o**, **2c**, **3o**, and **3c** are provided in the experimental section.
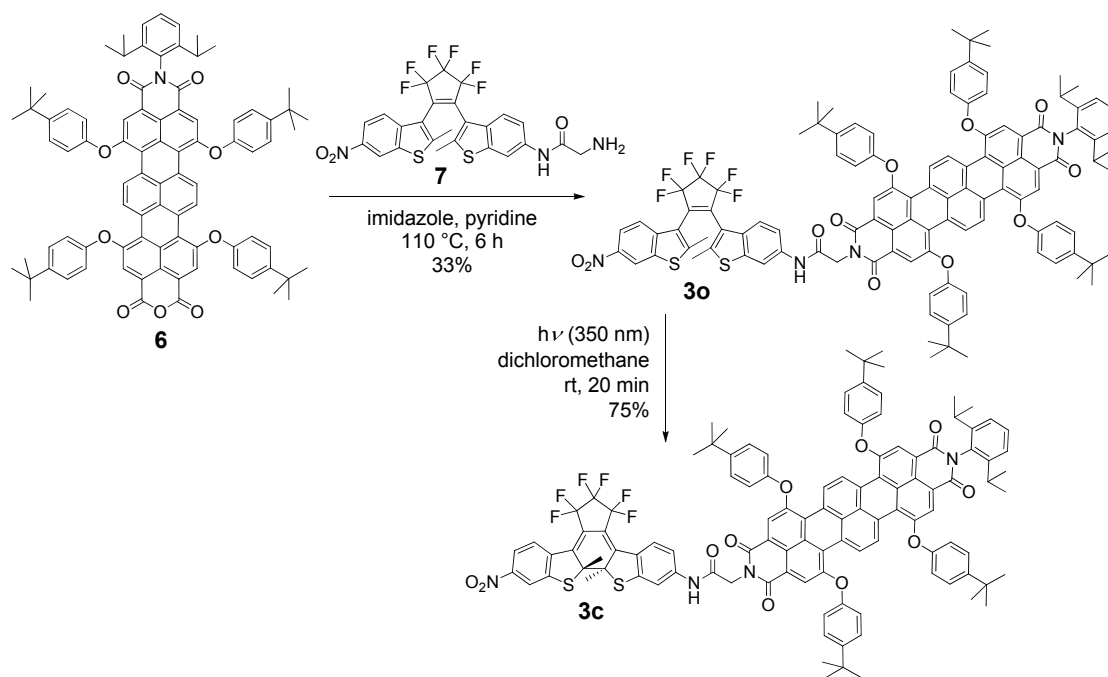
Scheme 2. Synthetic route for photochromic system **3o/3c** with glycine linker.

Absorption and Emission Studies

Initial UV/vis absorption and emission studies of dyad system **2o/2c** were performed in dichloromethane. The significant TBI band between 550 and 730 nm was observed for both ring-open and ring-closed form (see Figure 2) The absorption band of **2c** with a maximum at 683 nm revealed a slightly higher extinction than for **2o** at 681 nm. This behavior is similar to the TBI containing photochromic system of Chapter 4 and means a different influence of the directly linked systems compared to the glycine linked dyad (*vide infra*).

The fluorescence quantum yields of **2o** (31%) and **2c** (29%) in dichloromethane are almost equal within the measurement uncertainty and demonstrate that neither a PET process, which is unfeasible for this system due to thermodynamics, nor a disadvantageous FRET process causes fluorescence quenching. More importantly this shows that the fluorescence quenching observed in systems **1o/1c** (see Chapter 4) is most likely due to PET and not FRET.
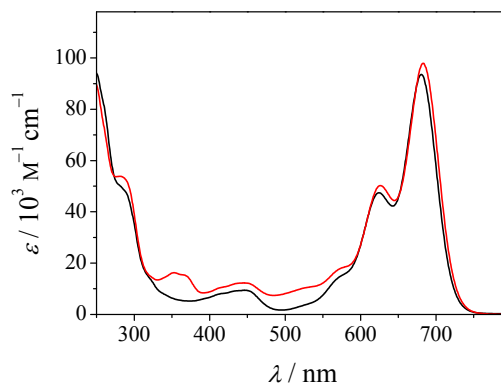
Figure 2. UV/vis absorption spectra of dyads **2o** (black line) and **2c** (red line) in dichloromethane (1×10^{-5} M) at 25 °C.

UV/vis absorption and emission studies of dyad system **3o**/**3c** with an incorporated glycine unit were performed and the influence of enduring excitation of the TBI unit on the fluorescence intensity of **3c** was investigated. The open form of the terrylene bisimide conjugate **3o** has an intense absorption between 550 and 730 nm with a maximum at 681 nm (Figure 3), almost identical to the absorption behavior of the dyad system without glycine linker (see Chapter 4.3). The closed form of dyad **3c** shows higher absorption between 350 and 650 nm, which corresponds to the absorption of the closed DAE moiety. In contrast to the system without the glycine linker (see Chapter 4 and compound **2o**/**2c**), the absorption of the terrylene bisimide moiety of dyad **3c** has a negligible increase of extinction with a maximum at 682 nm.
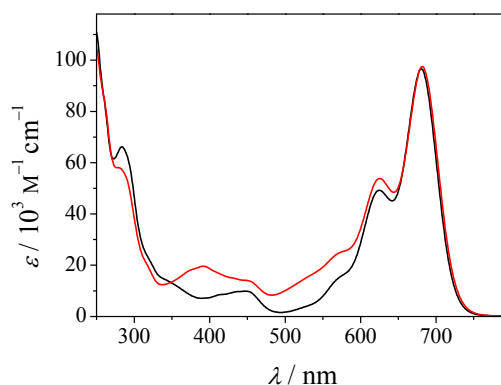
Figure 3. UV/vis absorption spectra of dyads **3o** (black line) and **3c** (red line) in dichloromethane (1×10^{-5} M) at 25 °C.

The fluorescence quantum yields of the open form **3o** (22%) and closed form **3c** (12%) in dichloromethane is in discrepancy with the dyad system without an incorporated linker (open form: 29%; closed form: 10%; see Chapter 4.3). Accordingly, the glycine linker itself has an influence on the fluorescence quantum yield for the open form of the dyad, which should not reveal any

fluorescence quenching behavior. This new quenching process by the glycine linker only takes place for the open form and not the closed form.

To verify and compare non-destructive read-out capability of photochromic system **3**, time-dependent fluorescence intensities of closed form dyad **3c** were measured upon excitation of the terrylene bisimide moiety with a light intensity of 4.3 mW/cm^2 at 720 nm for 1 h (see Figure 4). The emission intensity of **3c** increased dramatically by around 70% within the first 40 min. This 70% rise corresponds to a complete ring opening of **3c** and therefore, an increase of the fluorescence quantum yield from 12% (pure closed form **3c**) to 22% (pure open form **3o**).
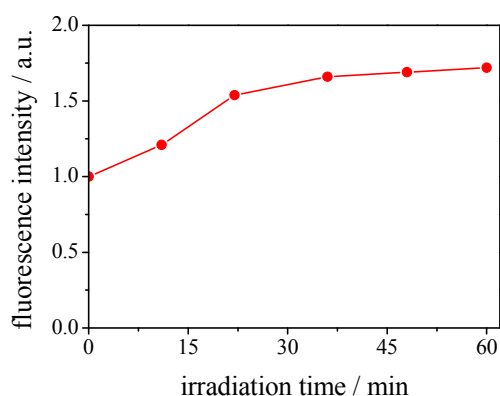
Figure 4. Time-dependent fluorescence intensities of **3c** in dichloromethane at 750 nm upon continuous excitation at 720 nm (±10 nm FWHM) with a 75 W Xenon short arc lamp (4.3 mW/cm^2) for 1 h (cut-off filter at 640 nm); FWHM = full width half maximum.

As a consequence, non-destructive read-out capability could not be improved by incorporation of a glycine linker between photochrome and emitter. Furthermore, the additional fluorescence quenching observed for the open form **3o** diminishes the performance of the system. These detrimental effects might be circumvented by incorporation of other spacers between DAE and TBI units.

Experimental Section

Materials and Methods

General: All solvents and reagents were purchased from commercial sources and were used as received without further purification, unless otherwise stated. 1-(6-Amino-2-methyl-1-benzo[*b*]thiophen-3-yl)-2-(2'-methyl-1'-benzo[*b*]thiophen-3'-yl)-perfluorocyclopentene (**5**) was prepared according to literature procedure.[1] An initial sample of *N*-(2,6-diisopropylphenyl)-1,6,9,14-tetra[4-(1,1,3,3-tetramethylbutyl)-phenoxy]terrylene-3,4:11,12-tetracarboxylic acid-3,4-anhydride-11,12-imide (**4**) was kindly provided by Dr. Neil G. Pschirer (BASF SE). Column chromatography was performed using silica gel 60M (0.04–0.063 mm) from Macherey-Nagel. Melting points were determined on an Olympus BX41 polarization microscope and a Linkam TP 94 heating stage and are uncorrected. High resolution mass spectra (ESI) were recorded on an ESI micrOTOF Focus

spectrometer from Bruker Daltonics. MALDI-TOF mass spectra were recorded on an Autoflex II spectrometer from Bruker Daltonics. The UV irradiation experiments were performed in a Rayonet Photoreactor RPR-100 (Southern New England Ultraviolet Company) with 16 UV lamps (24 W lamps with λ_{max} = 350 nm). A R64 filter (R64_.SP – 08.08.03 – 0.1 mm cuvette) from JASCO Corporation was used for filtering irradiation below 640 nm.

NMR spectroscopy: ^{1}H spectra were recorded on Bruker Advance 400 or Bruker Advance DMX 600 spectrometer and calibrated to the residual solvent peak (CD_2Cl_2: 5.32 ppm).

UV/vis absorption and fluorescence spectroscopy: For all spectroscopic measurements, spectroscopic grade solvents (Uvasol®) from Merck (Hohenbrunn, Germany) were used. UV/vis spectra were recorded on a Perkin Elmer UV/vis spectrometer Lambda 35 in combination with a Perkin Elmer PTP–1+1 peltier system and a Lauda ecoline RE306/E300 refrigeration circulator. Fluorescence spectra were recorded with a PTI QM-4/2003 using conventional quartz cells (light path 1 cm). All fluorescence measurements were performed under aerobic conditions and fluorescence spectra are corrected against photomultiplier and lamp intensity. The fluorescence quantum yields were determined as the average value for five different excitation wavelengths using Rhodamine 800 as reference (Φ_{fl} = 0.21 in ethanol) by applying the high dilution method (abs.: < 0.05).[3]

Cyclic voltammetry: Cyclic voltammetry measurements were performed on a standard, commercial electrochemical analyzer (EC epsilon; BAS Instruments, UK) in a three electrode single-compartment cell under argon atmosphere. Dichloromethane (HPLC grade) was dried over calcium hydride under argon and degassed prior to use. The supporting electrolyte tetrabutylammonium hexafluorophosphate (TBAHFP) was synthesized according to literature,[4] recrystallized from ethanol/water, and dried in high vacuum. The measurements were carried out under exclusion of air and moisture at a concentration of about 10^{-4} M with ferrocene as an internal standard for the calibration of the potential. Working electrode: Pt disc; reference electrode: Ag/AgCl; auxiliary electrode: Pt wire.

Open form of photochromic dyad 2o

This compound was synthesized according to a similar procedure previously reported for a 1,7-dipyrrolidinyl-perylene bisimide-diarylethene conjugate.[1] A mixture of 1-(6-amino-2-methyl-1-benzo[b]thiophen-3-yl)-2-(2'-methyl-1'-benzo[b]thiophen-3'-yl)-perfluorocyclopentene (**5**) (41.9 mg, 86.7 μmol), *N*-(2,6-diisopropylphenyl)-1,6,9,14-tetra[4-(1,1,3,3-tetramethylbutyl)-phenoxy]-terrylene-3,4:11,12-tetracarboxylic acid-3,4-anhydride-11,12-imide (**4**; 70.8 mg, 47.4 μmol), and 1 g imidazole was heated to 105 °C under an argon atmosphere for 7 h. Ethanol (8 mL) was carefully poured into the hot solution. The reaction mixture was then cooled down to room temperature and 20 mL dichloromethane and 20 mL aqueous HCl solution (2 N) were added. The layers were separated and the aqueous layer was extracted with dichloromethane (3 × 20 mL), dried over Na_2SO_4, and concentrated by rotary evaporation. The residue was purified by column chromatography on silica gel (CH_2Cl_2/*n*-hexane (2/1, v/v)) and the isolated product was dried at

10^{-3} mbar to yield 74.0 mg (37.8 µmol, 80%) of **2o** as a green solid. Mp: 213–214 °C (from dichloromethane).
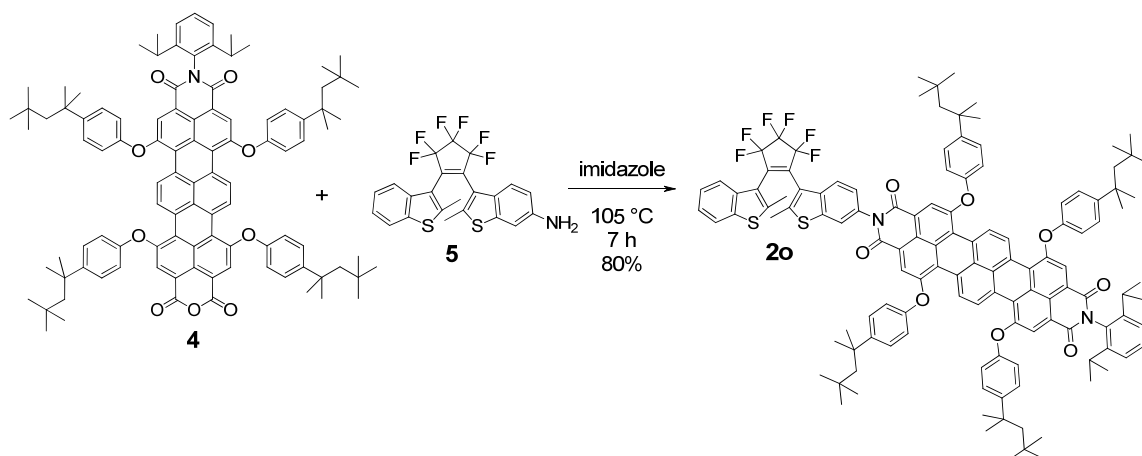
$C_{125}H_{122}F_6N_2O_8S_2$ (1958.435)

¹H NMR (400 MHz, CD_2Cl_2, 300 K): δ 9.53 (s, 4H), 8.17–8.21 (m, 4H), 7.55–7.80 (m, 4H), 7.42–7.49 (m, 9H), 7.20–7.40 (m, 5H), 7.07–7.15 (m, 8H), 2.70 (sept, ^3J(H,H) = 6.8 Hz, 2H), 2.63 (s, 1.1H), 2.63 (s, 1.1H), 2.54 (s, 1.9H), 2.53 (s, 1.9H), 1.75 (s, 4H), 1.74 (s, 4H), 1.39 (s, 24H), 1.08 (d, ^3J(H,H) = 6.8 Hz, 12H), 0.74 (s, 18H), 0.73 (s, 18H).

HRMS (ESI, pos. mode, acetonitrile/$CHCl_3$ 1:1): m/z: calcd for $C_{125}H_{123}F_6N_2O_8S_2$: 1957.8623 $[M+H]^+$; found: 1957.8620.

UV/vis (CH_2Cl_2): λ_{max}/nm (ε/M^{-1} cm^{-1}) = 448 (9400), 625 (47400), 681 (93600).

Fluorescence (CH_2Cl_2): λ_{max} = 717 nm (λ_{ex} = 651 nm), Φ_{fl} = 0.31.

CV (CH_2Cl_2, 0.1 M TBAHFP, vs. Fc/Fc⁺): $E_{1/2}^{red}$ (X/X^-) = –1.16 V, $E_{1/2}^{ox}$ (X/X^+) = 0.49 V, $E_{1/2}^{ox}$ (X^+/X^{2+}) = 0.79 V.

Closed form of photochromic dyad 2c

This compound was synthesized according to the procedure reported for the closed form of a 1,7-dipyrrolidinyl-perylene bisimide-diarylethene conjugate.[1] A solution of the open form of dyad **2o** (33.1 mg, 16.9 µmol) in 400 mL dichloromethane was irradiated in a Rayonet photoreactor RPR-100 with UV light (350 nm) for 1 h under vigorous stirring. The solution was concentrated by rotary evaporation in the dark, the resultant precipitate was purified in the dark by column chromatography on silica gel (acetone/n-hexane (1/10, v/v)), and the isolated product was dried at 10^{-3} mbar to yield 17.0 mg (8.68 µmol; 51%) of **2c** as a dark green solid.
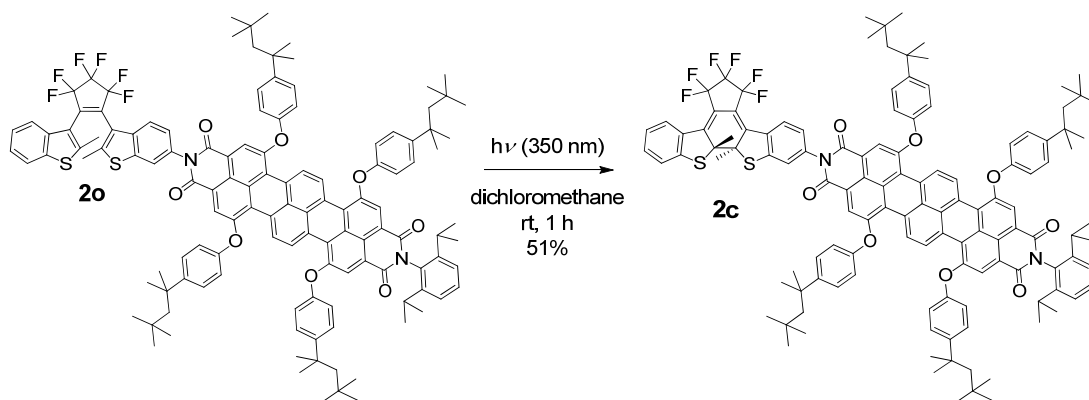
$C_{125}H_{122}F_6N_2O_8S_2$ (1958.435)

^{1}H NMR (600 MHz, CD$_2$Cl$_2$, 300 K): δ 9.51 (s, 4H), 8.16–8.19 (m, 4H), 8.01 (d, ^3J(H,H) = 8.5 Hz, 1H), 7.92 (d, ^3J(H,H) = 8.2 Hz, 1H), 7.42–7.48 (m, 9H), 7.33 (t, ^3J(H,H) = 8.0 Hz, 1H), 7.28–7.31 (m, 3H), 7.21 (d, ^4J(H,H) = 2.0 Hz, 1H), 7.17–7.20 (m, 1H), 7.08–7.13 (m, 8H), 7.05–7.08 (m, 1H), 2.68 (sept, ^3J(H,H) = 6.8 Hz, 2H), 2.70 (s, 3H), 2.05 (s, 3H), 1.75 (s, 4H), 1.74 (s, 4H), 1.38 (s, 24H), 1.08 (d, ^3J(H,H) = 6.8 Hz, 12H), 0.74 (s, 18H), 0.72 (s, 18H).

HRMS (ESI, pos. mode, acetonitrile/CHCl$_3$ 1:1): m/z: calcd for $C_{125}H_{123}F_6N_2O_8S_2$: 1957.8623 [M+H]$^+$; found: 1957.8599.

UV/vis (CH$_2$Cl$_2$): λ_{max}/nm (ε/M^{-1} cm^{-1}) = 281 (53900), 353 (16300), 447 (12300), 627 (50200), 683 (98000).

Fluorescence (CH$_2$Cl$_2$): λ_{max} = 719 nm (λ_{ex} = 651 nm), Φ_{fl} = 0.29.

Open form of terrylene bisimide-diarylethene dyad with glycine linker 3o

A mixture of 66.5 mg (52.4 µmol) N-(2,6-diisopropylphenyl)-1,6,9,14-tetra(4-$tert$-butylphenoxy)-terrylene-3,4,11,12-tetracarboxylic acid-3,4-anhydride-11,12-imide (**6**), 36.8 mg (62.9 µmol) of the slightly impure DAE precursor **7** (still contaminated with urea-derivative, see Chapter 3.6), 1 g imidazole and 1 mL distilled pyridine were heated for 6 h to 110 °C under an argon atmosphere. The reaction mixture was quenched with diluted hydrochloric acid and then extracted with dichloromethane (4 × 20 mL). The combined organic layers were dried over sodium sulfate and evaporated under reduced pressure. The crude product was purified by column chromatography on silica gel (dichloromethane/n-hexane/acetic acid 80:20:1 (v/v/v)) to yield a dark green solid (31.9 mg; 17.4 µmol; 33%). Mp: 259–260 °C (from dichloromethane).
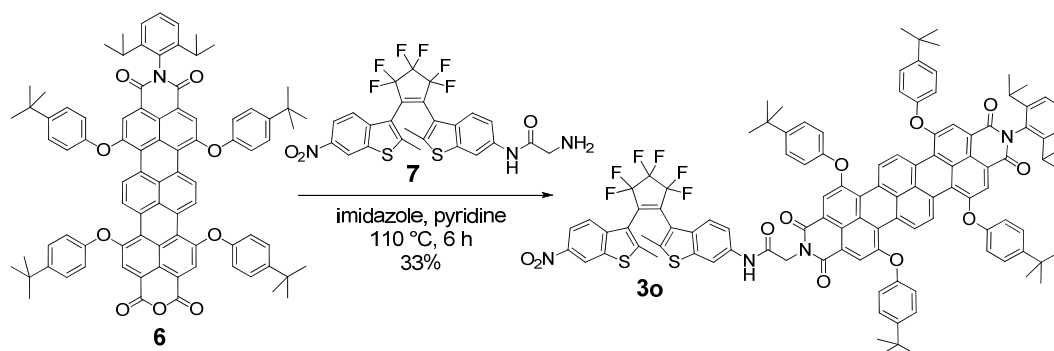
C$_{111}$H$_{92}$F$_6$N$_4$O$_{11}$S$_2$ (1836.109)

^{1}H NMR (600 MHz, CD$_2$Cl$_2$, 300 K): δ 9.24–9.31 (m, 4H), 8.60 (s, 0.6H), 8.51 (s, 0.4H), 8.19–8.22 (m, 0.6H), 8.12–8.17 (m, 2H), 7.96–8.03 (m, 2H), 7.89–7.95 (m, 2H), 7.84 (s, 0.4H), 7.68–7.73 (m, 0.6H), 7.57–7.61 (m, 0.4H), 7.22–7.49 (m, 12.6H), 6.99–7.12 (m, 8.4H), 4.73–4.81 (m, 2H), 2.76 (sept, ^3J(H,H) = 7.0 Hz, 2H), 2.53 (s, 1.3H), 2.41 (s, 1.3H), 2.25 (s, 1.7H), 2.12 (s, 1.7H), 1.32–1.36 (m, 36H), 1.07 (d, ^3J(H,H) = 6.8 Hz, 12H).

HRMS (ESI, pos. mode, acetonitrile/CHCl$_3$ 1:1): m/z: calcd for C$_{111}$H$_{93}$F$_6$N$_4$O$_{11}$S$_2$: 1835.6185 [M+H]$^+$; found: 1835.6163.

MS (MALDI, pos. mode, DCTB 1:3 in CHCl$_3$): m/z: calcd for C$_{111}$H$_{92}$F$_6$N$_4$O$_{11}$S$_2$: 1834.611 [M]$^+$; found: 1834.597.

UV/vis (CH$_2$Cl$_2$): λ_{max}/nm (ε_{max}/M^{-1} cm^{-1}) = 284 (66200), 448 (9900), 625 (49200), 681 (96600).

Fluorescence (CH$_2$Cl$_2$): λ_{max} = 721 nm (λ_{ex} = 651 nm), Φ_{fl} = 0.22.

Open form of terrylene bisimide diarylethene dyad with glycine linker 3c

This compound was synthesized according to the procedure reported for the closed form of a 1,7-dipyrrolidinyl-perylene bisimide-diarylethene conjugate.[1] A solution of the open form of dyad **3o** (25.4 mg, 13.8 μmol) in 300 mL dichloromethane was irradiated in a Rayonet photoreactor RPR-100 with UV light (350 nm) for 20 min under vigorous stirring. The solution was concentrated by rotary evaporation in the dark and the resultant precipitate was purified in the dark by column chromatography on silica gel (acetone/n-hexane (1/4, v/v)) and the isolated product was dried at 10^{-3} mbar to yield 38.8 mg (19.1 μmol; 75%) of **3c** as a dark green solid.
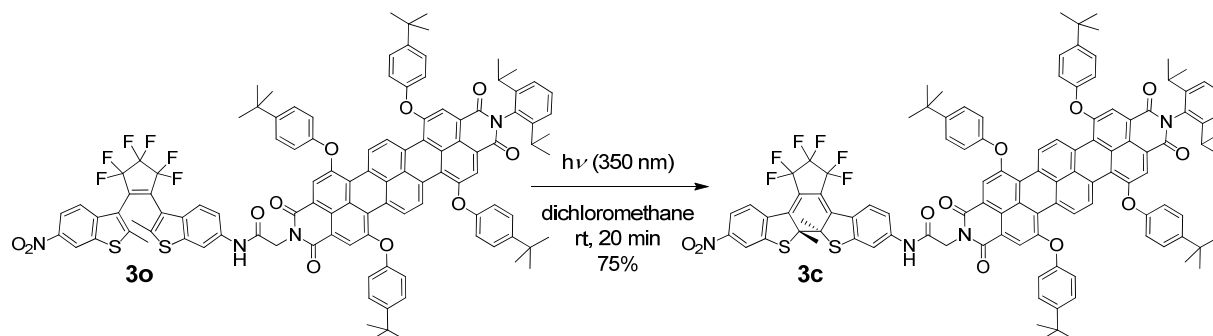
C$_{111}$H$_{92}$F$_6$N$_4$O$_{11}$S$_2$ (1836.109)

¹H NMR (600 MHz, CD_2Cl_2, 300 K): δ 9.32–9.37 (m, 4H), 8.16 (s, 2H), 8.10 (brs, 1H), 8.05 (d, ^4J(H,H) = 2.0 Hz, 1H), 8.01 (s, 2H), 7.91–7.96 (m, 2H), 7.80 (d, ^3J(H,H) = 8.8 Hz, 1H), 7.73 (d, ^4J(H,H) = 2.0 Hz, 1H), 7.41–7.47 (m, 9H), 7.29 (d, ^3J(H,H) = 7.9 Hz, 2H), 7.04–7.12 (m, 9H), 4.83 (s, 2H), 2.74 (sept, ^3J(H,H) = 6.8 Hz, 2H), 1.99 (s, 3H), 1.98 (s, 3H), 1.33 (s, 18H), 1.33 (s, 18H), 1.07 (d, ^3J(H,H) = 6.8 Hz, 12H).

HRMS (ESI, pos. mode, acetonitrile/$CHCl_3$ 3:1): m/z: calcd for $C_{111}H_{93}F_6N_4O_{11}S_2$: 1835.6185 $[M+H]^+$; found: 1835.6183.

UV/vis (CH_2Cl_2): λ_{max}/nm (ε/M^{-1} cm^{-1}) = 280 (58000), 392 (19600), 635 (53800), 682 (97500).

Fluorescence (CH_2Cl_2): λ_{max} = 723 nm (λ_{ex} = 651 nm), Φ_{fl} = 0.12.

References

[1]   M. Berberich, A.-M. Krause, M. Orlandi, F. Scandola, F. Würthner, *Angew. Chem. Int. Ed.* **2008**, *47*, 6616-6619.

[2]   F. Würthner, *Chem. Commun.* **2004**, 1564-1579.

[3]   a) R. Gvishi, R. Reisfeld, Z. Burshstein, *Chem. Phys. Lett.* **1993**, *213*, 338-344; b) *Principles of Fluorescence Spectroscopy* (ed. J. R. Lakowitz), 2nd ed., Kluwer Academic/Plenum, New York, **1999**, pp. 52-55.

[4]   A. J. Fry, *Laboratory Techniques in Electroanalytical Chemistry* (eds. P. T. Kessing, W. R. Heinemann), 2nd ed., Marcel Dekker Ltd, New York, **1996**, p. 481.

List of Publications

Communications and Articles

- *Towards Fluorescent Memories with Non-destructive Read-out: Photoswitching of Fluorescence by Intramolecular Electron Transfer in a Diarylethene-Perylene Bisimide Photochromic System*
  M. Berberich, A.-M. Krause, M. Orlandi, F. Scandola, F. Würthner, *Angew. Chem.* **2008**, *120*, 6718-6721; *Angew. Chem. Int. Ed.* **2008**, *47*, 6616-6619.

- *Terrylene bisimide-Diarylethene Photochromic Switch*
  M. Berberich, F. Würthner, *Chem. Sci.* **2012**, *3*, 2771-2777.

- *Non-destructive Photoluminescence Read-out by Intramolecular Electron Transfer in a Perylene Bisimide-Diarylethene Dyad*
  M. Berberich, M. Natali, P. Spenst, C. Chiorboli, F. Scandola, F. Würthner, *Chem. Eur. J.* **2012**, *18*, doi:10.1002/chem.201201484.

Poster and Oral Presentations

Various presentations with the title *Towards Fluorescent Memories with Non-destructive Read-out: Photoswitching of Fluorescence by Intramolecular Electron Transfer in a Diarylethene-Perylene Bisimide Photochromic System*:

- 5th International Workshop for Conjugated Polymers and Oligomers (KOPO 2007): From Synthesis to Electronic Function (poster presentation)
  Blaubeuren/Ulm, September 24–27, 2007
- 1. Chemistry-Symposium of the students of Mainfranken - Chem-SyStM 2007 (poster presentation)
  Würzburg, December 4, 2007
- PhD Student Lecture of the Organic Chemistry Department (oral presentation)
  University of Würzburg, July 7, 2008
- 118th BASF International Summer Course (poster presentation)
  Ludwigshafen, August 11–21, 2008
- International Conference of the Research Training School GRK1221: Electronic Processes in π-Conjugated Materials (poster presentation)
  Würzburg, October 7–10, 2008

- ISNA 13 – 13th International Symposium on Novel Aromatic Compounds
  Luxemburg, July 19–24, 2009 (poster presentation)
- XXIIIrd IUPAC Symposium on Photochemistry
  Ferrara, July 11–16, 2010 (poster presentation)
- 3. Chemistry-Symposium of the students of Mainfranken - Chem-SyStM 2010 (poster presentation)
  Würzburg, December 7, 2010
- International Conference of the Research Training School GRK1221: Electronic Processes in π-Conjugated Materials II (poster presentation)
  Würzburg, September 27–30, 2011

Curriculum Vitae

Personal Details

Name	Martin Berberich
Date of Birth	November 9, 1981
Place of Birth	Miltenberg, Germany

Education

09/92 – 05/01	Karl-Ernst-Gymnasium, Amorbach School leaving examination (Abitur); Degree: 1.4
08/01 – 07/02	Civilian service
10/02 – 08/07	Chemistry studies at the University of Würzburg Degree: Diploma (1.3)
11/06 – 08/07	Diploma work in the group of Prof. Dr. Frank Würthner at the Institute of Organic Chemistry, University of Würzburg: "*Photoschaltbare Diarylethen-Perylenbisimid-Konjugate:* *Synthese, optische und elektrochemische Eigenschaften*"
09/07 – 08/12	PhD studies in the group of Prof. Dr. Frank Würthner: "*Rylene Bisimide-Diarylethene Photochromic Systems* *for Non-destructive Memory Read-out*"

Professional Membership

Gesellschaft Deutscher Chemiker (GDCh, Society of German Chemists)

Danksagung